

ORE RESERVES ESTIMATION OF THE NAM NGA COAL DEPOSIT, LAO PDR, USING
GEOSTATISTICAL METHOD



A Thesis Submitted in Partial Fulfillment of the Requirements
for the Degree of Master of Engineering in Georesources and Petroleum Engineering
Department of Mining and Petroleum Engineering
Faculty of Engineering
Chulalongkorn University
Academic Year 2018
Copyright of Chulalongkorn University

การประเมินปริมาณสำรองแหล่งถ่านหินน้ำงา สปป. ลาว โดยวิธีการทางธรณีสถิติ



วิทยานิพนธ์นี้เป็นส่วนหนึ่งของการศึกษาตามหลักสูตรปริญญาวิศวกรรมศาสตรมหาบัณฑิต
สาขาวิชาวิศวกรรมทรัพยากรธรณีและปิโตรเลียม ภาควิชาวิศวกรรมเหมืองแร่และปิโตรเลียม

คณะวิศวกรรมศาสตร์ จุฬาลงกรณ์มหาวิทยาลัย

ปีการศึกษา 2561

ลิขสิทธิ์ของจุฬาลงกรณ์มหาวิทยาลัย

Thesis Title	ORE RESERVES ESTIMATION OF THE NAM NGA COAL DEPOSIT, LAO PDR, USING GEOSTATISTICAL METHOD
By	Mr. Tongvang Blichongvang
Field of Study	Georesources and Petroleum Engineering
Thesis Advisor	Assistant Professor Sunthorn Pumjan, Ph.D.
Thesis Co Advisor	Songwut Artittong, Ph.D.

Accepted by the Faculty of Engineering, Chulalongkorn University in Partial
Fulfillment of the Requirement for the Master of Engineering

..... Dean of the Faculty of Engineering
(Professor SUPOT TEACHAVORASINSKUN, D.Eng.)

THESIS COMMITTEE

..... Chairman
(Associate Professor Somsak Saisinchai)

..... Thesis Advisor
(Assistant Professor Sunthorn Pumjan, Ph.D.)

..... Thesis Co-Advisor
(Songwut Artittong, Ph.D.)

..... Examiner
(Dr. Raphael Bissen)

..... External Examiner
(Associate Professor Pinyo Meechumna, Ph.D.)

ทองวัง เบลีเยนทองวัง : การประเมินปริมาณสำรองแหล่งถ่านหินน้ำงา สปป. ลาว โดย
 วิธีการทางสถิติ. (ORE RESERVES ESTIMATION OF THE NAM NGA COAL
 DEPOSIT, LAO PDR, USING GEOSTATISTICAL METHOD) อ.ที่ปรึกษาหลัก : ผศ.
 ดร.สุนทร พุ่มจันทร์, อ.ที่ปรึกษาร่วม : ดร.ทรงวุฒิ อาทิตย์ทอง

การศึกษาวิจัยครั้งนี้มีวัตถุประสงค์เพื่อประเมินปริมาณ และคุณภาพของแหล่งถ่านหิน
 เช่นค่าความร้อนและปริมาณเถ้าของถ่านหินที่แหล่งถ่านหินน้ำงา สปป. ลาว โดยใช้วิธีการทางสถิติ
 เชิงเส้น (Ordinary Kriging; OK) และไม่ใช่เชิงเส้น (Sequential Gaussian Simulation;
 SGS) การประเมินเหล่านี้ใช้ข้อมูลวิเคราะห์คุณภาพถ่านหินจำนวน 295 ตัวอย่างที่รวบรวมจาก
 หลุมเจาะสำรวจจำนวน 51 หลุม จากบริษัทลาวพัฒนาเหมืองถ่านหิน ผลการวิจัยพบว่าวิธีการแบบ
 OK ให้ปริมาณสำรองทางธรณีวิทยา (Geological resource) ที่ 2.2 ล้านตัน โดยมีค่าความร้อน
 เฉลี่ยเท่ากับ 3,733 กิโลแคลอรีต่อกิโลกรัม และค่าปริมาณเถ้าเฉลี่ยเท่ากับ 48.68 เปอร์เซ็นต์
 ปริมาณสำรองที่ทำเหมืองได้ (Mineable reserve) ของแบบ OK เมื่อประเมินจากการออกแบบ
 เหมือง และบ่อเหมืองที่ปรับแล้วพบว่ามีปริมาณ 0.55 ล้านตัน วิธีการแบบ OK สามารถคำนวณ
 ปริมาณเปลือกดิน และหินที่ 9.32 ล้านตัน โดยมีค่าอัตราส่วนการเปิดเปลือกดินเท่ากับ 10.4:1
 ส่วนวิธีการแบบ SGS มีปริมาณสำรองทางธรณีวิทยาที่ 2.2 ล้านตัน โดยมีค่าความร้อนเฉลี่ยเท่ากับ
 3,769 กิโลแคลอรีต่อกิโลกรัม และค่าปริมาณเถ้าเฉลี่ยเท่ากับ 46.29 เปอร์เซ็นต์ วิธีการของ SGS
 คำนวณปริมาณสำรองที่ทำเหมืองได้ที่ 0.54 ล้านตัน จากออกแบบเหมือง และบ่อเหมืองที่ปรับแล้ว
 วิธีการของแบบ SGS คำนวณปริมาณเปลือกดิน และหินที่ 9.5 ล้านตัน โดยมีค่าอัตราส่วนการเปิด
 เปลือกดินเท่ากับ 10.1:1

อย่างไรก็ตามวิธีการแบบ OK และ SGS ให้ค่าผลลัพธ์ประเมินที่ใกล้เคียงกัน โดยค่า
 ประเมินจาก OK ใกล้เคียง แต่ในขณะที่การประเมินแบบ SGS จะยังคงรักษาโครงสร้างของความ
 แปรปรวนของข้อมูลเดิมไว้ โดยที่ค่าความแปรปรวนของข้อมูลที่ถูกจำลองจะมีค่าใกล้เคียงกับความ
 แปรปรวนของข้อมูลเดิม นอกจากนี้การประเมินแบบ SGS ยังให้ภาพจำลอง (realizations)
 หลากหลายภาพ ซึ่งจะเป็ประโยชน์ต่อการประเมินความเสี่ยงในการพัฒนาเหมืองแร่

สาขาวิชา วิศวกรรมทรัพยากรธรณีและ ลายมือชื่อนิสิต

ปีโตรเลียม

ปีการศึกษา 2561 ลายมือชื่อ อ.ที่ปรึกษาหลัก

ลายมือชื่อ อ.ที่ปรึกษาร่วม

6071202821 : MAJOR GEORESOURCES AND PETROLEUM ENGINEERING

KEYWORD: COAL QUALITIES ESTIMATION, ORDINARY KRIGING, SEQUENTIAL
GAUSSIAN SIMULATION, PIT OPTIMIZATION, MINEABLE RESERVE

Tongvang Bliachongvang : ORE RESERVES ESTIMATION OF THE NAM NGA
COAL DEPOSIT, LAO PDR, USING GEOSTATISTICAL METHOD. Advisor: Asst.
Prof. Sunthorn Pumjan, Ph.D. Co-advisor: Songwut Artittong, Ph.D.

This research study focuses on estimating the coal deposit quantity and qualities as CV and AC at Nam Nga coal deposit, Lao PDR using OK and SGS geostatistical methods. A total of 295 assays data from 51 exploration drill holes collected from LID Company were used. The results reveal that OK produces geological resource of 2.2 MT with an average CV of 3,733 kcal/kg and an average AC of 48.68 %. The mineable reserve computed from OK's ultimate pit design and pit adjustment are 0.55 MT. The OK method produces 9.32 MT of wastes, yielding a stripping ratio of 10.4:1. The SGS method produces 2.2 MT of geological resource with an average CV of 3,769 kcal/kg, and an average AC of 46 %. The SGS's ultimate pit design and pit adjustment generate 0.54 MT of mineable reserve. The SGS generates wastes 9.5 MT, yielding a stripping ratio of 10.1:1.

In comparison, the OK and SGS produce the very similar results for coal grades estimation, mineable reserve, and stripping ratio calculation. However, OK generates smoother maps when most of the estimated values moving toward the mean value. SGS method is better in preserving a local variation, as can be seen in the overall simulated variance closed to the original data variance. And SGS also provides a multiple realization maps which bring a benefit for accessing the risk involved.

Field of Study: Georesources and
Petroleum Engineering

Student's Signature

Academic Year: 2018

Advisor's Signature

Co-advisor's Signature

ACKNOWLEDGEMENTS

I would like to express my sincere acknowledgement for the financial support provided by the ASEAN University Network/Southeast Asia Engineering Education Development Network (AUN/SEED-Net) of the Japan International Cooperation Agency (JICA), who has offered me the opportunity to study within master's degree program in Georesources Engineering at Department of Mining and Petroleum, Faculty of Engineering, Chulalongkorn University.

I would like to express deep gratitude to my research advisor, Asst. Prof. Dr. Sunthorn Pumjan for his professional guidance, enthusiastic encouragement and valuable and constructive suggestions during the planning and development of this research work. I would also like to thank my co-advisor, Dr. Songwut Artittong for his advice, assistance, and valuable support.

I would like to express my very great appreciation to Assoc. Prof. Somsak Saisinchai, the chairman of the thesis committee, for his encouragement, useful critiques for this research. My grateful thanks are also extended to Dr. Raphael Bissen (thesis committee), and Assoc. Prof. Dr. Pinyo Meechumna (thesis external examiner) for their useful advice and suggestions for this research work.

I would like to extend my thanks to the Lao Integrated Development Group company for their assistance with the collection of my data and allow me to visit the mine site for this research.

I wish to thank Ms. Narumas Pajonpai and my friends at the Department of Mining and Petroleum Engineering for their insight and ideas during our discussion.

At last, I would like to acknowledge my beloved family members from the bottom of my heart, especially my mother, for their encouragement, advice and mental support to get through all obstacles since I have started my first schooling.

Tongvang Bliachongvang

TABLE OF CONTENTS

	Page
.....	iii
ABSTRACT (THAI).....	iii
.....	iv
ABSTRACT (ENGLISH).....	iv
ACKNOWLEDGEMENTS	v
TABLE OF CONTENTS.....	vi
LIST OF TABLES.....	x
LIST OF FIGURES	xiii
LIST OF ABBREVIATIONS	xix
LIST OF SYMBOLS	xx
CHAPTER 1 INTRODUCTION.....	1
1.1 Background.....	1
1.2 Location of the study area.....	2
1.3 General information of the LID’s concession area	4
1.3.1 Geography and access roads to the LID’s concession area	4
1.3.2 Local climate.....	6
1.3.3 Main rivers within the concession area.....	6
1.4 Geological setting and coal deposits within the concession area.....	7
1.4.1 Regional geology.....	7
1.4.2 Local geology	9
1.4.3 Volcanic rocks	10

1.4.4 Geological setting of coal basin	10
1.5 Statement of problem.....	15
1.6 Research objectives.....	16
1.7 Scope of study	16
1.8 Contributions	17
CHAPTER 2 THEORY AND LITERATURE REVIEW	18
2.1. Theory	18
2.1.1 Background of geostatistical applications	18
2.1.2 Summary of statistical analysis parameters.....	18
2.1.3 Histograms.....	23
2.1.4 Scatterplots.....	23
2.1.5 The Method of linear squares	25
2.1.6 Linear regression analysis.....	26
2.1.7 Drill holes composite	27
2.1.8 3D block modelling.....	28
2.1.9 Spatial analysis.....	29
2.1.10 Kriging estimation	35
2.1.11 Sequential Gaussian Simulation (SGS)	38
2.1.12 Pit limit	40
2.2. Literature review	41
CHAPTER 3 RESEARCH METHODOLOGY.....	45
3.1 Topography and drill holes data preparation.....	46
3.2 Database formatting and loading	47
3.3. Drill hole composites.....	51

3.4. Statistical analysis of composited data	53
3.5. 3D Solid zone construction	53
3.6. 3D block model development	56
3.7. Kriging estimation	57
3.7.1. Variogram calculation and modelling	57
3.7.2. Ordinary Kriging Estimation (OK)	58
3.7.3. The geological resource estimation.....	64
3.7.4. The Pit optimization and mineable reserve estimation	65
3.7.5. The pits adjustment and mineable reserve estimation	66
3.8. Sequential Gaussian Simulation (SGS)	67
3.8.1. Variogram calculation and modeling.....	67
3.8.2. SGS block grades simulation	69
3.8.3. SGS's geological resource estimation	77
3.8.4. SGS's Pit optimization and mineable reserves estimation	77
3.8.5. Pits adjustment and mineable reserves estimation	77
CHAPTER 4 RESULTS AND DISCUSSIONS	78
4.1. Drill hole data statistical analysis	78
4.2. Drill holes data compositing.....	79
4.3. 3D geological solid model	82
4.4. Ordinary Kriging (OK) Estimation.....	82
4.4.1. Variogram calculation and modelling	82
4.4.2. Variogram model validation	84
4.4.3. 3D block model and resources estimation.....	86
4.4.4. Pit optimization and mineable reserve estimation	93

4.4.5. Pits adjustment, mineable reserve and Grade Tonnage Curve	98
4.5. Sequential Gaussian Simulation (SGS)	108
4.5.1. Gaussian data transformation and variogram modelling.....	108
4.5.2. 3D block model and geological resources estimation.	110
4.5.3. SGS's Pit optimization and mineable reserves estimation	127
4.5.4. SGS's Pits adjustment, mineable reserve and Grade-Tonnage Curve	132
4.6. Compositing data, OK's and SGS's results comparison	143
CHAPTER 5 CONCLUSIONS AND RECOMMENDATIONS	146
5.1. Conclusions	146
5.2. Recommendations.....	147
REFERENCES	148
VITA.....	151

LIST OF TABLES

	Page
Table 3.1 Coal resource classification based on sampling spacing defined by the JORC Code 2012 system (De Souza et al., 2004)	59
Table 3.2 Kriging input parameters for coal quality parameters interpolation.....	60
Table 3.3 Geotechnical and economic parameters for pit optimization.....	65
Table 3.4 Coal prices at the LID mine mouth based on CV basis.....	65
Table 3.5 The pits adjustment parameters.....	67
Table 3.6 SGS's input parameters for block grades simulation.....	71
Table 4.1 Drill-hole data statistics.....	78
Table 4.2 Results of variogram model fitted for CV and AC.	83
Table 4.3 Comparison between composited and estimated CV statistical parameters.	84
Table 4.4 Comparison between composited and estimated AC statistical parameters.	86
Table 4.5 OK's input parameters and outputs of block grades estimation.....	87
Table 4.6 OK's geological resource classified by CV basis.....	88
Table 4.7 OK's geological coal resource classified by bench level.....	90
Table 4.8 OK's mineable reserve from nine optimal pits classified by CV basis.	96
Table 4.9 The OK's mineable reserve calculated from nine optimal pits classified by bench level.....	97
Table 4.10 OK's mineable reserve from the five adjusted pits based on the CV basis.	99
Table 4.11 Summary of the OK's mineable reserve in pit No.1.....	100

Table 4.12 Summary of OK's mineable reserve in pit No.2	101
Table 4.13 Summary of mineable coal reserve in pit No.3.....	102
Table 4.14 Summary of mineable coal reserve in pit No.3 (Continue).....	103
Table 4.15 Summary of OK's mineable reserve in pit No.4	105
Table 4.16 Summary of OK's mineable reserve in pit No.5.	106
Table 4.17 Variogram model results of normal transformed data for SGS simulation.	110
Table 4.18 SGS's input parameters and outputs of block grades simulation.	111
Table 4.19 SGS's geological resource estimation based on the CV basis.	112
Table 4.20 SGS's geological resource estimation by bench level.	112
Table 4.21 Comparison of statistical parameters of CV for 5 realizations.....	121
Table 4.22 Comparison of statistical parameters of AC for 5 realizations.....	121
Table 4.23 The SGS's mineable reserves from multiple optimal pits by CV basis. ...	130
Table 4.24 SGS's mineable reserve from nine optimum pits generated by LG algorithm by bench level.....	131
Table 4.25 SGS's mineable reserves after pits adjustment based on the CV basis. ...	135
Table 4.26 Summary of mineable reserve after SGS's pits adjustment for pit No.1. ...	136
Table 4.27 Mineable reserve after pits adjustment for SGS's pit No.2.	138
Table 4.28 Summary of mineable reserve after SGS's pits adjustment for pit No.3. ...	139
Table 4.29 Summary of mineable reserves after SGS's pits adjustment for pit No.4.	141
Table 4.30 Summary of mineable reserve after SGS's pits adjustment for pit No.5. ...	142
Table 4.31 Statistical parameters comparison among composited data, OK's results and SGS's results of CV.....	143

Table 4.32 Statistical parameters comparison among composited data, OK's results and SGS's results of AC.....	144
--	-----



LIST OF FIGURES

	Page
Figure 1.1 Location of the study area within the LID's concession area.....	2
Figure 1.2 Location of Lao Integrated Development Group Company.....	3
Figure 1.3 Three alternative access roads to LID exploration area.....	5
Figure 1.4 Elevation model map of LID's concession area and surrounding areas.....	6
Figure 1.5 Geologic structures map of Lao PDR and its neighboring countries.....	8
Figure 1.6 Geological map of the LID's concession area.	12
Figure 1.7 Geological map of coal bearing rock unit in the concession area.....	13
Figure 1.8 2D cross section of geological map of coal bearing rock units in within the LID's concession area.	14
Figure 1.9 The overall stratigraphic unit in the LID's concession area.....	15
Figure 2.1 A single peak and symmetric frequency distribution with mean, standard deviation.....	20
Figure 2.2 Histogram of AC (Wierzchowski, Chećko, & Pyka, 2017).	24
Figure 2.3 Histogram of CV (Olea, Luppens, Egozcue, & Pawlowsky-Glahn, 2016).	24
Figure 2.4 Example of scatter plot between calorific value and ash content (Lieskovský, Jankovský, Trenčiansky, & Merganič, 2017).....	25
Figure 2.5 Example of linear square method.....	26
Figure 2.6 Geometric parameters and boundary conditions of the numerical model of Baijiazhuang coal mine at Shanxi province, China (Bai et al., 2018).	28
Figure 2.7 Experimental variogram model shape (Saputra, 2008).....	31
Figure 2.8 Linear variogram model (Asmael, Dupuy, Huneau, Hamid, & Coustumer, 2015).....	32

Figure 2.9 Variogram models of Spherical, Exponential, Power, and Gaussian.....	34
Figure 2.10 Fundamental steps of SGS method (Asghari et al., 2009).....	40
Figure 2.11 The Open Pit Schematic.....	41
Figure 3.1 Flowchart of the research study.....	45
Figure 3.2 The contour map of 5-meter interval at NG exploration area.....	46
Figures 3.3 Flowchart of necessary files creation in MS3D software (Vang, 2015).....	48
Figure 3.4 Method of importing collar.csv to MS3D software.....	48
Figure 3.5 Method of importing survey.csv to MS3D software.....	49
Figure 3.6 Method of importing assay.csv to MS3D software (Data input).....	49
Figure 3.7 Method of importing assay.csv to MS3D software (Parameters loading)....	50
Figure 3.8 Method of importing geology.csv to MS3D software (Data input).....	50
Figure 3.9 Method of importing geology.csv to MS3D software (Lithology code).....	51
Figure 3.10 Drill hole composite in MS3D software (Composite limiting).....	52
Figure 3.11 Drill hole composite in MS3D software (Composite report).....	52
Figure 3.12 Exploration drill holes cross section determination.....	54
Figure 3.13 2D cross section of section-KK' of coal seams digitization.....	54
Figure 3.14 Flowchart of steps used to generate the 3D solid model.....	55
Figure 3.15 3D block model generated within 3D solid model of NG coal deposit. ..	56
Figure 3.16 Global vertical experimental variogram of CV.....	58
Figure 3.17 Global vertical experimental variogram of AC.....	58
Figure 3.18 OK method of CV in MS3D software (Data input).....	60
Figure 3.19 OK method of CV in MS3D software (Model parameters).....	61
Figure 3.20 OK method of CV in MS3D software (Kriging search parameters).....	61
Figure 3.21 OK method of CV in MS3D software (Interpolation control items).....	62

Figure 3.22 OK method of CV in MS3D software (Variogram model parameters)	62
Figure 3.23 OK method of CV in MS3D software (Optional search parameters).....	63
Figure 3.24 OK method of CV in MS3D software (block limiting).....	63
Figure 3.25 OK method of CV in MS3D software (Optional composite data selection)	64
Figure 3.26 The vertical experimental variogram of CV for SGS.....	68
Figure 3.27 The vertical experimental variogram of AC for SGS.....	68
Figure 3.28 Flowchart of Sequential Gaussian Simulation system.....	70
Figure 3.29 SGS method of CV simulation in MS3D software (Data input type).....	71
Figure 3.30 SGS method of CV simulation in MS3D software (Composited file input)	72
Figure 3.31 SGS method of CV simulation in MS3D software (composited items).....	72
Figure 3.32 SGS method of CV simulation in MS3D software (Data control).....	73
Figure 3.33 SGS method of CV simulation in MS3D software (Block model input).....	73
Figure 3.34 SGS method of CV simulation in MS3D software (Block model items)	74
Figure 3.35 SGS method of CV simulation in MS3D software (Block model limiting) .	74
Figure 3.36 SGS method of CV simulation in MS3D software (Searching pattern).....	75
Figure 3.37 SGS method of CV simulation in MS3D software (Ellipsoidal searching)..	75
Figure 3.38 SGS method of CV in MS3D software (Variogram model parameters).....	76
Figure 3.39 SGS method of CV in MS3D software (Conditioning Parameters)	76
Figure 4.1 Histogram of CV of composited data.	79
Figure 4.2 Histogram of AC of composited data.	80
Figure 4.3 Scatterplots of CV and AC.	80
Figure 4.4 3D display of topography map and drill hole data.....	81


Figure 4.5 Example of NG DHs composited data (Left = assays, Right = composited).	81
Figure 4.6 3D solid model view of major coal seams with topography and DHs data.	82
Figure 4.7 Variogram fitted model of CV.	83
Figure 4.8 Variogram fitted model of AC.	84
Figure 4.9 Scatterplot between composited data versus estimated values of CV.	85
Figure 4.10 Scatterplot between composited data versus estimated values of AC. ...	85
Figure 4.11 Histogram plot of CV's estimated values.....	88
Figure 4.12 Histogram plot of AC's estimated values.....	89
Figure 4.13 Scatterplot between estimated CV and AC.....	89
Figure 4.14 Top view of 3D estimated blocks model of CV.....	91
Figure 4.15 3D estimated blocks model showing CV's variance.	92
Figure 4.16 3D estimated blocks model of AC.....	92
Figure 4.17 3D estimated blocks model AC's variance	93
Figure 4.18 Nine optimum pits from pit optimization of NG coal deposit.....	94
Figure 4.19 Top views and 2D cross section view of optimum pits No. 1, 2, 3, and 4.	94
Figure 4.20 Top views and 2D cross section view of optimum pits No. 5.	95
Figure 4.21 Top views and 2D cross section view of optimum pits No. 6 and 7.....	95
Figure 4.22 Top views and 2D cross section view of optimum pits No. 9.	96
Figure 4.23 Top views of 5 adjusted pits (Pits No. 1, 2, 3, 4 and 5).....	98
Figure 4.24 Bottom views of 5 adjusted pits (Pits No. 1, 2, 3, 4 and 5).	99
Figure 4.25 2D cross section views of adjusted pits No. 1, 2 and 3.....	104
Figure 4.26 2D cross section views of adjusted pit No. 4.....	104

Figure 4.27 2D cross section view of adjusted pit No.5.....	107
Figure 4.28 OK's Grade Tonnage Curve of NG coal deposit.....	107
Figure 4.29 Normal scores distribution plot of CV.	108
Figure 4.30 Normal scores distribution plot of AC.	109
Figure 4.31 A vertical variogram model of CV.....	109
Figure 4.32 A vertical variogram model of AC.....	110
Figure 4.33 Map of realization No. 1 of CV.....	114
Figure 4.34 Map of realization No. 2 of CV.....	114
Figure 4.35 Map of realization No. 3 of CV.....	115
Figure 4.36 Map of realization No. 4 of CV.....	115
Figure 4.37 Map of realization No. 5 of CV.....	116
Figure 4.38 Map of E-Type Map (Mean) of CV.....	116
Figure 4.39 Map of variance map of CV.....	117
Figure 4.40 Map of realization No. 1 of AC.....	117
Figure 4.41 Map of realization No. 2 of AC.....	118
Figure 4.42 Map of realization No. 3 of AC.....	118
Figure 4.43 Map of realization No. 4 of AC.....	119
Figure 4.44 Map of realization No. 5 of AC.....	119
Figure 4.45 Map of E-Type Map (Mean) of AC.....	120
Figure 4.46 Map of variance map of AC.....	120
Figure 4.47 Histogram plot of CV's realization No.1.	122
Figure 4.48 Histogram plot of CV's realization No.2.	122
Figure 4.49 Histogram plot of CV's realization No.3.	123
Figure 4.50 Histogram plot of CV's realization No.4.....	123

Figure 4.51 Histogram plot of CV's realization No.5.	124
Figure 4.52 Histogram plot of AC's realization No.1.	124
Figure 4.53 Histogram plot of AC's realization No.2.	125
Figure 4.54 Histogram plot of AC's realization No.3.	125
Figure 4.55 Histogram plot of AC's realization No.4.	126
Figure 4.56 Histogram plot of AC's realization No.5.	126
Figure 4.57 SGS's nine ultimate pits from pit optimization.....	127
Figure 4.58 2D cross section views of SGS's pits No. 1, 2, 3, and 4.....	128
Figure 4.59 2D cross section views of SGS's pit No. 5.	128
Figure 4.60 2D cross section views of SGS's pits No. 6 and 7.....	129
Figure 4.61 2D cross section view of SGS's pit No. 9.....	129
Figure 4.62 2D cross section of long section views of SGS's pits.....	130
Figure 4.63 Top view of SGS's 5 adjusted pits generated by LG algorithm.	132
Figure 4.64 Bottom view of SGS's pit adjustment from multiple optimal pits.....	133
Figure 4.65 2D cross section views of SGS's pits No.1, 2 and 3.....	133
Figure 4.66 2D cross section views of SGS's pit No.4.	134
Figure 4.67 2D cross section view of SGS's pit No.5.	134
Figure 4.68 SGS's Grade Tonnage Curve of NG coal deposit.	143
Figure 4.69 Comparing GTC between OK's and SGS's results.	144
Figure 4.70 Comparing CV's histograms: (a). composited data, (b). OK's estimated values, (c). SGS's realization No.1.	145
Figure 4.71 Comparing AC's histograms: (a). composited data, (b). OK's estimated values, (c). SGS's realization No.1.	145

LIST OF ABBREVIATIONS

LXML	Lan Xang Minerals Limited
LID	Lao Integrated Development Group
NG	Nam Nga Coal Deposit
OK	Ordinary Kriging
SGS	Sequential Gaussian Simulation
CV	Calorific Value
AC	Ash Content
GTC	Grade Tonnage curve
LG	Lerch-Grossman
MS3D	MineSight 3D
SK	Simple Kriging
3DBM	3D Block Model
DH	Drill Hole
MSDA	MineSight Data Analysis
JORC	Joint Ore Reserves Committee
%M	Percent Moisture
VM	Volatile Matter
MT	Million Tonnes
SR	Stripping Ratio



LIST OF SYMBOLS

\bar{x}	Mean
Σ	Sigma, summation
x_i	Random variable
s^2	Variance, the square root of standard deviation
s	Standard deviation
IQR	Interquartile Range
Q_1	Lower quartile
Q_2	Middle quartile
Q_3	Upper quartile
σ	Coefficient of variation
Cov	Covariance
$\gamma(h)$	Semi-variograms
n	Number of random variables
c	A constant value
b_1	First regression coefficient
b_2	Second regression coefficient
k	Slope of linear model
N	Number of data pairs
$z(x_i)$	Sample value at location x_i
$z(x_i + h)$	Sample value at location $x_i + h$
C_0	Nugget effect
C_1	Partial sill
h	Separated distance between sample values
λ	Sample weight
$Z^*(x)$	Estimated value
μ	Lagrange multiplier
Q_c	Tonnage of coal
Q_w	Tonnage of waste

V_c	Volume of coal
V_w	Volume of waste
D_c	Density of coal
D_w	Density of waste
P	Total processing cost of coal in a block
y	Total processing cost per ton coal
C_c	Total cost in a block mining
q	Coal prices
R	Revenue from coal sales
r	Mining recovery
B_c	Block value of coal existed
B_w	Block value of waste existed
M_c	Total mining cost of coal in a block
m_c	Mining cost per ton coal
M_w	Total mining cost of waste in a block
m_w	Mining cost per ton waste

CHAPTER 1

INTRODUCTION

1.1 Background

Laos, officially the Lao People Democratic Republic (Lao PDR), is a landlock country in Southeast Asia bordered by China and Myanmar on the Northwest, Cambodia on the South, Vietnam on the East, and Thailand on the West. The population is estimated at 6.96 million people in 2018 with the area of 236,800 square kilometers. Laos currently is well-known of its abundance natural resources such as gold, copper, iron, lead, zinc, coal and limestone. There are numbers of mining companies invested in Lao PDR which comprise of the largest metal mining companies as Lan Xang Minerals Limited (LXML), Phu Bia Mining Company. Hongsa Power Company Limited is the biggest coal mine and coal-fired power plant in Laos. As a developing country, Laos needs to develop its infrastructure and economic growth, especially houses, schools, hospitals, roads, and electricity generation. Nevertheless, these development require primary resources which is produced from the mining industries in the upstream development and further supplies to the mid and downstream industry. Therefore, mineral resources development is one of the factors that plays a significant role for the development in Laos.

Since 1987, the Lao government has improved the renovation policy of economic growth and poverty reduction by adding varieties of exports and market-oriented economic. This expresses that the country opened up for the investment and development of the abundant natural resources and cooperated with foreign invested companies. Nowadays, Laos has an abundant natural resource that is still under exploration and development. Due to the lack of knowledge and expertise, the Lao government widely opened up for joint-venture from international investment mining companies. These are particularly in the development of precious metals, industrial minerals, and hydro-power generation.

1.2 Location of the study area

Lao Integrated Development Group (LID)'s concession area is located at the contact zone between Koua village, Sangthong district, Vientiane Capital and Nam Thom village, Hin Hoeup district, Vientiane Province. The LID's concession area comprises of 33.64 km², located at 78 km from Vientiane Capital. Based on the exploration phase, the concession area was divided into three blocks, which are called Block I (Nam Nga), Block II (Nam Thom), and Block III (Houy Tong Kob). This research study will be focused on Block I (Nam Nga exploration area) as shown in Figure 1.1. The location map of Lao Integrated Development Group Company is presented in Figure 1.2.

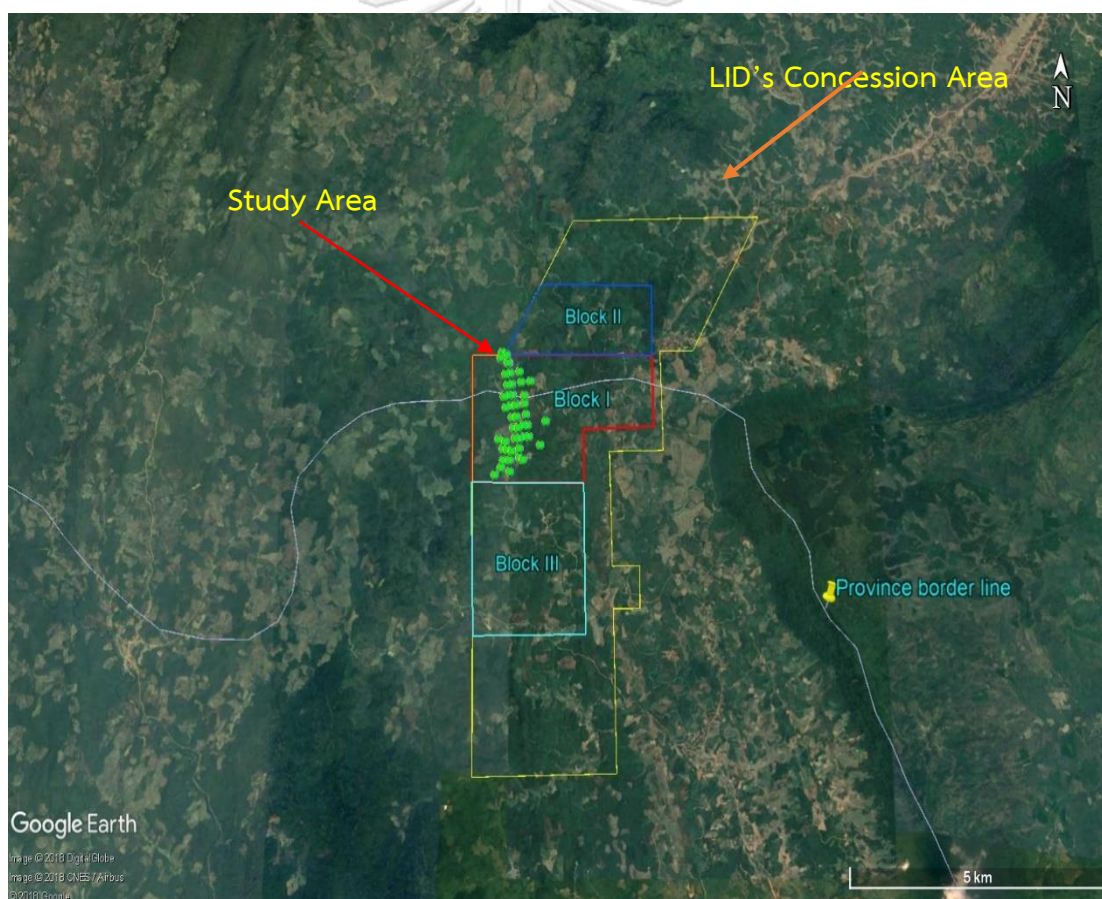


Figure 1.1 Location of the study area within the LID's concession area.

Source: Google Earth (2019)

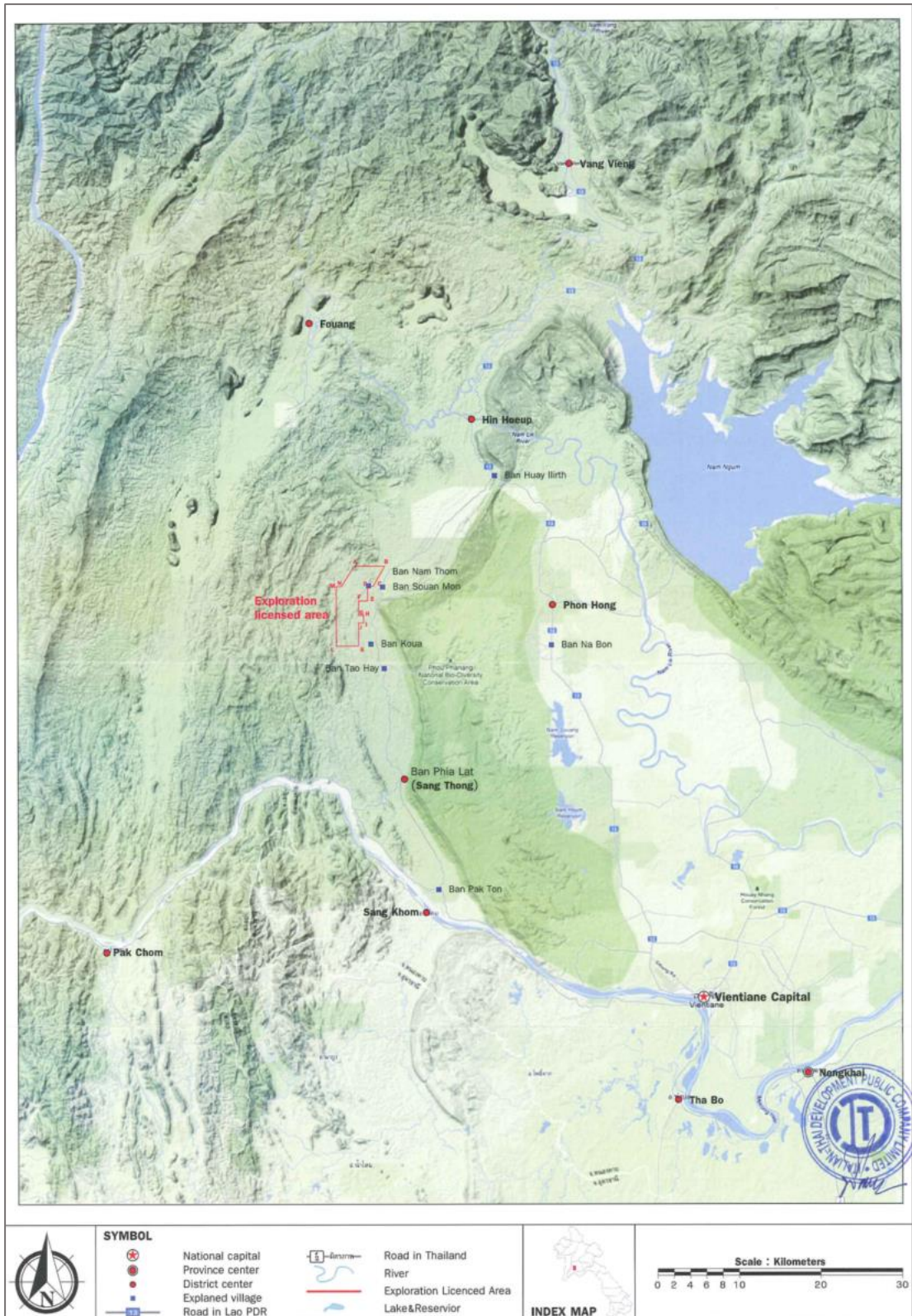


Figure 1.2 Location of Lao Integrated Development Group Company.

Source: Italian Thai Development Company (2012)

1.3 General information of the LID's concession area

1.3.1 Geography and access roads to the LID's concession area

The geography of the concession area was formed as undulating terrain along North-South direction, with the average elevation of 228 meters above mean sea level as shown in Figure 1.4. The concession area borders with Phou Pa Nang Biodiversity Conservation on the East, with Phou Kalai on the West, and with Phou Bo Jan on the North. Most areas nearby the concession area are rice fields belonging to the local farmer. There are three alternative access roads to the concession area as explained below. These three alternative access roads can be shown in Figure 1.3.

- 1) **Vientiane capital– Pak Ton village – Nam Thom village:** starting from Vientiane capital heads to Pak Ton village alongside Mekong river around 36 km, and then turn right to Sang Thong road via Phia Lak village to Nam Thom village about 42 km. It takes approximately 3 hours. The road condition is unpaved throughout.
- 2) **Vientiane capital– Nabon village – Tao Hai village – Nam Thom village:** starting from Vientiane capital heads to Hong Luey village along the 13 North road for 54 km. And then, turns left to Nabon village, Tao Hai village, Nam Thom village, respectively. This alternative route has a total distance of 85 km and takes approximately 2 hours. The 13 North road is a paved road ended at Nabon village, and the rest is a soil route.
- 3) **Vientiane capital– Houy Elerk village – Suan Mon village – Nam Thom village:** starting from Vientiane capital heads to Phon Hong village along 13 North road that follows Nam Xong river until reaching Houy Elerk village. At Elerk village, turns left and continues driving to Suan Mon village for around 25 km. At Suan Mon village, takes a left turn via Nam Thom village for about 4 km. This road has a longest distance for accessing to the concession area, but it is the most convenient one.

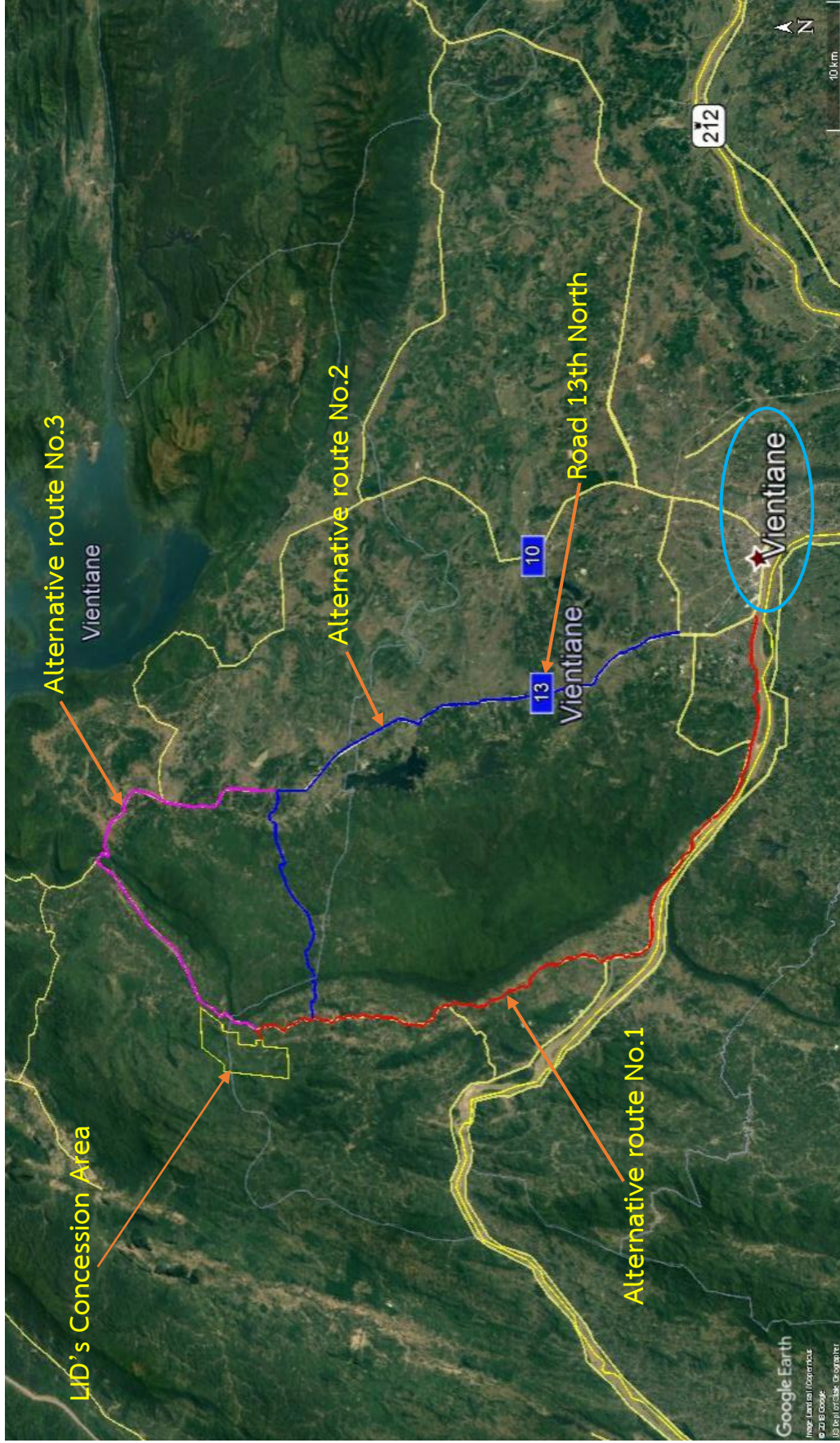


Figure 1.3 Three alternative access roads to LID exploration area.

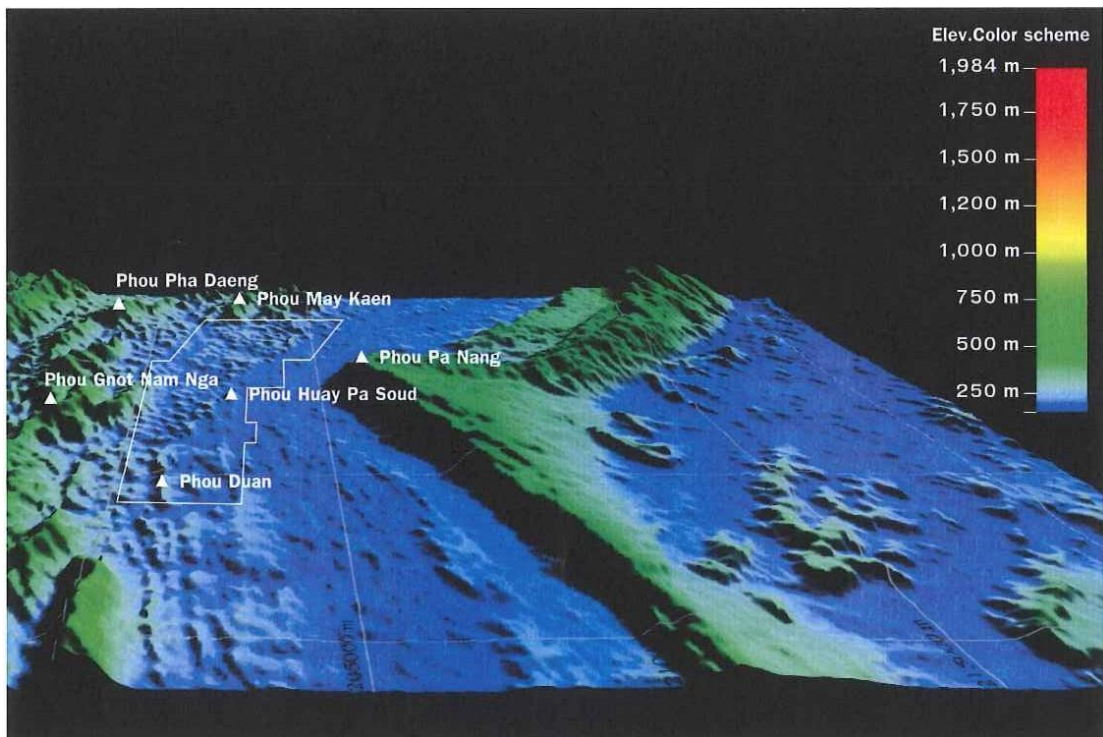


Figure 1.4 Elevation model map of LID's concession area and surrounding areas.

Source: Italian Thai Development Company (2012)

1.3.2 Local climate

The LID's concession area is categorized into tropical monsoon caused by the influences of the monsoon from South China sea. It comprises 3 seasons: dry season, rainy season and winter season. The dry season starts from early February to late May, and has the average temperature between 23.8 °c to 34.3 °c. The rainy season begins from early April to late September, which has the average rainfall between 245 - 334 mm. The winter season starts from early October to mid-February that has an average temperature between 16.4 °c - 30.3 °c.

1.3.3 Main rivers within the concession area

The main rivers surrounding the exploration area compose of 2 rivers such as Nan Ton river and Nam Thom river. Nan Ton river flows from the North to the South and connects to Mekong river at Pak Ton village. This river consists of 5 tributary streams such as Huay Ka Dan, Huay Nam Thom, Huay Som Phou, Huay Jaen Phila, and Huay Nam Ham.

1.4 Geological setting and coal deposits within the concession area

1.4.1 Regional geology

The geological formation belongs to the Paleozoic, Mesozoic, and Quaternary periods. Thus, the rock strata in the **Paleozoic** comprises of 5 rock formations ranking from the oldest to the youngest formation as: **1. Nam Xai Formation:** this is the lowest rock strata composed of shale, sericite-shale and quartzite, **2. Nam Sa Formation:** it is in early to late Devonian period, composed of thin limestone layer, moderate grain size sandstone layer, siltstone, and shale. This formation scatters along Lao and Thai border, **3. Nam Thom Formation:** this formation is in early to late Carboniferous period, it consists of sandstone layer, black siltstone infilled by lenticular limestone and black claystone combined with lenticular coal seam and conglomerate. It is covered by siltstone, and shale penetrating into conglomerate layer. This formation scatters from the North to the South of Vientiane province, **4. Na Lang Formation:** it is found in Carboniferous to Permian period. This formation composes of thick massive limestone layer and scatters on the Northwest of Vientiane province. Karst topography was formed and created a beautiful natural sightseeing especially natural tourist site in Vang Vieng city, and **5. Huay La Formation:** this formation is the marine limestone in Permian period which consists of sandstone, brown shale, conglomerate, and volcanic rock (basalt, andesite, andesitic basalt, and tuff in addition. The fault structures are found between the Huay La and Na Lang Formation.

The **Mesozoic** period consists of 5 formations as: **1. Phu Lek Phay Formation:** it is found in early to mid-Triassic period. It is characterized with sandstone infilling by claystone conglomerate and lenticular limestone penetrated with shale, **2. Nam Set Formation:** this is the marine rocks in late Triassic, and it composes of white-brown sandstone infilling by claystone, shale, and sandstone. The sandstone combines gypsum layer and lenticular coal seam, **3. Phu Phanang and Champa Formation:** It is the continent sedimentary rocks in Jurassic to Cretaceous period and generally found in Vientiane province. These two formations comprise of massive sandstone infilled by white thin sandstone-quartzite layer, and **4. Tha Ngon**

Formation: it consists of rock salt, which scatters throughout Vientiane province from the Middle to the East.

The **Quaternary** sediment deposit composes of the sediments found by the traces of rock accumulation incurred by the rivers and streams. The LID's concession area coincides with the Loei - Petchaboon fold belt, which formed from the collision of Shan - Thai and Indochina microcontinents in Triassic period. After the collision, the major Pangea plate had separated from each other and became various sub-continent in the Cretaceous period. This made the India plate moved into the North and collided with Eurasia plate in the middle Miocene of Tertiary period. This affected huge tectonic changes of Asia continent that made Himalayan mountain rising, opening of Gulf of Thailand, and opening of the South and North China sea. This is the source of Islands formed in the Pacific continent. Due to this change, the various continents have moved Northward as can be seen in nowadays. This tectonic change made the direction of rock strata fold belt align in the North - South direction along the Loei - Petchaboon fold belt. There were two major faults occurred as Northeast - Southwest (NE- SW) fault, and Northwest - Southeast (NW - SE) faults as shown in Figure 1.5.

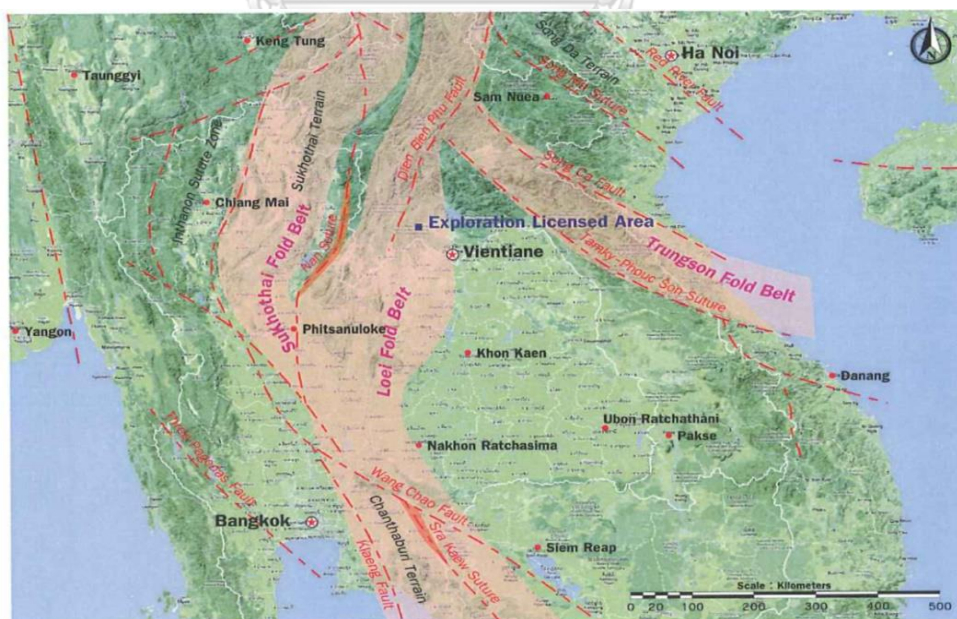


Figure 1.5 Geologic structures map of Lao PDR and its neighboring countries.

Source: Italian Thai Development Company (2012)

1.4.2 Local geology

A total of four sedimentary rock units was found within the entire of three blocks of exploration area ranging from upper to lower layers as follows:

1) Unconsolidated Sediment Unit: this rock unit was found in Quaternary period consisted of quartz, sand, sandy-silt, clay layer and other weathered rock types. Most of these sediment layers are scattered in a large area along the rivers of Nam Ton, Huay Nam Thom, Huay Som Phou, Huay Nam Nga, Huay Pa Pak, Huay Jaen Phi La, and Huay Nam Ham.

2) Red Bed Unit: It consists of three sub-rock units as demonstrated below.

- Upper red bed forms in middle to late Mesozoic period which is found most on Phou Pha Nang ridge in from North – South direction. It is also found in Phou Duen with a narrow area on the Southwest of the exploration area. Most rocks found in this unit are white – dark gray comprised of pebbly sandstone and conglomerate sandstone, which are infilled by siltstone and shale from thin to moderate layer.

- Middle Red Bed is found on the East of Nam Thom river and Phu Duen mountain with a large area composed of red to purple silicate-sandstone. It is infilled by quartz-sandstone and conglomerate layer.

- Lower Red Beds, which is formed as asymmetric folding with lenticular rock layer in the North – South direction. The folded rock strata on the West has a steep dip angle, while there is only a moderate dip angle on the East. This rock strata consists of coarse grain sandstone, conglomerate and brown to purple sandstone.

3) Coal Bearing Rock Unit composed of siltstone, sandstone, coarse-grain sandstone with gray to black color infilled by carboniferous shale and para-conglomerate. This combines split coal seams and lenticular coal seams, which are found in a large area from the North-South direction in the exploration area. The topography caused by this bearing rock unit is undulating terrain. Moreover, the fault contact zone is also found, which caused the discontinuities occurrence between coal bearing rock unit and sedimentary rock in the exploration area.

1.4.3 Volcanic rocks

The volcanic rocks found in the exploration area are divided into two rock units such as 1). Huay Pa Soud volcanic unit, consists of tuff, rhyolite, and thin andesite layer. These rocks are found at the Phu Houy Pa Soud and in the middle part of the exploration area, 2). Phou Ngot Huay Nam Nga volcanic unit, consists of tuff, rhyolite and thin green dacite strata. This rock unit scatters in Huay Nam Nga on the West of the concession area.

1.4.4 Geological setting of coal basin

1) Overview of coal accumulation in the concession area

The coal basin within the entire exploration area occurs in a transitional environment in Carboniferous period. A total of two major coal seams are found within the entire exploration area which demonstrated as upper and lower coal seams. The upper coal seam has a better quality than the lower coal seam. The coal deposits within the whole exploration area are ranking from Sub-bituminous C to Anthracite coal. The overburden is composed of fined-grain-sandstone, siltstone, and shale. The inter-burden consists of moderate to coarse grain size of sandstone, quartz sandstone, and conglomerate. The under-burden comprises of gray fine-grain sandstone, siltstone, shale and lenticular coal seam. The geologic map of coal accumulation within the exploration area is presented in Figures 1.6 - 1.7.

The occurrence of coal seams in the entire exploration area covers two main groups. The first group located on the West zone, covers the coal appearance area of 1.75 km². The second group located on the East zone covers coal appearance area of 0.3 km². These two groups cover a total coal appearance area of 2 km² as shown in Figure 1.7.

2) Coal seams

The coal deposits within the LID's concession area comprises of two major coal seams, the upper and the lower coal seam, and two minor coal seams. The cross section and overall stratigraphic units of coal accumulation are shown in Figure 1.8 - 1.9. The upper seam comprises of seam A and seam B incorporated with split

seams and sub-split seams. This upper coal seam is shiny black and brittle, which has the maximum and minimum appearance thickness of 4.58 meters and 0.34 meter, respectively. The coal seam dips toward the West with dip angle between 25° to 85° along the fault line.

The lower coal seam consists of seam C and seam D incorporated with split seams and sub-split seams, which are shiny black and brittle. It has the maximum and minimum appearance thickness of 5.07 meters and 0.35 meter, respectively. This coal seam dips toward the West of the concession area with dip angle between 25° to 85° along fault line.

The minor coal seam divides into two seams as seam O and seam U. The minor coal seam O exhibits in thin layer surrounded by fined-grain sandstone, siltstone, and shale. It is shiny black, and brittle which is found in block I (Nam Nga) on the Northwest, covering the area of 0.14 km². It has a low quality when interbedded with shale and mudstone. The minimum and maximum appearance thickness of this coal seam are 0.4 meter and 0.65 meter, respectively. This coal seam dips toward the West with dip angles between 25° to 85°. The minor seam U is interbedded with sandstone, siltstone, and gray shale, which is found in block II on the East covering the area of 0.89 km². It is shiny black and brittle with higher quality compared to minor seam O. The maximum and minimum appearance thickness of this coal seam are 1.44 meters and 0.30 meter, respectively. The minor seam U dips toward the East with dip angle between 25° to 65°.

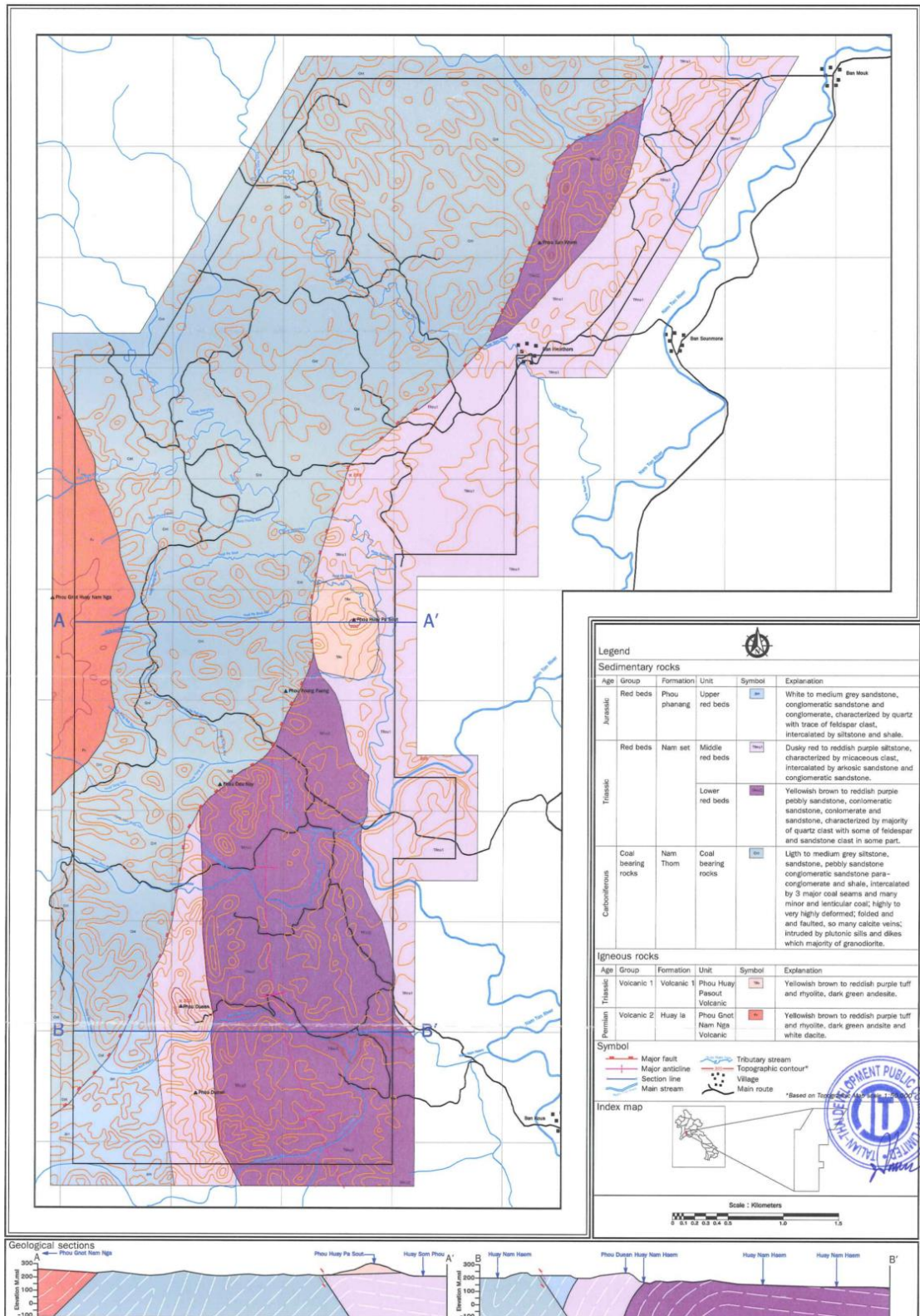


Figure 1.6 Geological map of the LID's concession area.

Source: Italian Thai Development Company (2012)

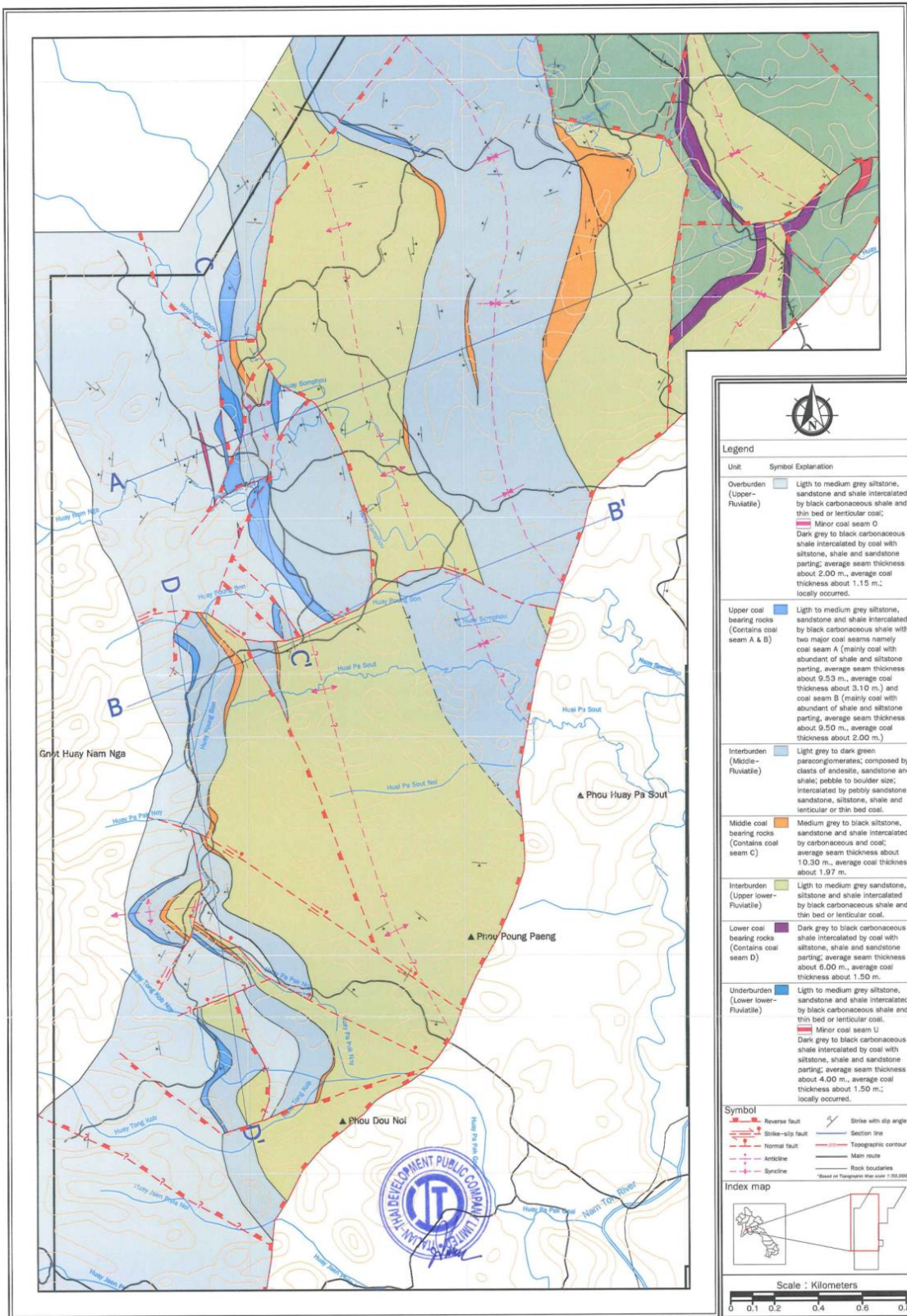


Figure 1.7 Geological map of coal bearing rock unit in the concession area

Source: Italian Thai Development Company (2012).

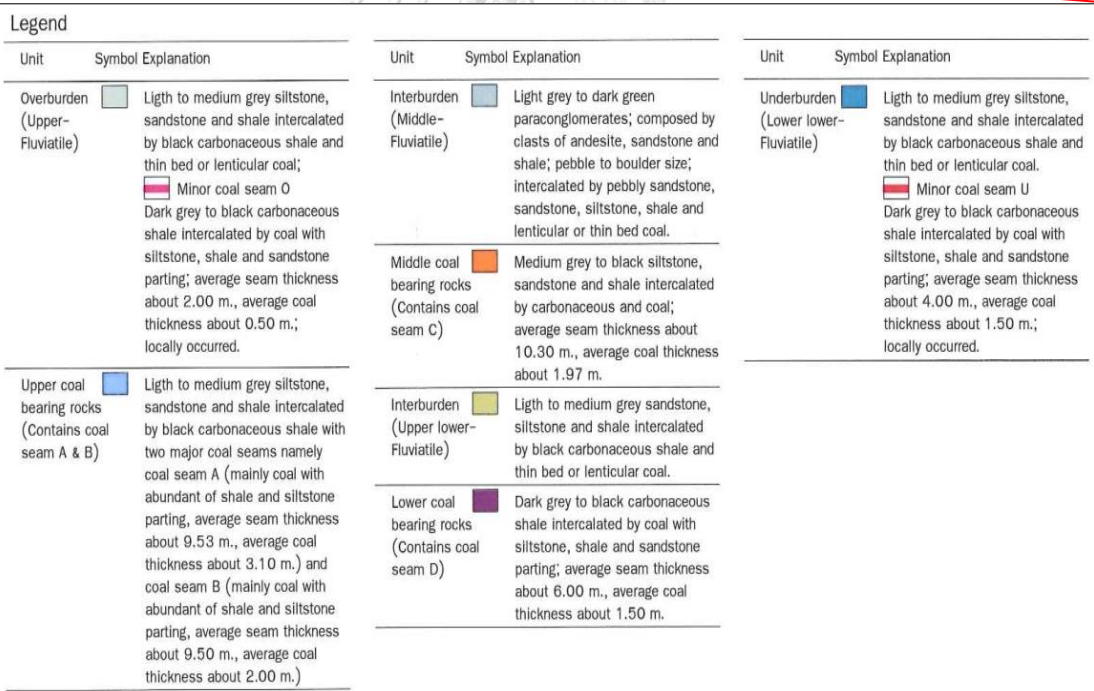
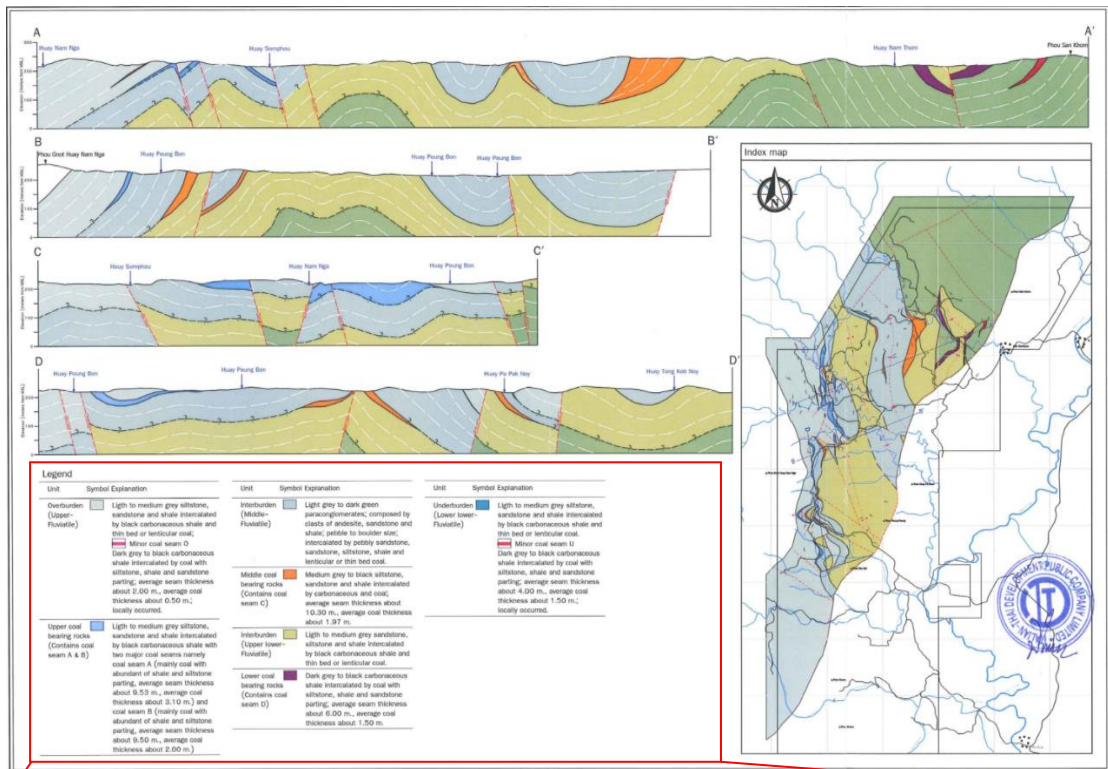


Figure 1.8 2D cross section of geological map of coal bearing rock units in within the LID's concession area.

Source: Italian Thai Development Company (2012).

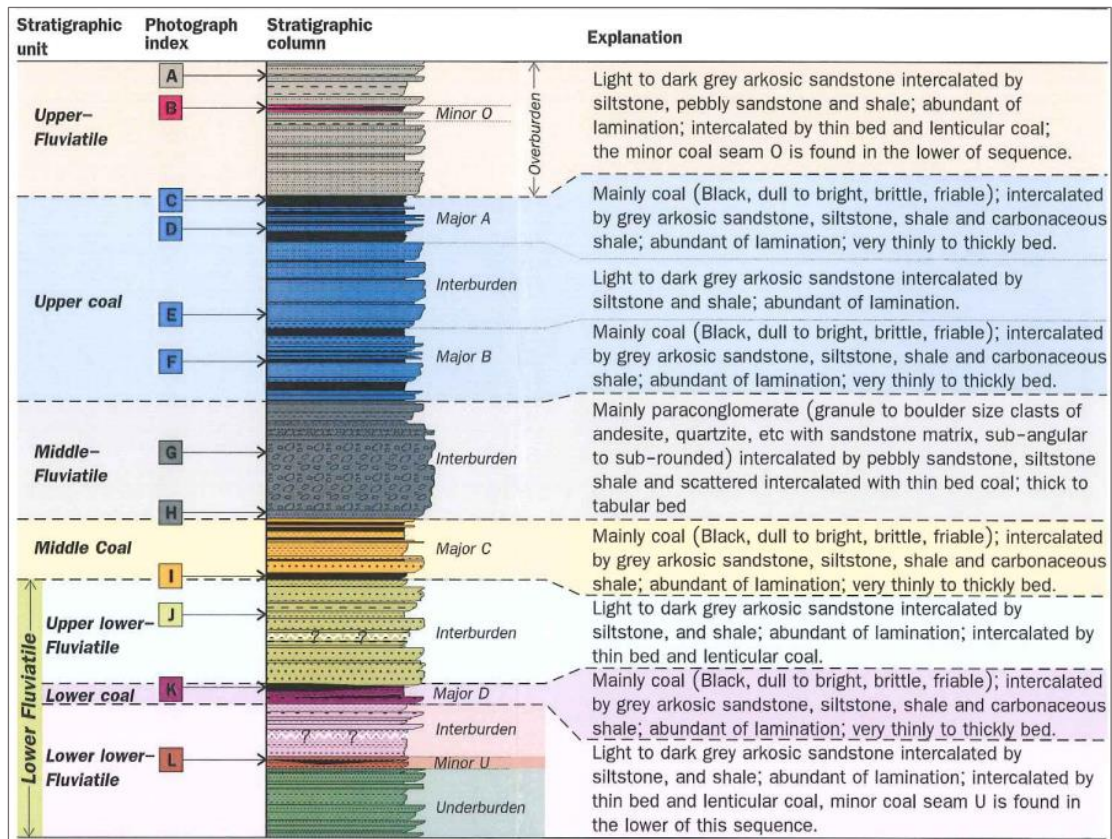


Figure 1.9 The overall stratigraphic unit in the LID's concession area.

Source: Italian Thai Development Company (2012).

1.5 Statement of problem

Natural resource extraction plays a very significant role in economic growth for the nation's development. Laos is known as a developing country, therefore the demand of coal utilization for electricity generation, steel-making, and cement factories is increasing simultaneously in recent development. In this attempt, the Ban Koua coal basin owned by LID is selected as the study area. The full development of NG coal basin is employed starting from 3D geological model development, resource, and reserve estimation, and mine design. However, the focus of this study is placed on the reserve estimation, when the initial mine pit layout was optimized. As mineral reserve estimation has played a very essential role for mine design, planning and day-to-day operation. Therefore, using the advanced geostatistical model for resource and reserve estimation in the exploration phase is highly necessary and required.

It is the fact that NG coal deposit presents complex geologic structures, resulting to high variation of coal thickness and qualities. The conventional reserve estimation approaches have a limitation when dealing with high variation characters of the coal grade. In order to model the high uncertainty data, the geostatistical approach poses some advantages. In this attempt, both linear (Ordinary Kriging) and non-linear model (Sequential Gaussian Simulation) will be adapted into this study with an expectation that the geostatistical models will carry the true statistical nature of the coal basin and the spatial information into the more accurate coal grades estimation model.

1.6 Research objectives

This research study focuses on estimating the coal qualities as Calorific Value (CV) and Ash Content (AC) at local blocks. The geostatistical linear (Ordinary Kriging) and non-linear (Sequential Gaussian Simulation) methods will be applied to the coal data of Ban Koua basin. The mineable reserve estimation will be calculated with the advent of the optimum mine plan, and the Grade-Tonnage Curve will be constructed. These findings will be used as a proposed guideline for mine planning and operations at NG coal mine.

1.7 Scope of study

The scopes of this work can be elaborated as follows:

- Drill holes data analysis; it involves in statistical analysis of composited data
- Structural analysis: it involves variogram calculation and modeling, and validation of composited data
- 3D block model constructions; Kriging estimation and Sequential Gaussian Simulation are required a 3D gridded block model.
- Estimation and Simulation subroutine; the coal qualities as CV and AC are estimated and simulated via linear (OK) and non-linear (SGS) geostatistical method, respectively.
- Geological coal resource estimation; the geological resource is calculated from OK's and SGS's estimated blocks.

- Ultimate pit layout; the pit optimization by Lerch-Grossman algorithm make use the estimated and simulated blocks. The mineable reserve is computed from the generated optimum pits.
- Practical pit limit; the ultimate pit layout is adjusted for the sake of practical operation, the final Grade-Tonnage Curve is then achieved.
- This study will be conducted using MineSight 3D software as a tool for 3D geological model construction, geostatistical analysis, pit optimization and mine design.

1.8 Contributions

Due to the fact that NG coal deposit presents a complex geologic structure environment, consequently using a geostatistical estimation method to access the coal qualities variation would be more advantage than a conventional method conceptually. In the later state, the results of geostatistical block model would be benefit to the mine planning and operation stages at NG coal mine. This research will be offered a guideline of coal qualities investigation via geostatistical model. The advantage of the model will be translated to an improvement of mine planning and operation.

CHAPTER 2

THEORY AND LITERATURE REVIEW

2.1. Theory

2.1.1 Background of geostatistical applications

Geostatistical approach is initiated from the work of mining engineering by D.G. Krige (1951). In the past, it has been applied to agronomy in early 1910s and meteorology in 1930s. It was then developed by Matheron (1963, 1968) in his theory of Regionalized Variables (Daya, 2015). Geostatistics can be described as a branch of statistics sciences that concerns of space phenomena and spatial correlation to interpolate the values of variables at unknown location using the surrounding values. Geostatistical estimation deals with the spatially autocorrelated data (Bohling, 2007). Geostatistics is a specialized scientific principle that provide a process to model the spatial continuity of regionalized variables (M. Abzalov, 2016). The applications of geostatistical techniques in mining industry play a significant role for mineral resources estimation to assess the uncertainty of the model and spatial relationship. This means it can be used to quantify the risks and measure the optimum drilling program and sampling grids (David, 1977).

The most popular geostatistical approaches are the linear univariate geostatistical estimators, Ordinary Kriging (OK) and Simple Kriging (SK). In Multivariate analysis, the methods of Co-kriging allows gathering the different types of data into a single coherent model (Deutsch & Journel, 1998). Geostatistical methods are also applied to estimate mining recovery by generating resources model in different scenarios of the mining selectivity (M. Z. Abzalov, 2006). As geostatistical approaches have been applied to many scientific fields since the past decades, the stochastic methods of geostatistics are generally used to define the continuity of geological and mineral resource models (Strebelle, 2002).

2.1.2 Summary of statistical analysis parameters

Statistical method has been applied to characterize the mineral deposit since 1945 (Alastair J, 2004). The applications of statistical analysis are the quantitative

numeric variables as metal grades and other characteristics. This is commonly concerned with the central tendency, dispersion of the values, histogram, sample correlation, autocorrelation, relations among group of variables, and a variety of probabilistic statements. In continuous distribution, the most common frequency distributions is the symmetrical bell-shape curve presented in Figure 2.1 with a single peak characterized by two parameters: the mean and the standard deviation. The mean of arithmetic mean is the point on the x-axis intersected by the axis symmetry of the “bell curve”. The standard deviation is measured for the width of “bell”. The summary of statistical analysis parameters is explained in the following according to (Alastair J, 2004):

1) Mean

The mean, \bar{x} , of equally weighted values of the samples or population is defined as the arithmetic mean. It is illustrated in equation (2.1).

$$\bar{x} = \frac{x_1 + x_2 + x_3 + \dots + x_n}{n} \quad (2.1)$$

Or shorten to:

$$\bar{x} = \frac{1}{n} \sum_{i=1}^n (x_i) \quad (2.2)$$

Whereby x_1, x_2 etc. are equivalent individual value of samples or measurements (i.e. they have the same sample support) and n is the total number of samples or measurements.

If the samples are not equivalent, and therefore each of the samples has a different support, then they must be weighted. Defined x_i as each sample value, and a_i is the weighting factor, for instance the core lengths of the analyzed sections. Then the mean value is:

$$\bar{x} = \frac{x_1 \cdot a_1 + x_2 \cdot a_2 + x_3 \cdot a_3 + \dots + x_n \cdot a_n}{a_1 + a_2 + a_3 + \dots + a_n} \quad (2.3)$$

Or shorten to:

$$\bar{x} = \frac{\sum_{i=1}^n (x_i \cdot a_i)}{\sum_{i=1}^n (a_i)} \quad (2.4)$$

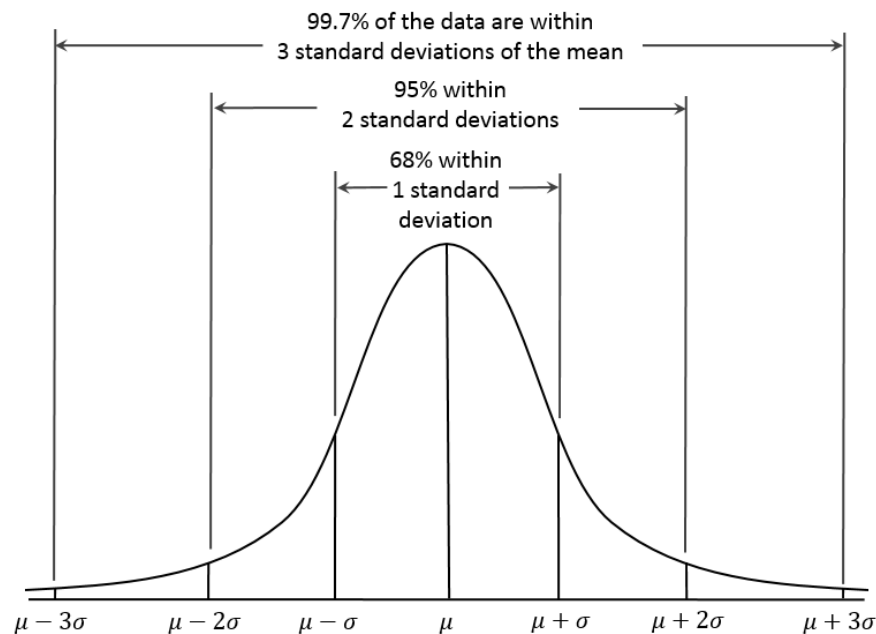


Figure 2.1 A single peak and symmetric frequency distribution with mean, standard deviation.

Source: <https://www.albert.io/blog/describing-distributions-ap-statistics/> (Access date: June 26, 2019)

2) Mode

The mode of a set of data is the most frequency occurring number in a dataset. A data set may have one mode, more than one mode, or no mode. If no entry is repeated the data set has no mode.

3) Median

The median is the midpoint value that divides a sample size or population into two equal halves, whereby, one half value less than the median and the other has values greater than the median.

4) Variances and Standard Deviation

Variance is the expectation of the squared deviation of a random variable from its average value. It measures the dispersion that how far a set of random numbers are spread out from their average value. Variance, s^2 , is defined as the mean square difference as shown in (2.5).

$$s^2 = \frac{\sum(x_i - \bar{X})^2}{(n - 1)} \quad (2.5)$$

Where x_i is any data value, \bar{X} is the mean of the data, and n is the total number of samples used. The term $(n - 1)$ referred to as degrees of freedom, originates in statistical theory which involved to the sampling distribution of s^2 .

The standard deviation (SD) is a measure that uses to determine the amount of variation or dispersion of a set of data values. It is the square root of variance as illustrates in (2.6).

$$s = \sqrt{s^2} = \sqrt{\frac{\sum(x_i - \bar{X})^2}{(n - 1)}} \quad (2.6)$$

5) Interquartile Range

The interquartile range or IQR is the difference between the maximum and minimum of data input in the data set. (2.7) denotes the interquartile range.

$$IQR = Q_3 - Q_1 \quad (2.7)$$

The IQR is a tool uses to measure the variability depends on the quartiles divided by the data set. Quartiles divide a rank-ordered data set into four equal parts. The values that separate parts are called the first, second, and third quartiles; and they are denoted by Q_1 , Q_2 , and Q_3 , respectively.

6) Coefficient of variation

Coefficient of variation is a statistical parameter that uses as a quick indicator of the variability of the data set. The coefficient of variation, σ , is defined by (2.8).

$$\sigma = \frac{s}{\bar{x}} \quad (2.8)$$

If the σ value is below 0.5, the distribution of the data set is likely to approach the normal distribution. Whereas, the σ above 0.5 is that the data distribution is becoming skewed and could be express better by a lognormal distribution or a combination of distributions.

7) Skewness and Kurtosis

Skewness characterizes the degree of asymmetry of a distribution around its mean. Positive skewness indicates a distribution with an asymmetric tail extending toward more positive values. Negative skewness indicates a distribution with an asymmetric tail extending toward more negative values.

Kurtosis characterizes the relative peakedness or flatness of a distribution compared with the normal distribution. Positive kurtosis indicates a relatively peaked distribution. Negative kurtosis indicates a relatively flat distribution. The skewness and kurtosis are defined as (2.9) and (2.10).

$$Skewness = \frac{n}{(n-1)(n-2)} \sum_{i=1}^k \left(\frac{x_i - \bar{x}}{s} \right) \quad (2.9)$$

$$Kurtosis = \left\{ \frac{n(n+1)}{(n-1)(n-2)(n-3)} \sum_{i=1}^k \frac{(x_i - \bar{x})^4}{s^4} \right\} - \frac{3(n-1)^2}{(n-2)(n-3)} \quad (2.10)$$

Where: n = number of sample values, x_i = sample values, \bar{x} = samples mean value, s = standard deviation.

8) Covariance

Covariance, s_{xy} , is a quantitative determinator of the systematic variability of two variables (x and y). The covariance equation is demonstrated in (2.11).

$$\text{Cov}(x, y) = \frac{\sum_{i=1}^n [(x_i - \bar{x})(y_i - \bar{y})]}{n - 1} \quad (2.11)$$

Where: x_i = Value of x-variable, y_i = Value of y-variable, \bar{x} = Mean value of x-variable, \bar{y} = Mean value of y-variable, n = Number of data points.

2.1.3 Histograms

Histogram is a graph used to express the numerical data distribution within continuous variable intervals that expand the range of variable. In order to demonstrate the attributes of mineral grades in simply and effectively, histogram analysis is a method that can be carried on. The distribution of histogram shape can be shown in various types such as positively skewness, symmetric and negatively skewness. This is to measure as a qualitative evaluation of dispersion and expand to the variables which can be clustered centrally with one or more modes. These all characteristics have to be noted as a shape of histogram or the distribution of data. The histogram shape of data distribution of CV and AC are shown in Figure 2.2 – 2.3. A histogram can be constructed from the samples class interval and this class interval should be in uniform (Arber & Ginn, 1991). Each histogram ought to contain the information, which include number of items, class interval, mean and standard deviation.

2.1.4 Scatterplots

A scatter plot is a two-dimensional data visualization that uses the dots as a representative of the sample values obtained for two different variables. The scatter plot can be shown as one variable is plotted along x-axis and the other is plotted along y-axis as shown in Figure 2.4. The use of scatter plot is to express the relationship between two variables as a correlation plot. Scatter plot is an essential

tool for carrying the relationship between two variables, but it has to be well-understood and interpreted properly by the practitioners.

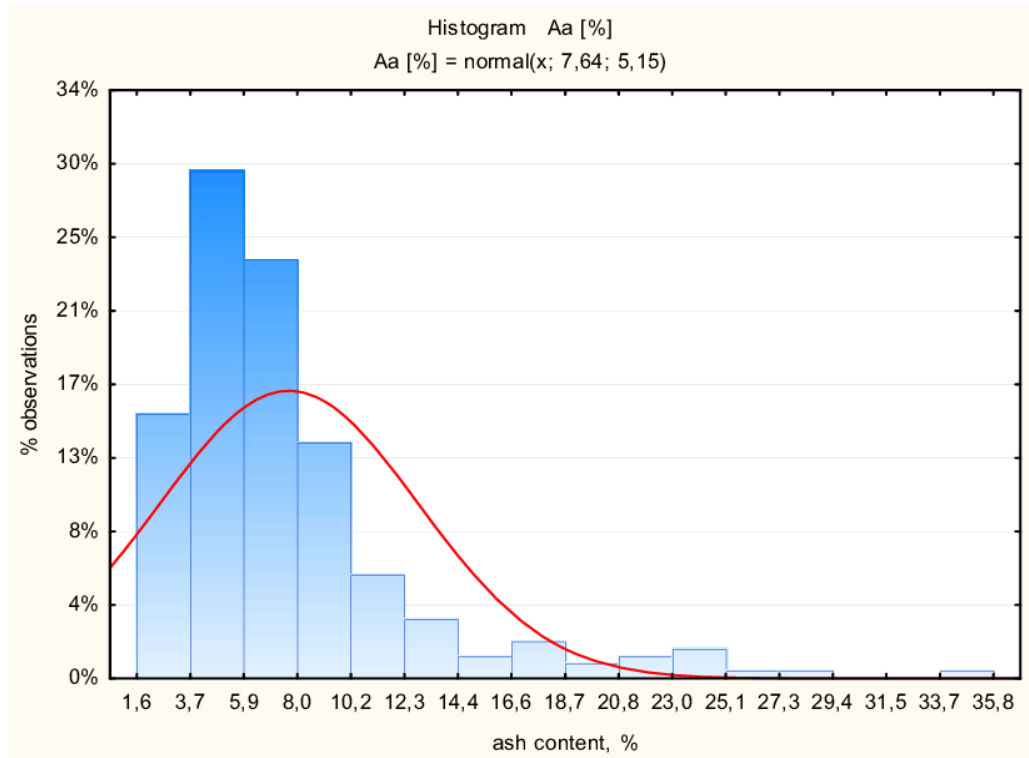


Figure 2.2 Histogram of AC (Wierchowski, Chećko, & Pyka, 2017).

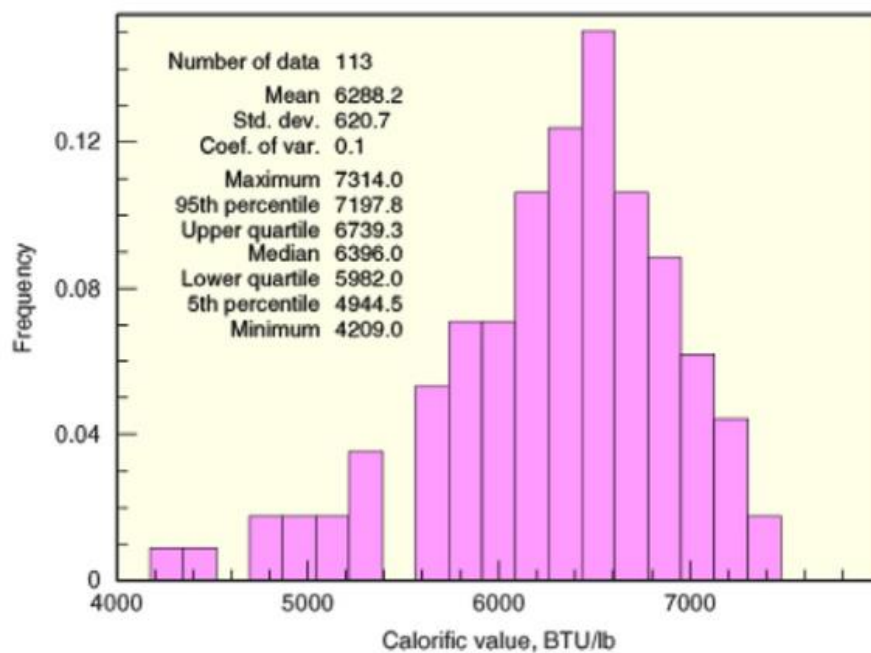


Figure 2.3 Histogram of CV (Olea, Luppens, Egozcue, & Pawlowsky-Glahn, 2016).

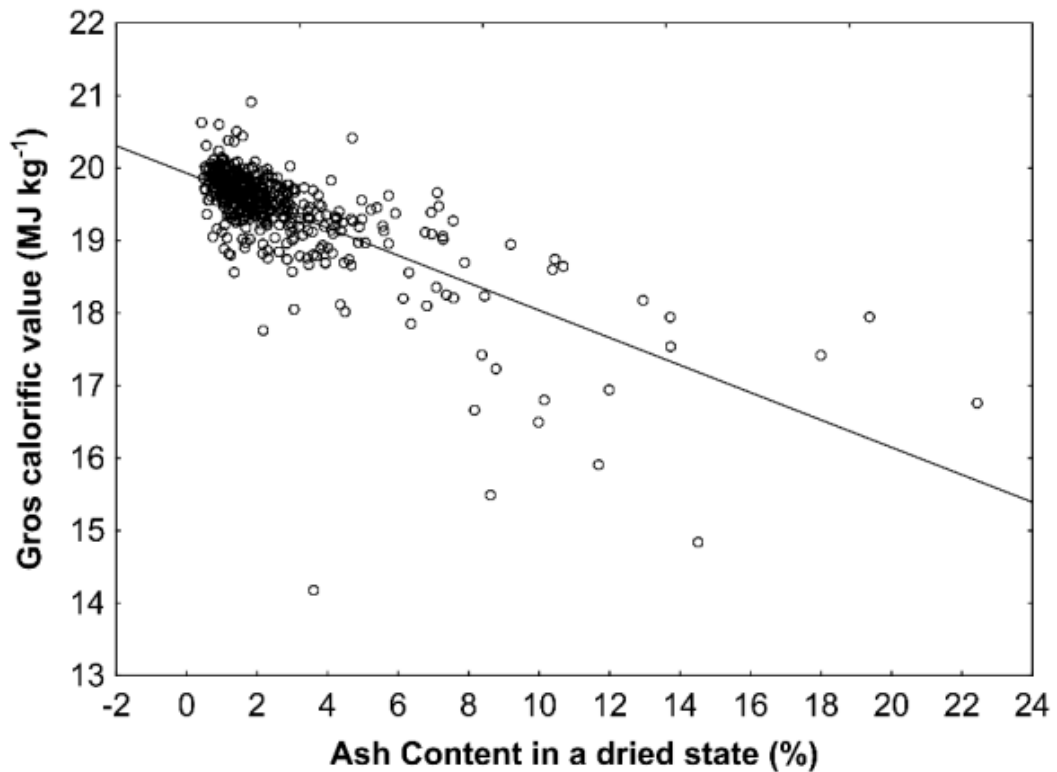


Figure 2.4 Example of scatter plot between calorific value and ash content (Lieskovský, Jankovský, Trenčianský, & Merganič, 2017)

2.1.5 The Method of linear squares

The least squares method is a form of mathematical regression analysis that finds the line of best fit for a dataset. It provides a visual showing of the relationship between the data points. Each point of data is representative of the relationship between a known independent variable and an unknown dependent variable.

The least squares method provides the overall rationale for the placement of the best fit line among the data points being investigated. The most common use of the least square method, referred to as linear or ordinary. It aims to create a straight line minimizing the sum of the squares of the errors generated by the results of the associated equations, such as the squared residuals resulting from differences in the observed value and the value anticipated based on the model as shown in Figure 2.5. The line of best fit equation and its components are demonstrated in Equation (2.12).

$$y = c + b_1(x_1) + b_2(x_2) \quad (2.12)$$

Where: y is the dependent variable, c is a constant, b_1 is the first regression coefficient, x_1 is the first independent variable. b_2 and x_2 the second coefficient and second independent variable.

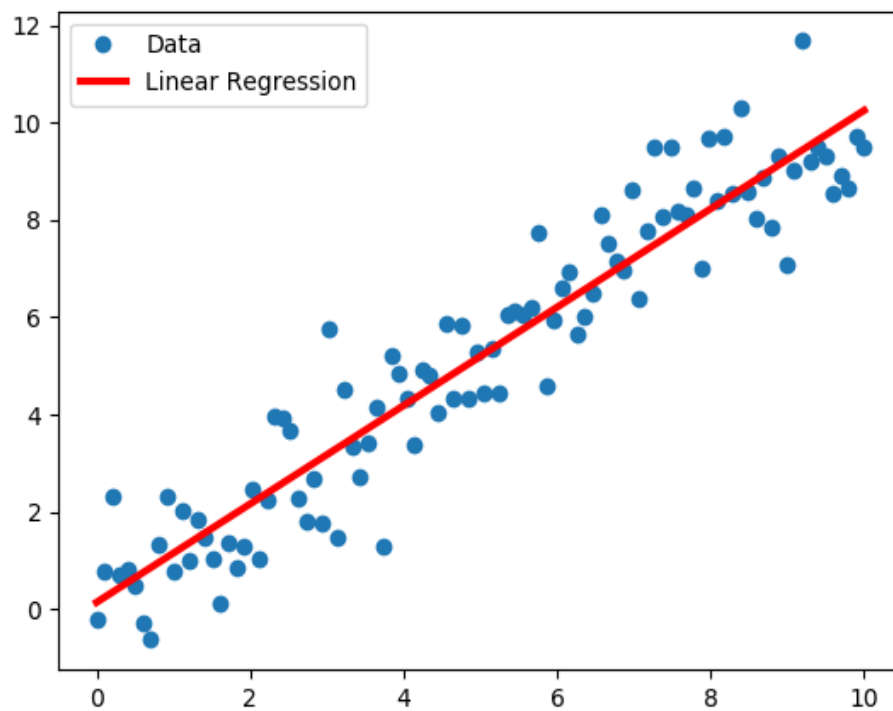


Figure 2.5 Example of linear square method.

Source: <https://alexisalulema.com/2018/01/18/linear-least-squares-regression-with-tensorflow/> (Access date: June 26, 2019).

2.1.6 Linear regression analysis

If there is a strong correlation between two variables, which can be shown by an equation, then one variable can be used to interpolate the other one if one of them is unknown. The commonly used method for this prediction is linear regression. It is assumed that the dependent variable on the other can be expressed by the (2.13) of a straight line such follows:

$$y = kx + b \quad (2.13)$$

Where: k is the slope, b is the constant of the line, and they are given by (2.16):

$$k = r \left(\frac{\sigma_y}{\sigma_x} \right); \quad b = m_y - am_x \quad (2.14)$$

The slope, k , is the correlation coefficient multiply by the ratio of standard deviations. σ_y is the standard deviation that is trying to predict, and σ_x is the standard deviation. When the slope is calculated. The constant, b , can be computed using the means of those two variables such as m_y and m_x . The linear regression line described the relation between two different variables can be illustrated in Figure 2.5.

2.1.7 Drill holes composite

In mineral deposits, raw data of assays compositing is required to produce such supports for mineral resources evaluation and mine operation phase by combining the assay samples into an appropriate fixed length. The term compositing used in mineral resource estimation is taken to the process by which the values of adjacent samples are matched. Therefore, the values of interval composited length can be estimated. Compositing is numerical methodology to compute the estimation weighted average grade over the bigger volumes than the original sample data (Revuelta, 2017). After the assay samples dataset was composited, the dataset is commonly validated. Samples data in mineral resource estimation are composited to standard lengths because of several reasons such as;

1. Decreases the number of samples.
2. Provides a representative for analysis where irregular length assay samples are presented.
3. Brings data to a common support; for instance, to gather drill core samples of different lengths to an appropriate fixed length.
4. Reduces the effect of isolated high-grade data.
5. Produces bench composites extending from the top of a bench to the base in an open-pit which will be provided for the design of the mine operations.

6. Incorporates dilution (e.g., in mining continuous height benches in an open-pit exploitation).
7. Provides equal-sized data for geostatistical analysis framework.

2.1.8 3D block modelling

3-D geological modeling of ore deposit is an approach developed for geological investigation, mineral resources and reserves estimation in mining and other fields (Wang & Huang, 2012). 3D block model is used for grade interpolation and tonnage calculation as the visualization of the mineral deposit (Hustrulid, Kuchta, & Martin, 2013). Nowadays, the block modeling of a deposit can be constructed throughout various types of mining engineering software which are the modern and advanced technologies provided for mineral deposit modeling. The 3D block model is also used for the measurement of 3D geological spatial continuities. The 3D block modeling is an essential process for mineral resources deposit and space variations modeling, which is used the mineral grades, rock properties and complex or irregular geological structures as presented in Figure 2.6.

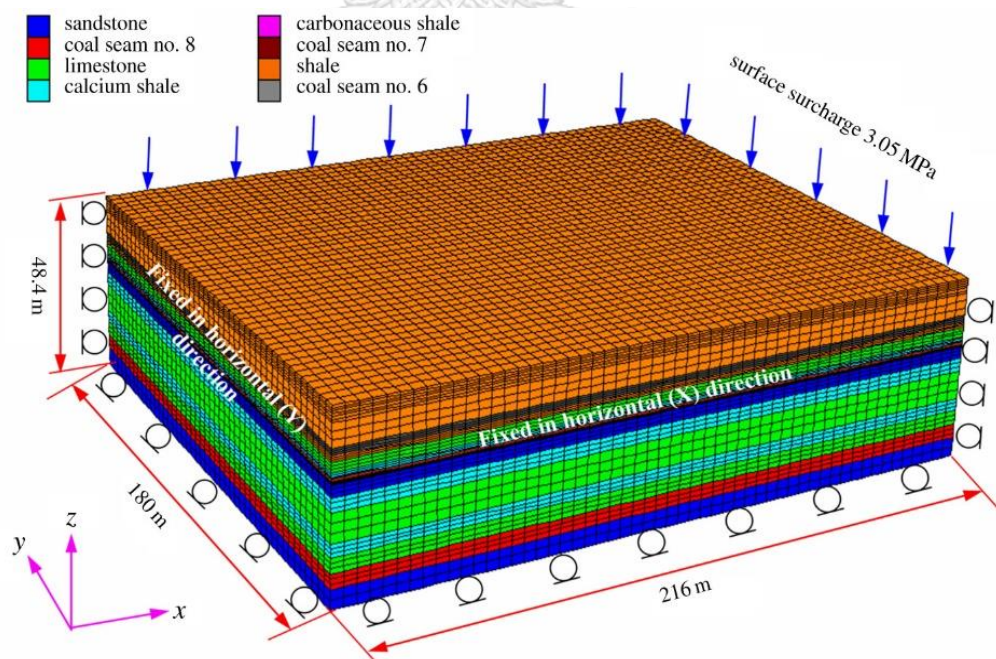


Figure 2.6 Geometric parameters and boundary conditions of the numerical model of Baijiazhuang coal mine at Shanxi province, China (Bai et al., 2018).

2.1.9 Spatial analysis

The spatial uncertainty measurement of a mineral deposit is very important for ore reserve estimation to define the variations of ore grade and geological structure conditions. The spatial continuity of ore deposit can be described by several geostatistical tools such as correlation function, covariance, and variogram model. These tools use the summary statistics parameters to demonstrate how the spatial uncertainty varies as a function of a distance and direction at specific area. Variogram measurement is widely used to quantify the space continuity in many fields such as mining, environment, geosciences and others. In geostatistical estimation and simulation methods, one of the most relevant parameters is variogram model. The sample variogram model is concluded from the existing data collected from any locations, which may be controlled the bias of a spatial and the effect of a proportional. Over this example variogram, a variogram is fitted and carried out through the procedure of estimation or simulation, that is usually do not respect to its discontinuities. The simulated realizations require an adequate input variogram model to reduce the bias in the simulation process (Ortiz Cabrera & Leuangthong, 2007).

Geostatistical estimation and simulation methods are based on the variogram model, which characterizes the spatial uncertainty that used the random function values calculated from the available sample data. The kriging estimation methods use the variogram model to determine the closeness and redundancy of the dataset with individual location being interpolated. In simulation model, the variogram model is used to interpolate the conditional data distributions within the location, which the simulated values are drawn randomly.

2.1.9.1. Variogram model

Geostatistical estimation such as kriging estimation and simulation, frequently request a semi-variogram or covariance model as the input for the interpolation. Apart from the initial decision of stationary, the appropriate variogram model is the most essential decision in a geostatistical estimation. General practice composes of experimental variograms' fitting with a nested combination of proven models like the

spherical, exponential, and Gaussian models. These models perform well in most cases (Pyrcz & Deutsch, 2006). The empirical model provides a description of how the data are related (correlated) with a distance. The semi-variogram function, $\gamma(\mathbf{h})$, was originally defined by Matheron (1963) as half the average squared difference between points separated by a distance h . Given a geostatistical model, $Z(\mathbf{x})$, its variogram $\gamma(\mathbf{h})$ is formally defined as in (2.15):

$$\begin{aligned}\gamma(h) &= \frac{1}{2} \text{var}[Z(\mathbf{x}) - Z(\mathbf{u})] \\ &= \frac{1}{2} \iint [Z(\mathbf{x}) - Z(\mathbf{u})]^2 f(\mathbf{x}, \mathbf{u}) d\mathbf{x} d\mathbf{u}\end{aligned}\quad (2.15)$$

where $f(\mathbf{x}, \mathbf{u})$ is the joint probability density function of $Z(\mathbf{x})$ and $Z(\mathbf{u})$.

For an intrinsic random field, the variogram can be estimated using the method of moments estimator, as follows:

$$\gamma(h) = \frac{1}{2N} \sum_{i=1}^N [Z(\mathbf{x}_i) - Z(\mathbf{x}_i + \mathbf{h})]^2 \quad (2.16)$$

where \mathbf{h} is the distance separating sample locations \mathbf{x}_i and $\mathbf{x}_i + \mathbf{h}$, N is the number of distinct data pairs. In an isotropic case, \mathbf{h} should be written as a scalar h , representing magnitude.

The main aim of variogram analysis is to construct a variogram model that best estimate the autocorrelation structure of the underlying stochastic process. Most variograms are defined through several parameters namely: the nugget, sill and range. According to Saputra (2008), the range, sill and nugget can be described as follows and the variogram model is shown in Figure 2.7:

- **Range:** At some offset distance, the variogram values will stop changing and reach a “plateau”. The distance at which this occurs is called the range.
- **Sill:** The “plateau” value at which the variogram stops changing.
- **Nugget:** The discontinuity at the origin. Although this theoretically should be zero, sampling error and short scale variability can cause it to be nonzero.

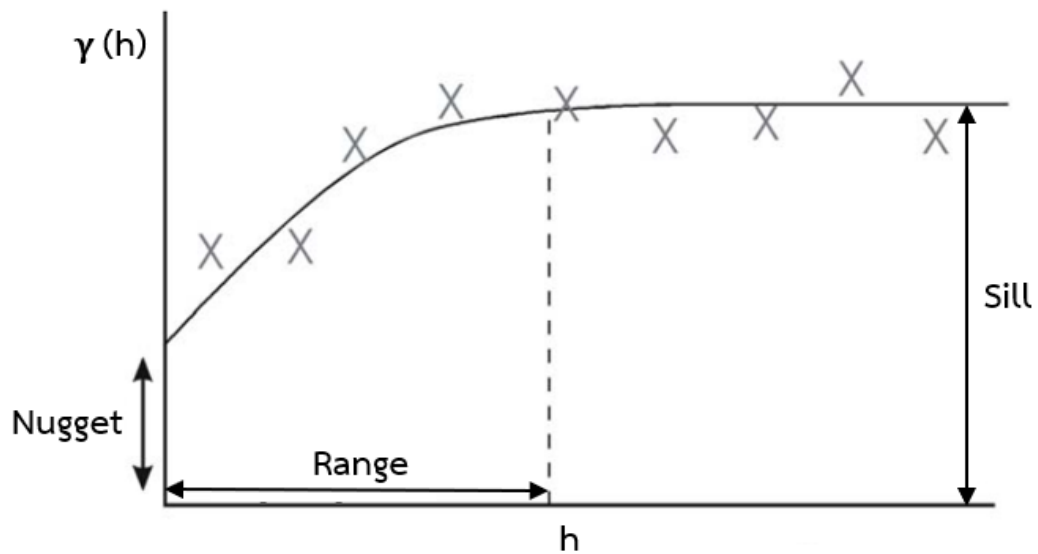


Figure 2.7 Experimental variogram model shape (Saputra, 2008).

The variogram offer a significant tool for explaining how the spatial data are related with distance. As we have known, it is determined in terms of dissimilarity in sample values between two locations separated by a distance h .

There are two reasons we need to fit a model to the empirical model such as:

1. Spatial prediction (kriging) requires estimates of the variogram $\gamma(\mathbf{h})$ for those \mathbf{h} 's which are not available in the data.
2. The empirical variogram cannot guarantee the variance of predicted values to be positive, but a variogram model can ensure the variance positive. Several parametric variogram models have been used in the literature and those are:

a) Linear Model

The linear model is expressed as linear function in (2.17)

$$r(\mathbf{h}) = c_0 + kh \quad (2.17)$$

where c_0 is the nugget effect, \mathbf{h} is a distance separating of sample points. The linear model has no sill, and so the total variance of the process does not reach its limit. The existing linear variogram is taken into account when the variogram point data exhibits a linearity as shown in Figure 2.8.

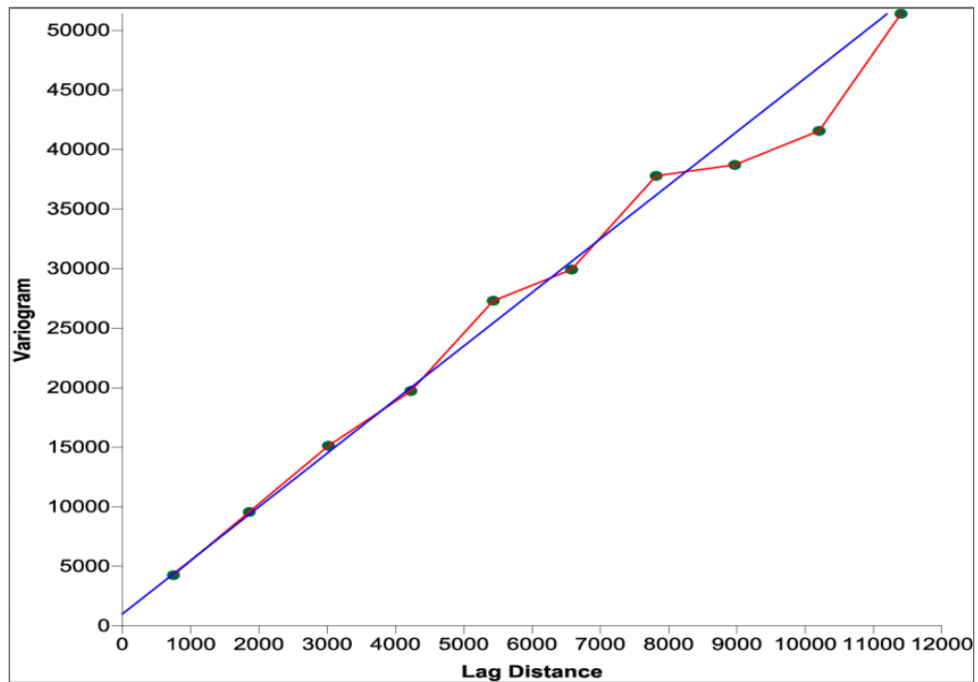


Figure 2.8 Linear variogram model (Asmael, Dupuy, Huneau, Hamid, & Coustumer, 2015).

b) Power Model

The power model is expressed as power function in (2.18)

$$r(h) = C_0 + bh^\alpha \quad (2.18)$$

where C_0 is the nugget effect. The power model has no sill, therefore, the variance of the process still does not match its limit. The linear variogram is considered as a special case of the power model as shown Figure 2.9.

c) Exponential Model

Mathematically, the exponential semi-variogram model is defined as (2.19):

$$r(h) = \begin{cases} 0 & h = 0 \\ C_0 + c \left[1 - \exp\left(-\frac{\|h\|}{a}\right) \right] & h \neq 0 \end{cases} \quad (2.19)$$

Where: $C_0 \geq 0, c > 0$ and $a > 0$.

The exponential semi-variogram model has a nugget effect of C_0 and Journel and Huijbregts (1978:164) clarified that the exponential model reaches its sill value of $C_0 + C$ asymptotically. Armstrong (1998:37) adds that the range of the exponential semi-variogram model is practically defined as $3a$ (The distance at which 95% of the sill value is reached if $C_0 = 0$). The exponential variogram model is shown in Figure 2.9.

d) Spherical Model

Base on Armstrong (1998:37), the spherical semi-variogram model is probably the most commonly used model in geostatistical estimation as shown in Figure 2.9. In mathematical, the spherical semi-variogram model is measured as (2.20):

$$r(h) = \begin{cases} 0 & h = 0 \\ C_0 + C \left[\frac{3h}{2a} - \frac{1}{2} \left(\frac{h}{a} \right)^3 \right] & 0 < h \leq a \\ C_0 + C & h \geq a \end{cases} \quad (2.20)$$

$$C_0 \geq 0, C > 0 \text{ and } a > 0$$

Where: C_0 is the nugget effect, a is the range and $C_0 + C$ is the sill value.

e) Gaussian Model

The Gaussian model is used to represent extremely continuous phenomena (i.e. phenomena that have strong dependencies over short distance), since the model illustrates a parabolic behavior near the origin (Isaaks & Srivastava, 1989:375). The Gaussian semi-variogram model is measured as (2.21):

$$r(h) = \begin{cases} 0 & h = 0 \\ c_0 + c \left[1 - \exp \left(-\frac{h^2}{a^2} \right) \right] & h \neq 0 \end{cases} \quad (2.21)$$

$$c_0 \geq 0, c > 0 \text{ and } a > 0$$

Where: c_0 is the nugget effect, a is the range, and $c_0 + c$ is the sill value. According to Journel & Huijbregts (1978:165), a sill value reached asymptotically at a practical range of $\sqrt{3}a$ as shown in Figure 2.9.

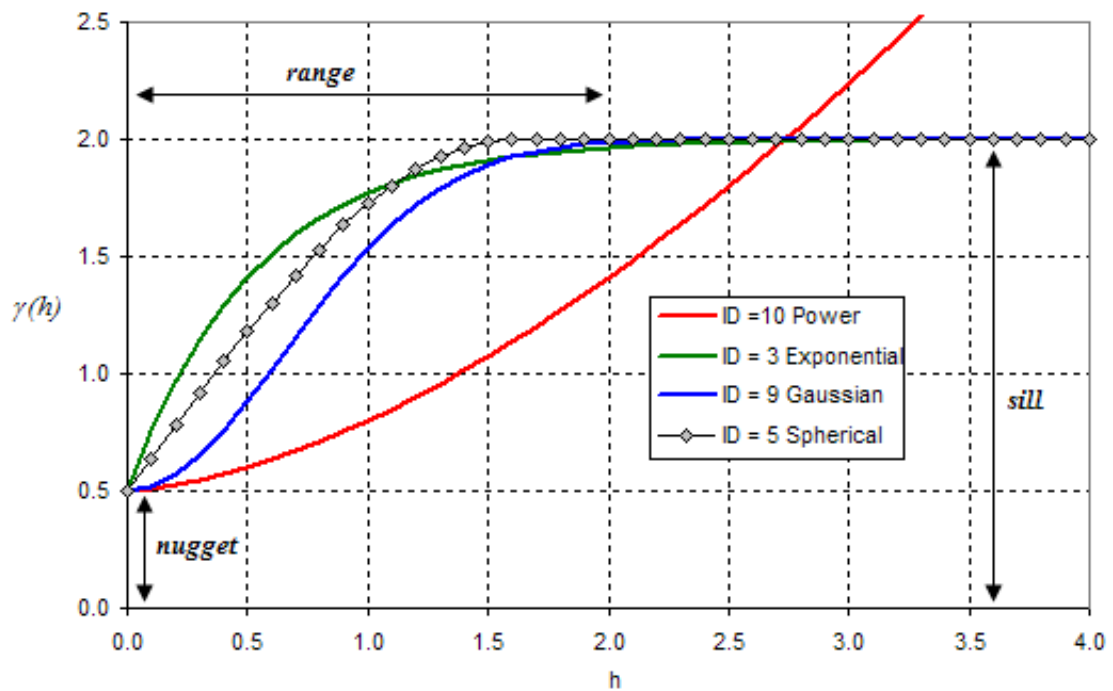


Figure 2.9 Variogram models of Spherical, Exponential, Power, and Gaussian.

Source: <http://xongrid.sourceforge.net/GpVariogram.htm> (Access date: June 26, 2019)

f) Nested Model

Nested structures of the ore deposit sometimes can be found when looking at the experimental variogram. They point out the presence of the operating process at different scales. For instance, there might be measurement at the level of a sample, i.e. for $h=0$. At the petrographic scale (i.e. $h < 1\text{cm}$), there can be discontinuity because of a transition from a mineralogical constituent to another. At the level of strata or mineralized lenses (i.e. for $h < 100\text{m}$), a third type of variability comes into play as the points pass from ore to waste or from ore facies to another.

The shorter range could be differentiated by the characteristics that change in the curvature. This change is obvious when the two ranges are quite different. If they are not, the change is more gradual and need not be obvious.

2.1.9.2. Regionalized Variables

The regionalized variables theory was developed by Matheron, which forms the mathematical basis of geostatistics. The essential point of this theory is that the geological or mineralogical process acted in the formation of ore deposit is

interpreted as a random process. Therefore, the grade at any locations within the deposit is taken into account as a specific result of this random process. The probabilistic interpretation of a natural process is significant to find a solution of the practical issues of the grade estimation in an ore deposit. Such as the interpretation is a simple conceptualization of facts and valid so far. It creates a great result of the reality and allows the practical problems to be modified.

The regionalized variables are random variables that have a space correlation in time. For instances, the regionalized variables are the metal grades and quality of coal seams. In geostatistical estimation, variables can be classified as random variables, but in term of regionalized is used to demonstrate that the variables are correlated spatially to some degree.

Geostatistical approach aims to quantify the spatial variation of the regional variable as the variogram model. And in the follow up process, the variogram model will be used as conditioning information in the estimation or simulation process.

2.1.10 Kriging estimation

Geostatistical modeling does not provide the description of the physical process thus it is not widely used in extrapolative predictions beyond the spatial bounds of the given data. The geostatistical approaches are largely depended on the interpolative predictions based on inferred spatial continuity of the existing data (i.e. variogram models) and therefore these methods are widely applied for estimating the grade and tonnage of mineral resources and ore reserves.

The estimation is usually applied using Ordinary Kriging (OK) or Simple Kriging (SK), which are the variants of linear regression methods allowing estimation of a single regionalized variable in unsampled points. Kriging technique defines the following special limitations on the estimation:

- It minimizes an estimation error.
- It assures that mathematical expectation of the estimate error is equal to zero.

These characteristics provide advantage to kriging comparing to other linear estimators. Geostatistical techniques have become the most popular used methods applied for estimating grade and tonnage of mineral resources and ore reserves (Krige

1951; Matheron 1963, 1968; David 1977, 1988; Journé and Huijbregts 1978; Cressie 1990; Annels 1991; Goovaerts 1997; Sinclair and Blackwell 2002; Rossi and Deutsch 2014). The most commonly used approaches are linear estimators which is known as Kriging system.

Kriging is a variable of the basic linear regression techniques allowing a single regionalized variable at the unsampled locations to be estimated (Cressie 1990). Apart from the use in the linear regression such as Ordinary Kriging (OK) and Simple Kriging (SK), the Kriging equations also underly the non-linear estimators and conditional simulation techniques (Lantuejoul 2002).

The specific essential point of kriging technique is the special conditions determined to estimate as a constraining factor. These conditions can be seen as follows: Kriging estimate minimizes an estimation error, $\varepsilon = Z_{TRUE} - Z_{KRIGING}$. Kriging approach guaranties that the mathematical expectation of the estimation error is equal to zero, $E(\varepsilon) = (Z_{TRUE} - Z_{KRIGING}) = 0$.

These both characteristics provide advantage to Kriging when being compared with other linear estimators as it is concluded to be the Best Linear Unbiased Estimator (BLUE) (Cressie 1990; Annels 1991; Sinclair and Blackwell 2002). Quality of the Kriging estimate bases on many factors, including parameters that should be defined by a practitioner and used in the Kriging equations. Those parameters are commonly variogram model, search neighborhood and model grid dimension.

2.1.10.1. Ordinary Kriging

Ordinary Kriging (OK) is a widely used estimation technique for mineral resources estimation ((Journé & Huijbregts, 1978). It is a univariate linear estimator which is allowed to estimate a single regionalized variable at the unsampled locations by using the surrounding known samples. OK methodology is a representative of a variant of the basic linear regression estimator, and in general forms. The Ordinary Kriging equation is demonstrated in (2.22):

$$\begin{cases} Z^*(x) = \sum_{i=1}^n [\lambda_i Z(x_i)] \\ \sum_{i=1}^n \lambda_i = 1 \end{cases} \quad (2.22)$$

Where λ_i is the weight of OK assigned to each datum $Z(x_i)$, which are interpreted as a realization of the regionalized variable of interest $Z(x)$, $Z^*(x)$ is the estimated value and $Z(x_i)$ is the sample value at location i .

The OK system of linear equations allows to compute the sample weights in case of the intrinsic distribution model which is assured the optimal and unbiased conditions of the estimator ((Dhaene & Goovaerts, 1997; Journel & Huijbregts, 1978), as shown in (2.23).

$$\begin{cases} \sum_{\beta=1}^n \lambda_{\beta} \gamma(x_{\beta} - x_{\alpha}) - \mu = \gamma(x_0 - x_{\alpha}) \\ \sum_{\beta=1}^n \lambda_{\beta} = 1 \end{cases} \quad (2.23)$$

Where λ_i are the Ok weights; μ is the lagrange multiplier associated with the constraint $\sum_{\beta=1}^n \lambda_{\beta} = 1$. $\gamma(x_{\beta} - x_{\alpha})$ are the semi-variogram between data points, $\gamma(x_0 - x_{\alpha})$ is a semi-variogram between each datum and block.

The estimation error variance is also known as Ordinary Kriging variance and it is calculated as (2.24):

$$s^2(x) = s_0^2 - \sum \lambda_{\alpha} \gamma(x_0 - x_{\alpha}) - \mu \quad (2.24)$$

Where s_0^2 is the point variance of the regionalized variable $Z(x)$ and the matrix notation of OK system can be represented as follows:

$$[K] \times [\lambda] = [M_2] \quad (2.25)$$

The matrix of $[K]$, $[\lambda]$ and $[M_2]$ are illustrated as Equation (2.26) and (2.27):

$$[K] = \begin{bmatrix} \gamma(0) & \dots \dots & \gamma(x_1, x_n) & 1 \\ \dots \dots & \gamma(x_\alpha, x_\beta) & \dots \dots & 1 \\ \gamma(x_n, x_\beta) & \dots \dots & \gamma(0) & 1 \\ 1 & 1 & 1 & 0 \end{bmatrix} \quad (2.26)$$

$$[\lambda] = \begin{bmatrix} \lambda_1 \\ \vdots \\ \lambda_n \\ \mu \end{bmatrix} \quad \text{and} \quad [M] = \begin{bmatrix} \gamma(x_1, x_0) \\ \dots \\ \gamma(x_\alpha, x_0) \\ \dots \\ \gamma(x_n, x_0) \\ 1 \end{bmatrix} \quad (2.27)$$

The sample weights are estimated as Equation (2.28):

$$[\lambda] = [M] \times [K]^{-1} \quad (2.28)$$

2.1.11 Sequential Gaussian Simulation (SGS)

According to (M. Abzalov, 2016), Sequential Gaussian Simulation (SGS) is a based Gaussian method of conditional simulation, and it uses the transformed data from the original data, which has zero mean and a unit variance. These transformed data will be used to simulate the spatial variability of the interested variable. To produce realizations, the random path through grid nodes were defined including the conditional data, which is considered as hard data. A sequential neighborhood of the grid node is constructed by using the original data and simulated data. The original and simulated data are combined and used to compute the local conditioning distribution and obtain the simulated value at the target node. SGS method is widely used for modeling metal grades at different deposit types and mineralization styles (M. Abzalov, 2016).

SGS is an algorithm which simulates the grid nodes by each other sequentially, and subsequently the simulated values are used as conditional data for simulating other grid nodes. In SGS method, it requires the transformation of original data to normal score distribution data, therefore the original data known as composited data

is transformed into Gaussian data before they are used in the next process (Asghari, Soltani, & Amnieh, 2009).

The fundamental steps in SGS approach are demonstrated as follows:

1. Computes the histogram and statistical parameters of original data.
2. Transforms original data into normal score distribution data.
3. Calculates the variogram experimental and fit the model of the transformed data.
4. Defines a grid pattern.
5. Selects random path.
6. Kriges a value at each node using the known and previously simulated values and define Gaussian distribution.
7. Draws a value from Gaussian distribution, which is known as simulated value.
8. Simulates other grid nodes sequentially.
9. Back transform the simulated values into the original data (a realization was produced in this step).
10. To generate another realization, repeat step 6 until 9.

The variogram model of the transformed data are computed and used as spatial variability parameters in simulation process. The establishment of a grid for simulation and a random path is an essential to simulate each value at grid nodes. Based on the kriging mean and variance, the distribution of Gaussian probability is defined in individual node. It is very important to select a random path for estimation value at each node. A random value drawing from Gaussian probability distribution is conserved as a simulated value in each node. The basic steps in SGS algorithm are illustrated in Fig 2.12. (Deutsch & Journel, 1992).

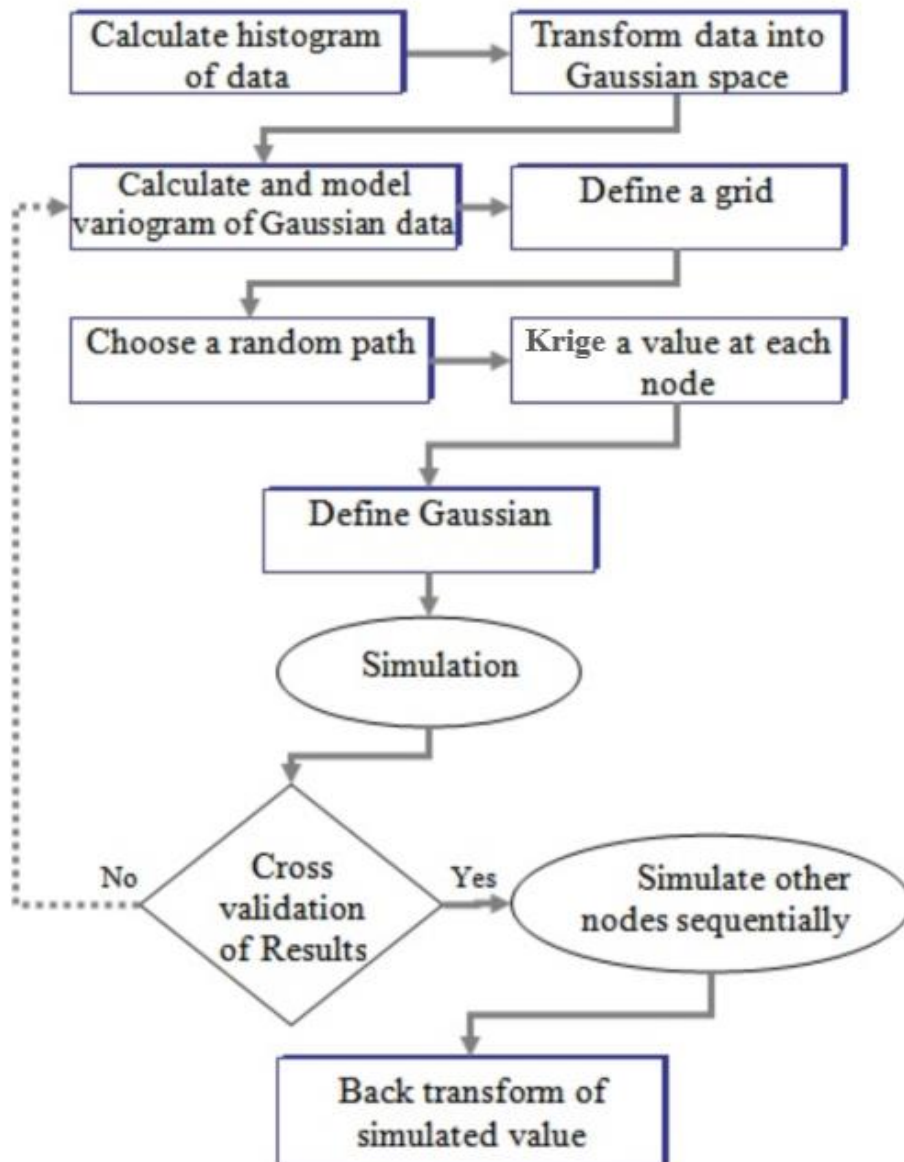


Figure 2.10 Fundamental steps of SGS method (Asghari et al., 2009)

2.1.12 Pit limit

The processes related to the development of a geometric surface which is called a pit onto the mineral deposit. When the pit limit was calculated, the mineable reserves volume will be lying within the pit boundaries. A vertical section which is taken through a pit limit is demonstrated in Figure 2.11. The size and shape of the pit are based on the economic factors and design/production constraints. If the price of minerals increases, the pit might expand in size by defining all other

factors remained constant. In contrast, when the price of minerals decreases the pit's size and shape would move in or narrower assuming all other factors remained constant. The pit existed at the end of mining phase is named the final or the ultimate pit.

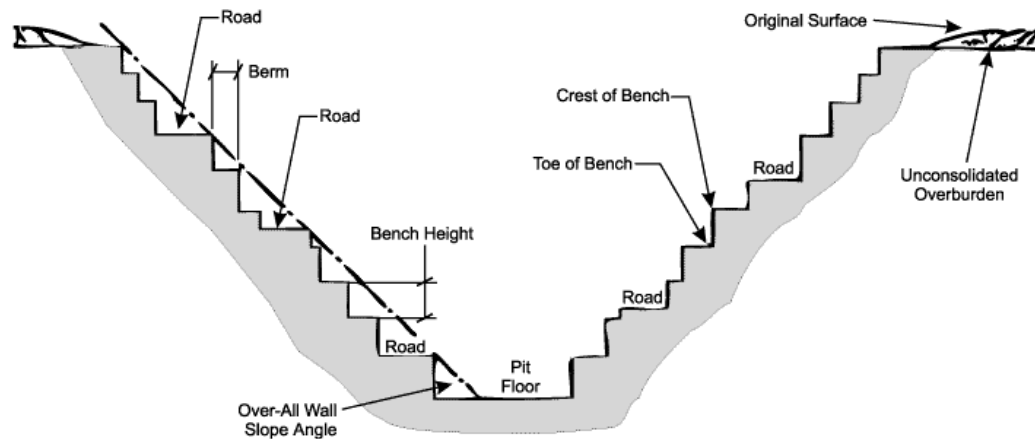


Figure 2.11 The Open Pit Schematic.

Source: <http://www.vbnc.com/eis/chap3/chap3.htm> (Access date: June 26, 2019)

Within the pit, different values of materials are found. To produce the final pit, the economic criteria are applied to define the objectivity for these materials depending upon their values (i.e. mill, waste dump, leach dump, stock pile, etc.). Once the pit limits have been determined and rules established for classifying the in-pit materials, then the ore reserves (tonnage and grade) can be calculated. The ore grade and tonnage will be used as the inputs in the follow up process such as reserve estimation, mine design, mine production, and mine life calculation.

2.2. Literature review

- Lesmana and Hitch (2013) discussed the modelling and spatial variability of three coal parameters, namely calorific value, ash content and sulfur content of a coal seam in Malinau, East of Kalimantan, Indonesia. The author concluded that the use of Kriging approach is strongly influenced by the amount of drill hole data and the area distribution of them. The results are more realistic when there are more drill holes available, and the variables distribution is performed well. Therefore, it can be

concluded that geostatistical estimation of the three coal parameters interpolated in this study is incorporated into mine planning and mine operation in Malinau coal mine.

- Wood (1979) evaluated low-ash coal reserves in No. 2 seam in Witbank, South Africa. This seam composes of several zones with different qualities and physical occurrences characteristics. The spherical variogram model was used in this variography study, and the typical value for the range was from 150 to 320 m. It is concluded that a consideration of the geological structure of the coal seam provides a deeper insight into the problems that could be predicted when the coal is mined. This makes the possibility of the estimation of low-ash coal reserves more realistic with more confidence. Geostatistical estimation method provides the most appropriate for reserves estimation and be placeable to confidences limits on all the estimates.

- Pardo-Igúzquiza, Dowd, Baltuille, and Chica-Olmo (2013) studied on geostatistical modelling of a coal seam for resource risk assessment. The study area is located in the North-West of Iberian Peninsula, which consists of several basins along dextral strike-slip fault zones. Based on the coal deposit, sampling density and spatial variability of seam thickness, the uncertainty in the semi-variogram are small. The consequences of selecting from the distribution of possible resources is very important. The variability of thickness in the simulation and kriging models were compared and summarized that simulation model is more effective than kriging estimated field. The total resources calculated from simulation is 245 million cubic meters with 95% confidences interval. Geostatistical simulation is an alternative approach that provides a mean of quantifying the uncertainty and resources risk assessment.

- De Souza, Costa, and Koppe (2004) investigated the methods capable of incorporating uncertainty to the estimates of resources and reserves via OK, Sequential Gaussian Simulation and Sequential Indicator Simulation. The coal deposit of this study is located in the Southern Santa Catarina coal basin, Brazil. It has been exploited since the early 1900's. The authors concluded that both methodologies,

OK and Simulation methods, led to similar results in term of tonnages within each class. However, the spread of the error derived from simulation is different from the interval obtained via Kriging variance. The OK variance may be used as a measure for spread of the estimates that depends on spatial continuity of dataset and spatial configuration of the observations. The conditional simulation methods had illustrated that the error associated with estimates can be evaluated using multiple simulated scenarios to define confidence levels, and these can then use in the classification process. Stochastic simulation allows reproduction of statistics (histogram, semi-variogram and scatter-gram) inferred from the data, therefore the model or realization looks more realistic than a smooth estimate.

- Irfan Manrwanza (2016) studied on coal resources classification using variogram to describe the spatial variability. The coal deposit in this study area was named Sangatta Coalfield containing high volatile bituminous coal, and it is occupied in the Northern Kutei Basin, Indonesia. This coal basin is divided into two zones (west zone and east zone). The research aimed using the range of variogram of calorific value to calculate distance between drill holes spacing for resources classification. After studied, the author reported that variogram may assist in defining distances of continuity between points observation. The coal measured resources distances between drill holes in west zone is 60 m. It is shorter than the variogram range expressed with 116 m. Then the distance can be extended according to the variogram. In east zone, the distance between drill holes is relatively similar to the practical drilling spaces. The acceptable confidence of drill holes spacing is required in a resource estimates and this is based on the geological conditions and range of variogram.

- Olea and Luppens (2012) applied Sequential Simulation approach for modeling of multi-seam coal deposits with an application to the assessment of a Louisiana lignite. The author reported that Stochastic simulation allows both detailed geological characterization of coal deposits and a quantification of associated uncertainties inherent to the modelling. Geological factors considered in the modeling can be bed boundaries, erosion, oxidation, bed thickness and coal density.

The modeling provides detailed as well as synoptic results for uncertainties at both the deposit and the local cell level. For total resources, a probability distribution provides total resources and associated probabilities. At the cell level, it is possible to map cell tonnage generated probability distributions cell by cell and summarized the expected cell tonnage in the form of cumulative distribution as a function of cell uncertainties.

- COSTA, Zingano, and KOPPE (2000) studied on comparing the methods used in ore reserves estimation between the conventional method and geostatistical simulation method as FGT method (F=Fault, G=Grade and T=Thickness). This study area is located in Eastern portion of Central Iran. After the studies, the authors reported that a new method as FGT method can be applied into Parvadeh III coal deposit to access a particular aspect of the fault existence risk. The results of conventional method and FGT method were compared to verify the resources classification. The comparison indicated that the areas which should be rejected from the region in FGT method are less and more distinguishable than those determined with the conventional method. Therefore, the inferred resources can be differentiated from indicated and measured resources with high resolution. The conventional method cannot distinguish between these three categories at this level of resolution. Thus, the FGT approach has high precision in classifying the coal resources compared to the conventional method.

CHAPTER 3

RESEARCH METHODOLOGY

The methodology of this study is expressed by the flowchart in Figure 3.1:

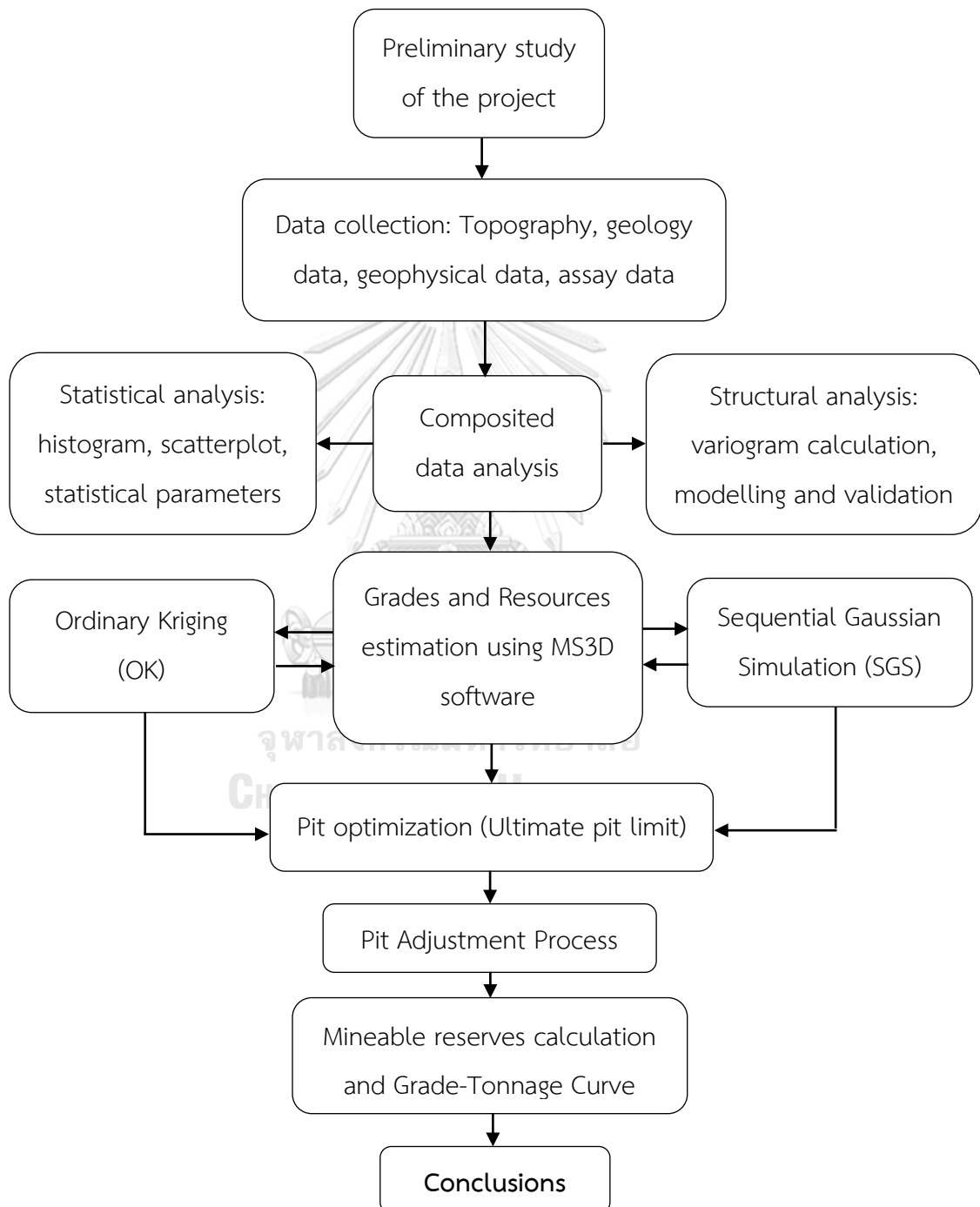


Figure 3.1 Flowchart of the research study.

3.1 Topography and drill holes data preparation.

The x, y, z coordinates of assay data collected within NG exploration area represent in Easting, Northing and Elevation. In this study, the data points were edited in excel spreadsheet and saved into csv (comma-separated values) format. This prepared csv file was imported to MS3D as point data and then triangulated to wireframe and 2D surface. The 5-meter interval was used to create a contour map within the NG exploration area as shown in Figure 3.2. The topography is setting within the coordinate of 200133.2 - 204124.31 Easting, and 2037413.07 - 2042116.35 Northing. The elevation (Z) is ranging from 200 to 320 m above msl. A total of 295 assays data from 51 exploration drill holes (DH) which collected from the Lao Integrated Development Group (LID) company were used for coal grades, resource and reserve estimation.

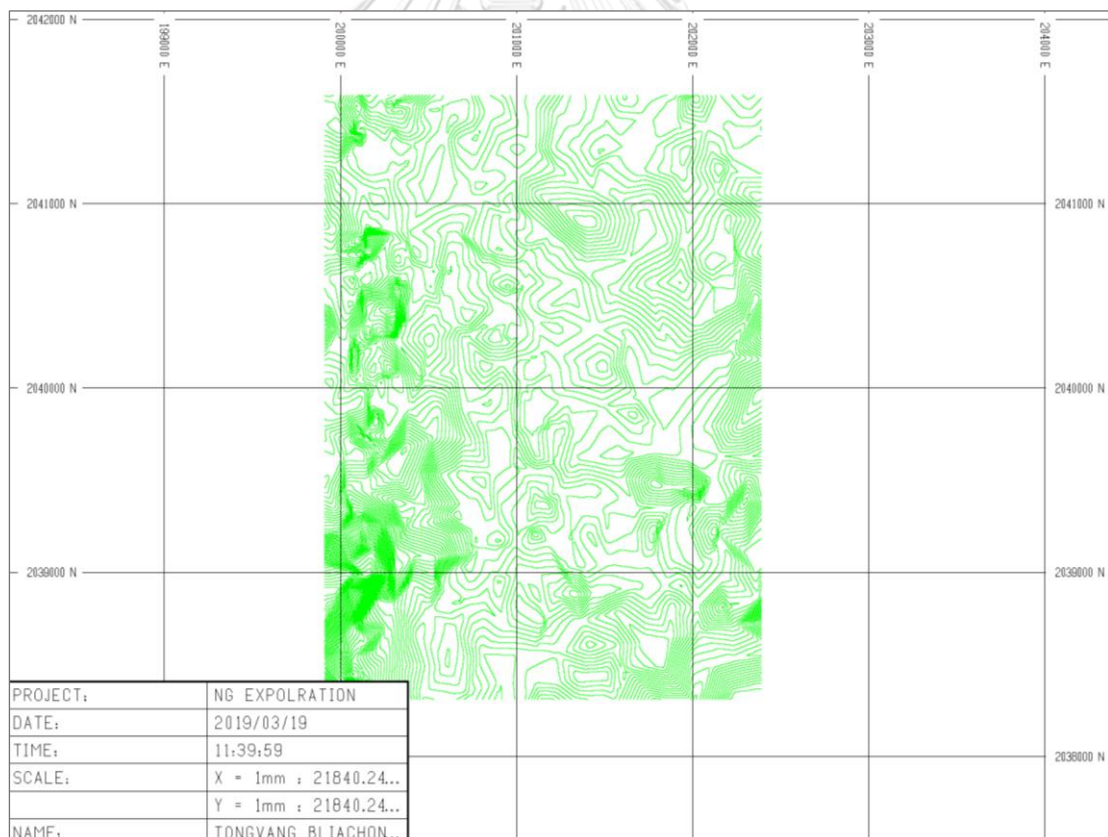


Figure 3.2 The contour map of 5-meter interval at NG exploration area.

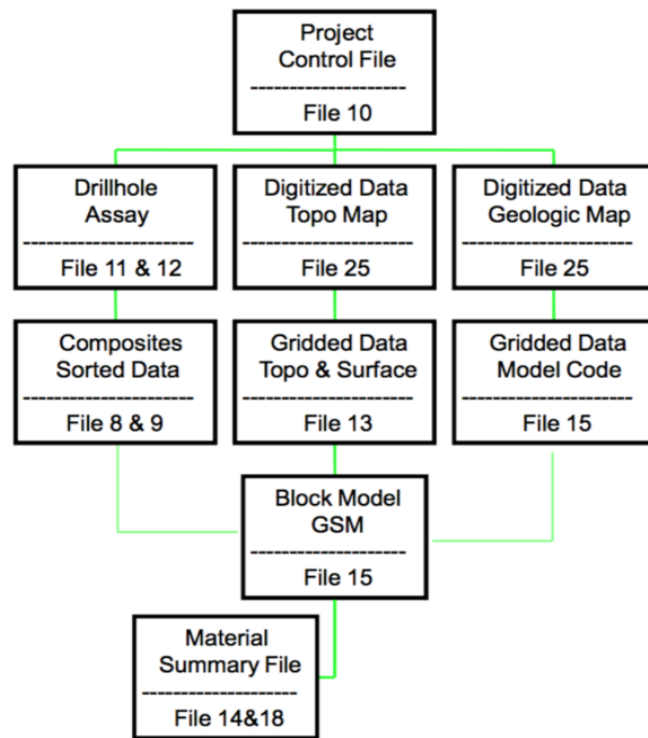
3.2 Database formatting and loading

The prepared DH data files of csv format were imported into MS3D software by a procedure called conca.dat. This procedure was used to convert and combine the DH data files into a main database, which kept all DH information ready for loading and displaying after the completely converting process. After importing, the DH data validation was followed up to check for any bias occurred in the running process or prior. These validations included DH coordinates or collar, assay information, and lithology logging information.

In order to complete a project in MS3D software, there are some required files to be created during the processes. The characters of those files are explained below:

- File 10 (F10) is a MS main data file as a project control file, which is be used to store all information about the project created such as a project control area and other minor files creation later.
- File 11 (F11) is a MS assay file that contains all the information of coal qualities in term of a coal deposit.
- File 12 (F12) is a MS survey file containing the DH survey information or orientation such as DH dip and azimuth.
- File 8 and 9 (F8 and F9) are MS unsorted and sorted composite files that are used to store the DH composited data.
- File 25 (F25) is a MS digital file containing the topography data
- File 13 (F13) is a MS gridded surface file (GSF) or 3D surface model that uses to store the elevation data for surface and pit optimization.
- File 15 (F15) is a MS 3D block model (3DBM) file which is used to store the 3DBM information such as block size, density, grades and other attributes required for other purpose such as mining cost, block value, milling cost and others.

These required files and the processes of a complete project construction in MS3D software are denoted in Figure 3.3.



Figures 3.3 Flowchart of necessary files creation in MS3D software (Vang, 2015).

Figures 3.4 - 3.9 display the method of importing the collar, assay, survey and geology files to MS3D software, respectively.

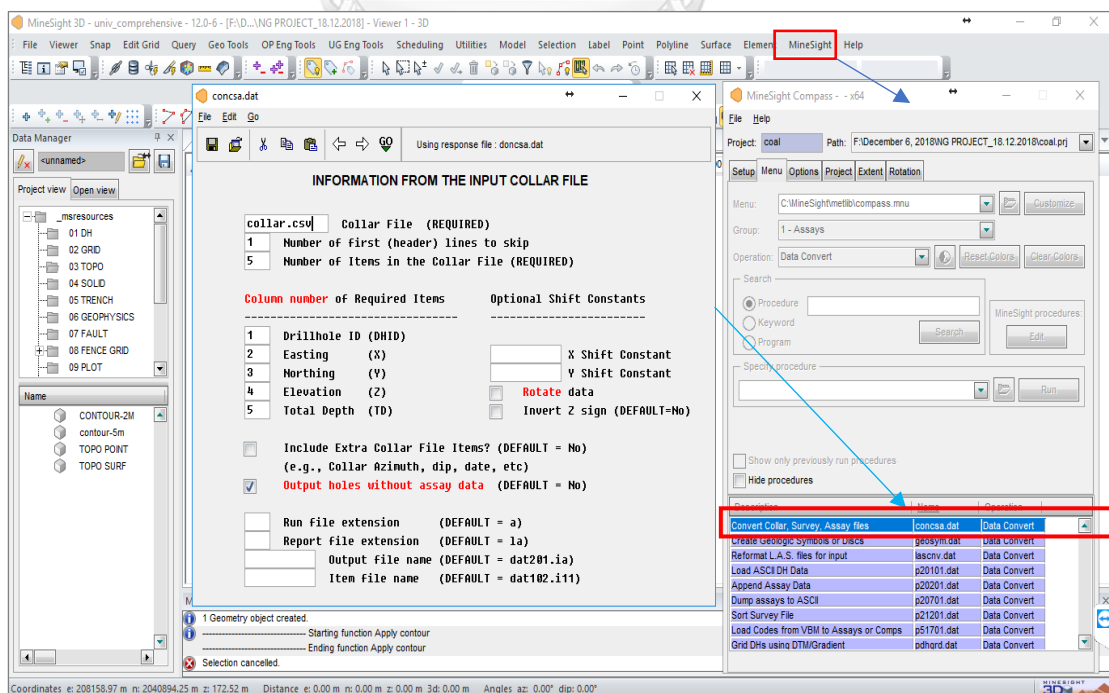


Figure 3.4 Method of importing collar.csv to MS3D software.

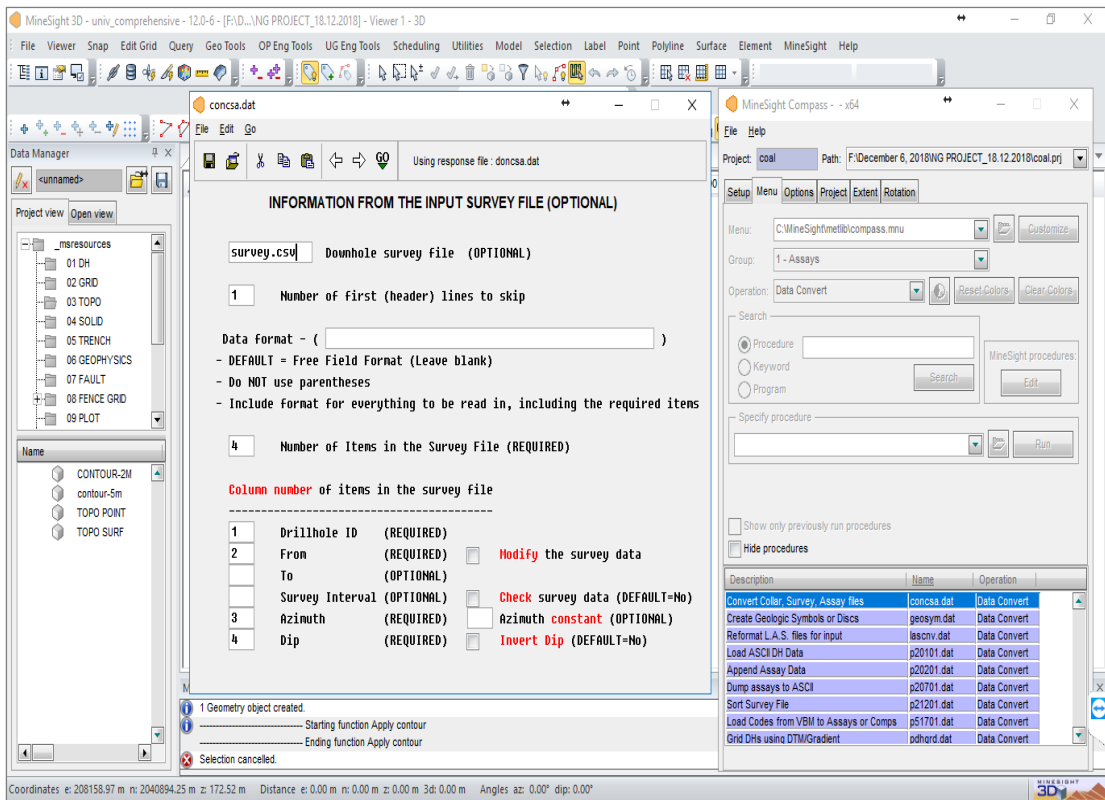


Figure 3.5 Method of importing survey.csv to MS3D software.

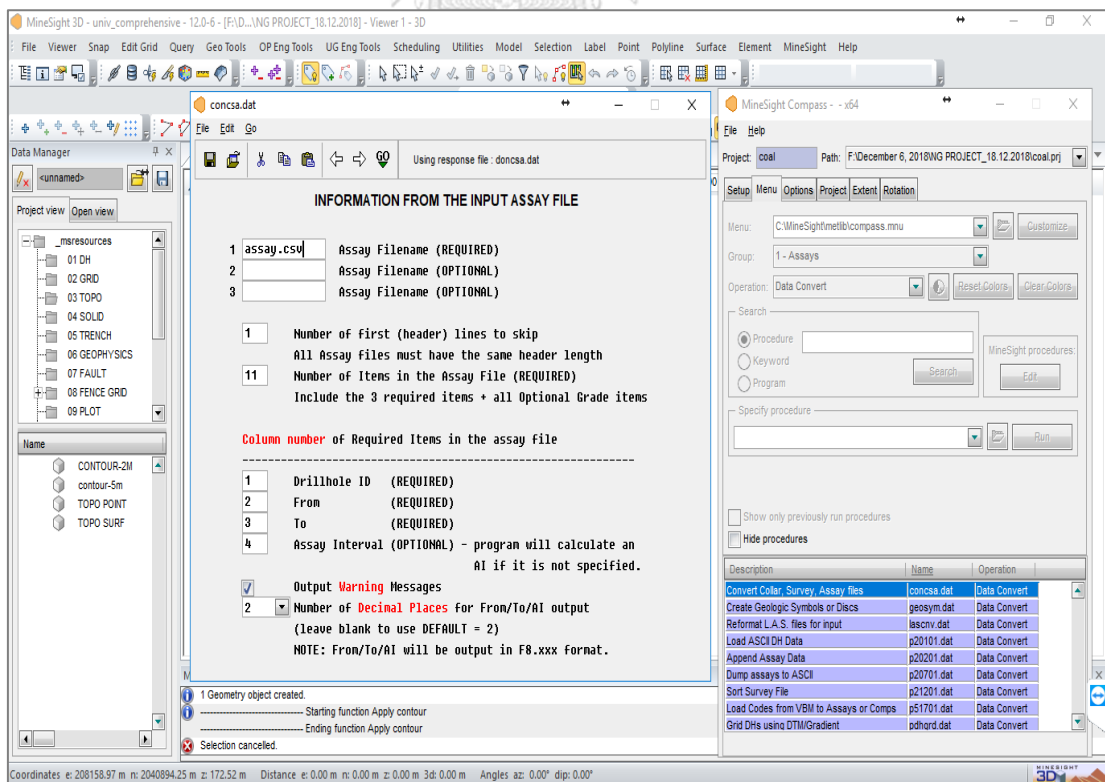


Figure 3.6 Method of importing assay.csv to MS3D software (Data input)

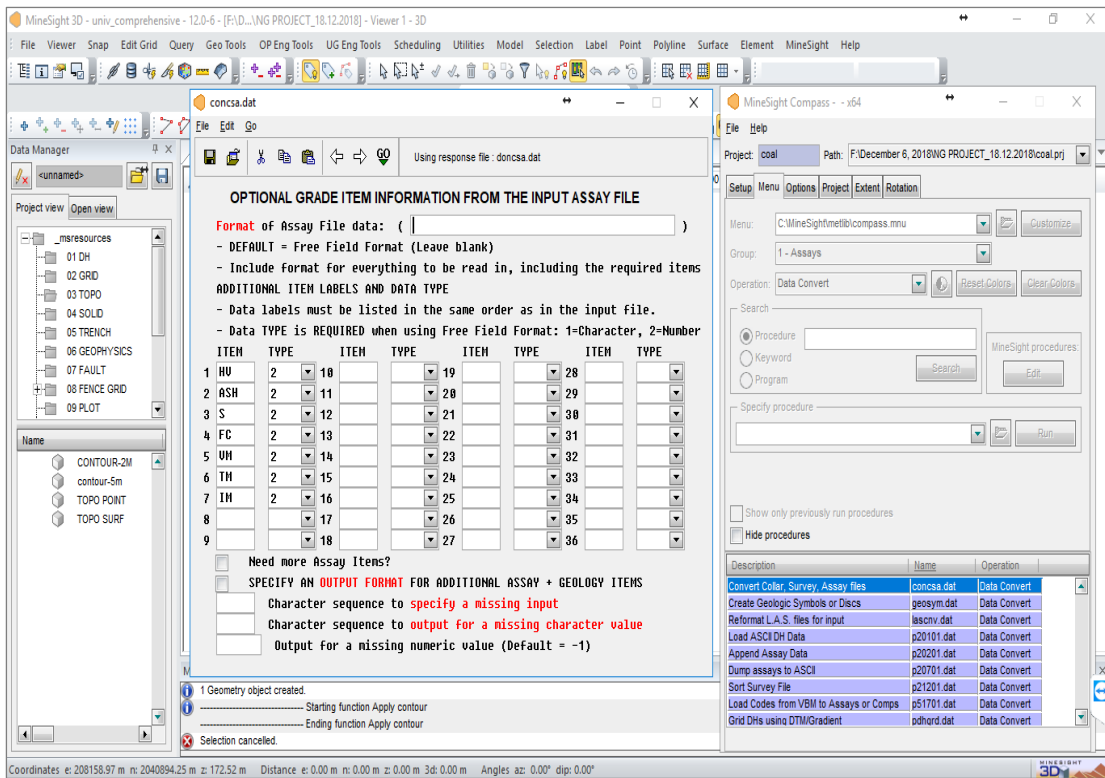


Figure 3.7 Method of importing assay.csv to MS3D software (Parameters loading)

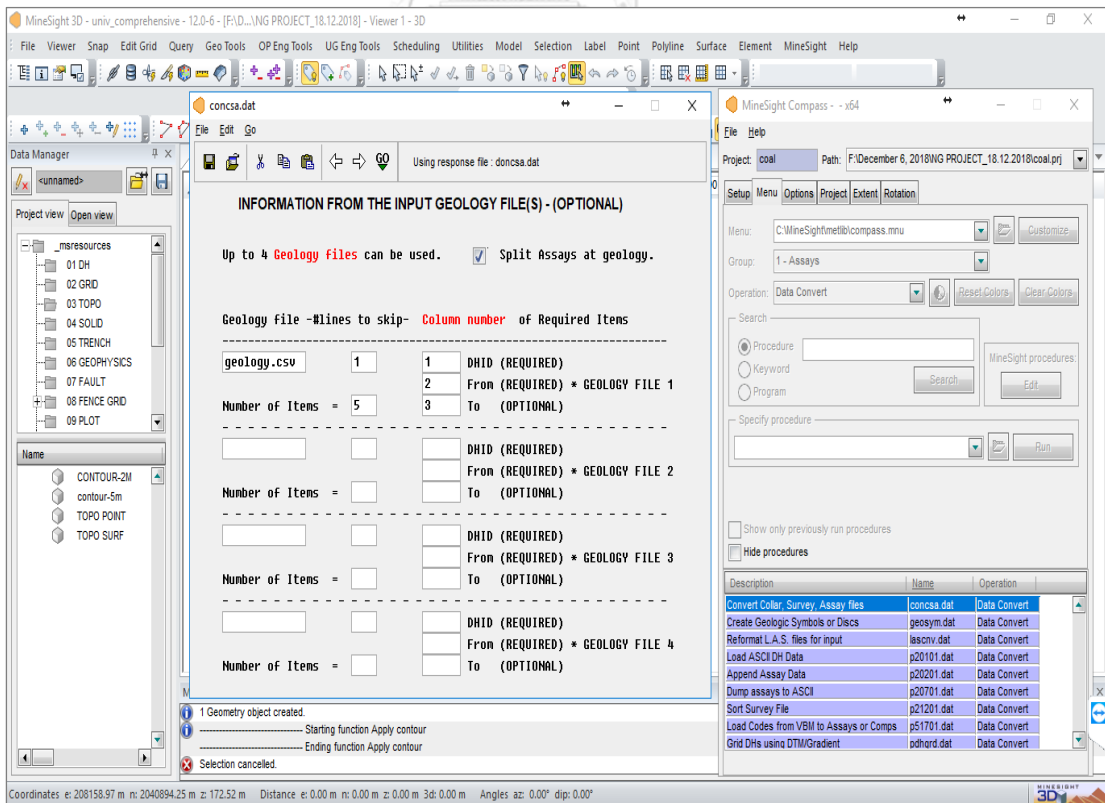


Figure 3.8 Method of importing geology.csv to MS3D software (Data input).

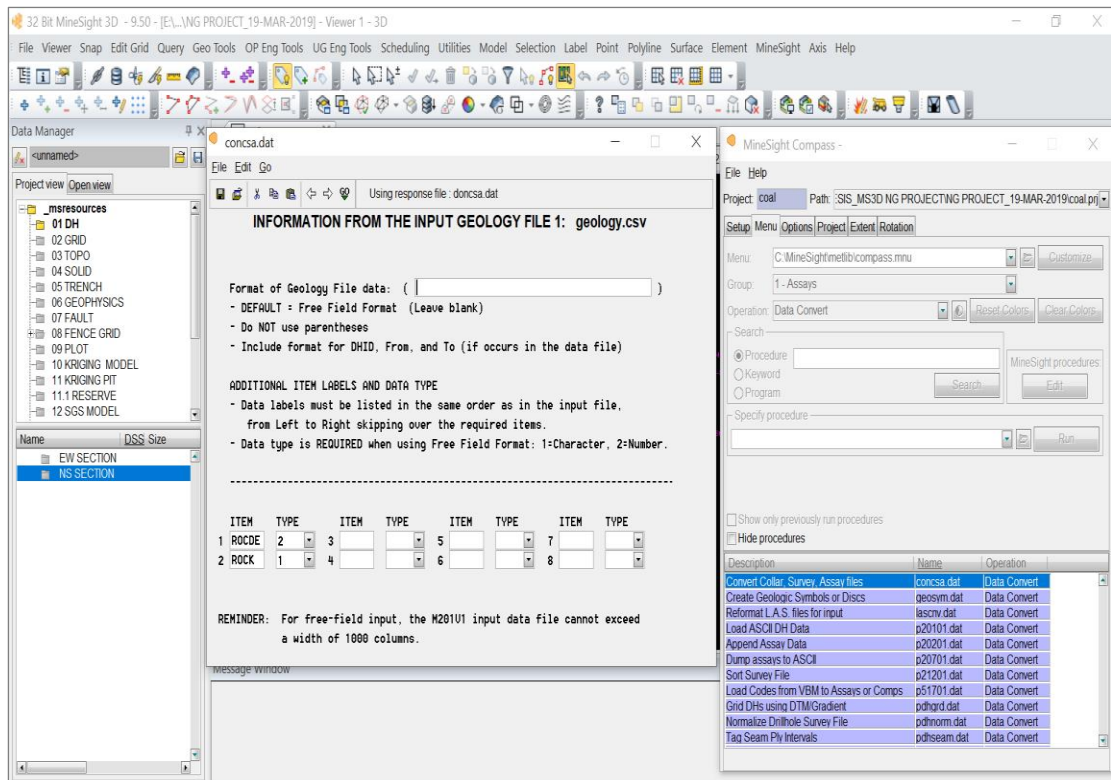


Figure 3.9 Method of importing geology.csv to MS3D software (Lithology code).

After the four DH data files were imported into MS3D software, the initialize of assay data was carried out, and then the DH database (dat201.txt) was loaded to display DH information and validation.

3.3. Drill hole composites

Drill hole composite was accomplished using a bench compositing method in MS3D. In order to provide an appropriate interpolation of coal quality parameters such CV and AC for geostatistical estimation, a fixed length of 1 m interval was considered as a suitable composite length for DH composite in this study. This is because of the high variations of coal seam thickness within NG exploration area. Gross calorific value and ash content are the chosen parameters used for DH compositing and furthermore process like Ordinary Kriging estimation and Sequential Gaussian simulation. The drill hole composite was succeeded by the following steps: MineSight > MScompass > Group: 2 – Composites, Operation: Calculation > Bench compositing. DH composite procedures are presented in Figure 3.10 – 3.11.

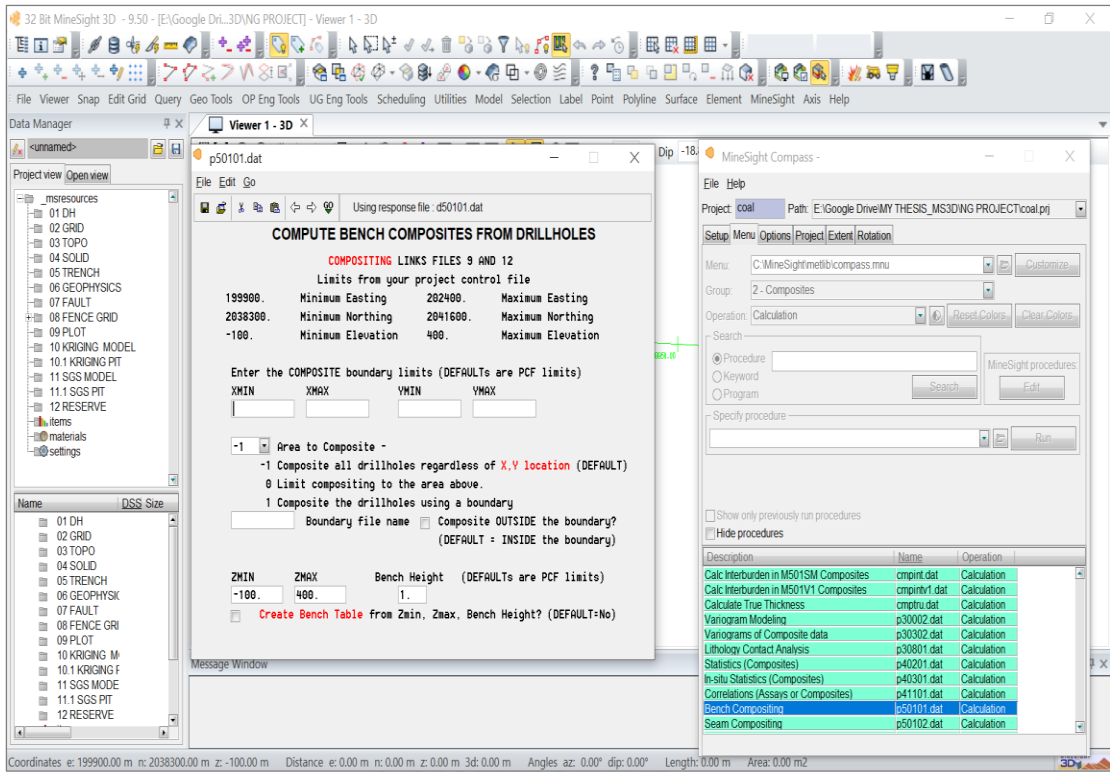


Figure 3.10 Drill hole composite in MS3D software (Composite limiting).

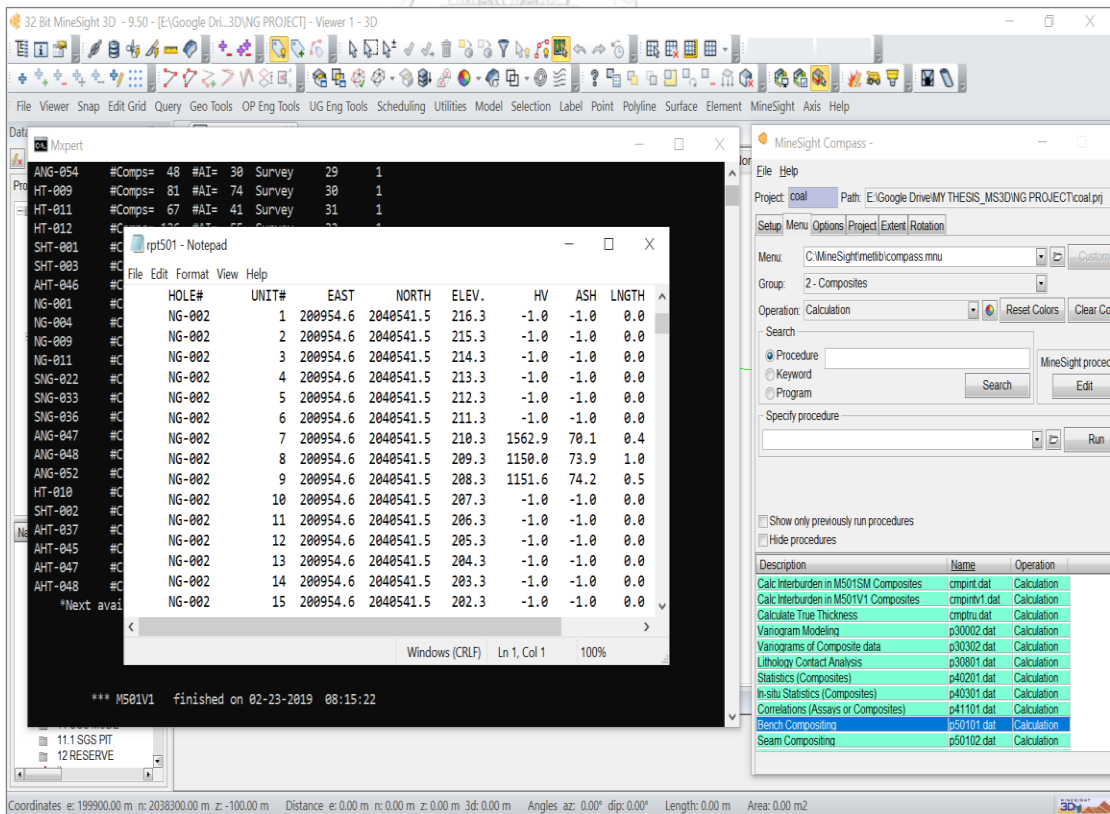


Figure 3.11 Drill hole composite in MS3D software (Composite report).

3.4. Statistical analysis of composited data

The composited data of CV and AC were used to calculate the statistical parameters such as minimum, maximum, mean, variance, standard deviation, coefficient of correlation and other required parameters. The statistical analysis of these two variables were accomplished using histogram plot and scatterplot by a tool called MineSight Data Analysis (MSDA) in MS3D software. This is to show the distribution characteristics of each parameter and a correlation between them.

3.5. 3D Solid zone construction

The cross-sectional method was used to define drill holes section for creating 3D solid model of NG coal deposit. There was a total of 15 cross sections of drill holes defined along East-West direction within NG exploration area. The 2D cross section view of drill holes data were used for creating a closed segment based on each coal seam, which had a correlation to each other from one drill hole to others. The geological structures such as fault and fold, and geophysical information were used to assist the coal seams interpretation. The maximum distance of coal seams interpretation is 75 meters. The closed segments from each DH section were connected together to construct a wireframe model of the domain. The wireframe model was then validated and saved to generate a solid model of each coal seam for the entire deposit. In this study, the cross section spacing is varied from 50 meters to 200 meters similarly to the exploration drilling program.

Due to NG coal deposit exhibits a complex geological setting area, resulted in a high variation of coal seam thickness and qualities. The coal seam thickness has demonstrated as a thin, moderate and thick layer with multiple seams within the entire NG exploration area. In this research study, the minimum thickness of 0.3 meter was considered for 3D solid model construction. For a practical consideration, a group of split seams and sub-split seams occurred near each other with partings less than 0.3 meter were then grouped together. And for a group of split seams and major seams having thickness greater 1 meter, which consisted of partings less than 0.45 meter were also grouped together. The cross-sections determination within NG exploration drill holes are illustrated in Figure 3.12, and Figure 3.13 represents a 2D

cross-section of section-KK'. The procedures of constructing a 3D solid model of NG coal deposit can be seen in Figure 3.14.

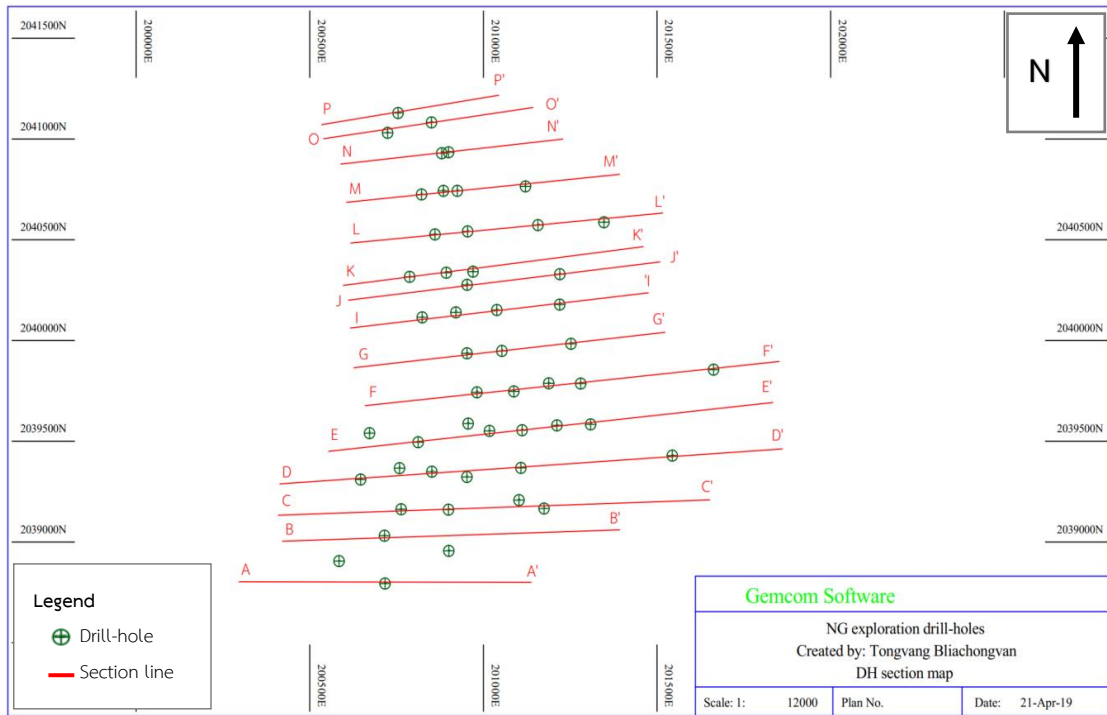


Figure 3.12 Exploration drill holes cross section determination.

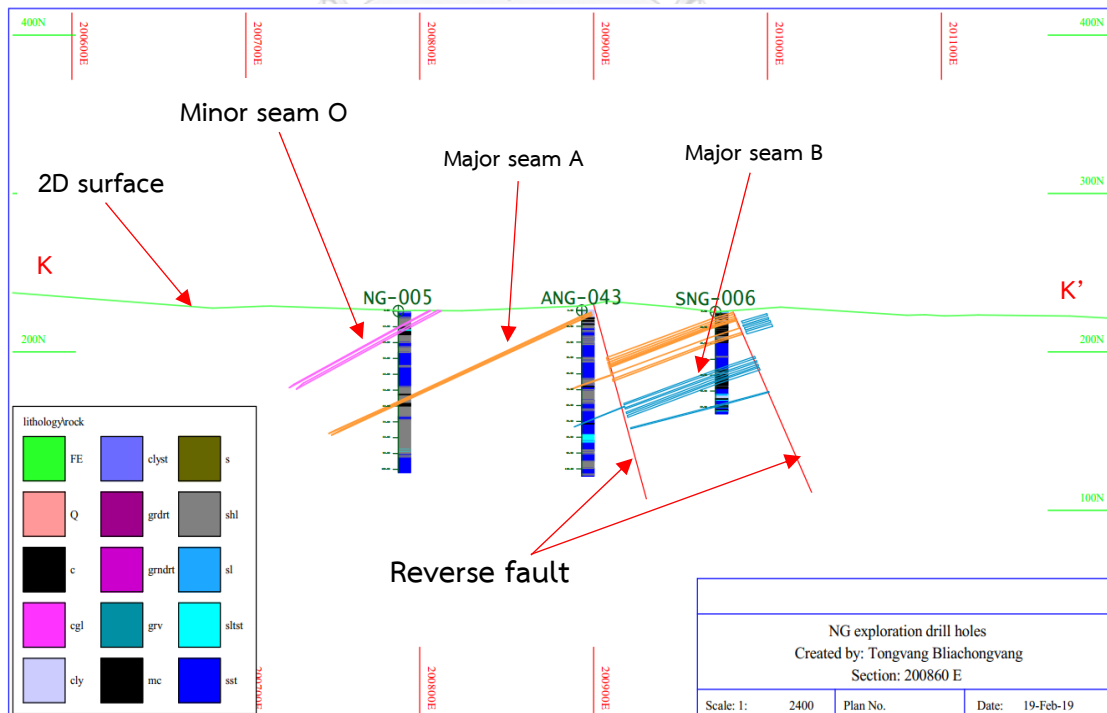


Figure 3.13 2D cross section of section-KK' of coal seams digitization.

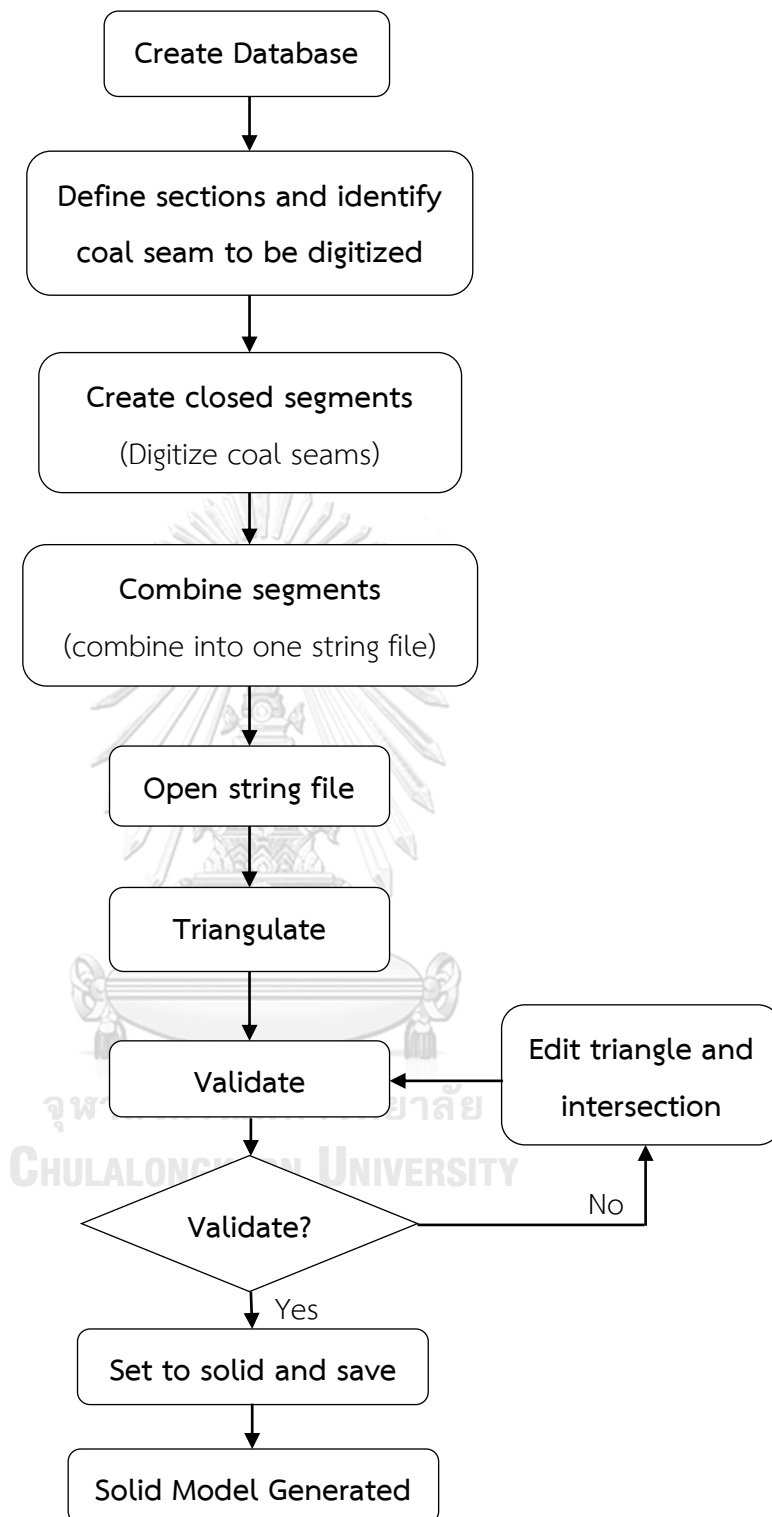


Figure 3.14 Flowchart of steps used to generate the 3D solid model.

3.6. 3D block model development

The 3D block model used for OK estimation and SGS was created by defining the block size interval based on bench dimension. Then, the attributes and required economic parameters used for pit optimization were added into the block model. In this study, the block size discretization was defined as $20 \times 20 \times 5$ (in x, y and z dimension) cubic meters for coal quality parameters as CV and AC interpolation. The 3D block model of NG coal deposit is demonstrated in Figure 3.15. The 3D solid model of NG coal deposit was used for block model coding to determine the percentage of solid model volume intersected within the entire block model volume. In this study, a minimum 8 percent of solid model volume intersected within the entire 3D block model volume was considered to be coal and used for the interpolation. The 3D block model containing the percentage less than 8 percent were classified as waste. There is a total of 4,796 blocks generated within the 3D solid zone model of this coal deposit. These blocks were used for coal quality parameters as CV and AC interpolation, geological resource and mineable reserve computation.

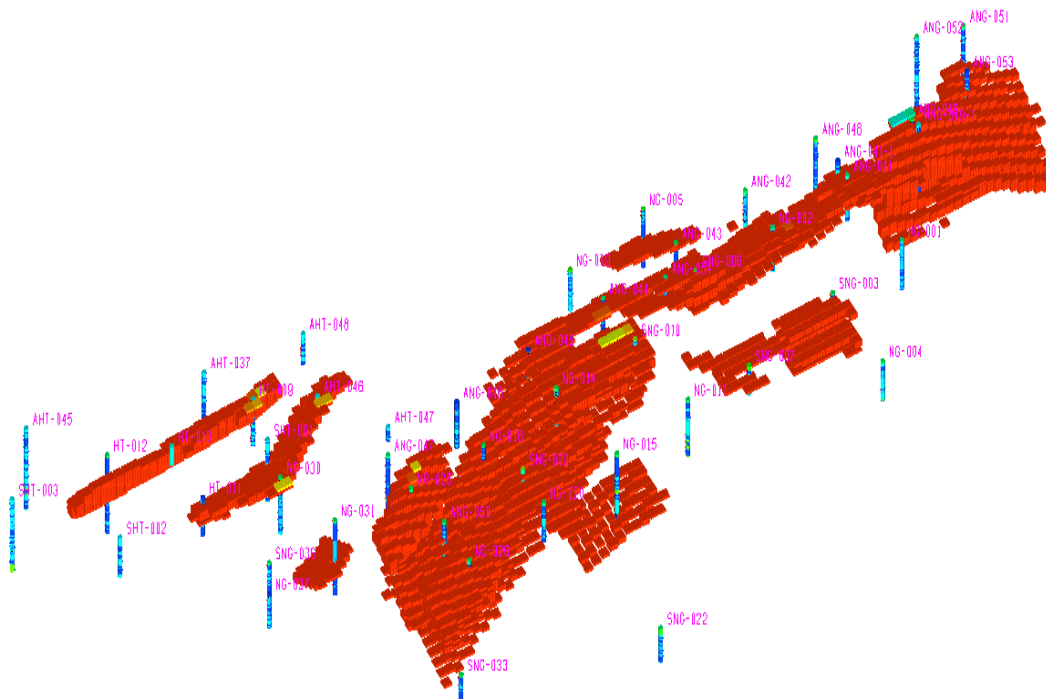


Figure 3.15 3D block model generated within 3D solid model of NG coal deposit.

3.7. Kriging estimation

Kriging estimation is a popular and widely used geostatistical tool applied to mining industries and other geoscience fields. Kriging methods comprise of many estimators used for metal grades and coal quality parameters interpolation which will be used for mineral resource and reserve estimation. Kriging estimation methods use neighboring sample values to interpolate the unknown values at unsampled locations. It minimizes the error variance into minimum and no biased when the sum of sample weights equal to one. In this study, Ordinary kriging (OK), a Best Linear Unbiased Estimator (BLUE), was used to interpolate coal quality parameters such as CV and AC at NG coal deposit.

3.7.1. Variogram calculation and modelling

The exploration drill holes spacing grid pattern within NG exploration area and other blocks varies from 50 meters × 50 meters to 200 meters × 200 meters. The DH drilling direction is assumed as vertical direction with dip angle of 90° based on the exploration stage. In this research, the experimental variogram calculations of CV and AC were carried out using azimuth ranging from 0° to 225° with 45° increasement in order to observe the anisotropic characteristics. The dip angle is ranging from 0° to 90° with 30° increasement for both parameters. In this case, only the vertical experimental variogram calculations were constructed for both variables by a tool called MSDA in MS3D software as presented in Figure 3.16 – 3.17. Consequently, the vertical experimental variogram calculation was used for fitting a best variogram model based on the practitioner's observation. The best fitted model provides the range, the nugget effect, and partial sill included CV and AC. These parameters will be stored and retrieved for the subsequent related process.

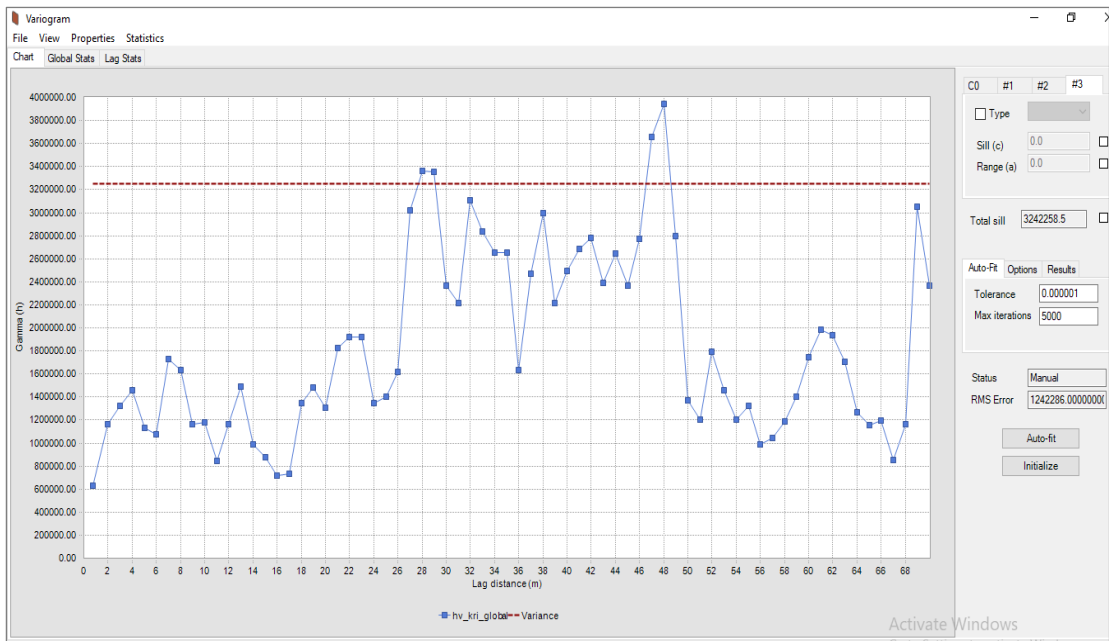


Figure 3.16 Global vertical experimental variogram of CV.

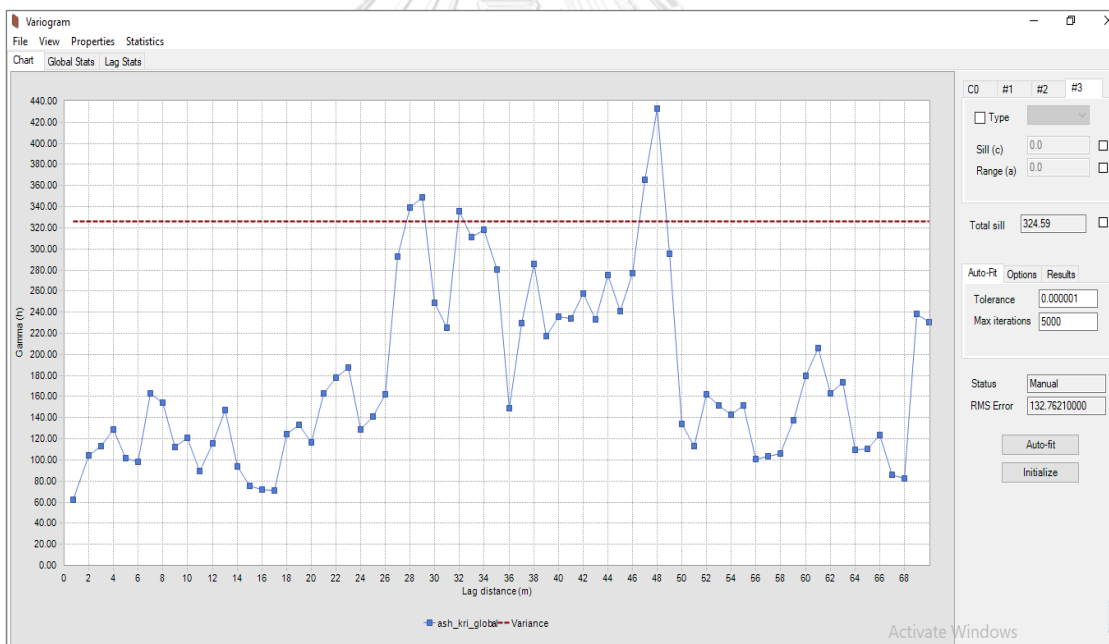


Figure 3.17 Global vertical experimental variogram of AC.

3.7.2. Ordinary Kriging Estimation (OK)

The interpolation of CV and AC within each block in the entire 3D block model of NG coal deposit was implemented using Ordinary Kriging approach, which is demonstrated in Equation (3.1). The Ordinary Kriging method provided in MS3D

software is a module used for metal grades and coal quality parameters interpolation. Then the estimated block model was used for geological resource, pit optimization, and mineable reserve calculation. In this study, the fitted variogram model as spherical model from the composited data was applied as the input of the uncertainty determination for Ordinary Kriging estimation. This fitted variogram model minimized the error variance and defined the anisotropic characteristics. There is a total of 4,796 blocks used for CV and AC interpolation within NG coal deposit. Prior to the interpolation, the attributes such as CV's mean, AC's mean, CV's variance and AC's variance were added into the 3D block model to store the interpolated results.

In accordance with the fitted vertical variogram model, the ranges for CV and AC fitted were very close to each other. Therefore, the vertical search distance of 100 m was used. However, the searching dimension criteria along Easting and Northing for this interpolation is 250 m based on JORC Code 2012 as shown in Table 3.1. Ordinary Kriging input parameters for coal quality parameters interpolation are demonstrated in Table 3.6.

$$Z^*(x) = \sum_{i=1}^n [\lambda_i Z(x_i)] \quad (3.1)$$

Where: $Z^*(x)$ = estimated value at location x

λ_i = sample weight from the estimated value to known sample value

$Z(x_i)$ = sample value at location x_i

Table 3.1 Coal resource classification based on sampling spacing defined by the JORC Code 2012 system (De Souza et al., 2004)

Classes of resource	Maximum extrapolation distance	Maximum spacing between points of observation	Degree of uncertainty
Measured	500 meter	+ 1 km; <500 meter	0 – 10%
Indicated	1,000 meter	+ 2 km; < 1 km	10 – 20 %
Inferred	2,000 meter	+ 4 km	> 20%

Table 3.2 Kriging input parameters for coal quality parameters interpolation.

Input files	Composited data of CV and AC				
Grid discretization	20 meter × 20 meter × 5 meter				
Variogram model (Spherical Model)	Variable	Structure	Nugget (C_0)	Partial Sill (C_1)	Range (a)
	CV	1 st	669,322.7	1,075,697.2	9.37
		2 nd		1,497,238.5	48.5
	AC	1 st	63.13	105.98	9.04
2 nd			155.48	40.08	
Searching dimension	x = 250-meter, y = 250-meter, z = 100 meter				
Conditional data	Min = 1, Max = 7				

The Ordinary Kriging estimation in MS3D software is as followed; MineSight > MScompass > Group: 5a – 3D Modeling, Operation: Calculation > Ordinary Kriging. This procedure is shown in Figure 3.18 – 3.27.

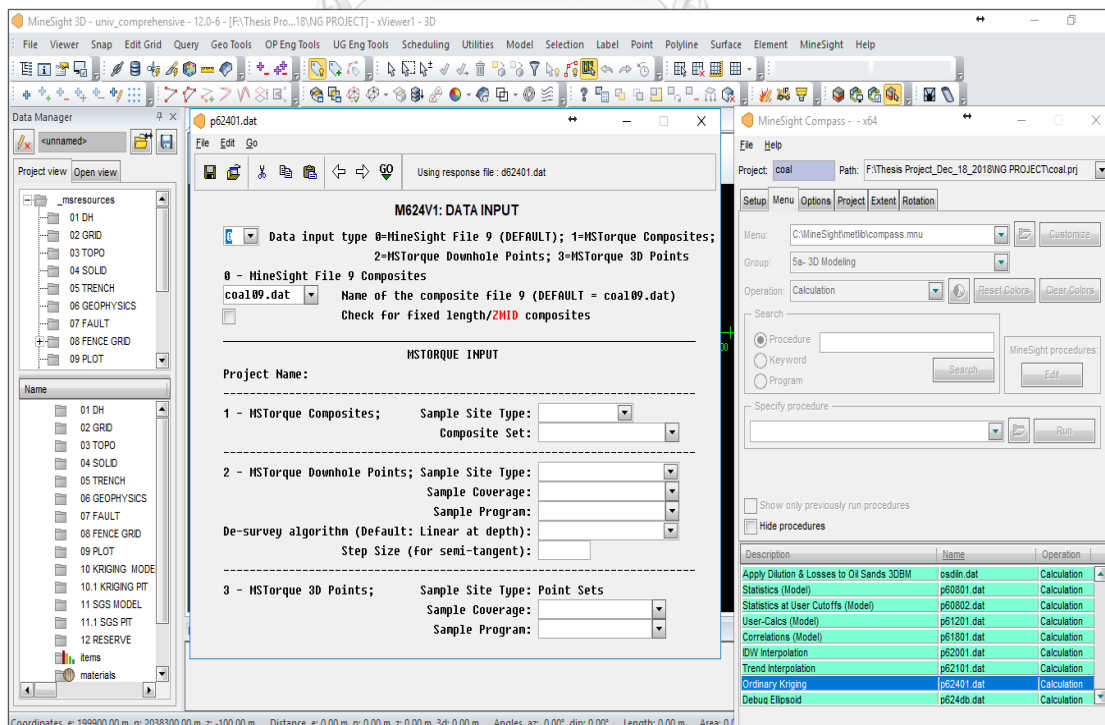


Figure 3.18 OK method of CV in MS3D software (Data input)

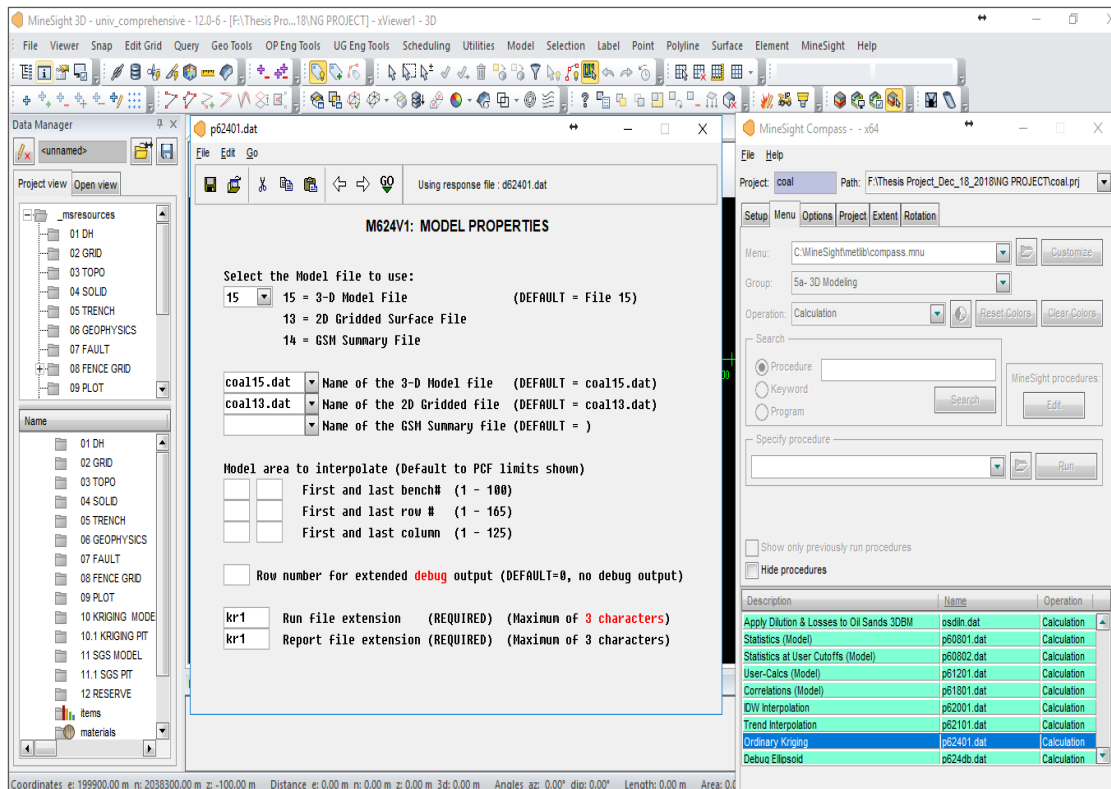


Figure 3.19 OK method of CV in MS3D software (Model parameters)

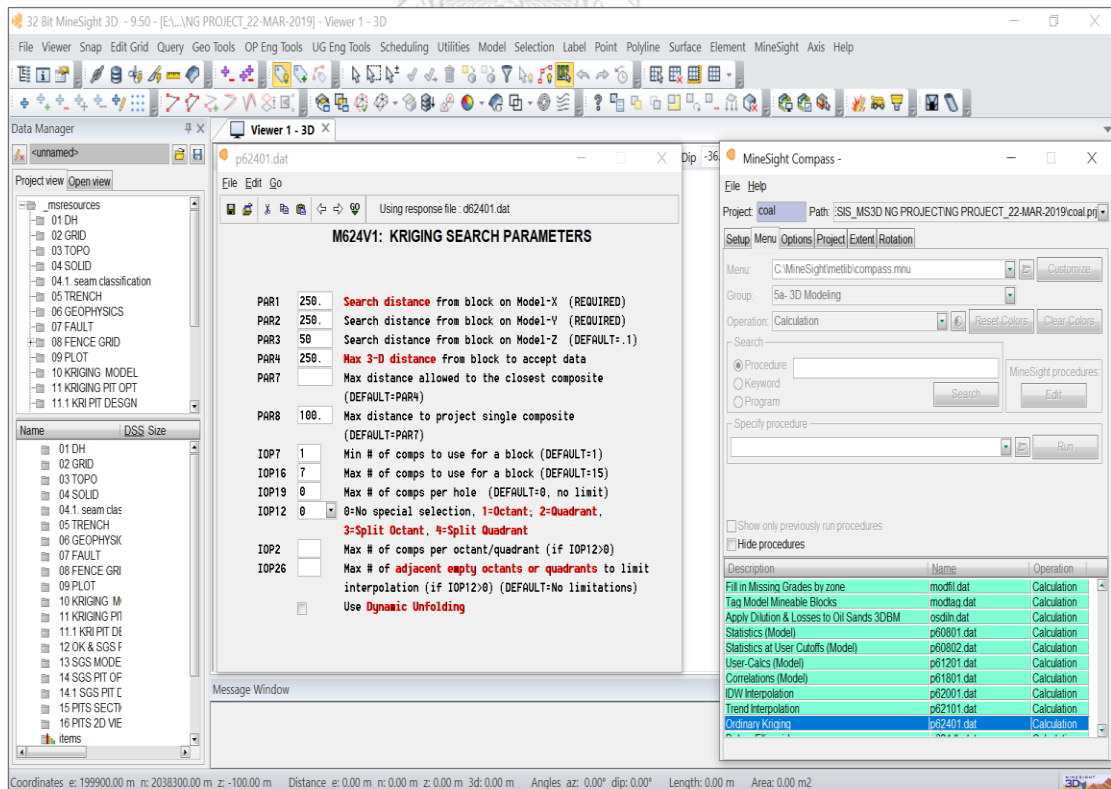


Figure 3.20 OK method of CV in MS3D software (Kriging search parameters)

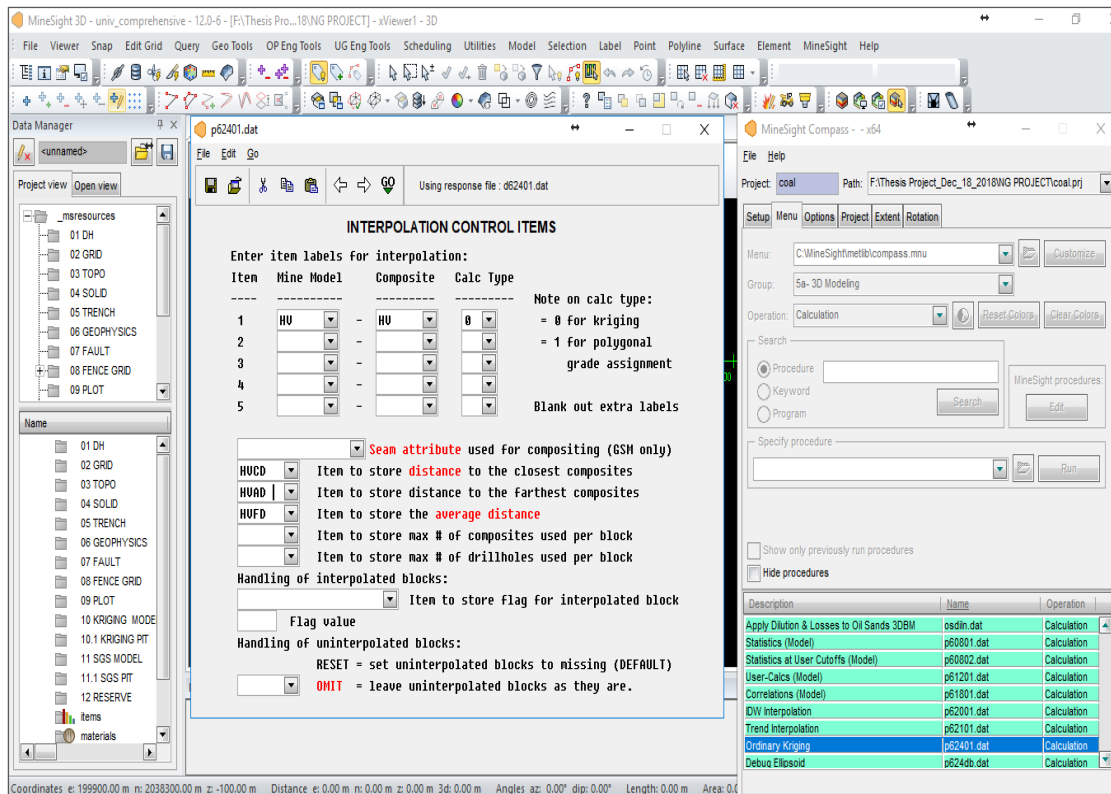


Figure 3.21 OK method of CV in MS3D software (Interpolation control items)

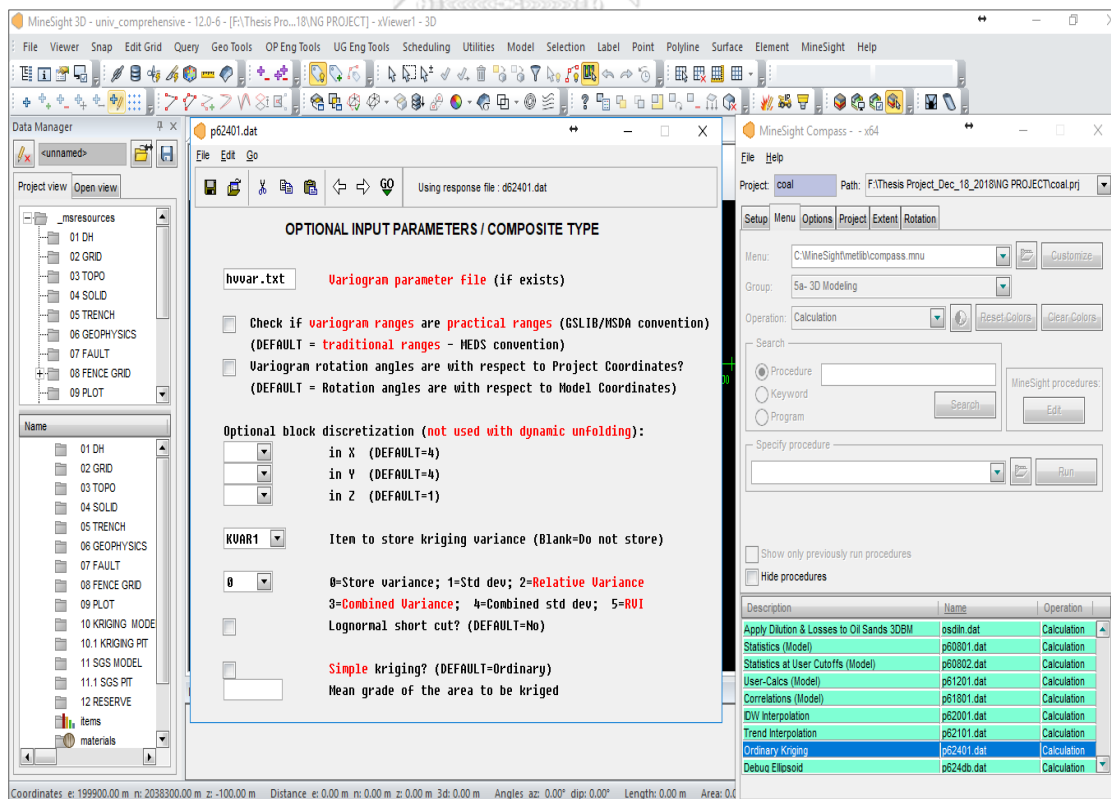


Figure 3.22 OK method of CV in MS3D software (Variogram model parameters)

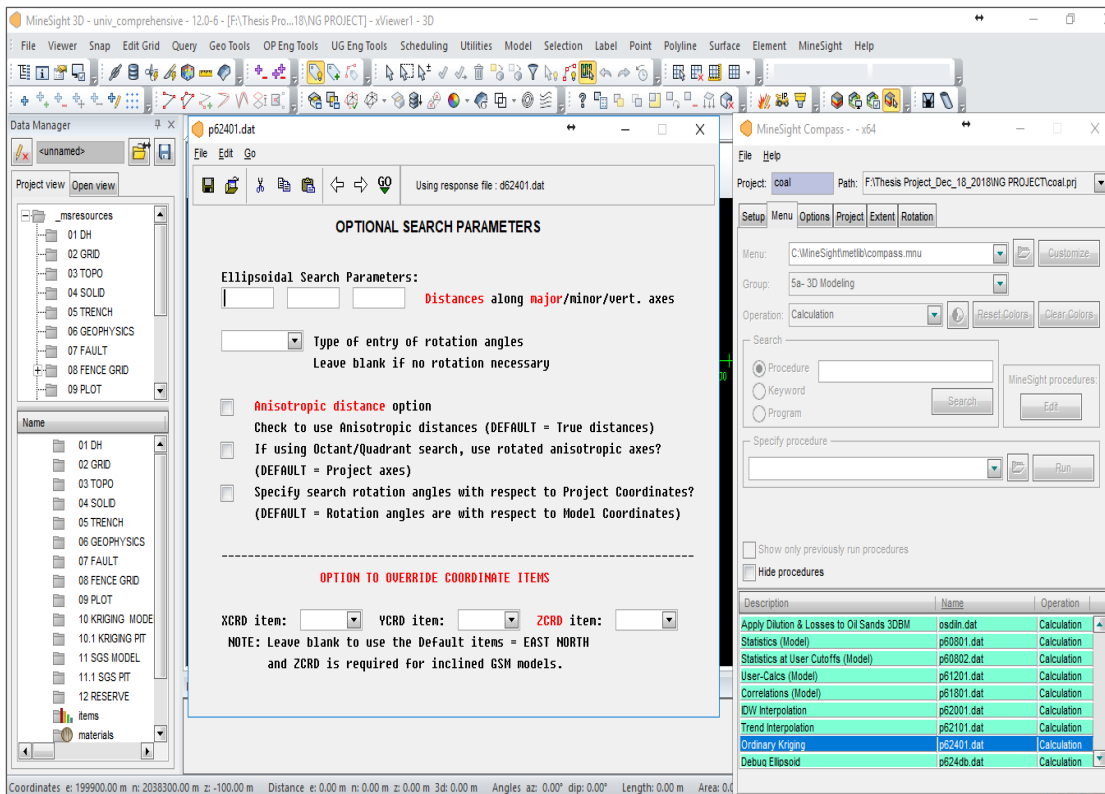


Figure 3.23 OK method of CV in MS3D software (Optional search parameters)

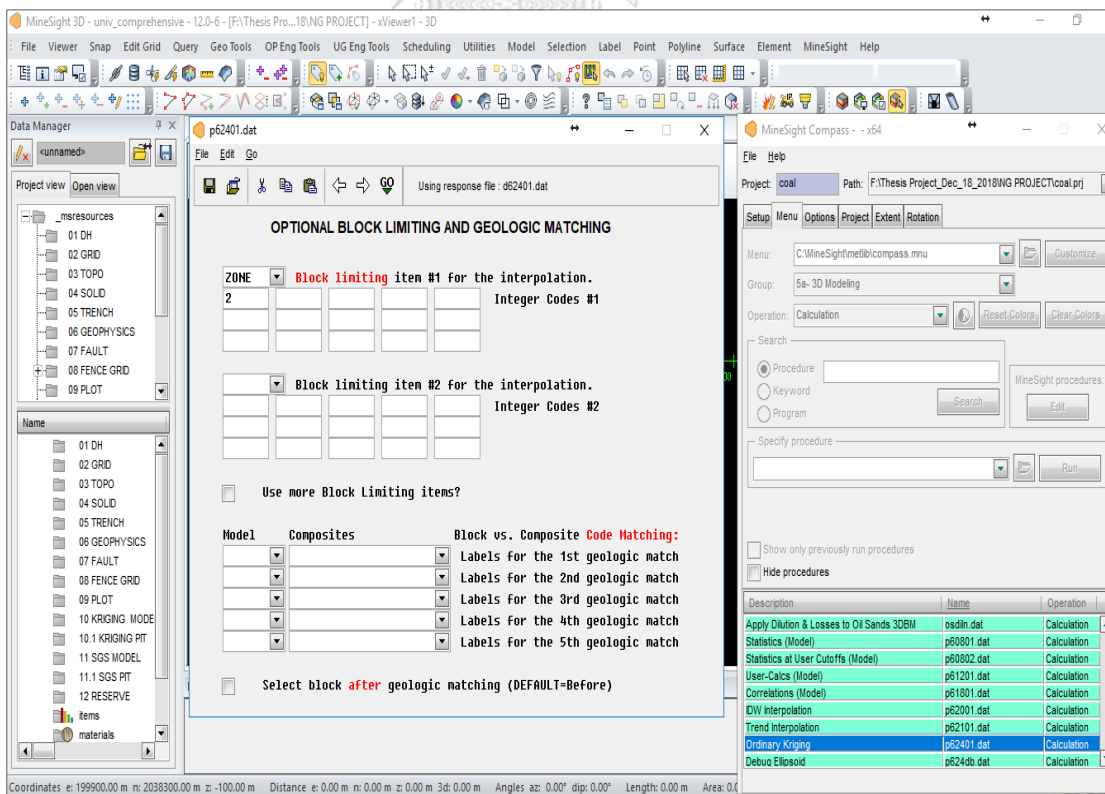


Figure 3.24 OK method of CV in MS3D software (block limiting)

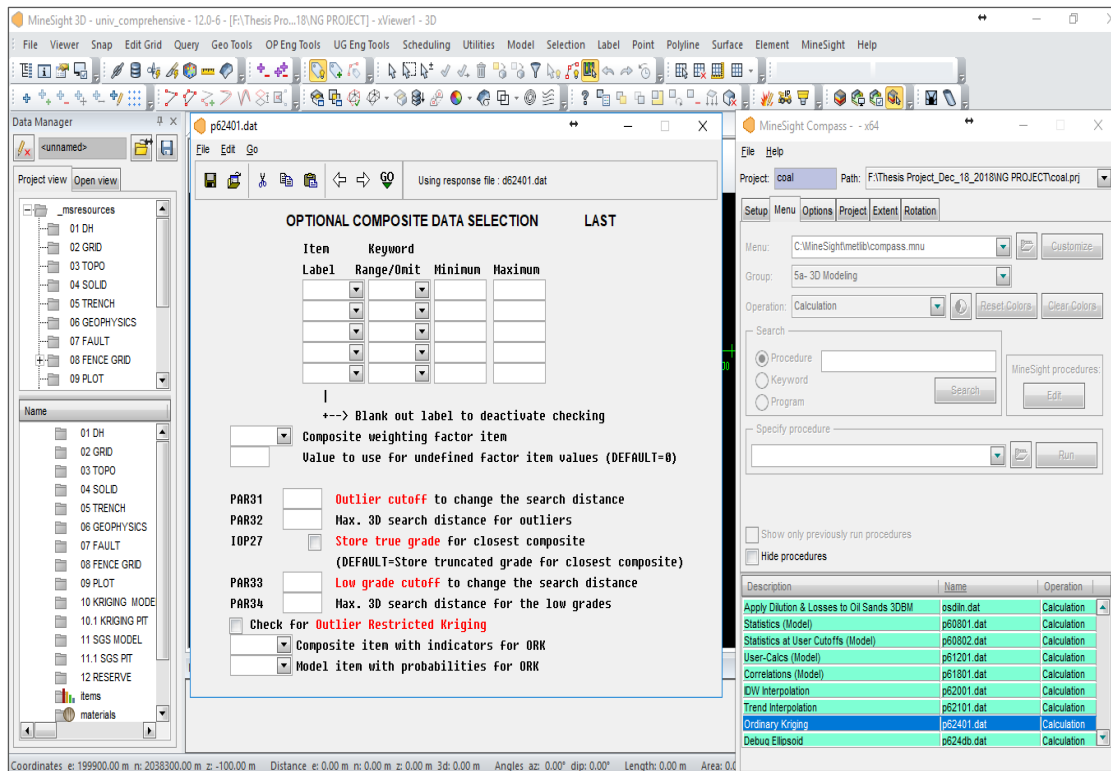


Figure 3.25 OK method of CV in MS3D software (Optional composite data selection)

3.7.3. The geological resource estimation

The geological resource of NG coal deposit was calculated using the 3D block model method, which coded from the 3D solid model of deposit. The equation used for geological resource calculation is denoted in Equations (3.2). In this research, the 3D solid model was coded within the 3D block model to compute the coal volume, which defined in percentage that intersected inside a full block volume. These coal percentages were applied to geological resource computation. The coal density of 1.15 ton/m³ adopted from LID coal mine was employed for geological resource calculation.

$$Q_c = V_c \times D_c \quad (3.2)$$

Where: Q_c = Tonnage of coal (T)
 V_c = Volume of coal (m³)
 D_c = Density of coal (T/m³)

3.7.4. The Pit optimization and mineable reserve estimation

Pit optimization was employed by applying the geotechnical and economic parameters into the 3D block model of NG coal deposit. The net profit in the block model is a main parameter used for running pit optimization to produce the optimal pits for pit design and mineable reserve calculation. Those parameters were calculated using user-calc (Model) tool in MS3D software and stored in 3DBM. Lerch-Grossman algorithm, the most popular algorithm for pit optimization in mining industries, was applied for pit optimization in this case. The geotechnical and economic parameters used for pit optimization are represented in Table 3.3. The coal prices selling at the LID mine mouth is shown in Table 3.4. The computed equations of calculating costs and revenues for pit optimization are illustrated in Equation (3.3) – [3.10]. The pit optimization will generate the optimal pits for mineable reserve computation.

Table 3.3 Geotechnical and economic parameters for pit optimization.

Parameter	Cost (US\$)
Mining cost per ton coal and waste	1.63
Processing cost per ton coal	15
Mining recovery	80 %
Overall pit slope angle	45°
Density of coal	1.15 T/m ³
Density of waste	1.8 T/m ³

Table 3.4 Coal prices at the LID mine mouth based on CV basis.

CV bin (kcal/kg)	Price (US\$)
500 - 4000	46.6
4001 - 5000	53.6
5001 - 5500	58.4
5500 – up	65.8

$$Q_w = V_w \times D_w \quad (3.3)$$

$$M_c = Q_c \times m_c \quad (3.4)$$

$$M_w = Q_w \times m_w \quad (3.5)$$

$$P = Q_c \times y \quad (3.6)$$

$$C_c = M_c + P \quad (3.7)$$

$$R = Q_c \times q \times r \quad (3.8)$$

$$B_c = R - C_c \quad (3.9)$$

$$B_w = -M_w \quad (3.10)$$

Where:

- Q_c = Tonnes of coal (T)
 R = Revenue of coal sales,
 Q_w = Tonnes of waste (T),
 V_w = Volume of waste (m³)
 D_w = Density of waste (T/m³),
 M_c = Total mining cost of coal in a block (US\$)
 m_c = Mining cost of coal (US\$/T),
 M_w = Total mining cost of waste in a block (US\$)
 m_w = Mining cost waste (US\$/T),
 P = Total processing cost of coal in a block (US\$)
 y = Processing cost of coal (US\$/T)
 C_c = Total cost of coal mining and processing (\$)
 q = Coal price (US\$)
 r = Mining recovery (%)
 B_c = Block value of coal exists (US\$)
 B_w = Block value of waste (US\$)

3.7.5. The pits adjustment and mineable reserve estimation

The pits adjustment was implemented in order to achieve the practical pit operation. The pits adjustment for NG coal deposit was carried out using a pit

expansion tool in MS3D software. This is a required process allowing to access and excavate the ore material to the full extent of the coal seams. The pits adjustment parameters derived from the current LID coal mine are presented in Table 3.5. The mineable reserves and waste materials from individual adjusted pit were computed and classified depending on CV basis and bench level.

Table 3.5 The pits adjustment parameters

Parameters	Value
Overall pit slope angle (°)	45
Bench slope angle (°)	60
Bench height (meter)	5
Berm width (meter)	5
Ramp width (meter)	8
Ramp gradient	1:10
Pit floor width (meter)	23

3.8. Sequential Gaussian Simulation (SGS)

SGS is a non-linear geostatistical method which is widely used in mineral resource simulation in mining industries and others. It produces realizations (maps) of grades distribution in a block model within the deposit. SGS is a method that requires a normal score data transformation, which used the drill holes composite data as original input data. The Gaussian normal scores data was used to calculate experimental variogram and fit by an appropriate model which will be used as inputs for SGS process.

3.8.1. Variogram calculation and modeling

For variogram experimental calculation of CV and AC in SGS, the drill holes composited data of them were transformed to Gaussian normal scores data in MS3D software. Then Gaussian normal scores data was validated using statistical analysis (histogram) of both variables to check for a standard normal score distribution such a unit variance and mean value equal to zero were produced. In this study, variogram

model constructions were implemented by different azimuth directions ranging from 0° to 225° with 45° increasement, and dip angle ranging from 0° to 90° with 30° increasement. The experimental vertical variogram calculation of transformed data, CV and AC, were fitted by spherical model which was considered as the best and appropriate model that provides the least error of nugget effect. Both vertical experimental variogram calculation of CV and AC are presented in Figure 3.26 – 3.29.

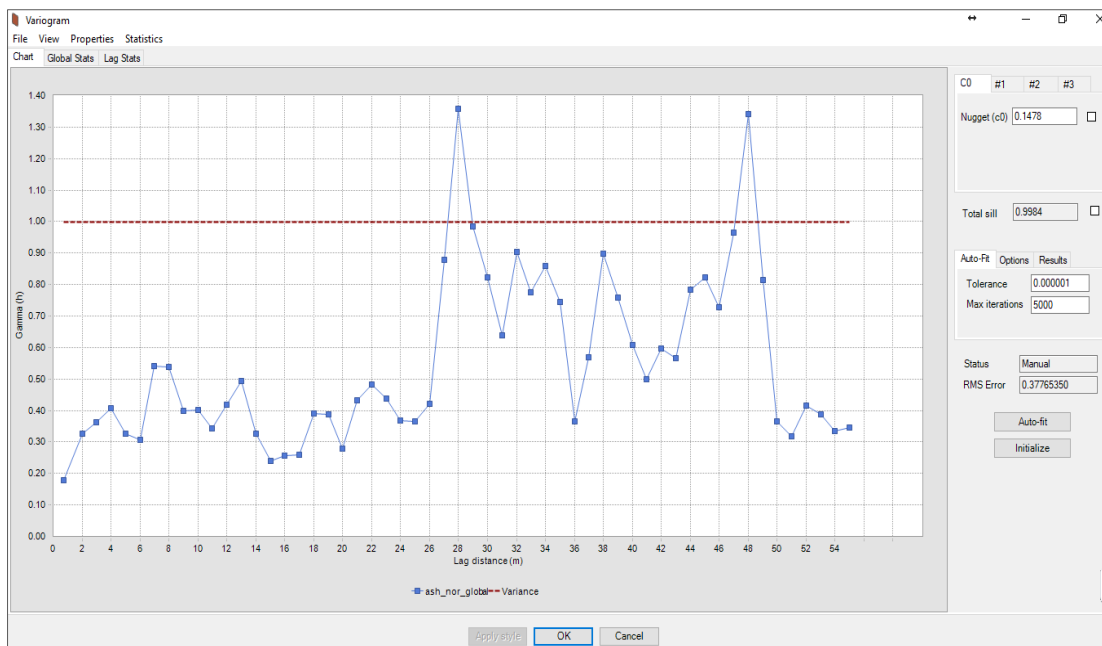


Figure 3.26 The vertical experimental variogram of CV for SGS.

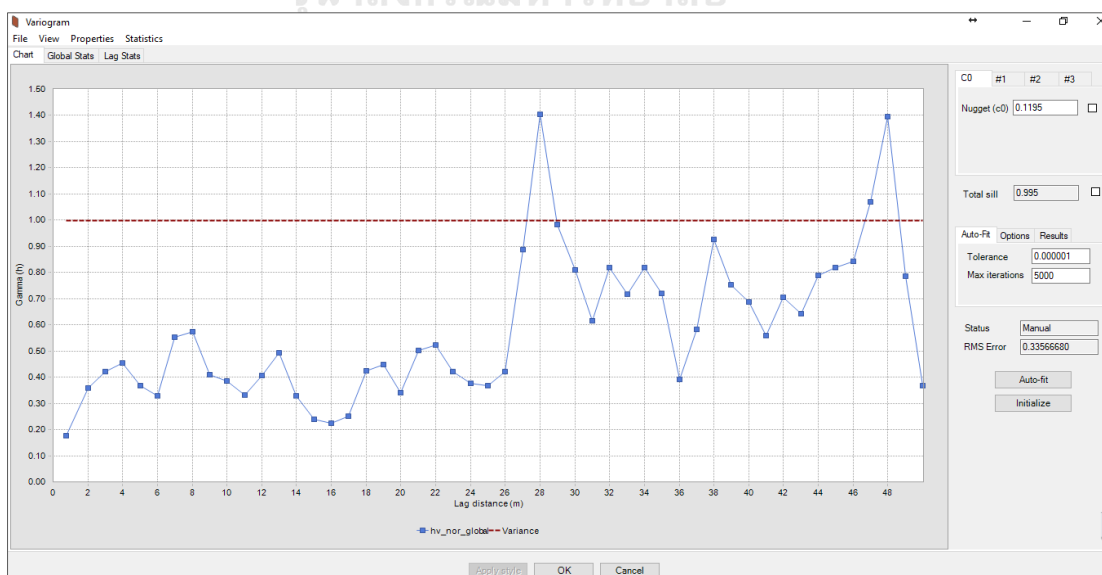


Figure 3.27 The vertical experimental variogram of AC for SGS.

3.8.2. SGS block grades simulation

Sequential Gaussian Simulation was used to estimate the probability distribution function (pdf) for all blocks within NG coal deposit using the (3.11):

$$f [Z^*(x_\alpha)] = \sum_{i=1}^n \lambda_\alpha f [Z(x_\sigma)] \quad (3.11)$$

Where:

$f [Z^*(x_\alpha)]$ = estimated distribution function (pdf) at location x_σ

λ_α = sample weight for function at location x_σ

This simulation process involves with two steps: (1) Estimation of statistical inference (μ, σ^2) of the assumed pdf, and (2) Draws a realization from the estimated pdf. The block grades simulation using SGS was carried out by the following steps as the flowchart Figure 3.28 . The Sequential Gaussian Simulation input parameters are determined in Table 3.6. There are 5 realizations (Maps) generated for each CV and AC in this case. The post-simulation processing (E-type map) was accomplished to calculate the mean and unit variance (μ, σ^2) of each block. The mean value of CV here was used for economic evaluation of pit optimization in order to compute the mineable reserves for NG coal deposit. The procedures of SGS in MS3D software were employed by the flowing Figure 3.29 - 3.41.

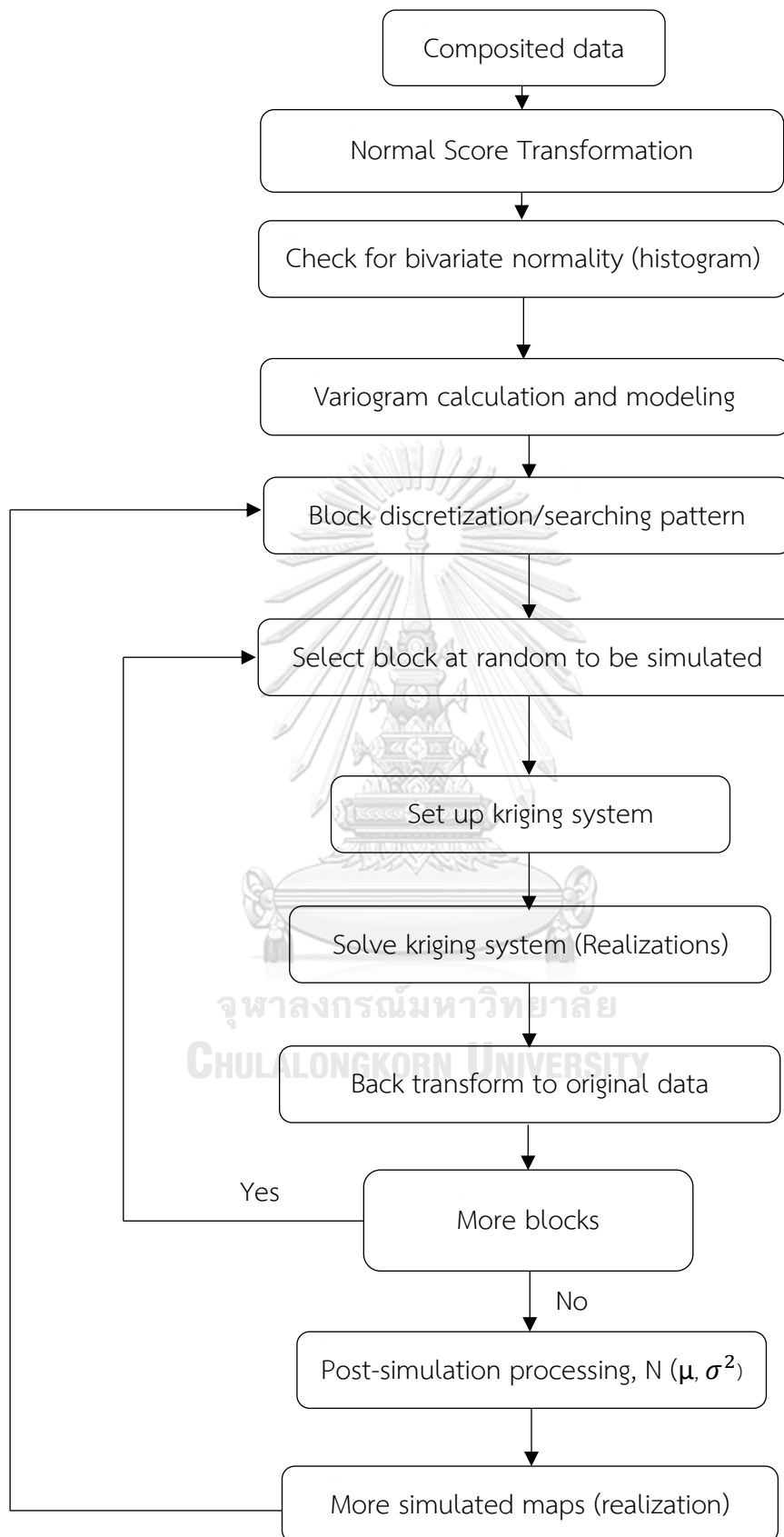


Figure 3.28 Flowchart of Sequential Gaussian Simulation system.

Table 3.6 SGS's input parameters for block grades simulation

Input file	Composited data of CV and AC				
Grid discretization	20 meter × 20 meter × 5 meter				
Variogram model (Spherical model)	Variable	Nugget (C_0)	Partial Sill (C_1)	Range (a)	No. of Realizations
	CV	0.1195	0.8755	10.679	5
	AC	0.1478	0.8506	11.313	5
Searching dimension	x = 250-meter, y = 250-meter, z= 125 meter				
Conditional data	Min = 1, Max = 7				

The SGS method in MS3D software is demonstrated by the following steps: MineSight > MScompass > Group: 3a – Advanced Geostatistics, Operation: Calculation > Conditional Simulation-SGS.

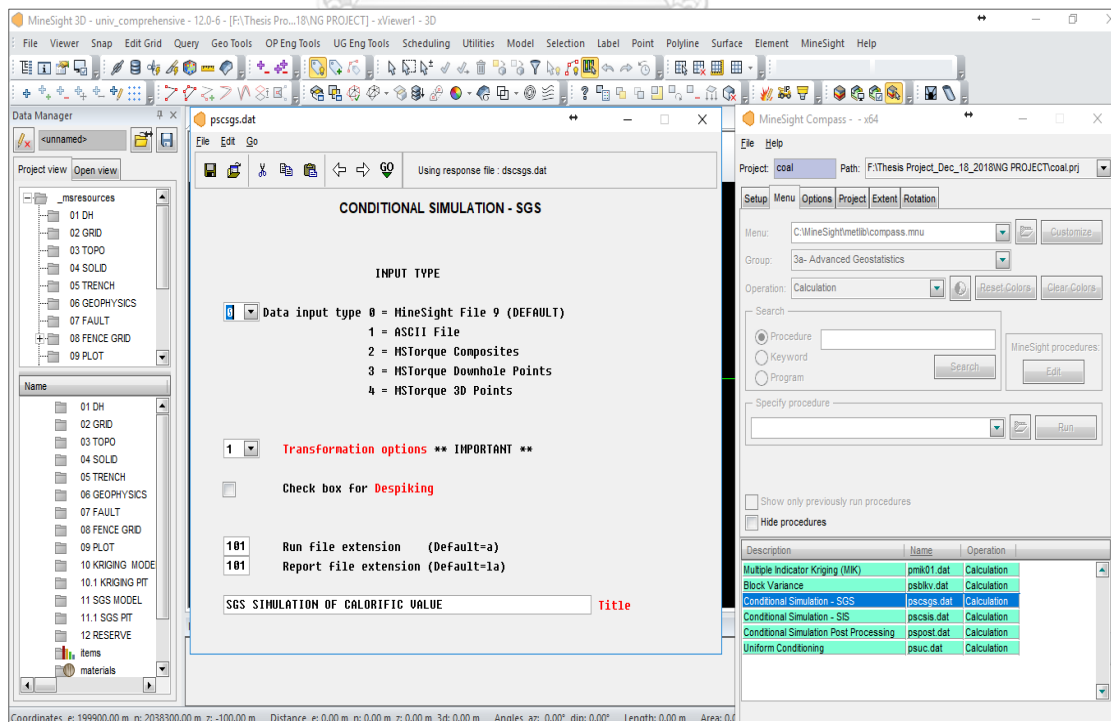


Figure 3.29 SGS method of CV simulation in MS3D software (Data input type)

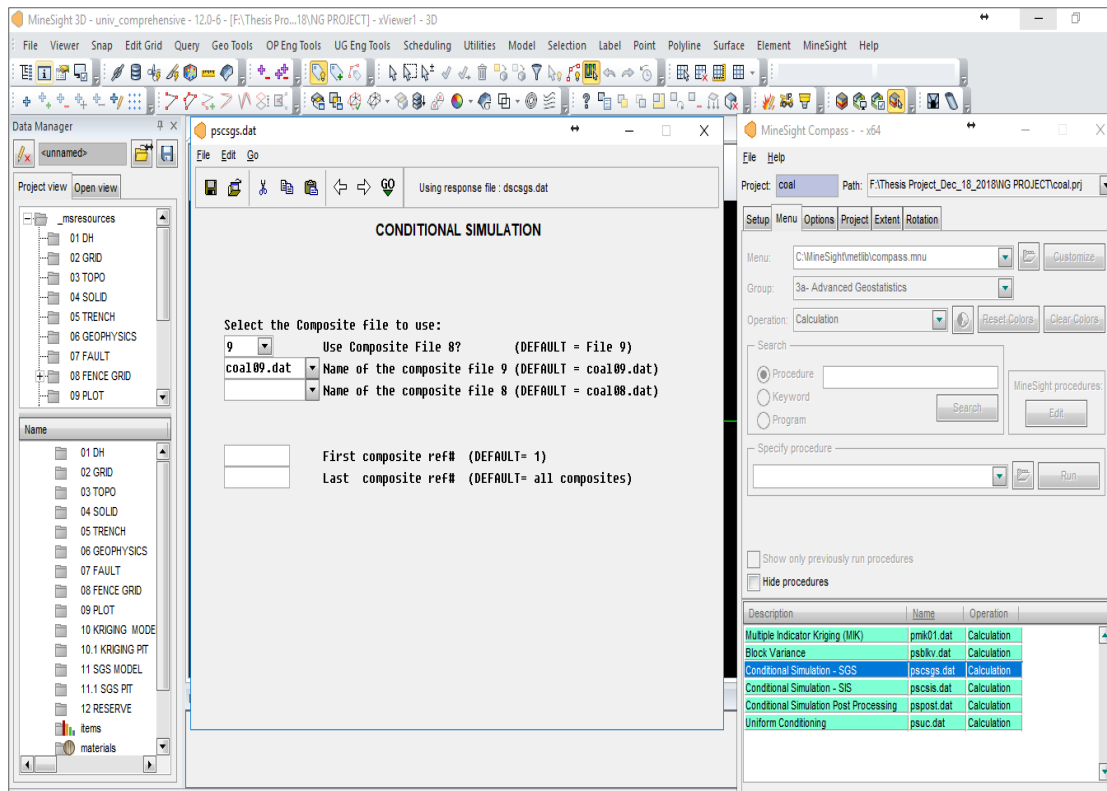


Figure 3.30 SGS method of CV simulation in MS3D software (Composited file input)

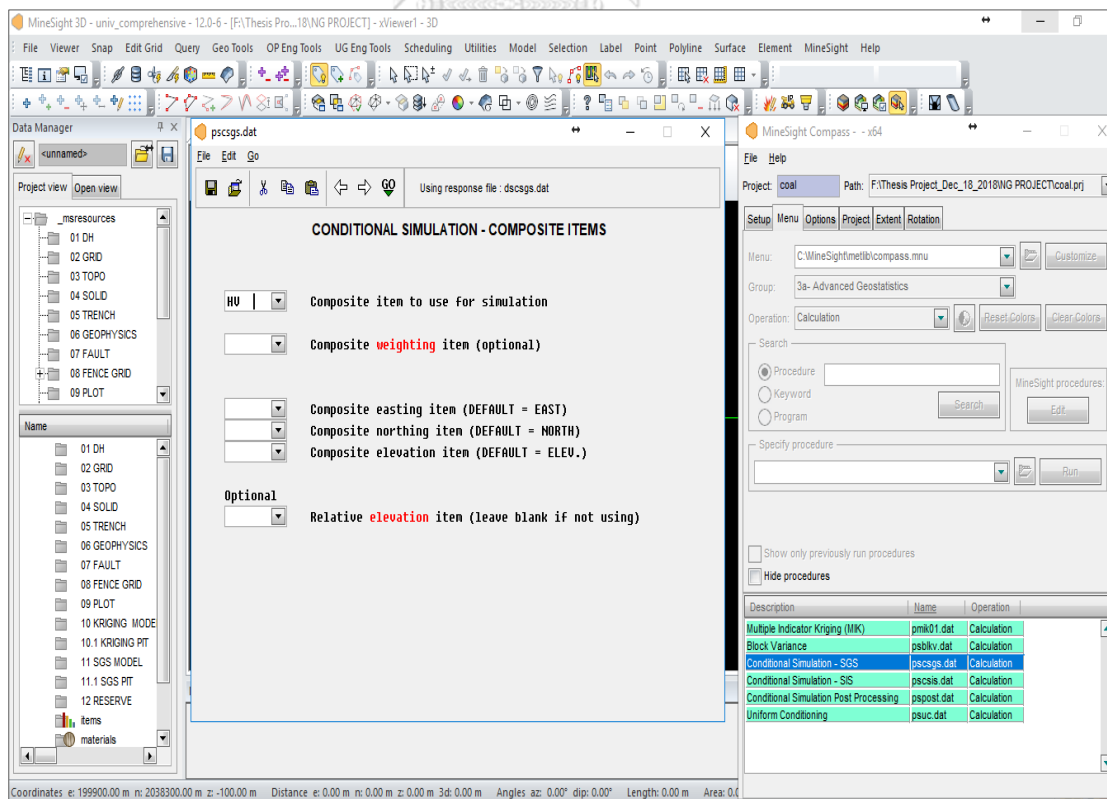


Figure 3.31 SGS method of CV simulation in MS3D software (composited items)

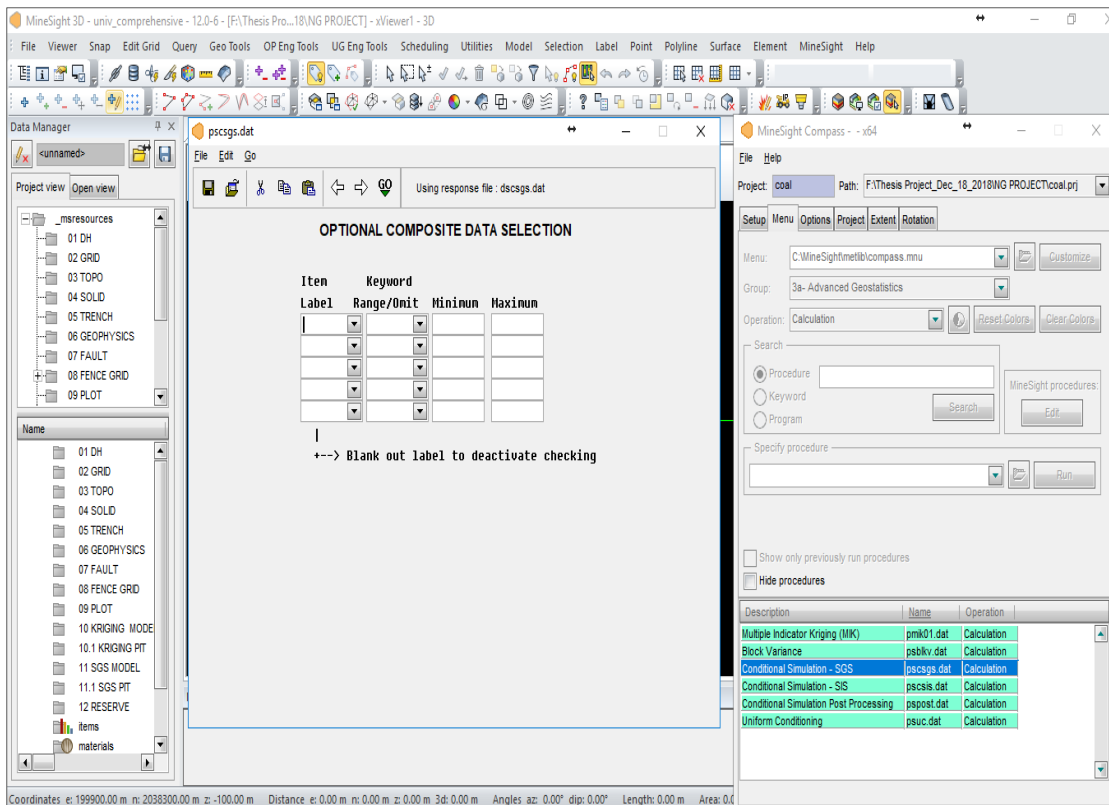


Figure 3.32 SGS method of CV simulation in MS3D software (Data control)

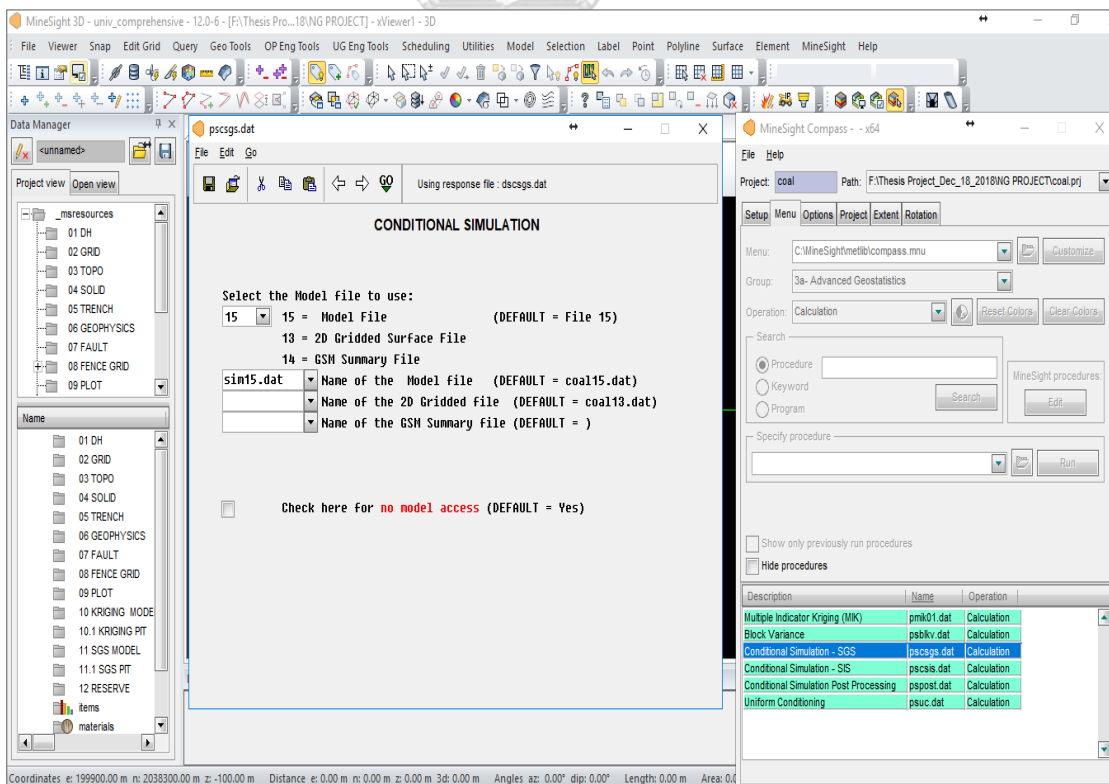


Figure 3.33 SGS method of CV simulation in MS3D software (Block model input)

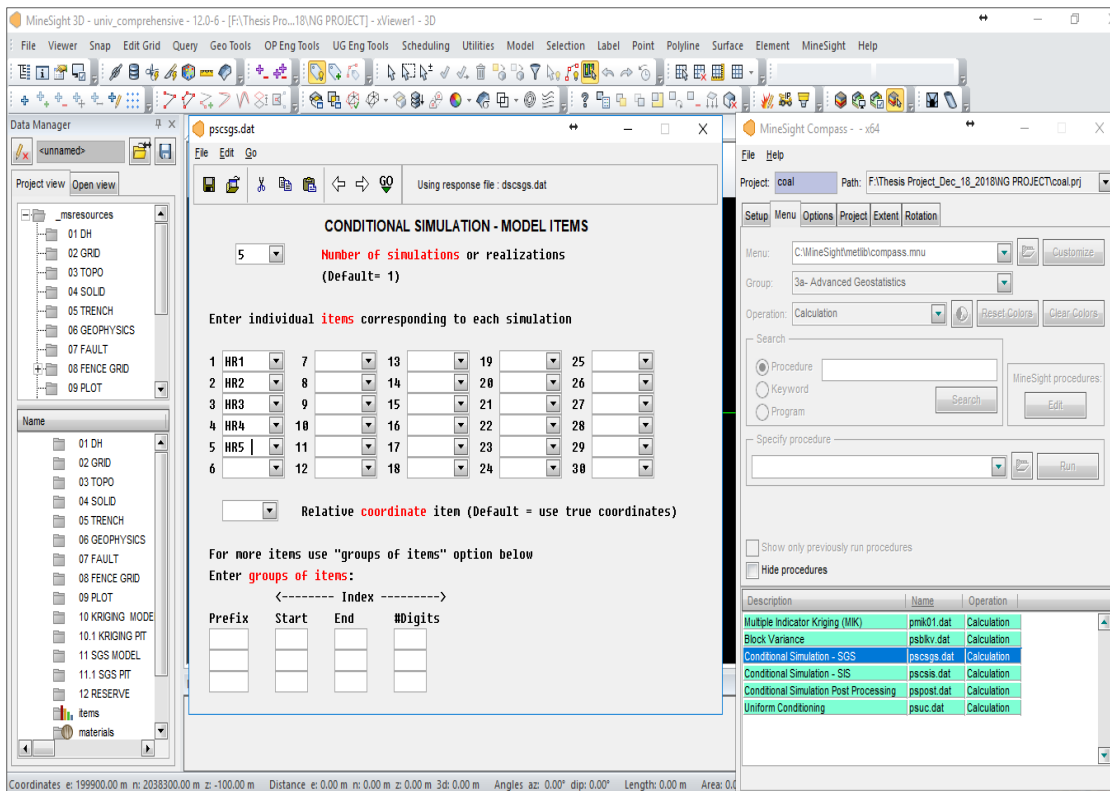


Figure 3.34 SGS method of CV simulation in MS3D software (Block model items)

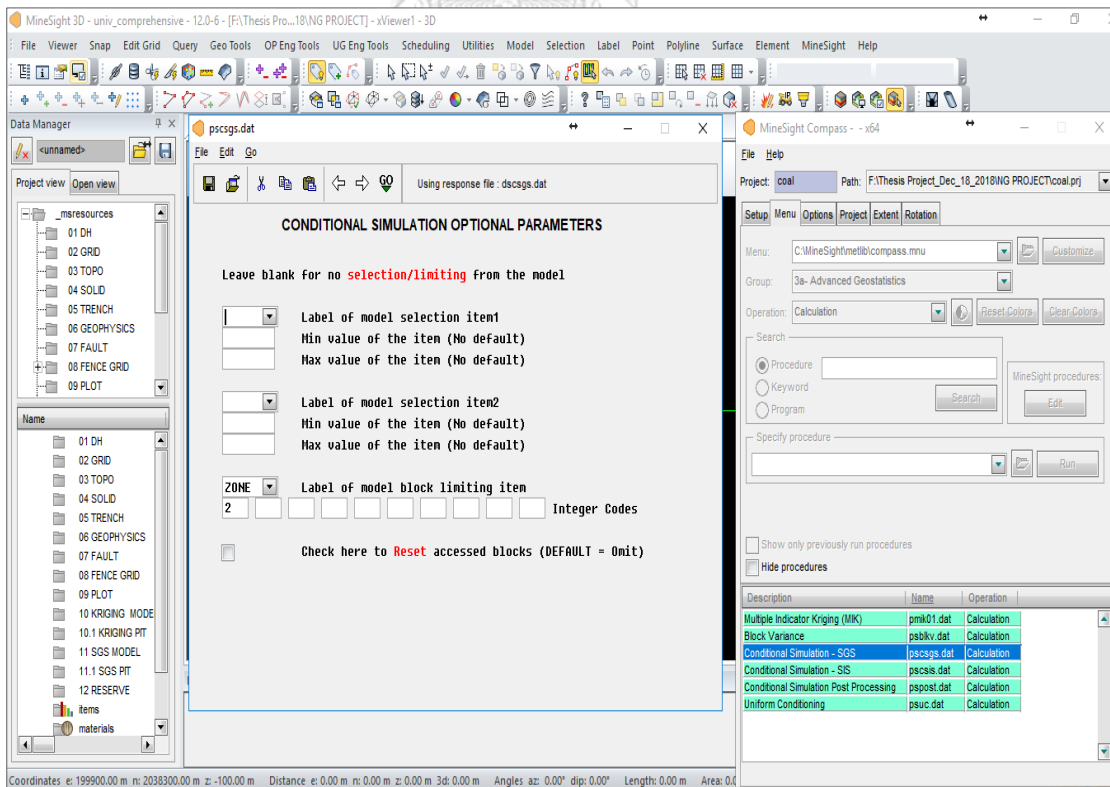


Figure 3.35 SGS method of CV simulation in MS3D software (Block model limiting)

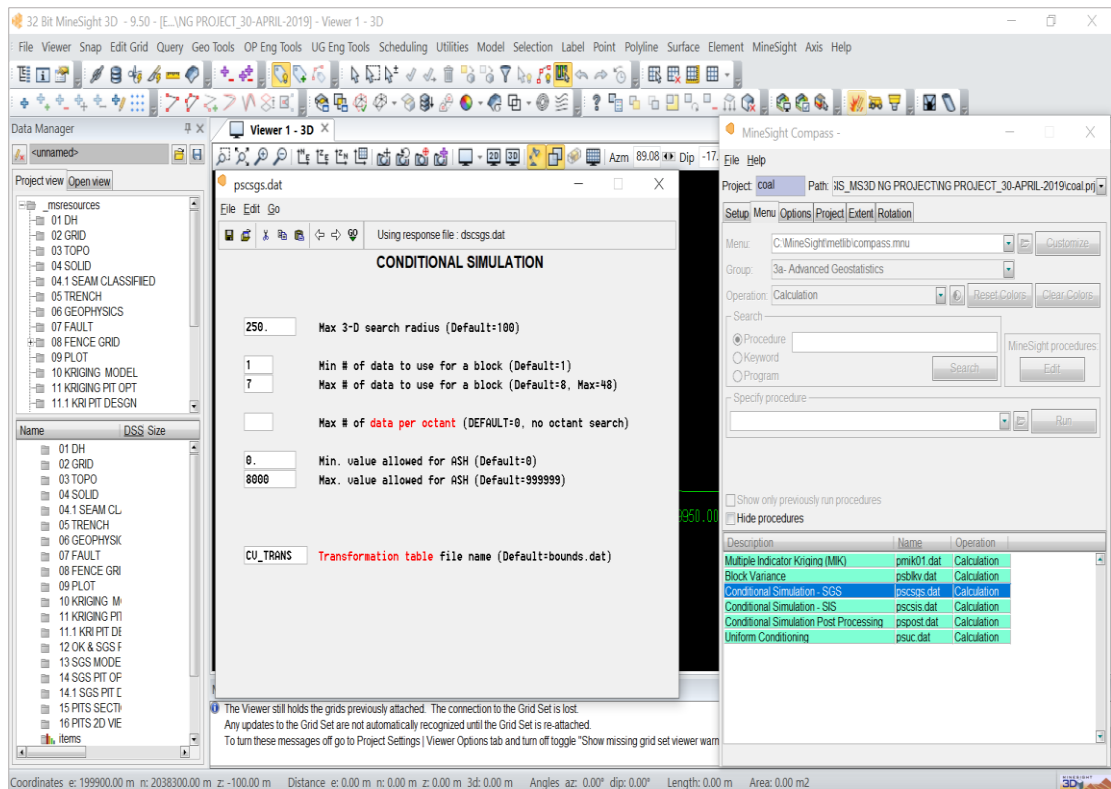


Figure 3.36 SGS method of CV simulation in MS3D software (Searching pattern)

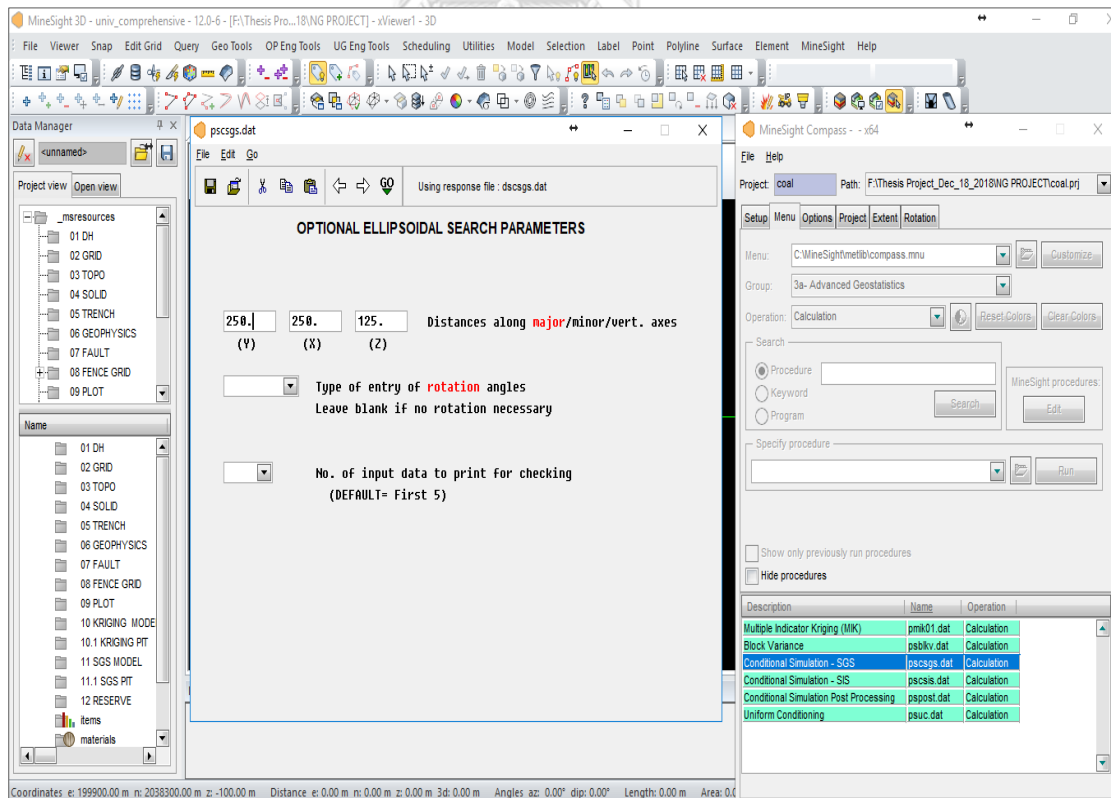


Figure 3.37 SGS method of CV simulation in MS3D software (Ellipsoidal searching)

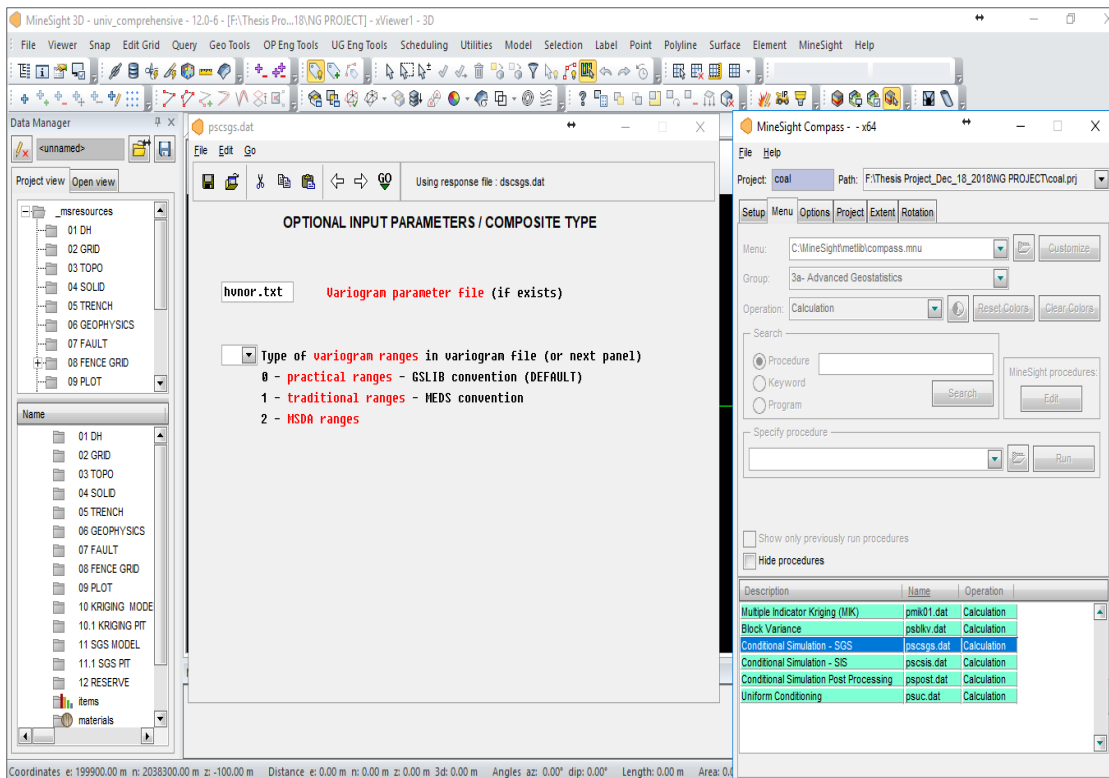


Figure 3.38 SGS method of CV in MS3D software (Variogram model parameters)

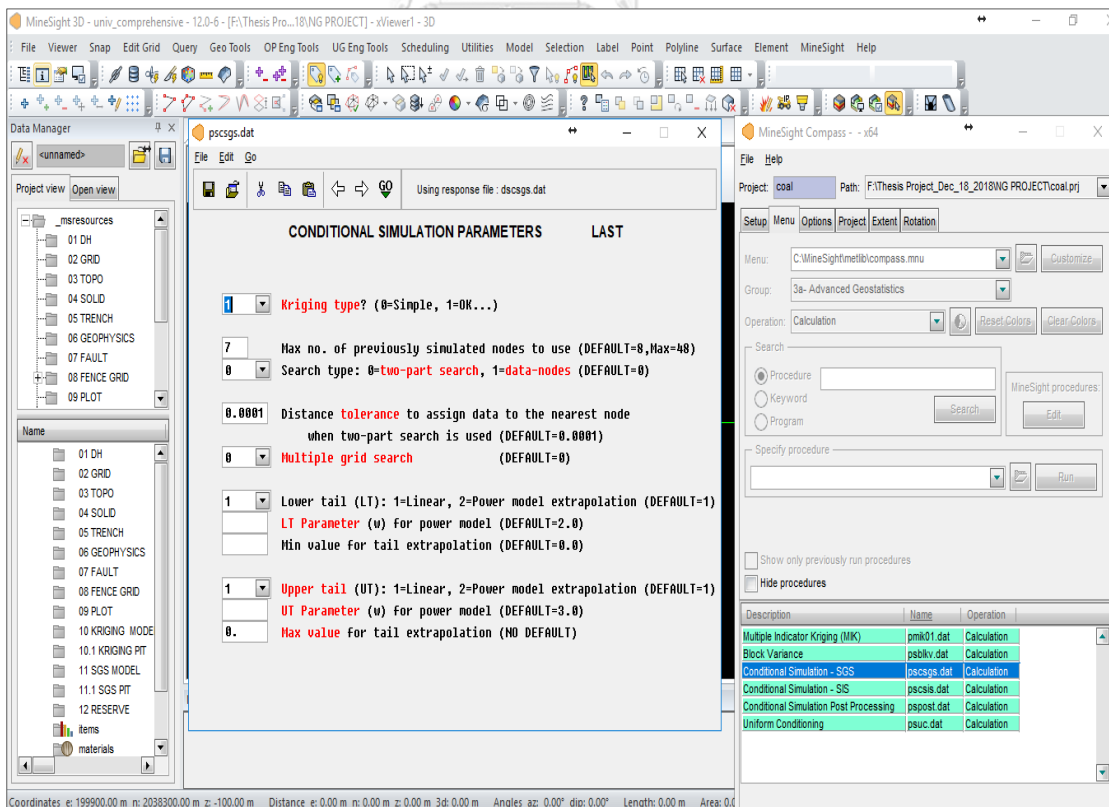


Figure 3.39 SGS method of CV in MS3D software (Conditioning Parameters)

3.8.3. SGS's geological resource estimation

The geological resource calculation based on SGS approach was computed using simulated block model. SGS's geological resource was calculated using the Equation (3.1). The geological resource was classified based on the CV basis for NG coal deposit. It also was summarized based on the bench level basis. The coal density of 1.15 ton/m^3 was used for the calculation.

3.8.4. SGS's Pit optimization and mineable reserves estimation

SGS's pit optimization was employed using LG algorithm to produce optimal pits for mineable reserves calculation. The SGS's pit optimization uses the calorific values calculated from multiple realizations (E-type map). The economic parameters were used for pit optimization especially net profit value of each block. The geotechnical parameter such as overall pit angle was used. These multiple optimized pits were used for mineable reserves computation. The economic and geotechnical parameters used for SGS's pit optimization can be seen in Table 3.3, and the coal prices are illustrated in Table 3.4. The computation of costs and revenues for SGS's pit optimization is illustrated in Equations (3.3)– (3.11).

After the pit optimization has been accomplished and generated multiple optimal pits for NG coal deposit. The optimum pits were used for mineable reserves computation. A mineable reserve was computed from each generated pit and then combined together as total mineable reserves for NG coal deposit.

3.8.5. Pits adjustment and mineable reserves estimation

SGS's optimum pits adjustment was implemented in order to apply the open pit design parameters to the generated optimal pits. A pit expansion tool in MS3D software was used to adjust the optimal pits generated from LG algorithm for NG coal deposit. This process allows us to access and excavate the ore materials to the full extent. The optimal pits adjustment parameters used for SGS's optimal pits are presented in Table 3.5. Furthermore, the mineable reserves and waste materials from individual adjusted pit was computed and classified based on CV and bench level basis.

CHAPTER 4

RESULTS AND DISCUSSIONS

4.1. Drill hole data statistical analysis

In the coal washing plant of LID Coal Mine, there are few main parameters must be quantified as a coal shipment and sales qualities which are CV, %M, and VM. CV is a main parameter used for price negotiation between producer and buyers. In accordance with DH statistical analysis, CV and AC parameters have a very strong negative correlation. In this study, CV and AC were chosen as studied variables. The AC displays highly varied percentage which could decrease the CV. The DH boundary and average values of variables are summarized in Table 4.1. In order to demonstrate the coal quality parameters distribution, histograms of both CV and AC are plotted. The histograms of CV, AC and other parameters are shown in Figure 4.1 – 4.2. The scatterplot between CV and AC was plotted to demonstrate the correlation of these two variables as shown in Figure 4.3

Table 4.1 Drill-hole data statistics

Variable	Min	Max	Average	DH No.
Easting (m)	200,584.32	201,662.94	-	-
Northing (m)	2,038,794	2,041,129.21	-	-
Elevation (m. MSL)	214.69	236.84	-	-
Calorific Value (kcal/kg)	373	7,486	3,745.91	-
Fixed carbon (%)	6.05	80.37	42.38	-
Ash content (%)	9.64	85.58	48.32	-
Sulphur (%)	0.01	11.34	0.80	-
Volatile matter (%)	4.30	26.44	8.32	-
Total moisture (%)	1.27	30.45	6.80	-
Inherent moisture (%)	0.04	30.55	2.21	-
Total	-	-	-	51

The DH composited statistical analysis of CV and AC demonstrate similar distribution of symmetrical shape. The statistical parameters of CV such as minimum, maximum, mean, standard deviation and coefficient of variation are 373 kcal/kg, 7,403.3 kcal/kg, 3,793.49 kcal/kg, 1,803.66, and 0.5, respectively. The AC statistical parameters such as minimum, maximum, mean, standard deviation and coefficient of variation are 11.5 %, 83.7 %, 47.83 %, 18.07, 0.4, respectively. The correlation coefficient between CV and AC is - 0.98, which indicates that these two variables have a high negative correlation.

4.2. Drill holes data compositing

In this study, the coal seam thickness varies from 0.05 meter to 5.5 meters and the average thickness of coal seams within NG exploration area is 0.5 meter. To provide the best input data for geostatistical estimation model, the 1-meter interval was used for DHs composited in this case. The DHs locations and composited data are shown in Figure 4.4 – 4.5. The CV and AC are used for DHs composited, which will later use for the interpolation. The entire assays data of CV and AC were composited into 317 sample values by length weighting method. The composited data were used for DH statistical analysis, and geostatistical estimation and simulation.

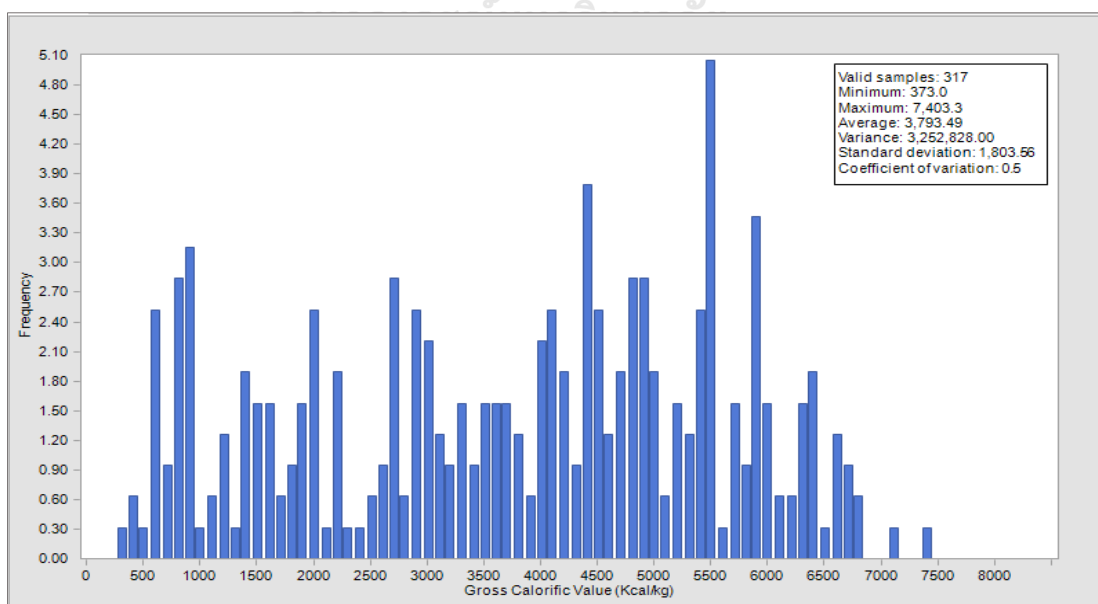


Figure 4.1 Histogram of CV of composited data.

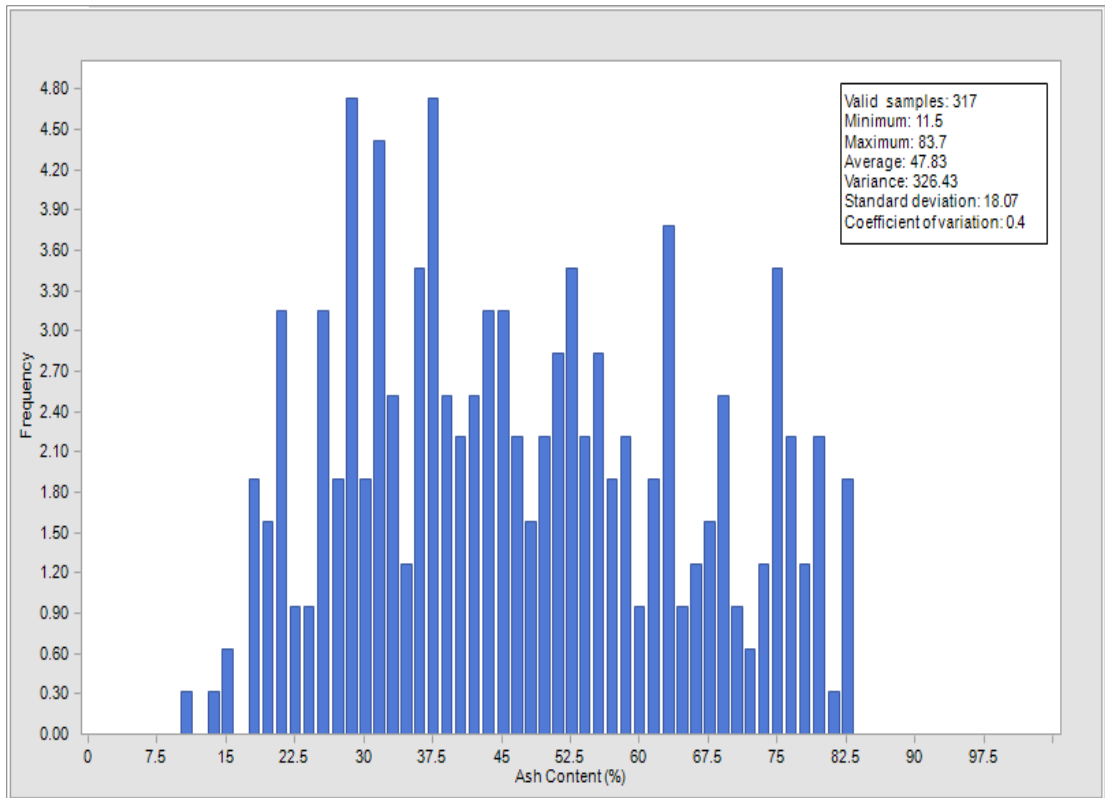


Figure 4.2 Histogram of AC of composited data.

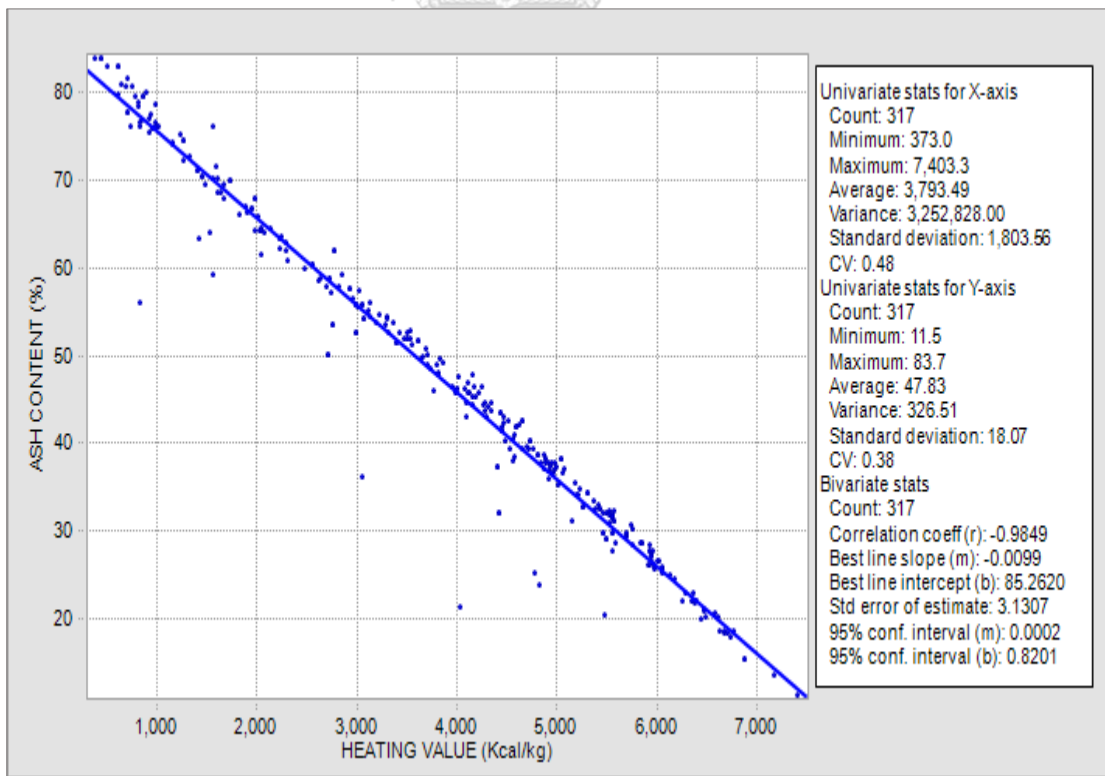


Figure 4.3 Scatterplots of CV and AC.

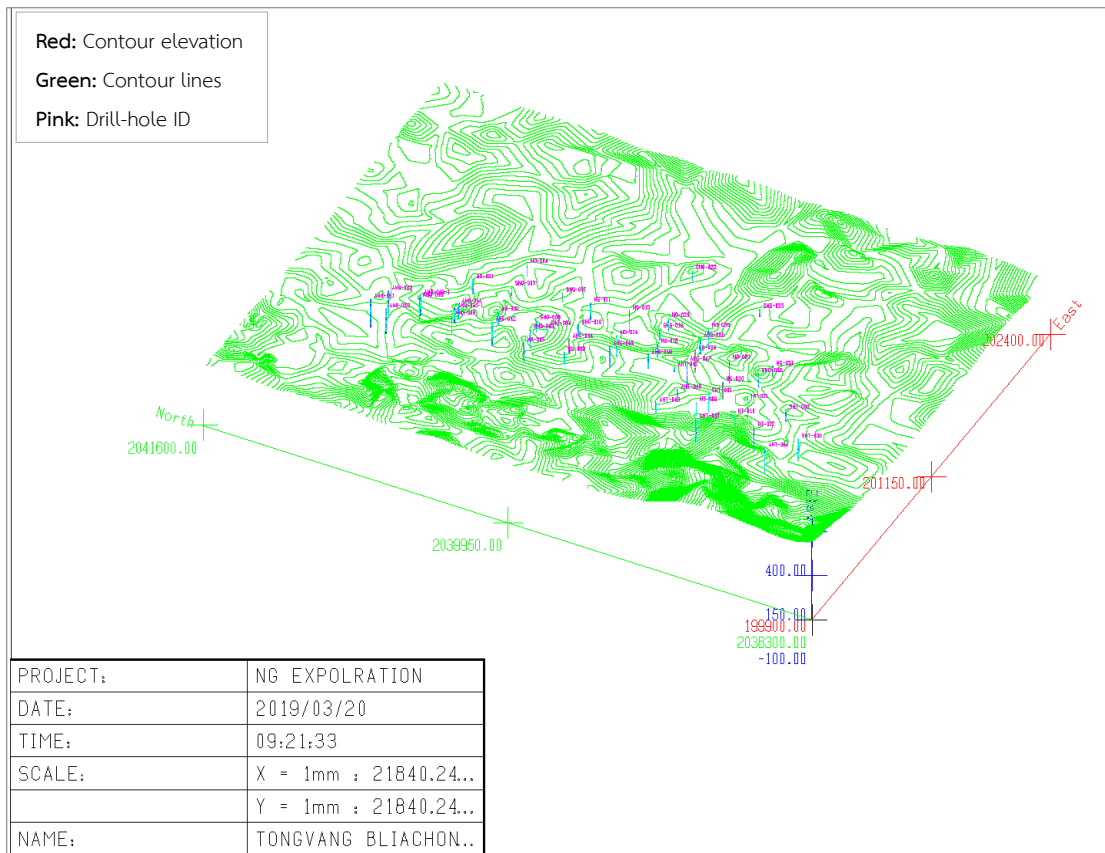


Figure 4.4 3D display of topography map and drill hole data.

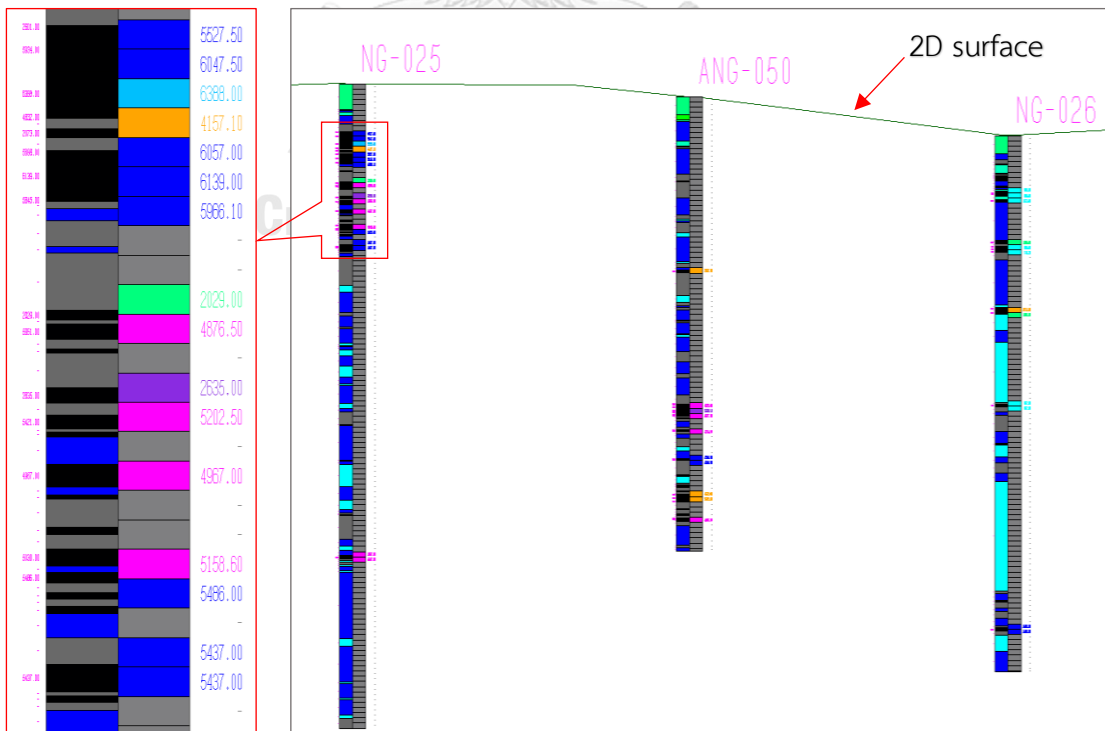


Figure 4.5 Example of NG DHs composited data (Left = assays, Right = composited).

4.3. 3D geological solid model

The 3D geological solid model of the NG coal deposit was created by a cross sectional method from the exploration drill-hole database, which has the boundary in 2038769 - 2041241 Northing and 200671 - 201438 Easting. Due to the high variations of coal seam thickness, there were multiple 3D solid models generated for major coal seams and split-seams. The 3D solid models were colored based on the major coal seams (A, B and C) including its split seams and sub-split-seams. The 3D major coal seams (A, B and C) and minor seam (O) distribution can be seen in Figure 4.6 – 4.7.

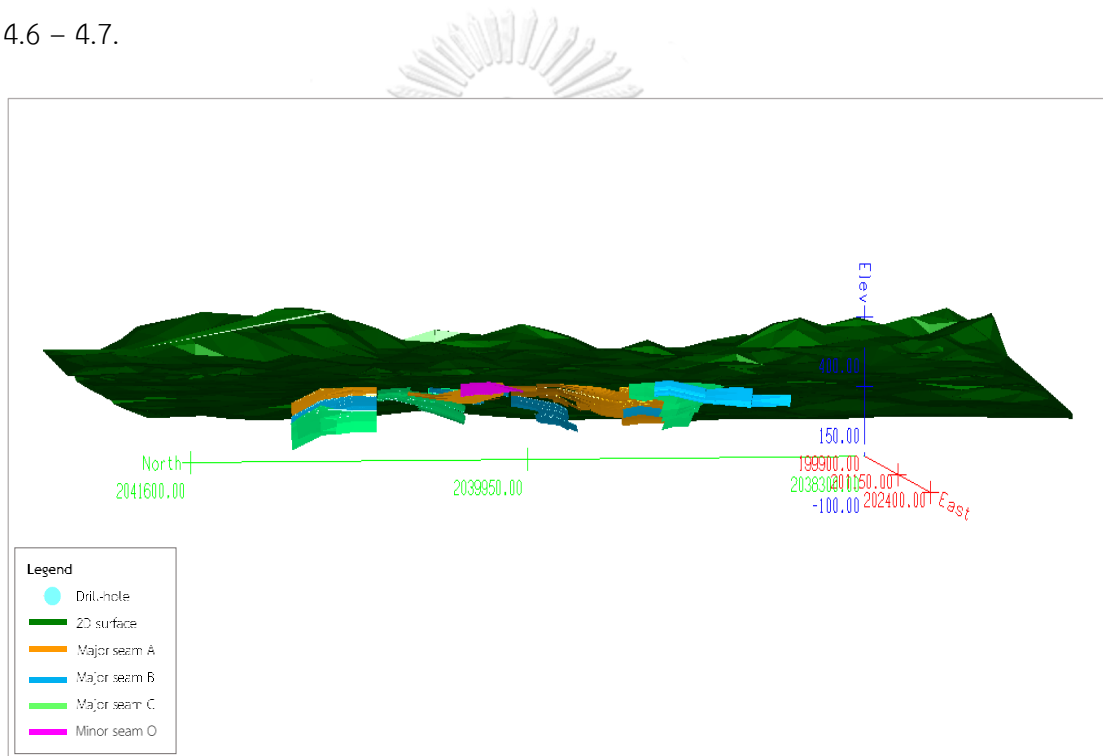


Figure 4.6 3D solid model view of major coal seams with topography and DHs data.

4.4. Ordinary Kriging (OK) Estimation

4.4.1. Variogram calculation and modelling

The vertical experimental variogram calculations for both CV and AC were carried out using DHs composited data. The best fitted variogram model was selected as spherical model of both parameters. The variogram results present a nest structure for these two variables. The variogram structures of CV and AC are presented in Table 4.2. It was concluded that the variogram models of CV and AC

are zonal anisotropic variogram. The CV's variogram model shows the range of 9.37 meter for the 1st structure and 48.5 meter for the 2nd structure. And the AC's variogram model shows the range of 9.04 meter for the 1st structure and 40.08 meter for the 2nd structure.

In general, the variogram model of both CV and AC are comparable and illustrated that they provide a similar range in vertical direction. Due to the exploration drilling program is systematically controlled in vertical direction. The dip angle is set equal to 90°. The horizontal variogram calculation shows an erratic result, therefore it will not be used in this OK's estimation. The azimuths parameters do not have any impacts for variogram calculations. The vertical experimental variogram and their best fitted models for CV and AC are shown in Figure 4.7 – 4.9.

Table 4.2 Results of variogram model fitted for CV and AC.

Variable	Structure	Nugget (C_0)	Partial Sill (C_1)	Range (a)	Variogram Model
CV	1 st	669,322.7	1,075,697.2	9.37	Spherical
	2 nd		1,497,238.5	48.5	Spherical
AC	1 st	63.13	105.98	9.04	Spherical
	2 nd		155.48	40.08	Spherical

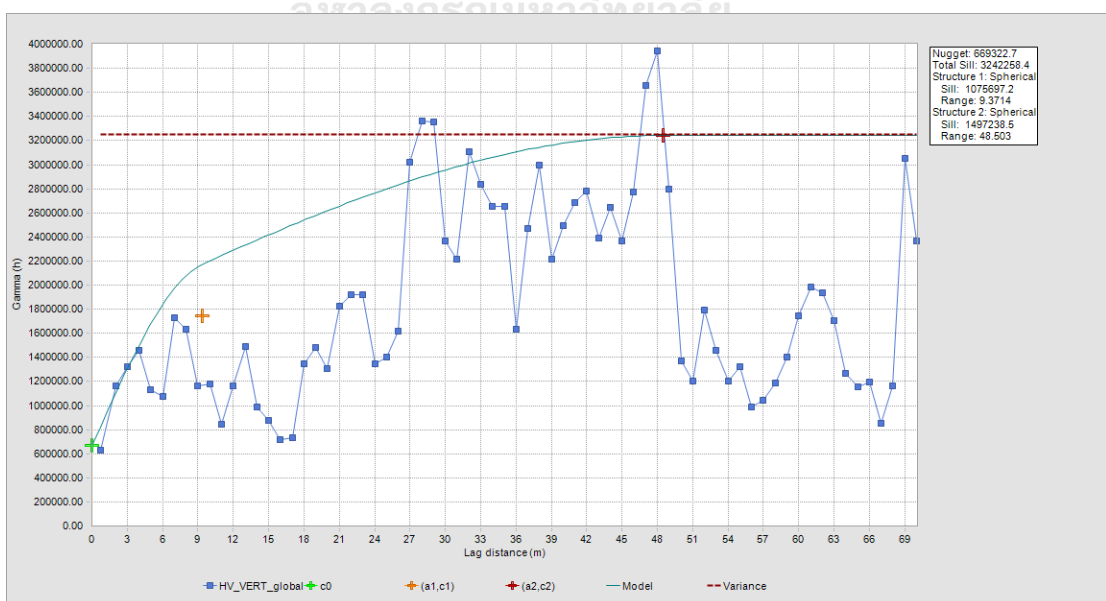


Figure 4.7 Variogram fitted model of CV.

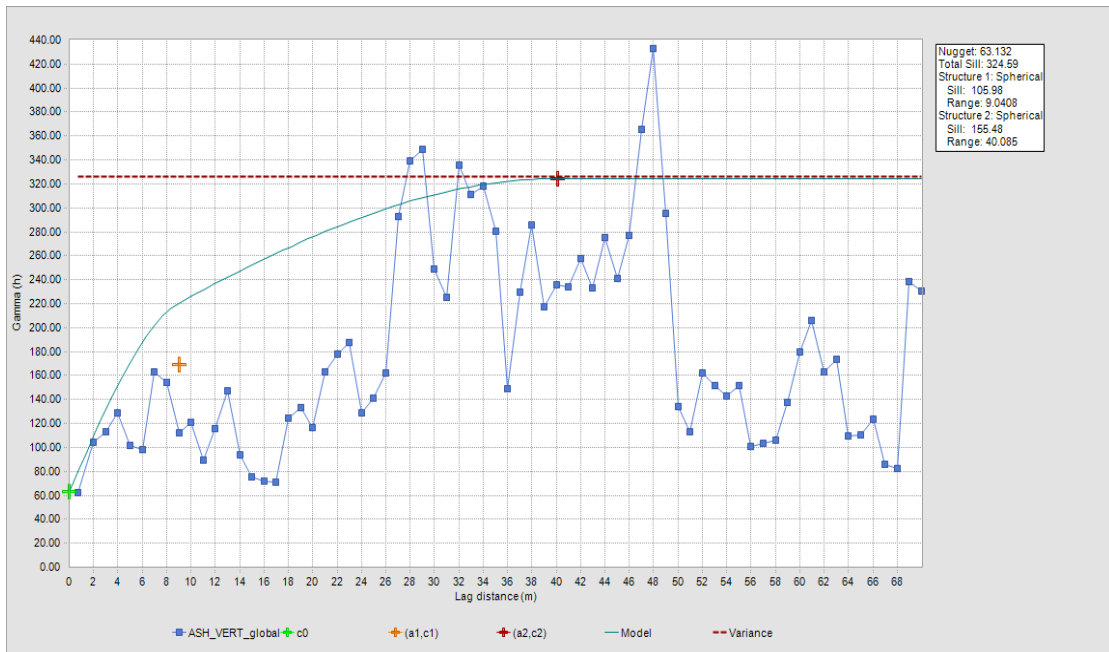


Figure 4.8 Variogram fitted model of AC.

4.4.2. Variogram model validation

The fitted variogram models of CV and AC were validated using a point validation tool in MS3D software. To keep in mind that the interpolation used the composited data as the original data, the validation process starts with the comparison between the composited data to the estimated ones. The scatterplot is used for the sake of comparison. The scatterplot of both variables can be seen in Figure 4.9 – 4.11. The statistical parameters comparison between composited data and point estimated values for CV and AC are demonstrated in Table 4.3 – 4.4. The comparison of mean values was used as a main criterion to justify the adopted variogram model.

Table 4.3 Comparison between composited and estimated CV statistical parameters.

No	Parameters	Composited data	Point estimated	% Different
1	Min	373	433	16.09
2	Max	7403	6875	7.13
3	Mean	3845	3854	0.23
4	Standard. Dev	1789	1549	13.42
5	Median	4156	4018	3.32

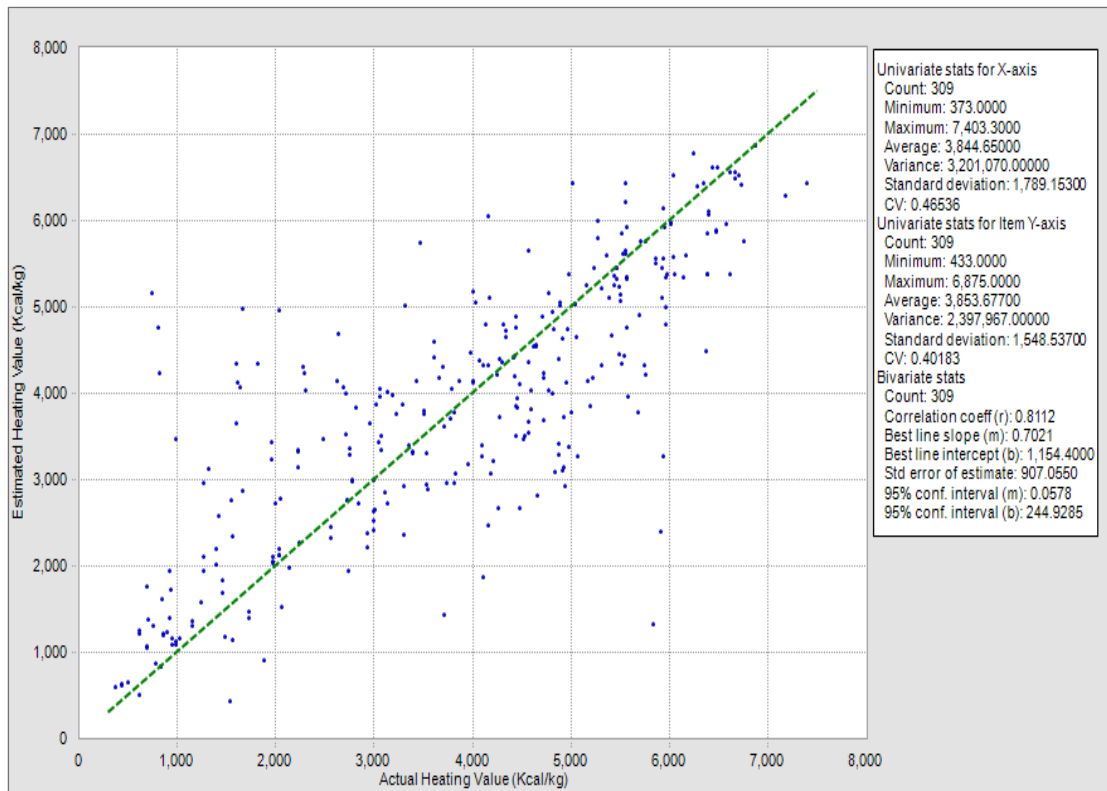


Figure 4.9 Scatterplot between composited data versus estimated values of CV.

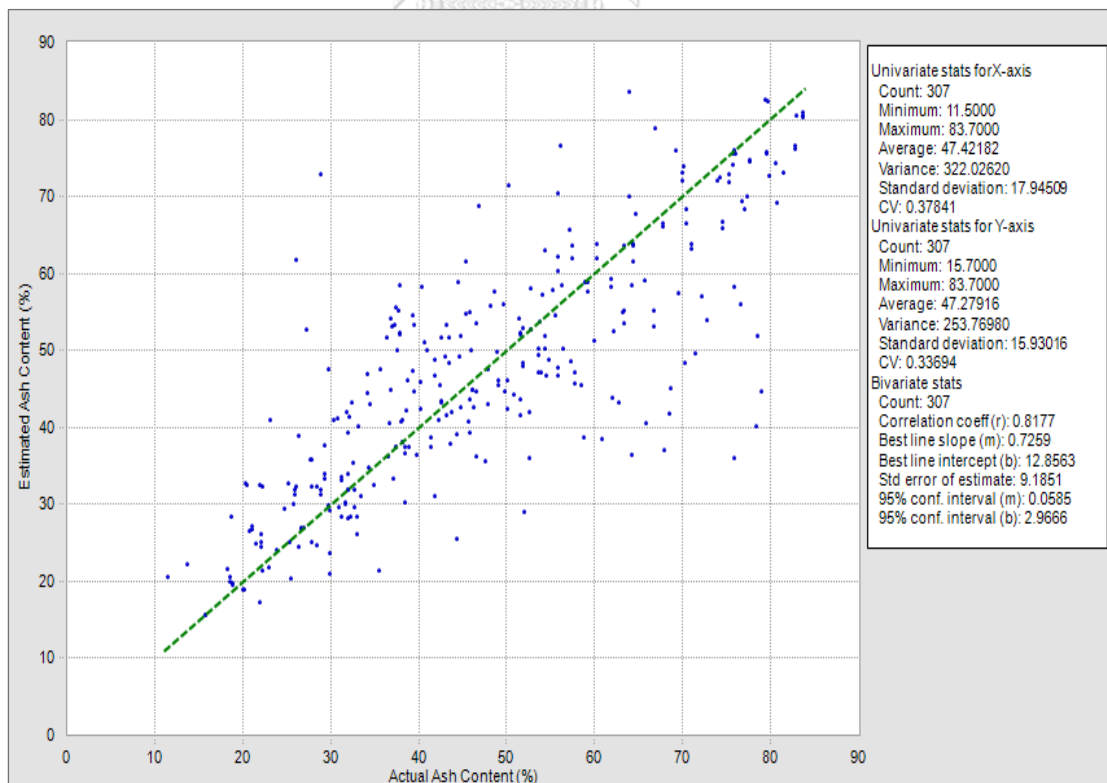


Figure 4.10 Scatterplot between composited data versus estimated values of AC.

Table 4.4 Comparison between composited and estimated AC statistical parameters.

No	Parameters	Composited data	Point estimated	% Different
1	Min	11.5	15.7	36.52
2	Max	83.7	83.7	0.00
3	Mean	47.42	47.28	0.3
4	Standard. Dev	17.95	15.93	11.23
5	Median	45.7	46.2	1.09

It can be observed that it provides a comparable result between the composited data and the point estimated values for both CV and AC parameters. The mean value of the composited and estimated CV are 3,844.6 kcal/kg and 3,853.68 kcal/kg, respectively. The mean values of the composited data and estimated AC are 47.42 % and 47.28 %, respectively. It can be seen that the average values between the composited data and estimated value for both CV and AC are very close to each other. Therefore, it can be concluded that the two variogram fitted models can be applied for the block grades estimation using Ordinary Kriging method.

4.4.3. 3D block model and resources estimation

A total of 4,796 blocks were used for coal grades, CV and AC, estimation by the Ordinary Kriging method. The variogram fitted models of both CV and AC were applied into the estimation model. The OK's output and variogram input parameters are presented in Table 4.5 – 4.6. The histograms of estimated CV and AC from 3D block models were produced to show the grades distribution within the NG coal deposit. A scatterplot between estimated CV and AC was carried out to observe their correlation.

The statistical analysis results of 3DBM showed that the histograms for both CV and AC are multimodal and symmetric shape. The minimum, maximum, mean, standard deviation, coefficient of variations of CV are 998 kcal/kg, 6,457.03 kcal/kg,

3,733.84 kcal/kg, 1,258.23 and 0.34, respectively. The minimum, maximum, mean, standard deviation, coefficient of variations of AC are 20.91 %, 76.01 %, 48.68 %, 12.48 and 0.26, individually. The histograms of CV and AC are represented in Figure 4.11 – 4.12. The scatterplot between CV and AC is shown in Figure 4.13. The geological resource of NG coal deposit was computed into 2.2 Mts with an average CV of 4,018.12 kcal/kg and an average AC of 45.891 %. The summary of OK's geological resource classified by CV basis can be seen in Table 4.7 by bench level. The 3D block model results of CV and its variance estimation are presented in Figure 4.14– 4.15, and the 3D block model results of AC and its variance is shown in Figure 4.16– 4.17, respectively.

Table 4.5 OK's input parameters and outputs of block grades estimation

Input file	Composite data file of CV and AC				
Grid discretization	20 meter × 20 meter × 5 meter				
Variogram model	Variable	Structure	Nugget (C_0)	Partial Sill (C_1)	Range (a)
	CV	1 st	669,322.7	1,075,697.2	9.37
		2 nd		1,497,238.5	48.5
	AC	1 st	63.13	105.98	9.04
2 nd			155.48	40.08	
3D Searching dimension	x = 250-meter, y = 250-meter, z = 100 meter				
Conditional data	Min = 1, Max = 7				
Output data	Block (x = 200770, y = 2039350, z = 207.5)	CV= 5650.01 kcal/kg, var= 2,051,303.88			
		AC content = 30.39 %, var = 224.44			

Table 4.6 OK's geological resource classified by CV basis.

CV basis (kcal/kg)	V_c (m ³)	D_c (T/m ³)	Q_c (T)	Average grade	
				CV (kcal/Kg)	AC (%)
500-4000	815,716	1.15	938,073.40	2,753.34	58.42
4000-5000	679,628		781,572.20	4,516.42	41.003
5000-5500	64,708		74,414.20	5,147.35	35.049
>=5500	337,803		388,473.45	5,853.42	27.537
Total	1,897,855		2,182,533.25	4,018.12	45.891

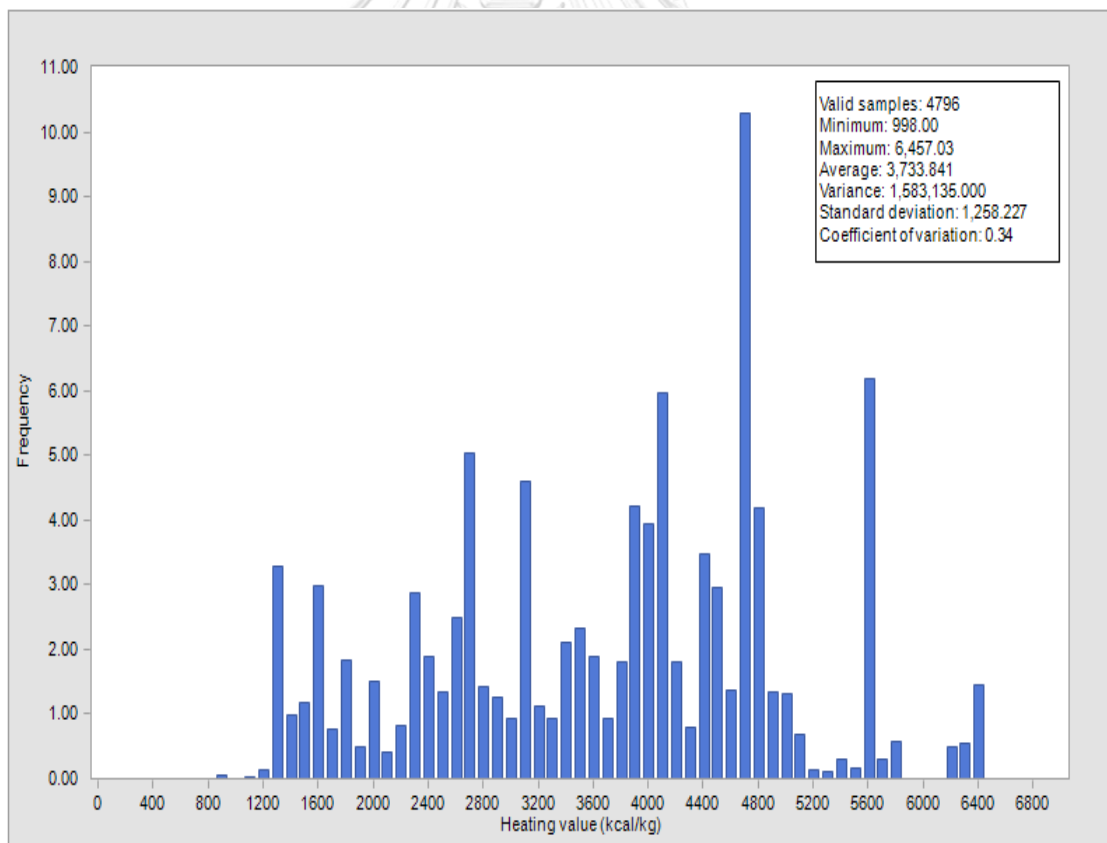


Figure 4.11 Histogram plot of CV's estimated values.

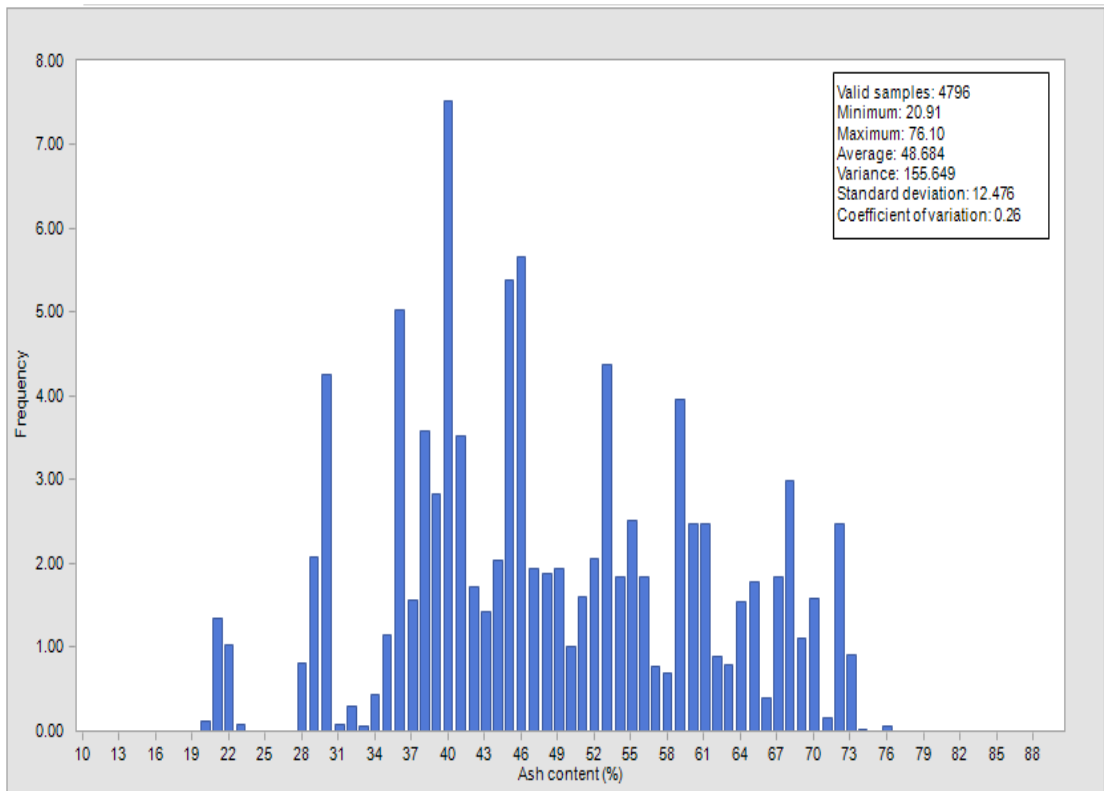


Figure 4.12 Histogram plot of AC's estimated values.

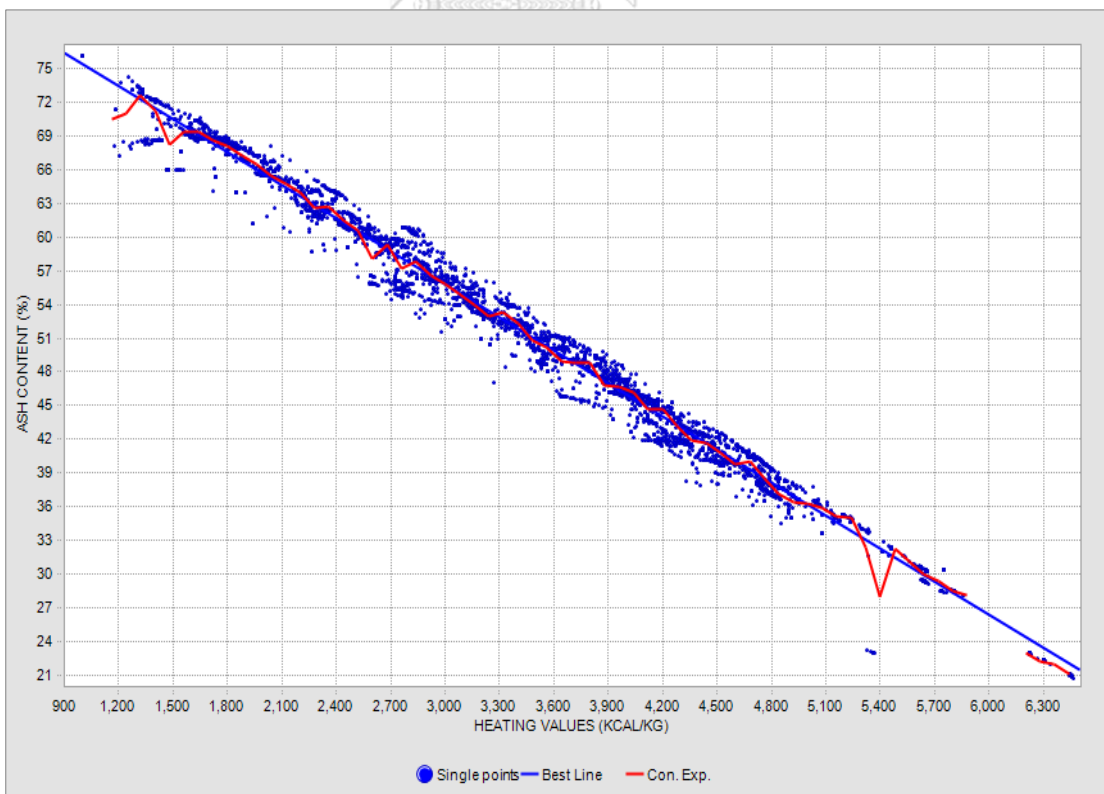


Figure 4.13 Scatterplot between estimated CV and AC.

Table 4.7 OK's geological coal resource classified by bench level.

Bench No	Bench level	V _c (m ³)	D _c (T/m ³)	Q _c (T)	Average grade	
					CV (kcal/kg)	AC (%)
1	225	550	1.15	632.50	3,529.13	48.53
2	220	16,283		18,725.45	4,043.48	42.94
3	215	49,382		56,789.30	4,295.06	42.88
4	210	82,508		94,884.20	3,887.24	47.25
5	205	120,015		138,017.25	3,607.39	50.10
6	200	136,644		157,140.60	3,645.16	49.23
7	195	140,623		161,716.45	3,636.89	49.45
8	190	130,702		150,307.30	3,687.64	49.14
9	185	114,188		131,316.20	3,864.39	47.53
10	180	113,571		130,606.65	3,843.23	47.68
11	175	113,834		130,909.10	4,008.70	46.06
12	170	98,104		112,819.60	4,190.07	44.20
13	165	87,539		100,669.85	4,278.25	43.13
14	160	78,573		90,358.95	4,370.29	42.16
15	155	68,079		78,290.85	4,324.98	42.58
16	150	63,530		73,059.50	4,287.04	42.92
17	145	54,570		62,755.50	4,306.96	42.68
18	140	41,175		47,351.25	4,258.04	43.10
19	135	32,429		37,293.35	4,006.22	45.73
20	130	29,659		34,107.85	3,943.04	46.56
21	125	32,813		37,734.95	4,449.08	41.73
22	120	31,689		36,442.35	4,232.68	44.19
23	115	31,811		36,582.65	4,360.52	43.01
24	110	31,389		36,097.35	4,414.02	42.59
25	105	29,890		34,373.50	4,281.84	43.81
26	100	27,352		31,454.80	4,195.50	44.80
27	95	26,099		30,013.85	4,244.61	44.36
28	90	24,704		28,409.60	4,251.58	44.26
29	85	21,418		24,630.70	4,307.23	43.87
30	80	18,401		21,161.15	4,354.86	43.44
31	75	14,635		16,830.25	4,406.21	43.05

Table 4.7 OK's geological coal resource classified by bench level (Continue).

32	70	11,729	1.15	13,488.35	4,413.11	43.05
33	65	8,207		9,438.05	4,486.76	42.35
34	60	3,874		4,455.10	4,560.55	41.72
35	55	3,148		3,620.20	4,606.17	41.25
36	50	1,972		2,267.80	4,639.68	40.95
37	45	2,031		2,335.65	4,651.00	40.85
38	40	1,467		1,687.05	4,700.72	40.41
39	35	1,206		1,386.90	4,700.72	40.41
40	30	951		1,093.65	4,700.72	40.41
41	25	589		677.35	4,175.25	45.6
42	20	341		392.15	3,950.24	47.32
43	15	182		209.3	3,950.24	47.32
Total		1,897,856			2,182,534.40	4,018.12

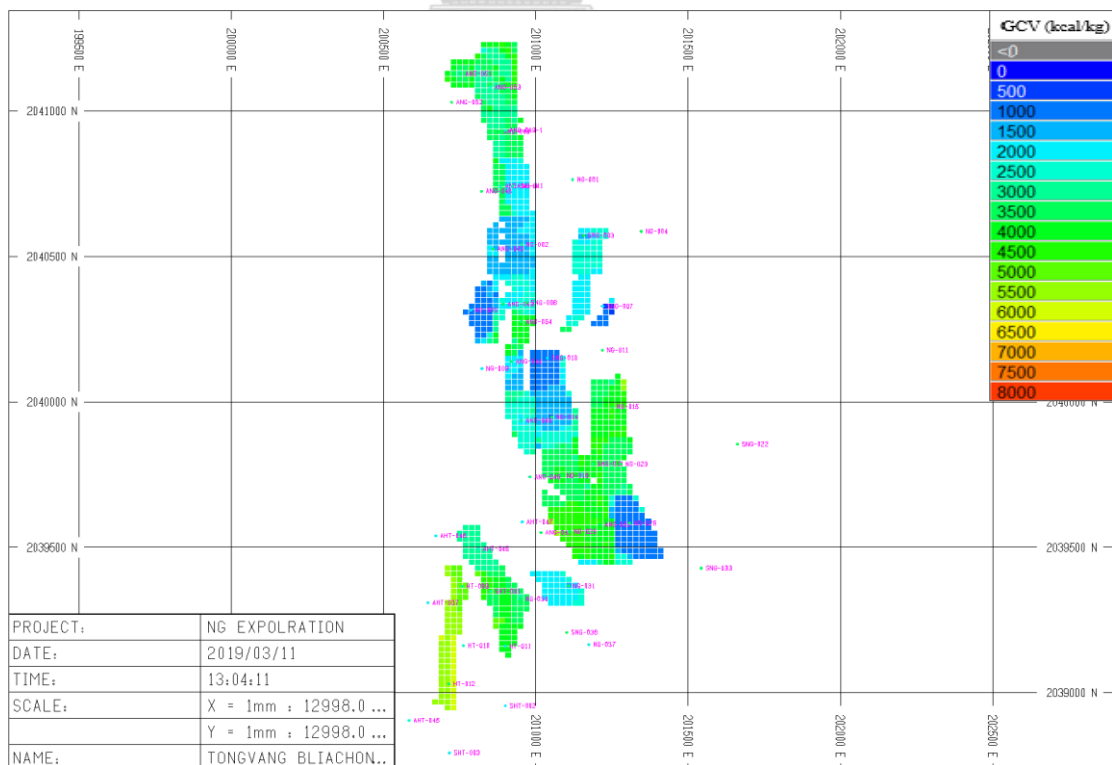


Figure 4.14 Top view of 3D estimated blocks model of CV.

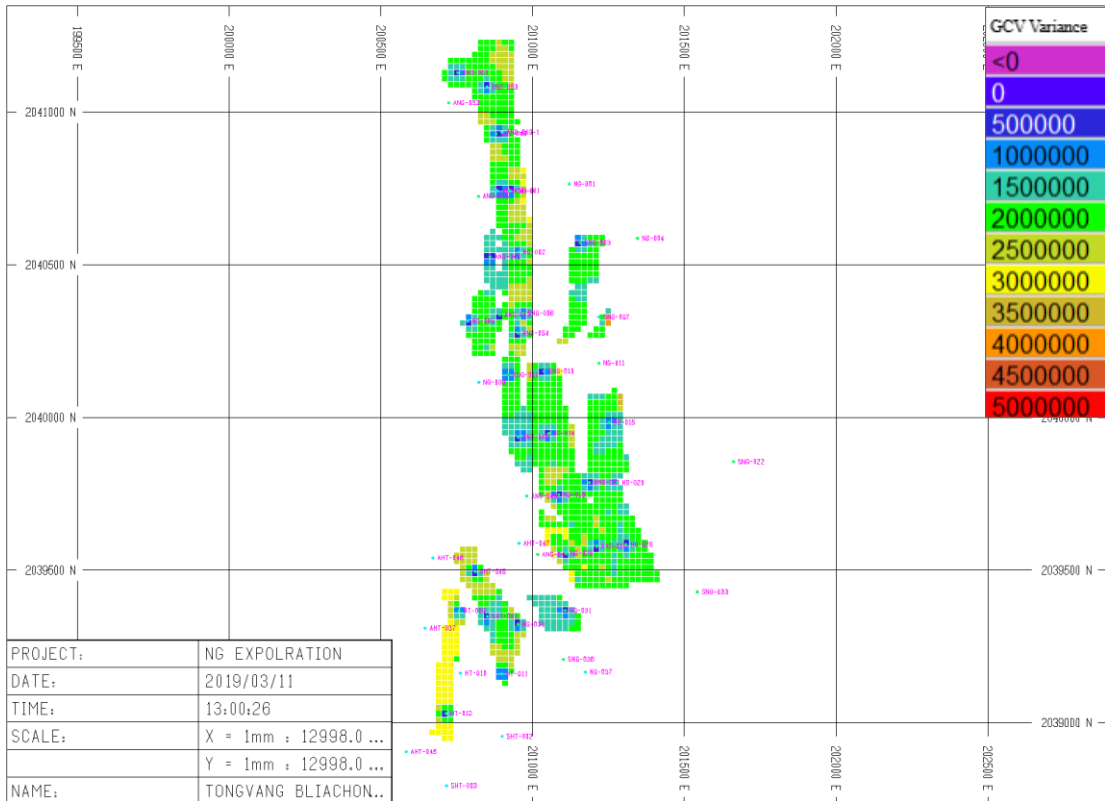


Figure 4.15 3D estimated blocks model showing CV's variance.

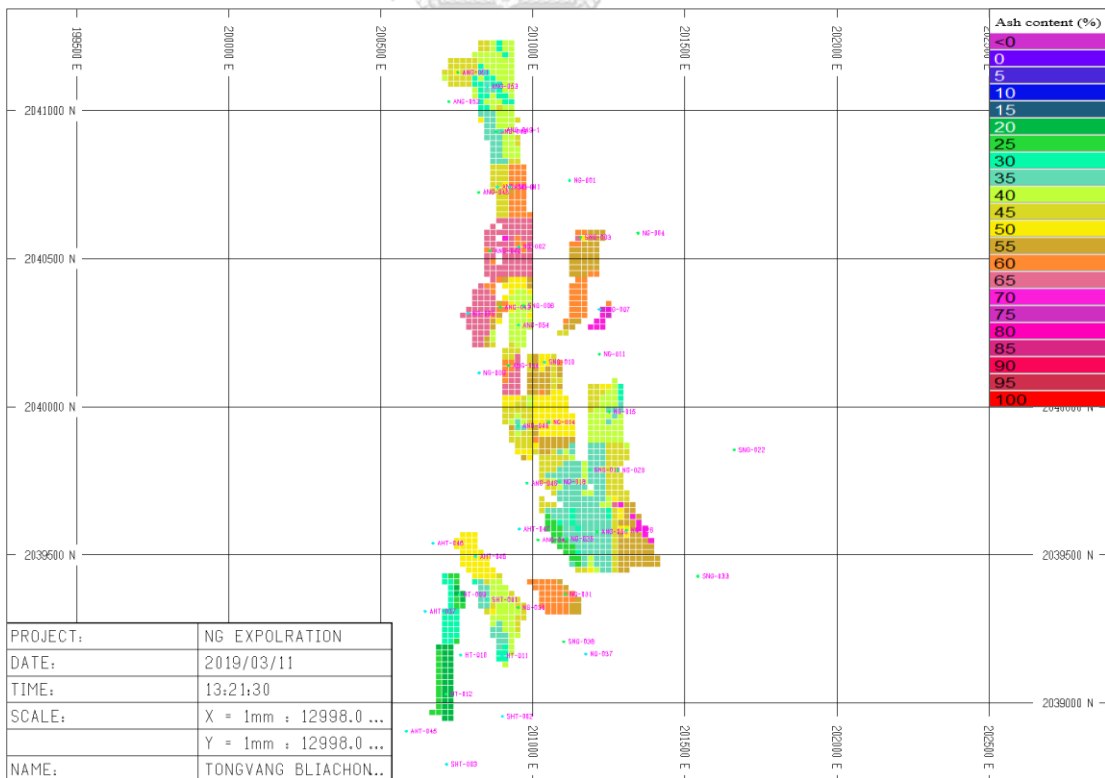


Figure 4.16 3D estimated blocks model of AC.

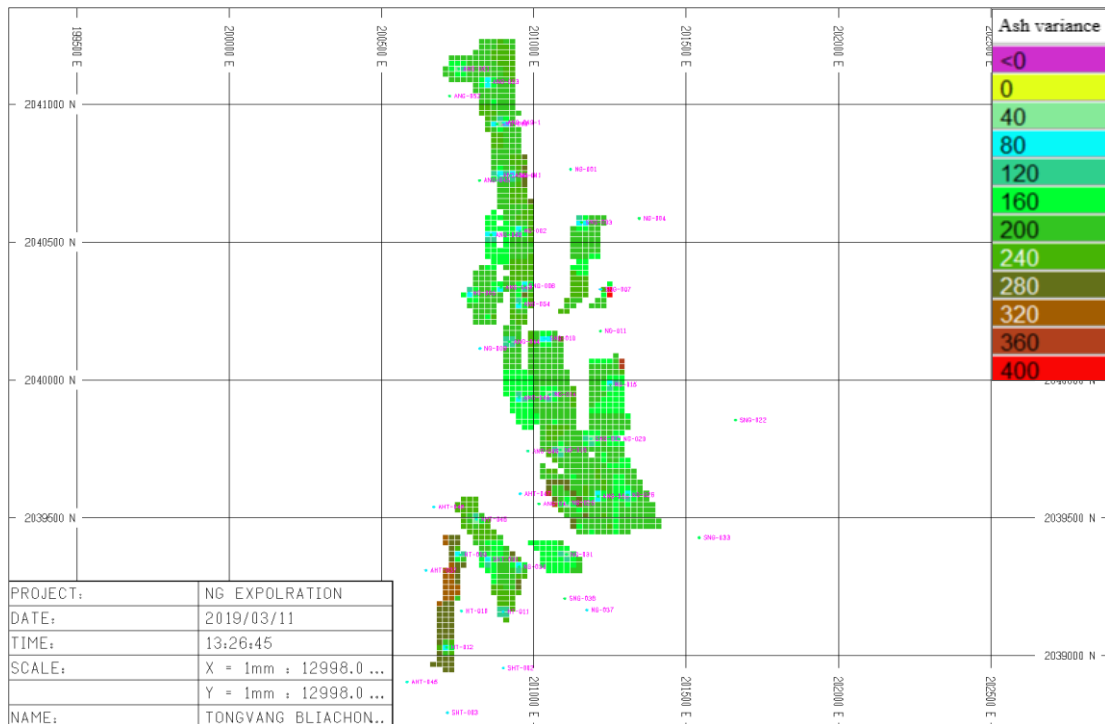


Figure 4.17 3D estimated blocks model AC's variance

4.4.4. Pit optimization and mineable reserve estimation

The pit optimization was carried out using the Lerch-Grossman algorithm in MS3D software. The economic parameters, overall pit slope angle and coal prices were used as conditioned data. The results have shown that there are nine optimum pits produced for NG coal deposit. These nine optimum pits will be used for mineable reserve calculation. It can be observed that the nine optimal pits consist of narrow pit floor as shown in Figure 4.18, which resulted to a lower mineable reserve computation. The top view and 2D cross sections of them are displayed in Figure 4.19 – 4.26. This could cause by the inclined coal seams which comprise of thin, and many split seams. The mineable reserve calculated from nine optimal pits are 0.68 Mts with an average CV of 4,073.21 kcal/kg, and an average AC of 45.24 % yielding a stripping ratio of 5:1. It can be seen that the mineable reserve generated by LG algorithm presents only 31 % from the original geological resource. This could reduce the mine life and impact to the mine feasibility study. The summary of mineable reserve is presented in Table 4.8, classified by CV basis, and in Table 4.9 classified by bench level.

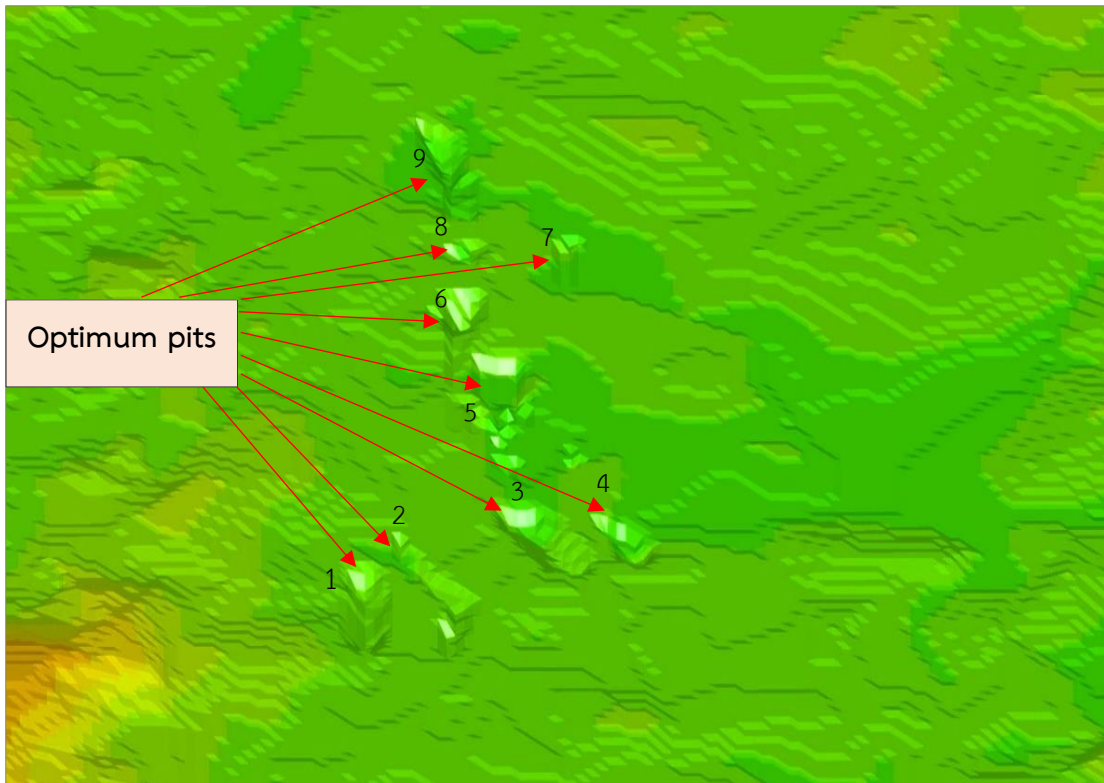


Figure 4.18 Nine optimum pits from pit optimization of NG coal deposit.

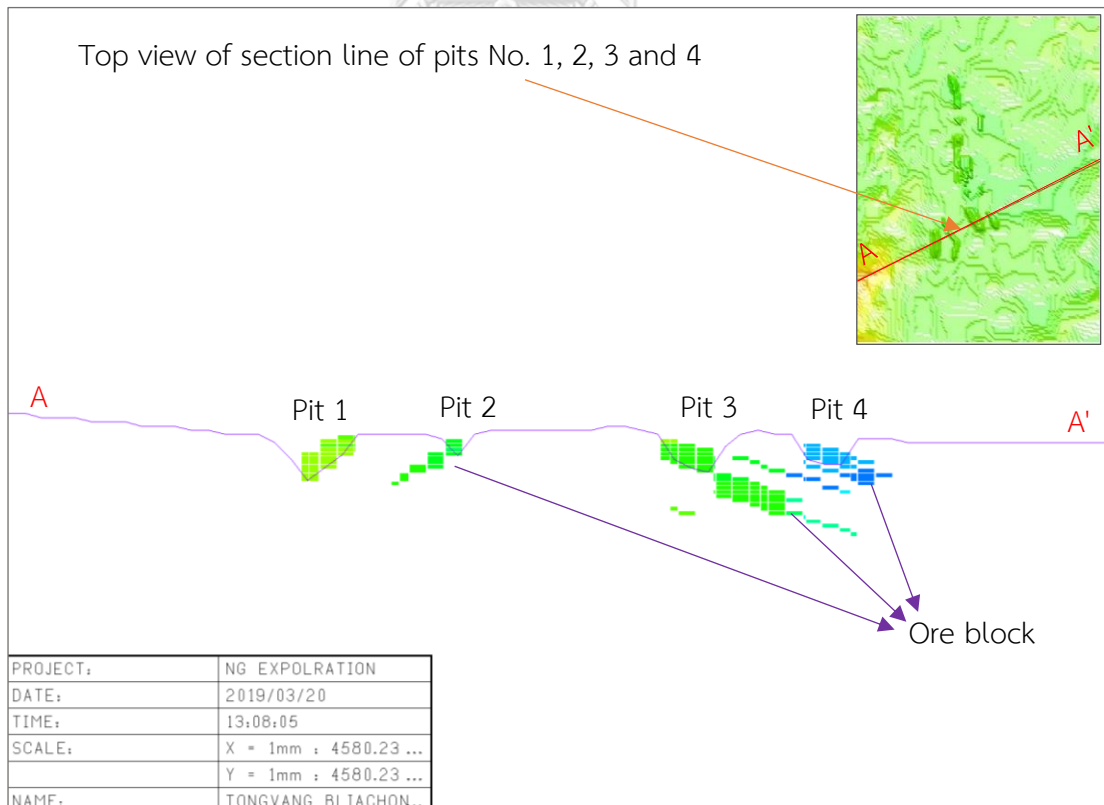


Figure 4.19 Top views and 2D cross section view of optimum pits No. 1, 2, 3, and 4.

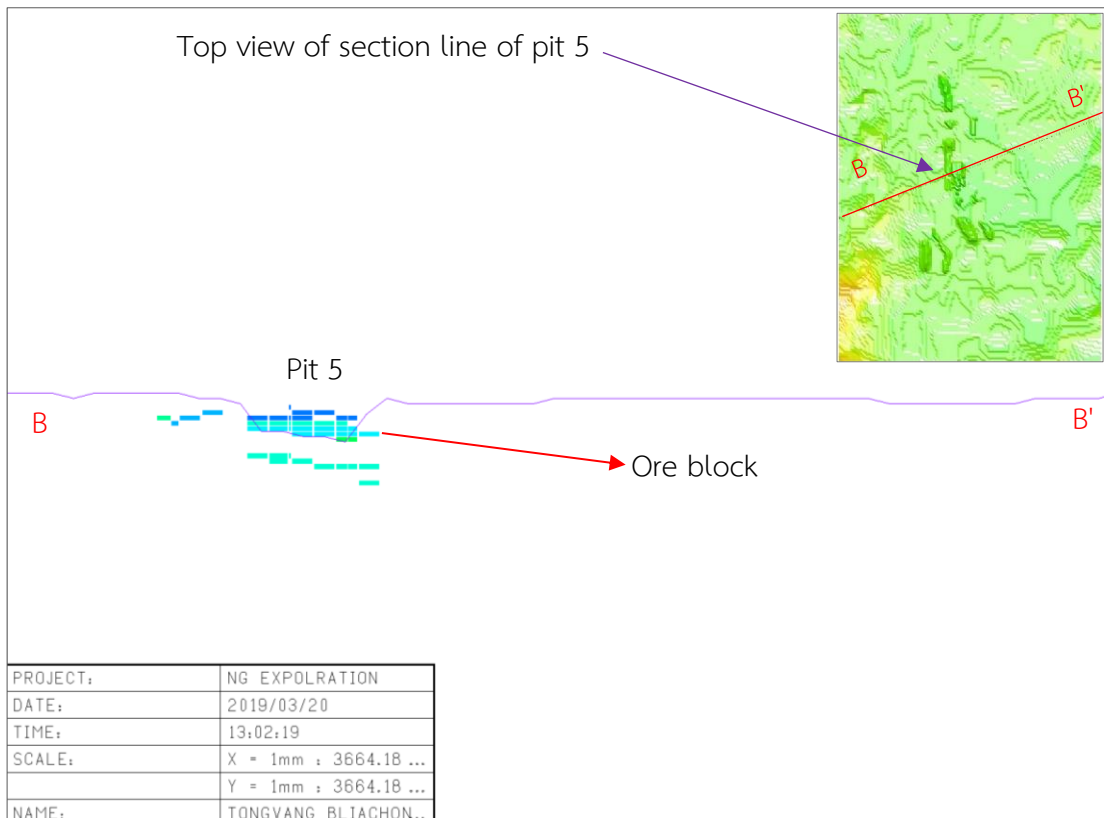


Figure 4.20 Top views and 2D cross section view of optimum pits No. 5.

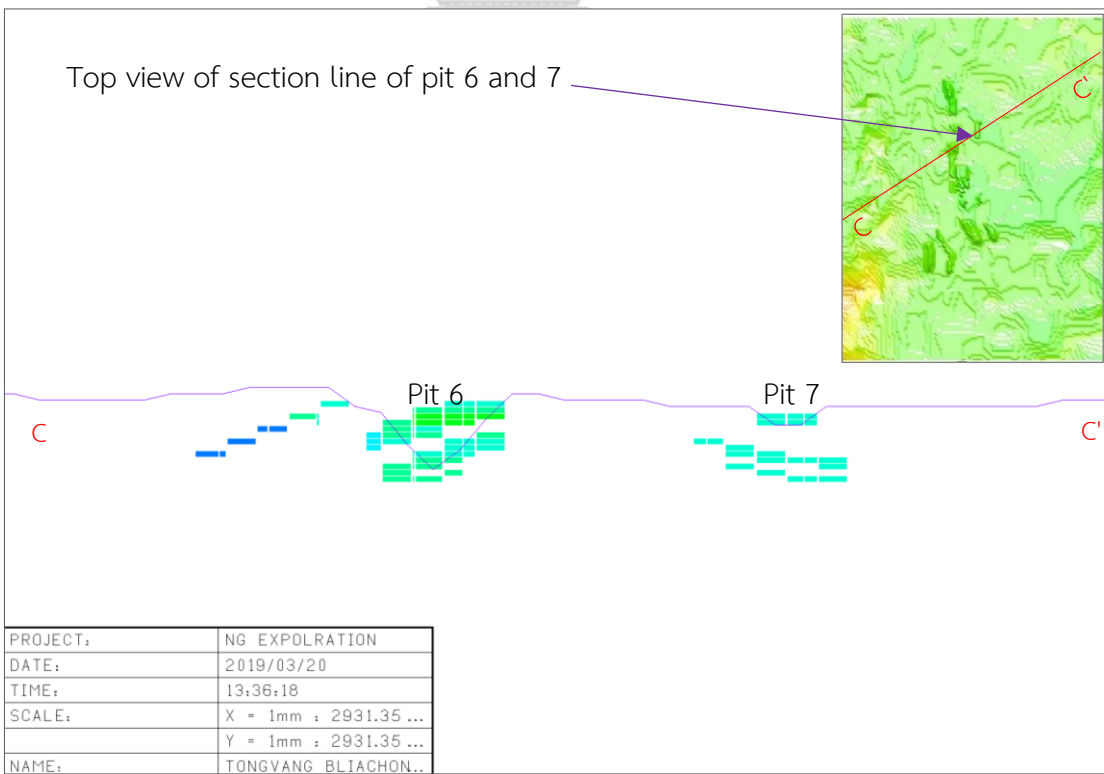


Figure 4.21 Top views and 2D cross section view of optimum pits No. 6 and 7.

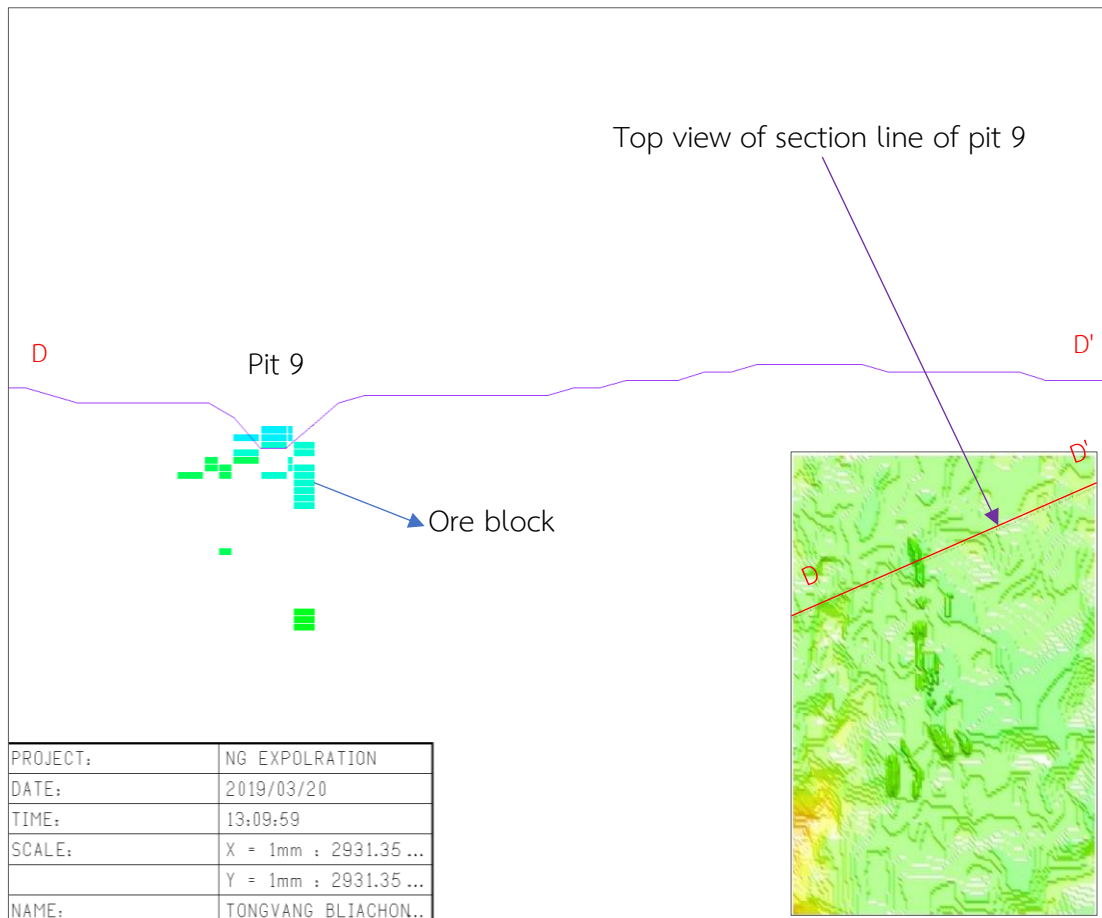


Figure 4.22 Top views and 2D cross section view of optimum pits No. 9.

Table 4.8 OK's mineable reserve from nine optimal pits classified by CV basis.

CV basis (kcal/kg)	V_c (m ³)	D_c (T/m ³)	Q_c (T)	Average grade	
				CV (kcal/kg)	AC (%)
500 - 4000	244,354.00	1.15	281,007.10	2,705.56	58.95
4000 - 5000	207,899.00	1.15	239,083.85	4,607.75	39.51
5000 - 5500	11,394.00	1.15	13,103.10	5,431.70	31.16
>= 5500	130,948.00	1.15	150,590.20	5,658.43	29.96
Total	594,595.00	1.15	683,784.25	4,073.21	45.24

Table 4.9 The OK's mineable reserve calculated from nine optimal pits classified by bench level.

Bench level (meter)	V _c (m ³)	D _c (T/m ³)	Q _c (T)	CV (kcal/kg)	AC (%)	V _w (m ³)	D _w (T/m ³)	Q _w (T)	SR (BCM: T)
230	-	-	-	-	-	8,500	1.8	15,300	-
225	550	1.15	632.50	3,529.13	48.53	151,530	1.8	272,754	275.51
220	15,912	1.15	18,298.80	4,071.40	42.66	438,068	1.8	788,522.4	27.53
215	47,298	1.15	54,392.70	4,351.07	42.37	667,282	1.8	1,201,107.6	14.11
210	78,804	1.15	90,624.60	3,937.47	46.79	641,016	1.8	1,153,828.8	8.13
205	103,709	1.15	119,265.35	3,760.37	48.70	518,291	1.8	932,923.8	5.00
200	108,935	1.15	125,275.25	3,830.94	47.42	377,065	1.8	678,717	3.46
195	96,902	1.15	111,437.3	3,926.99	46.56	281,098	1.8	505,976.4	2.90
190	62,343	1.15	71,694.45	4,238.34	43.66	163,657	1.8	294,582.6	2.63
185	39,754	1.15	45,717.10	4,708.44	39.06	102,246	1.8	184,042.8	2.57
180	21,530	1.15	24,759.50	4,828.21	38.17	50,470	1.8	90,846	2.34
175	14,024	1.15	16,127.60	5,029.90	36.40	29,976	1.8	53,956.8	2.14
170	4,833	1.15	5,557.95	5,245.68	34.08	11,167	1.8	20,100.6	2.31
Total	594,594	1.15	683,783.1	4,073.21	45.24	3,440,366	1.8	6,192,658.8	5.03

4.4.5. Pits adjustment, mineable reserve and Grade Tonnage Curve

As a results from pit optimization, there are nine optimum pits generated by LG algorithm with very narrow pit floor width. Thus, the minimum pit floor width of 23 meter adopted from the current LID's coal mine was applied for pits design and adjustment. The pit design and adjustment will allow the practical excavation and transportation activities in the mining pit and the smooth overall operation in the operating phase. Due to the proximity of the generated pits, thereby they were combined to generate a bigger pit resulting a higher mineable reserve and feasibility of the mine development. After an adjustment, there were five pits generated from the previously LG's pits as shown in Figure 4.23. The bottom view of the five adjusted pits are shown in Figure 4.24. The mineable computed from five adjusted pits based on CV basis is shown in Table 4.10, and Table 4.11 – 4.15, based on bench level.

The Grade-Tonnage Curve (GTC) is an important criterion for mine production phase in terms of defining various grades. In this case, there are 21 grades ranging from 500 kcal/kg to 5500 kcal/kg by 250 kcal/kg increasement were defined for Grade-Tonnage Curve construction as presented in Figure 4.28.

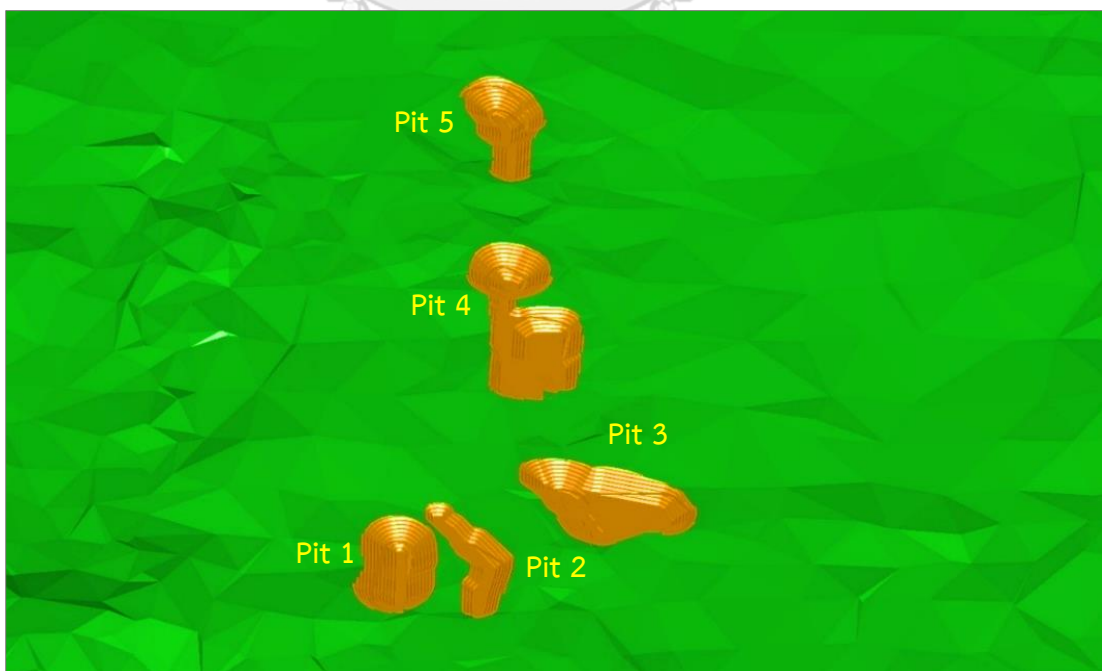


Figure 4.23 Top views of 5 adjusted pits (Pits No. 1, 2, 3, 4 and 5).

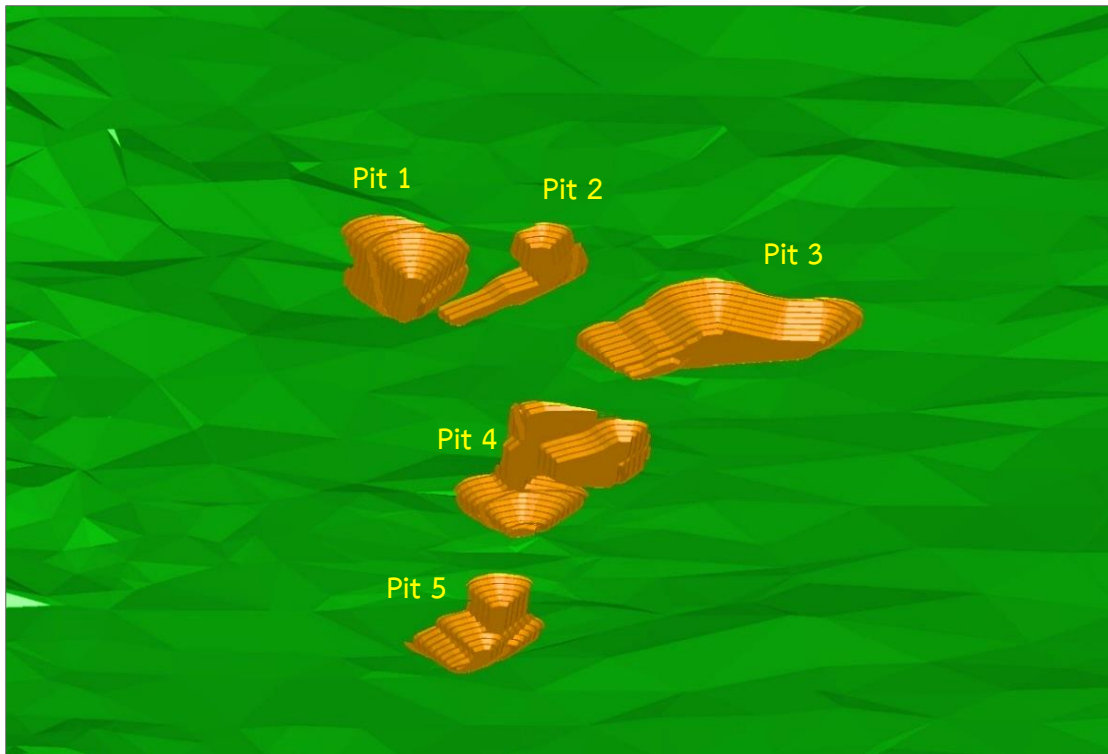


Figure 4.24 Bottom views of 5 adjusted pits (Pits No. 1, 2, 3, 4 and 5).

Table 4.10 OK's mineable reserve from the five adjusted pits based on the CV basis.

CV basis (kcal/kg)	V_c (m ³)	Q_c (T)	CV (kcal/kg)	AC (%)
500 - 4000	177,859.66	204,538.62	2,692.37	59.03
4000 - 5000	175,548.78	201,881.10	4,636.50	39.20
5000 - 5500	373.60	429.64	5,125.95	35.65
≥ 5500	124,664.14	143,363.77	5,635.40	30.10
Total	478,446.18	550,213.13	4,174.44	44.20

The waste materials calculated from five adjusted pits consist of 9.3 Mts, yielding a stripping ratio of 10.36:1. The 2D cross section of pits No. 1 - 5 are shown in Figure 4.25 – 4.31, respectively.

Table 4.11 Summary of the OK's mineable reserve in pit No.1

Bench level	CV bin (kcal/kg)	Mineable reserve		Average grade		Waste material		SR (BCM: T)
		V _c (m ³)	Q _c (T)	CV (kcal/kg)	AC (%)	V _w (m ³)	Q _w (T)	
240	-	-	-	-	-	180.00	324.00	
235	-	-	-	-	-	4,309.34	7,756.81	
230	-	-	-	-	-	19,680.08	35,424.14	
225	-	-	-	-	-	41,850.53	75,330.95	
220	>= 5000	1,629.60	1,874.04	5,350.14	23.14	194,768.59	350,583.45	
215	>= 5000	6,069.20	6,979.58	5,742.10	28.50	209,177.23	376,519.05	
210	>= 5000	9,390.40	10,798.96	5,458.02	32.37	172,977.93	311,360.25	
205	>= 5000	13,231.60	15,216.34	5,650.05	30.39	138,407.37	249,133.27	
200	>= 5000	16,244.00	18,680.60	5,619.87	30.36	106,503.08	191,705.54	
195	>= 5000	19,001.20	21,851.38	5,614.21	30.41	76,877.27	138,379.07	
190	>= 5000	18,568.00	21,353.20	5,614.07	30.41	52,277.49	94,099.45	
185	>= 5000	14,623.74	16,817.31	5,613.91	30.42	33,649.06	60,568.34	
180	>= 5000	9,308.59	10,704.88	5,613.53	30.42	19,056.25	34,301.24	
Total		108,066.33	124,276.29	5,608.95	34.91	1,069,714.22	1,925,485.56	8.61

Table 4.12 Summary of OK's mineable reserve in pit No.2

Bench level	CV bin (kcal/kg)	Mineable reserve		Average grade		Waste material		SR (BCM: T)
		V _c (m ³)	Q _c (T)	CV (kcal/kg)	AC (%)	V _w (m ³)	Q _w (T)	
225	500 - 4000	550.00	632.50	3,529.13	48.52	43,820.53	78,876.94	
220	500 - 4000	3,496.26	4,020.70	3,551.03	48.60	118,289.80	212,921.66	
215	500 - 4000	5,961.42	6,855.64	3,413.41	50.44	128,394.02	231,109.24	
	4000 - 5000	931.25	1,070.94	4,424.43	42.46			
210	500 - 4000	6,036.35	6,941.79	3,425.93	50.36	91,427.91	164,570.22	
	4000 - 5000	2,748.91	3,161.25	4,406.45	42.53			
205	500 - 4000	1,838.27	2,114.02	3,239.32	53.24	55,526.31	99,947.35	
	4000 - 5000	6,931.07	7,970.73	4,223.51	43.48			
Total		28,493.53	32,767.57	3,749.85	47.62	437,458.57	787,425.41	13.35

Table 4.13 Summary of mineable coal reserve in pit No.3

Bench level	CV bin (kcal/kg)	Mineable reserve		Average grade		Waste material		SR (BCM: T)
		V _c (m ³)	Q _c (T)	CV (kcal/kg)	AC (%)	V _w (m ³)	Q _w (T)	
235	-	-	-	-	-	210.44	378.78	
230	-	-	-	-	-	9,809.99	17,657.98	
225	-	-	-	-	-	85,271.52	153,488.75	
220	>= 5500	3,537.85	4,068.53	5,806.44	28.48	218,065.29	392,517.52	
215	500 - 4000	404.80	465.52	3,765.44	48.38	308,538.15	555,368.67	
	>= 5500	13,059.96	15,018.95	5,807.93	28.47			
210	500 - 4000	4,882.51	5,614.89	2,388.10	62.51			
	4000 - 5000	18,332.44	21,082.31	4,946.50	36.35	294,756.67	530,562.05	
	5000 - 5500	373.60	429.64	5,125.95	35.65			
205	500 - 4000	7,933.93	9,124.02	2,207.99	64.16			
	4000 - 5000	22,974.91	26,421.15	4,916.20	36.96	246,246.33	443,243.39	

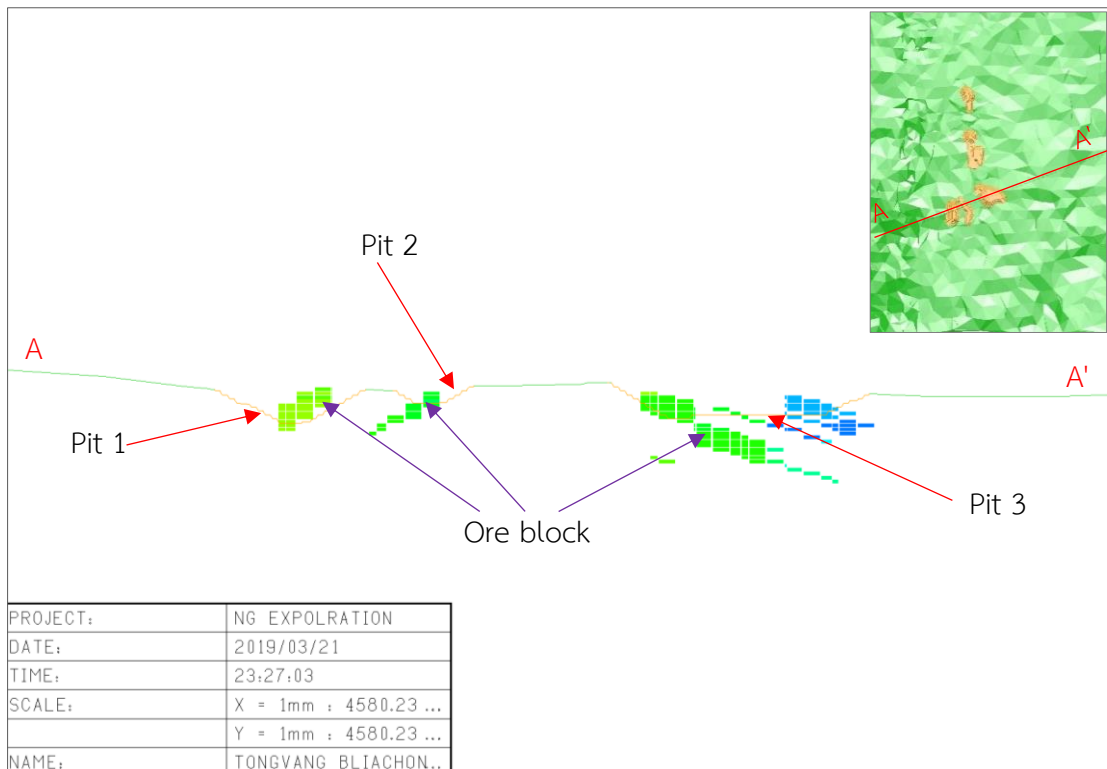


Figure 4.25 2D cross section views of adjusted pits No. 1, 2 and 3.

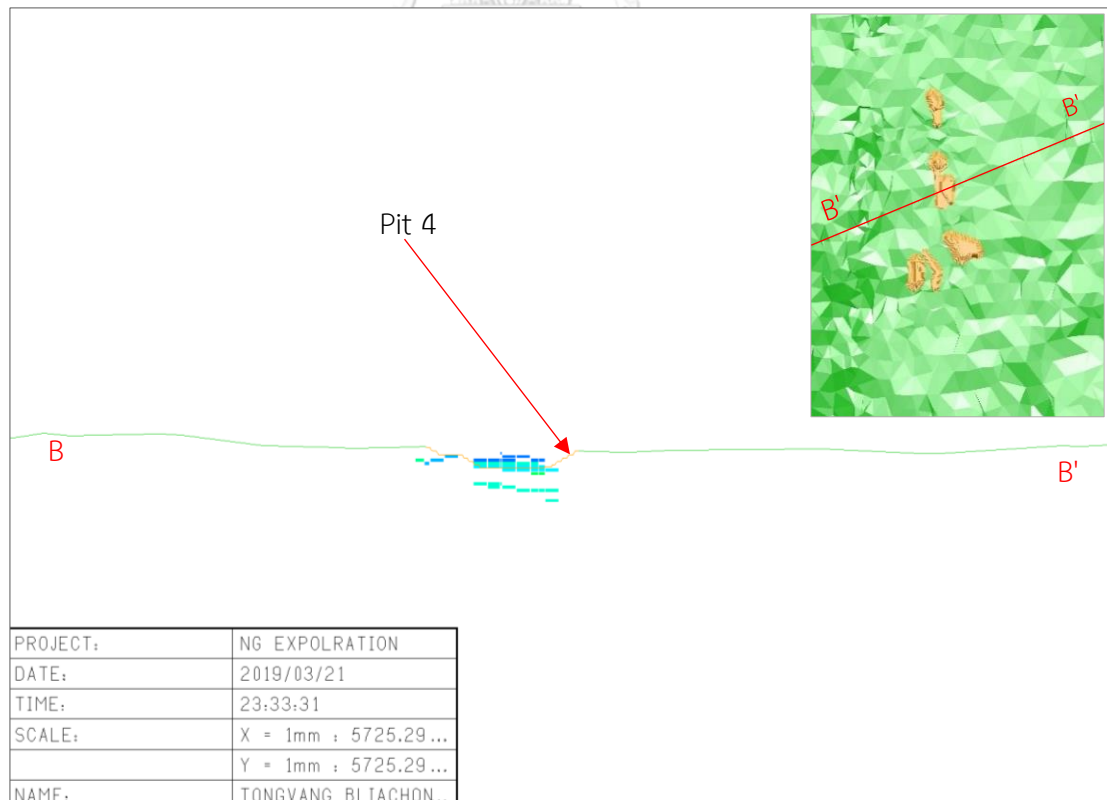


Figure 4.26 2D cross section views of adjusted pit No. 4.

Table 4.15 Summary of OK's mineable reserve in pit No.4

Bench level	CV bin (kcal/kg)	Mineable reserve		Average grade		Waste material		SR (BCM: T)
		V _c (m ³)	Q _c (T)	CV (kcal/kg)	AC (%)	V _w (m ³)	Q _w (T)	
230	-	-	-	-	-	9,875.40	17,775.72	
225	-	-	-	-	-	114,647.40	206,365.33	
220	500 - 4000	5,086.52	5,849.49	2,788.75	55.07	205,611.43	370,100.61	
	4000 - 5000	2,073.75	2,384.81	4,106.52	41.96			
215	500 - 4000	16,093.47	18,507.48	3,044.51	55.85	314,967.89	566,942.21	
	4000 - 5000	3,471.30	3,991.99	4,182.20	41.72			
210	500 - 4000	3,285.73	3,778.59	1,515.90	70.87	219,704.96	395,468.95	
	4000 - 5000	10,721.07	12,329.23	4,183.60	44.08			
205	500 - 4000	12,718.60	14,626.39	1,741.42	68.35	165,489.36	297,880.82	
	4000 - 5000	8,266.48	9,506.45	4,181.85	44.36			
200	500 - 4000	6,510.69	7,487.29	2,630.69	60.44	118,072.81	212,531.05	
	500 - 4000	17,475.65	20,097.00	2,555.59	59.37			
195	4000 - 5000	1,369.49	1,574.92	4,218.12	42.14	80,480.09	144,864.15	
	500 - 4000	24,074.59	27,685.79	2,605.24	59.26			
190	4000 - 5000	455.80	524.17	4,178.58	41.91	15,190.35	27,342.64	
	500 - 4000	2,605.52	2,996.35	2,805.86	58.44			
185	500 - 4000	817.80	940.47	2,878.28	57.82	7,622.57	13,720.62	
Total		115,026.46	132,280.42	2,909.08	56.39	1,251,662.26	2,252,992.10	9.46

Table 4.16 Summary of OK's mineable reserve in pit No.5.

Bench level	CV bin (kcal/kg)	Mineable reserve		Average grade		Waste material		SR (BCM: T)
		V _c (m ³)	Q _c (T)	CV (kcal/kg)	AC (%)	V _w (m ³)	Q _w (T)	
225	-	-	-	-	-	180.00	324.00	
220	-	-	-	-	-	14,244.62	25,640.30	
215	4000 - 5000	585.00	672.75	4,547.94	41.48	136,665.06	245,997.08	
210	500 - 4000	2,395.29	2,754.58	2,381.61	63.92	169,709.86	305,477.76	
	4000 - 5000	4,062.60	4,671.99	4,498.27	42.12			
205	500 - 4000	10,831.08	12,455.74	3,095.46	56.54	130,252.73	234,454.88	
	4000 - 5000	1,279.80	1,471.77	4,012.10	46.65			
200	500 - 4000	8,521.61	9,799.84	2,625.69	61.56	97,604.16	175,687.49	
	4000 - 5000	4,468.48	5,138.75	4,051.38	45.85			
195	500 - 4000	8,184.94	9,412.68	3,175.40	55.44	72,795.55	131,032.01	
190	500 - 4000	3,750.59	4,313.18	3,856.93	47.57	42,305.84	76,150.50	
185	500 - 4000	3,605.93	4,146.84	3,826.83	47.96	26,167.69	47,101.83	
180	500 - 4000	64.19	73.82	2,767.72	60.81	12,254.74	22,058.52	
	4000 - 5000	3,596.01	4,135.41	4,134.70	45.57			
Total		51,345.52	59,047.35	2,311.80	41.35	702,180.25	1,263,924.37	11.9

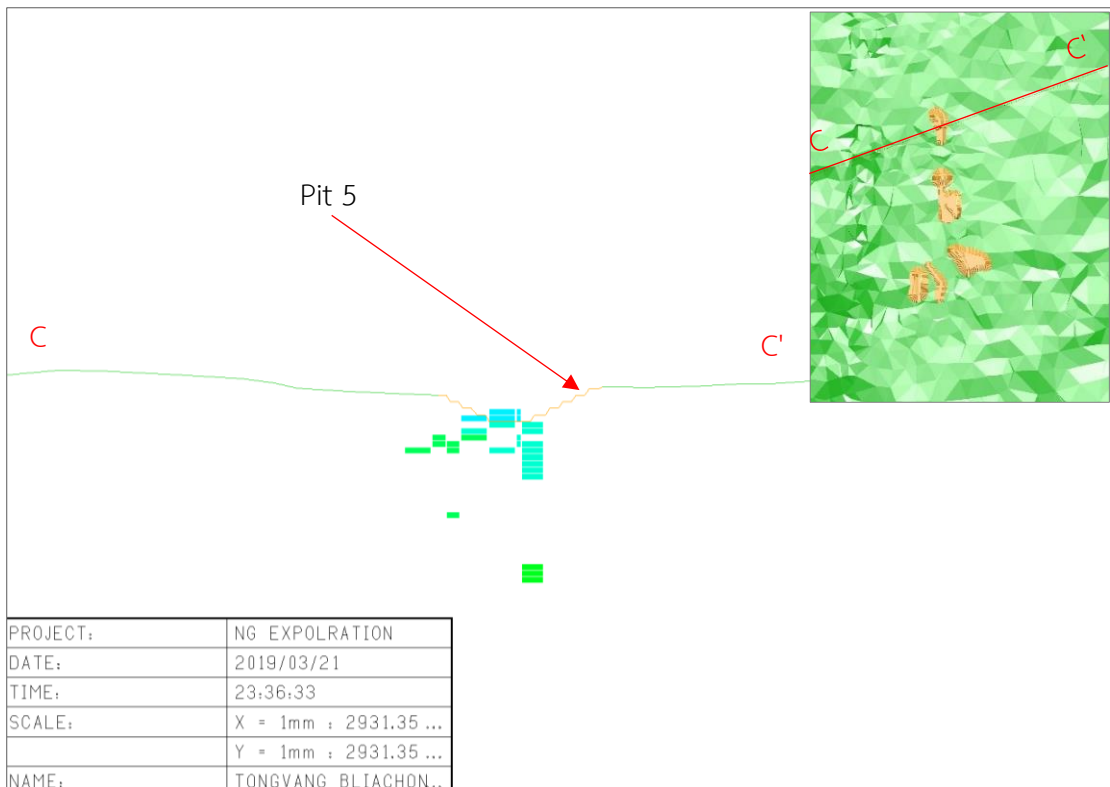


Figure 4.27 2D cross section view of adjusted pit No.5.

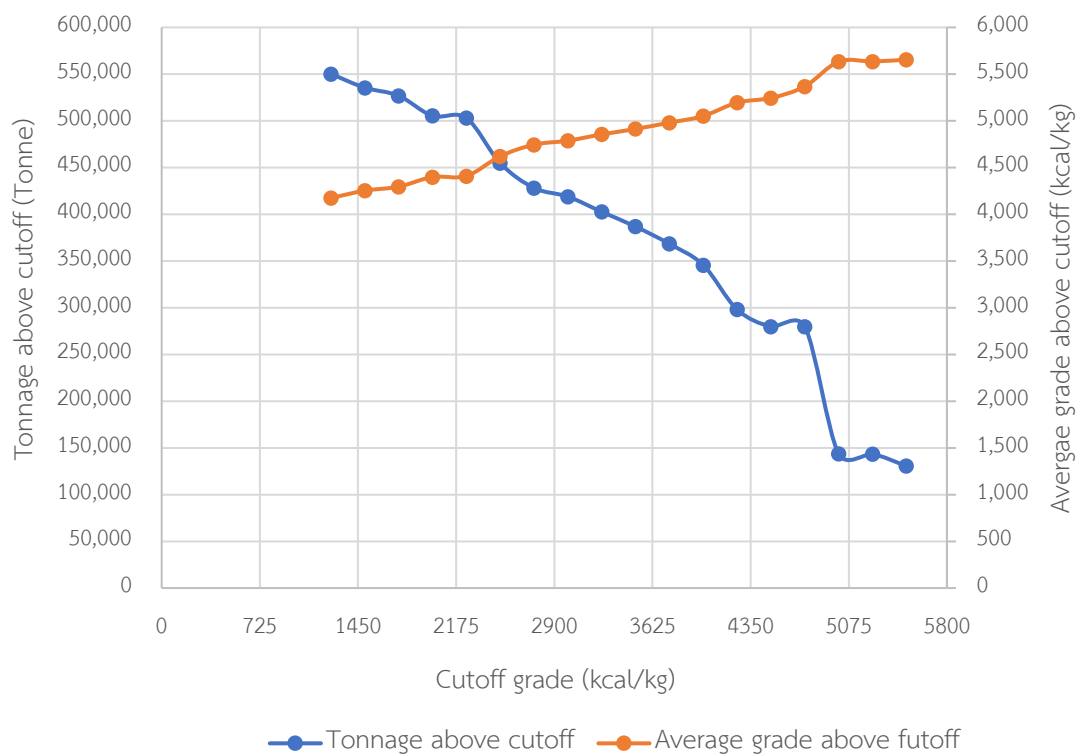


Figure 4.28 OK's Grade Tonnage Curve of NG coal deposit.

4.5. Sequential Gaussian Simulation (SGS)

4.5.1. Gaussian data transformation and variogram modelling

According to SGS criterion, the composited data must be transformed into Gaussian data values. The Gaussian data contains of zero mean and a unit variance as of standard normal distribution. In this study, the composited data of CV and AC were transformed into Gaussian data using MS3D software. The univariate analysis was followed up to check the normality of the transformed data. As the results of both CV and AC, the histogram plots of Gaussian transformed data display a normal score distribution with a unit variance and zero mean as demonstrated in Figure 4.29 – 4.34.

After the Gaussian data was validated, the transformed data were used to calculate experimental variogram and modeling. In this case, spherical model was chosen for modeling CV and AC experimental variograms. The variogram models have shown that both variables exhibit a very close range in comparison. CV's variogram model shows the range of 32 meters and AC's variogram model gives the range of 33 meters. The variogram models for CV and AC can be seen in Figure 4.31 - 4.36 and the summary of variogram model parameters of both CV and AC is shown in Table 4.17.

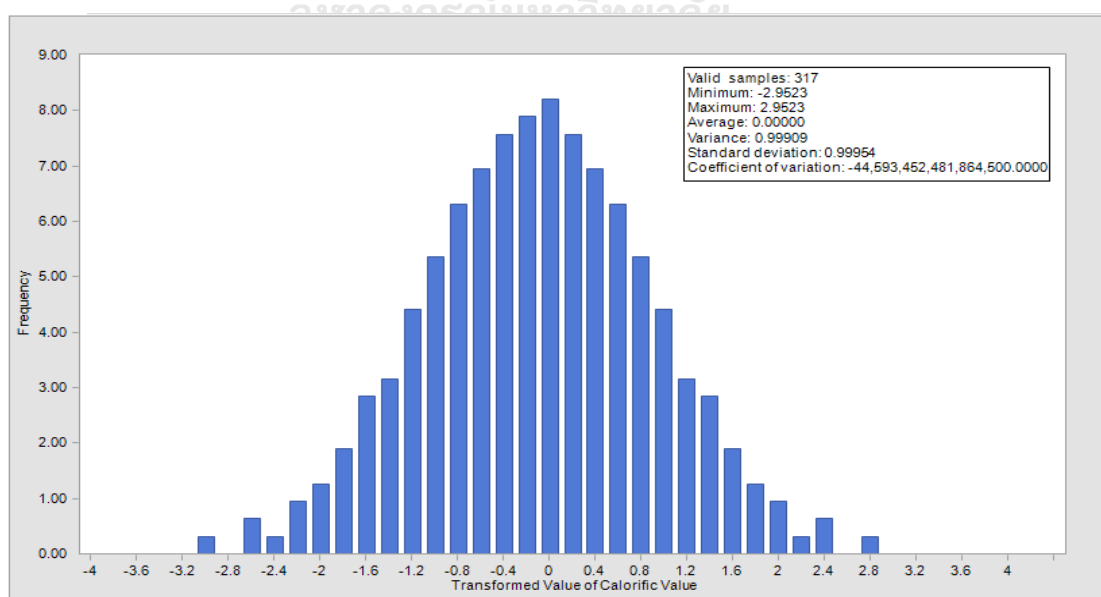


Figure 4.29 Normal scores distribution plot of CV.

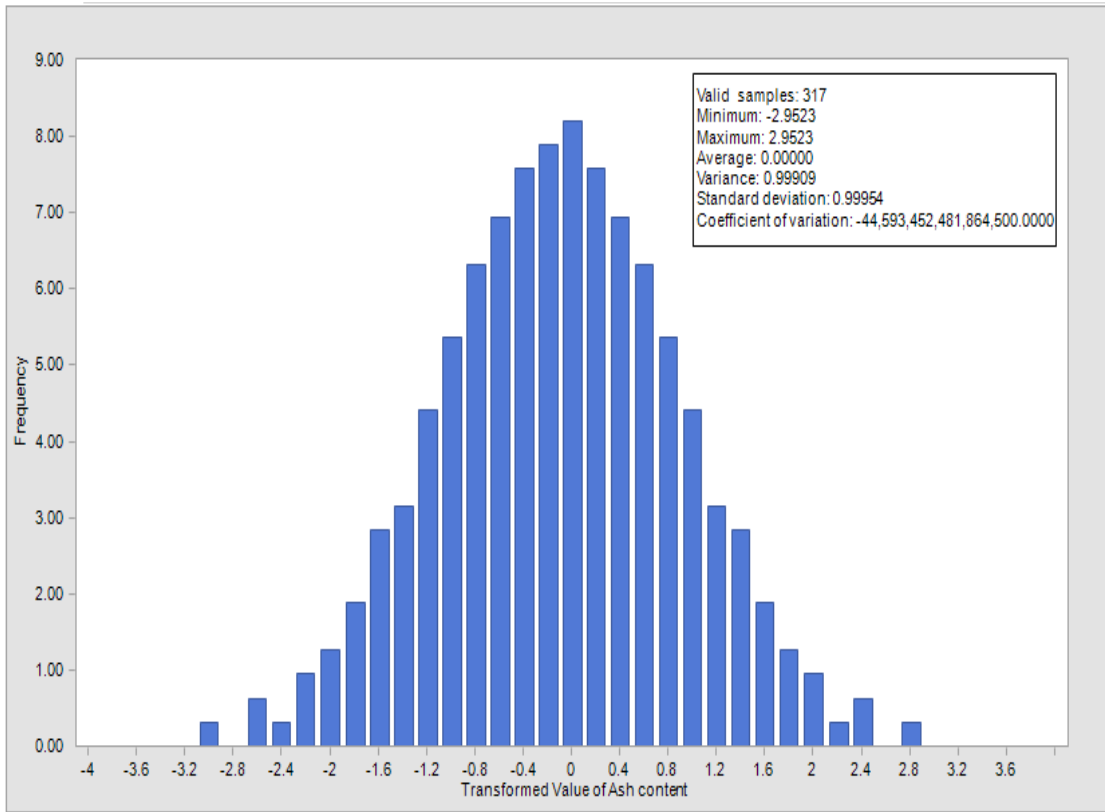


Figure 4.30 Normal scores distribution plot of AC.

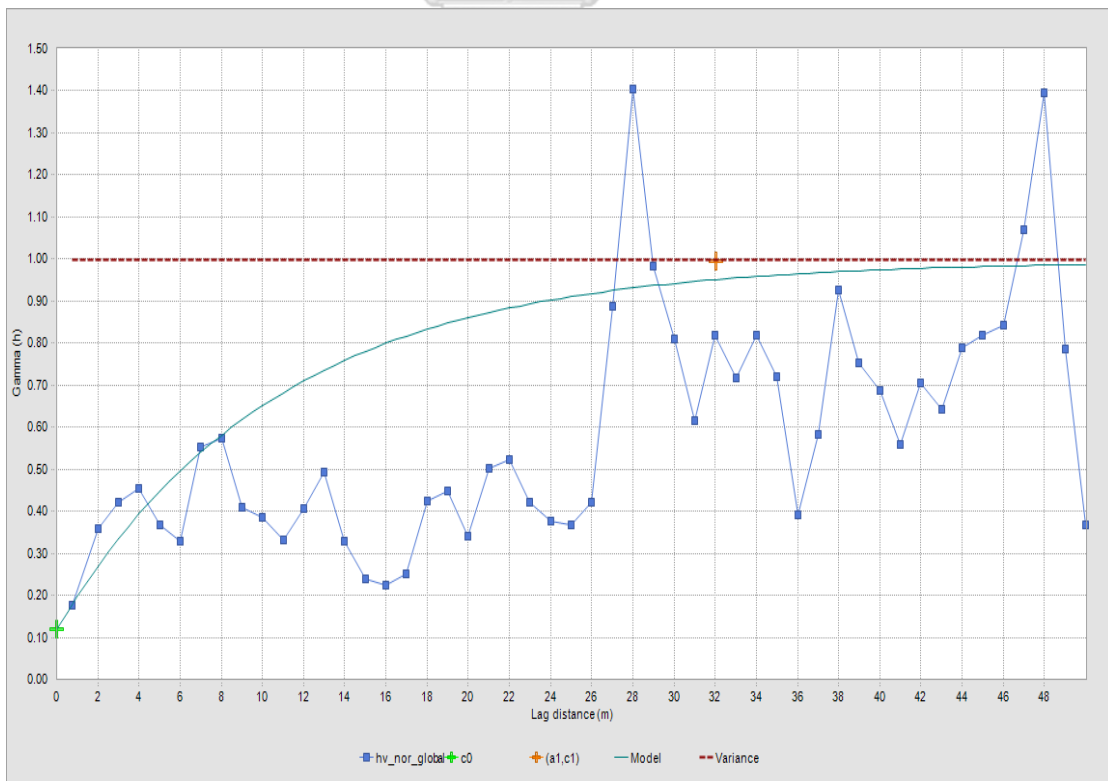


Figure 4.31 A vertical variogram model of CV.

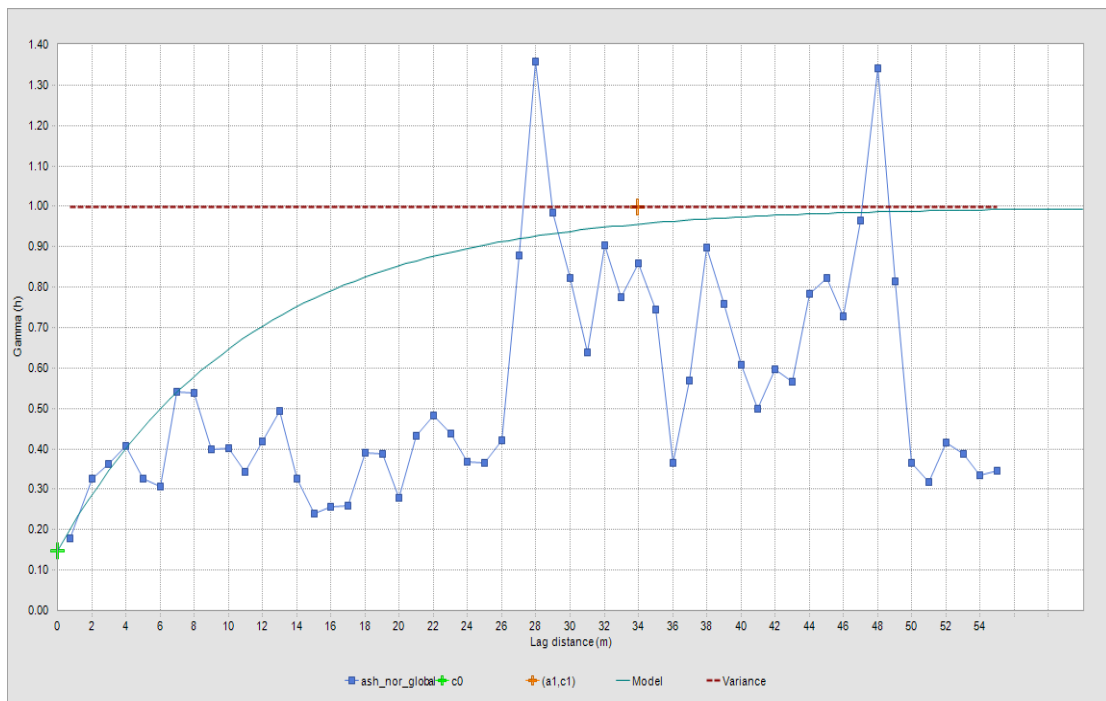


Figure 4.32 A vertical variogram model of AC.

Table 4.17 Variogram model results of normal transformed data for SGS simulation.

Variable	Nugget effect (C_0)	Partial Sill (C_1)	Range (a)	Model	Variogram equation
CV	0.1195	0.8755	32.037	Spherical	$\gamma(h) = C_0 + C_1 \left(\frac{3h}{2a} - \frac{1}{2} \left(\frac{h}{a} \right)^3 \right)$ $0 < h < a$
AC	0.1478	0.8506	33.933	Spherical	

4.5.2. 3D block model and geological resources estimation.

The 3D block model initialized from the previous grid discretization step was used for SGS of CV and AC. A total of 4,796 blocks were simulated for both CV and AC. The inputs and outputs-controlled parameters of SGS are represented in Table 4.18. There are five realizations (maps) were produced for CV and AC separately. The E-Type maps of each variable were produced by combining these realizations together to calculate the mean and variance, sequentially. The CV's five realization maps and E-Type map are illustrated in Figure 4.33 – 4.38. The AC's five realizations and E-Type map are presented in Figure 4.40 – 4.45. The variance maps of CV and AC are shown in Figure 4.389 and Figure 4.46.

For SGS's geological resource calculation, the same criteria as Ordinary Kriging was applied and the coal density of 1.15 ton/m³ was used. SGS's geological resource contains 2.2 Mts (the same as OK's geological resource) with an average CV of 3,769 kcal/kg and an average AC of 46.3 %. In comparison, SGS's and Ok's geological resource are the same in terms of quantity, but they both have different CV's and AC's statistics. This can be explained that the same number of blocks was computed for both OK's and SGS's model, resulting in the same resource quantities. However, the grade distributions are differentiated when comparing Ok's and SGS's model. The SGS's geological resource is presented in Table 4.19 by CV basis, and Table 4.20 by bench level.

The statistical analysis of individual five realizations of CV and AC were carried out for the comparison purpose as shown in Table 4.21 – 4.22. The CV's five realizations' histogram plots are shown in Figure 4.47 - 4.51, and AC's five realizations' histogram plots are shown in Figure 4.52 - 4.56.

Table 4.18 SGS's input parameters and outputs of block grades simulation.

Input data	Gaussian transformed data of CV and AC				
Grid discretization	20 meter × 20 meter × 5 meter				
Variogram model	Variable	Nugget (C_0)	Partial sill (C_1)	Range (a)	Model
	CV	0.1195	0.8755	32.037	Spherical
	AC	0.1478	0.8506	33.933	Spherical
Searching dimension	X=250 m, Y= 250 m, Z= 125 m				
Conditional data	Min = 1, Max = 7				
Output data	CV = Realization 1, 2, 3, 4, 5 and E-Type Map				
	AC = Realization 1, 2, 3, 4, 5 and E-Type Map				

Table 4.19 SGS's geological resource estimation based on the CV basis.

CV basis (kcal/kg)	V _c (m ³)	D _c (T/m ³)	Q _c (T)	Average grade	
				CV (kcal/kg)	AC (%)
500-4000	1,079,380	1.15	1,241,287.00	2,918.75	47.71
4000-5000	512,570		589,455.50	4,482.11	44.89
5000-5500	158,963		182,807.45	5,231.36	44.67
>= 5500	146,943		168,984.45	5,945.32	42.47
Total	1,897,856		2,182,534.40	3,769.01	46.29

Table 4.20 SGS's geological resource estimation by bench level.

Bench No.	Bench level	V _c (m ³)	D _c (T/m ³)	Q _c (T)	Average grade	
					CV (kcal/kg)	AC (%)
1	225	550	1.15	632.50	4,689.97	54.68
2	220	16,281		18,723.15	3,603.08	45.27
3	215	49,381		56,788.15	3,731.71	46.58
4	210	82,507		94,883.05	3,478.12	46.63
5	205	120,015		138,017.25	3,313.69	48.29
6	200	136,644		157,140.60	3,339.11	48.72
7	195	140,623		161,716.45	3,322.61	48.53
8	190	130,702		150,307.30	3,363.52	47.85
9	185	114,189		131,317.35	3,516.86	47.27
10	180	113,571		130,606.65	3,609.31	47.96
11	175	113,833		130,907.95	3,576.06	45.39
12	170	98,106		112,821.90	3,844.20	43.71
13	165	87,539		100,669.85	3,926.37	43.15
14	160	78,572		90,357.80	4,208.89	44.92
15	155	68,079		78,290.85	4,229.54	43.33

Table 4.20 SGS's geological resource estimation by bench level (Continue)

16	150	63,530		73,059.50	4,193.96	43.76
17	145	54,571		62,756.65	4,322.65	44.94
18	140	41,175		47,351.25	4,275.04	44.23
19	135	32,429		37,293.35	4,124.53	45.52
20	130	29,660		34,109.00	4,205.19	48.44
21	125	32,812		37,733.80	4,071.02	47.69
22	120	31,690		36,443.50	4,102.26	47.21
23	115	31,811		36,582.65	3,988.38	45.52
24	110	31,389		36,097.35	4,168.96	47.32
25	105	29,890		34,373.50	4,009.59	45.18
26	100	27,351		31,453.65	4,144.03	45.85
27	95	26,100		30,015.00	4,283.44	45.71
28	90	24,704		28,409.60	4,216.12	44.96
29	85	21,418		24,630.70	4,343.73	45.22
30	80	18,401	1.15	21,161.15	4,455.19	46.03
31	75	14,636		16,831.40	4,327.77	43.43
32	70	11,730		13,489.50	4,147.25	41.49
33	65	8,207		9,438.05	4,477.39	43.46
34	60	3,874		4,455.10	4,297.74	40.28
35	55	3,148		3,620.20	4,508.37	42.48
36	50	1,972		2,267.80	4,238.78	40.13
37	45	2,030		2,334.50	4,562.36	44.03
38	40	1,466		1,685.90	4,543.10	46.03
39	35	1,207		1,388.05	4,866.01	49.73
40	30	951		1,093.65	4,538.75	44.23
41	25	589		677.35	4,525.46	45.72
42	20	341		392.15	4,542.95	46.13
43	15	182		209.3	6,090.51	69.65
Total		1,897,856		2,182,534.4	3,769.01	46.29

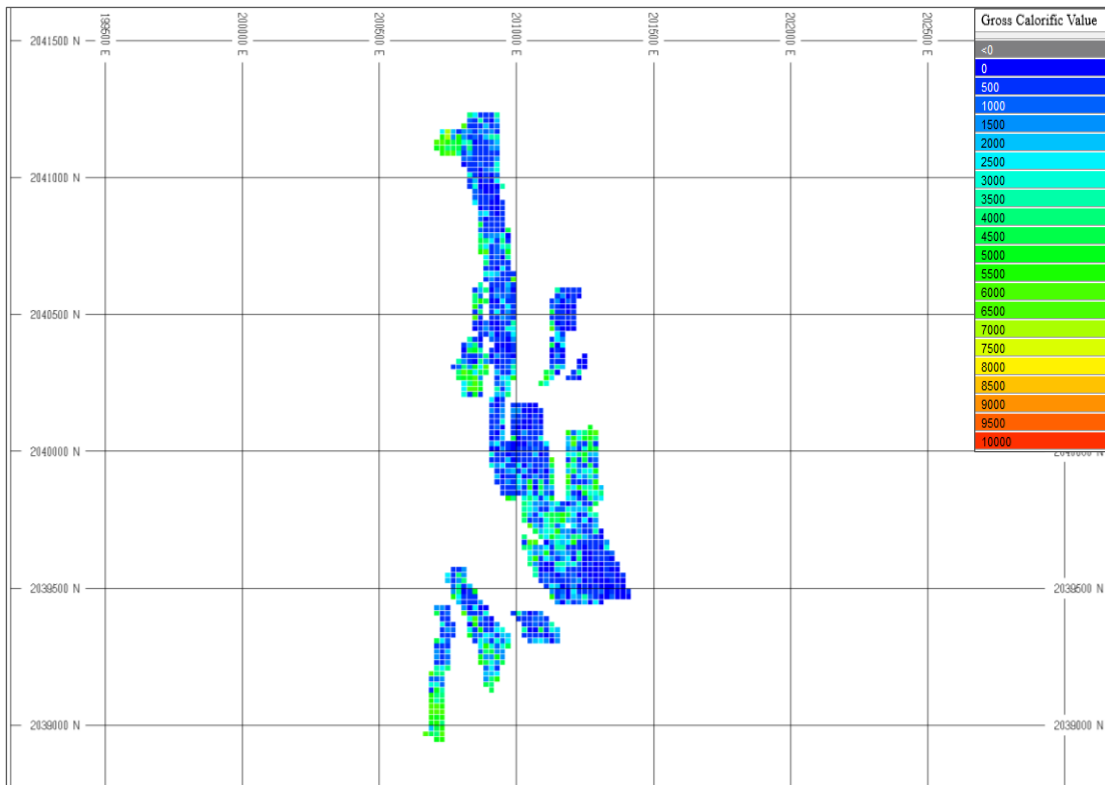


Figure 4.33 Map of realization No. 1 of CV.

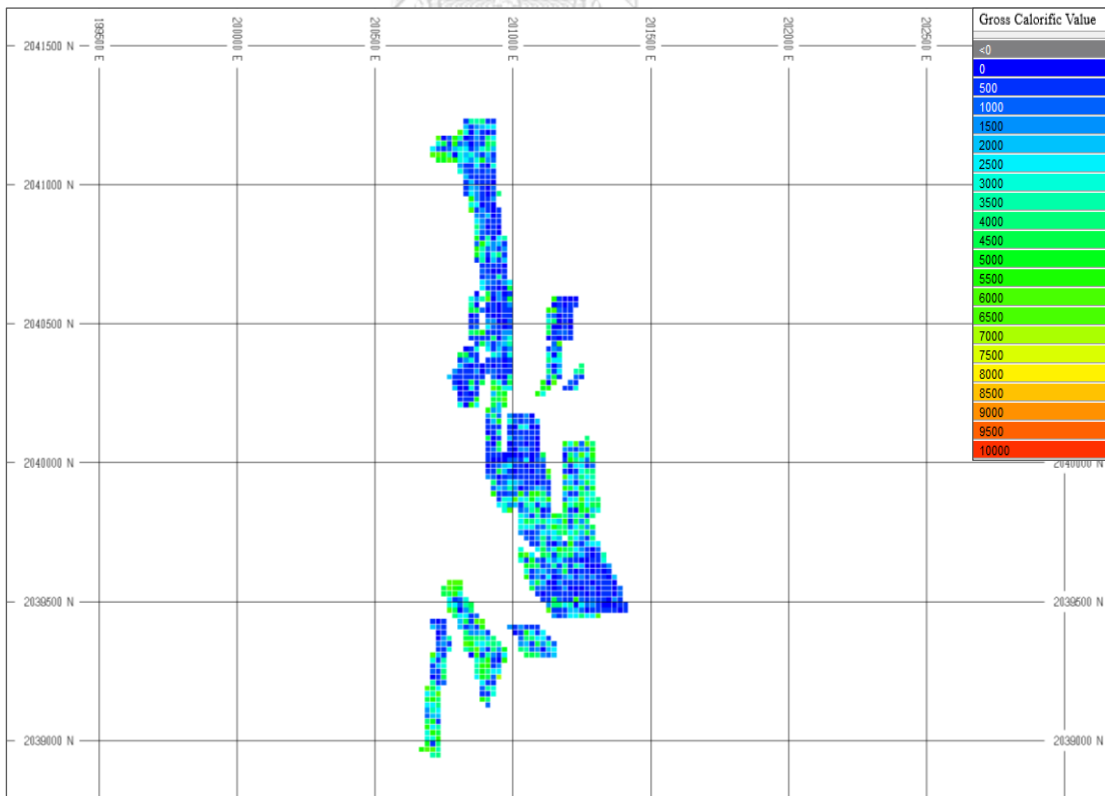


Figure 4.34 Map of realization No. 2 of CV.

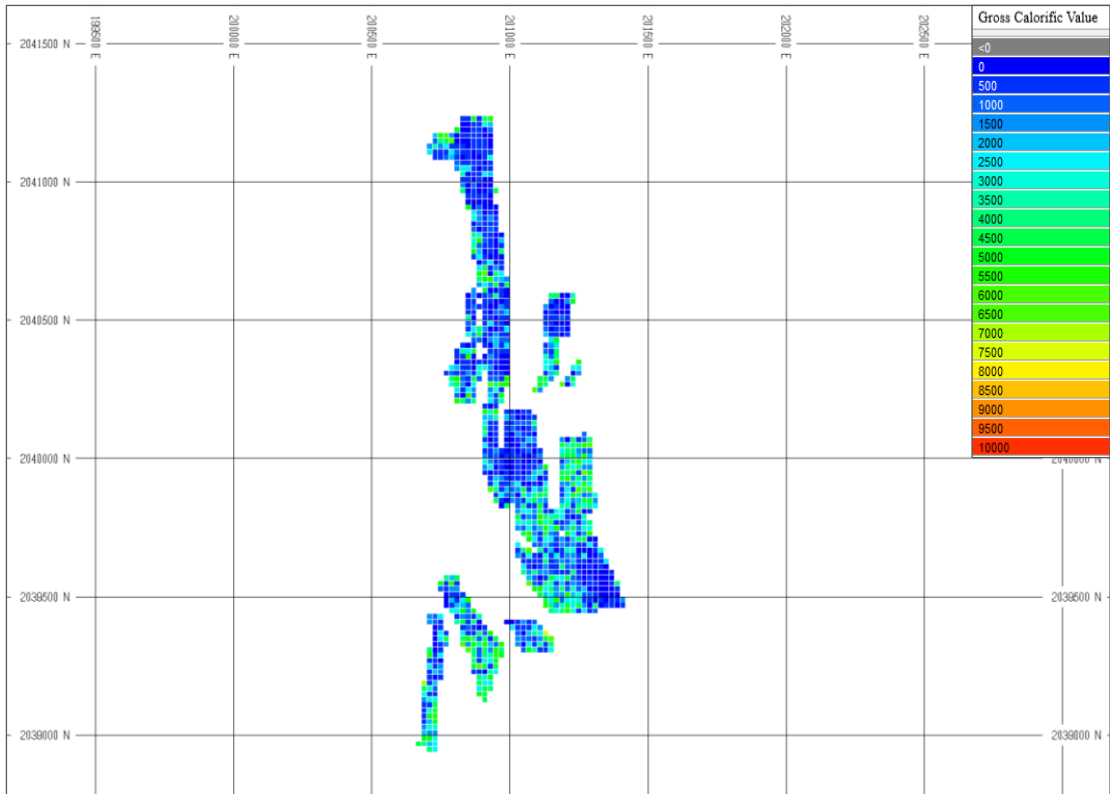


Figure 4.35 Map of realization No. 3 of CV.

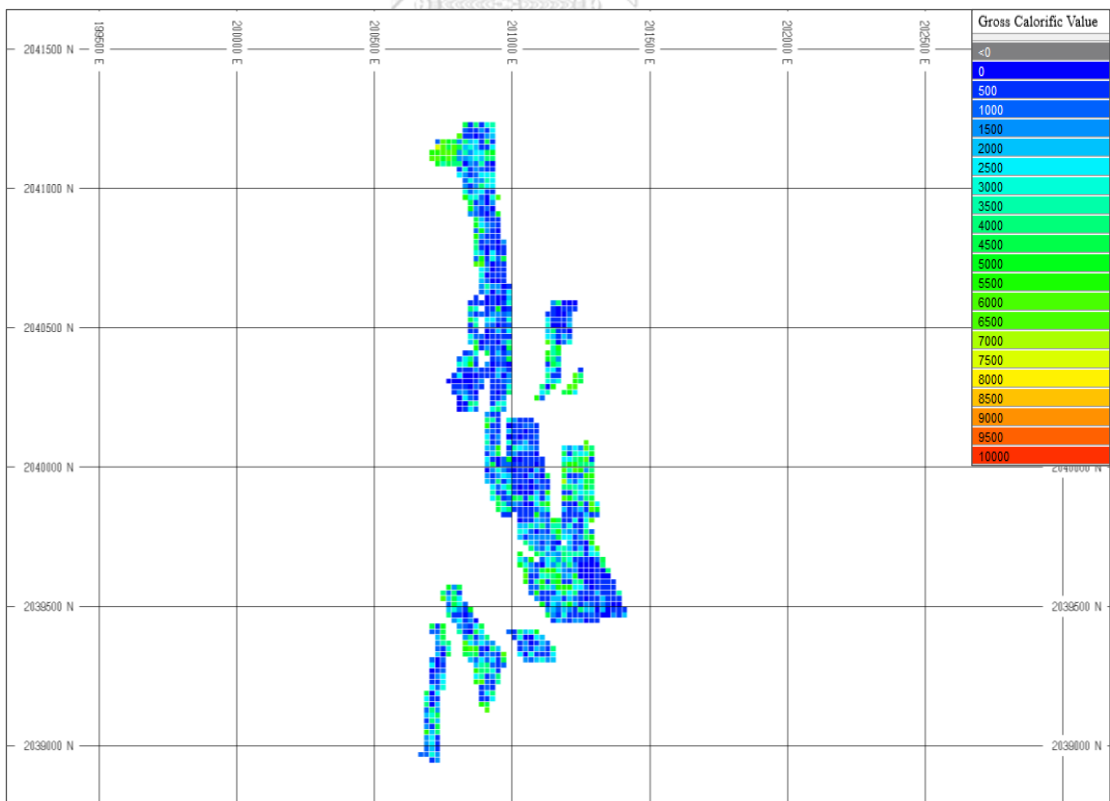


Figure 4.36 Map of realization No. 4 of CV.

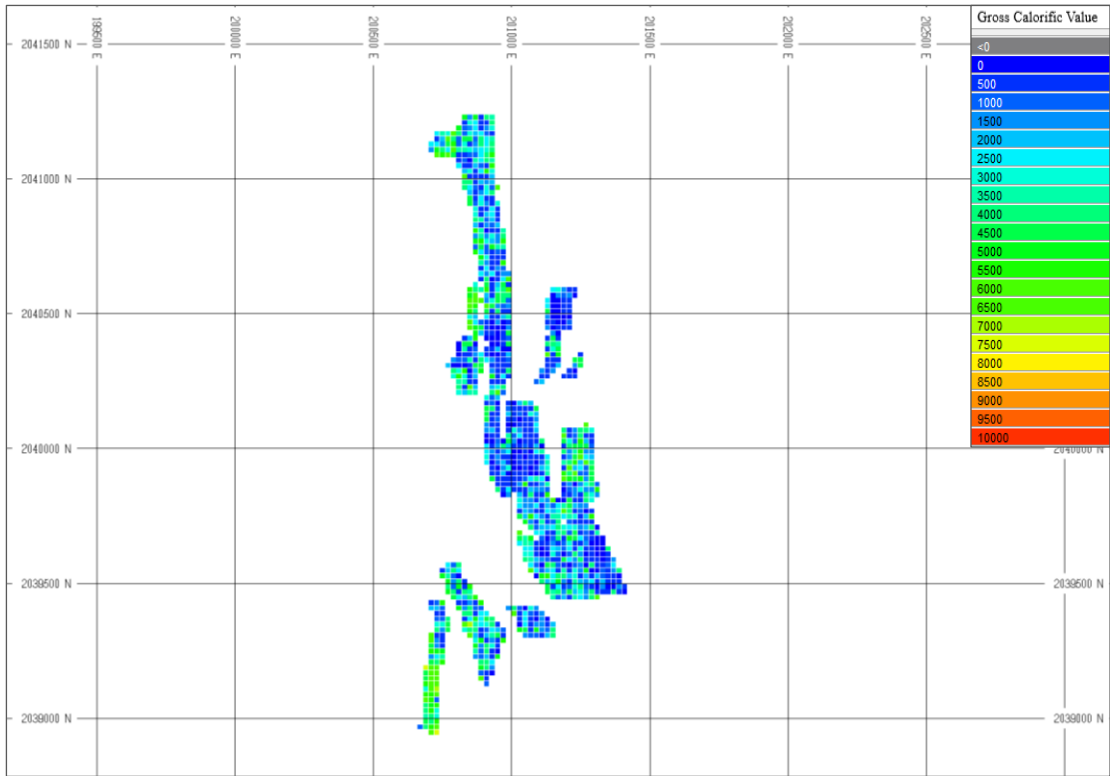


Figure 4.37 Map of realization No. 5 of CV.

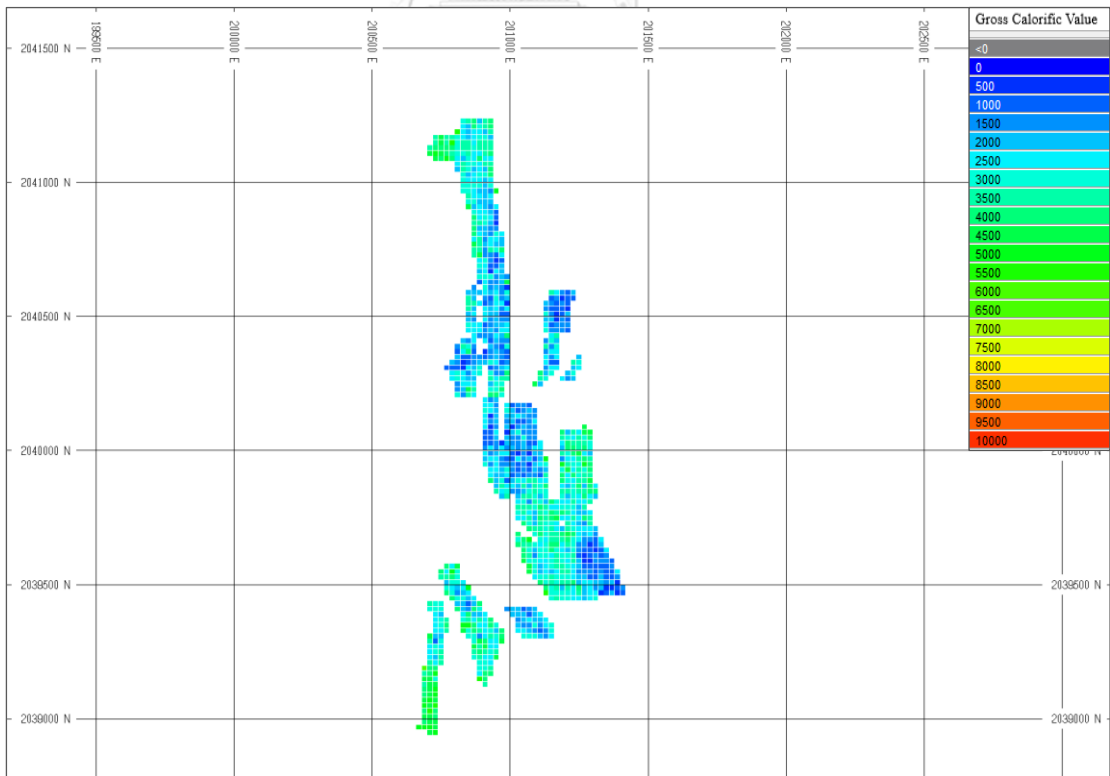


Figure 4.38 Map of E-Type Map (Mean) of CV.

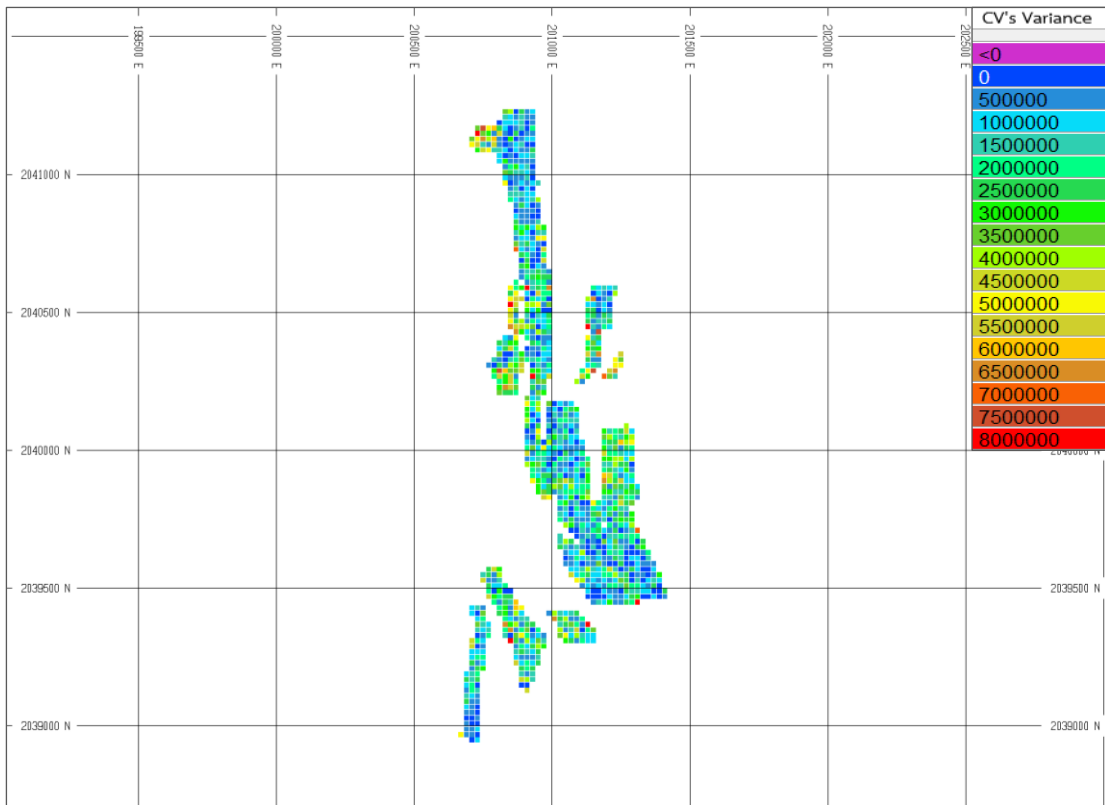


Figure 4.39 Map of variance map of CV.

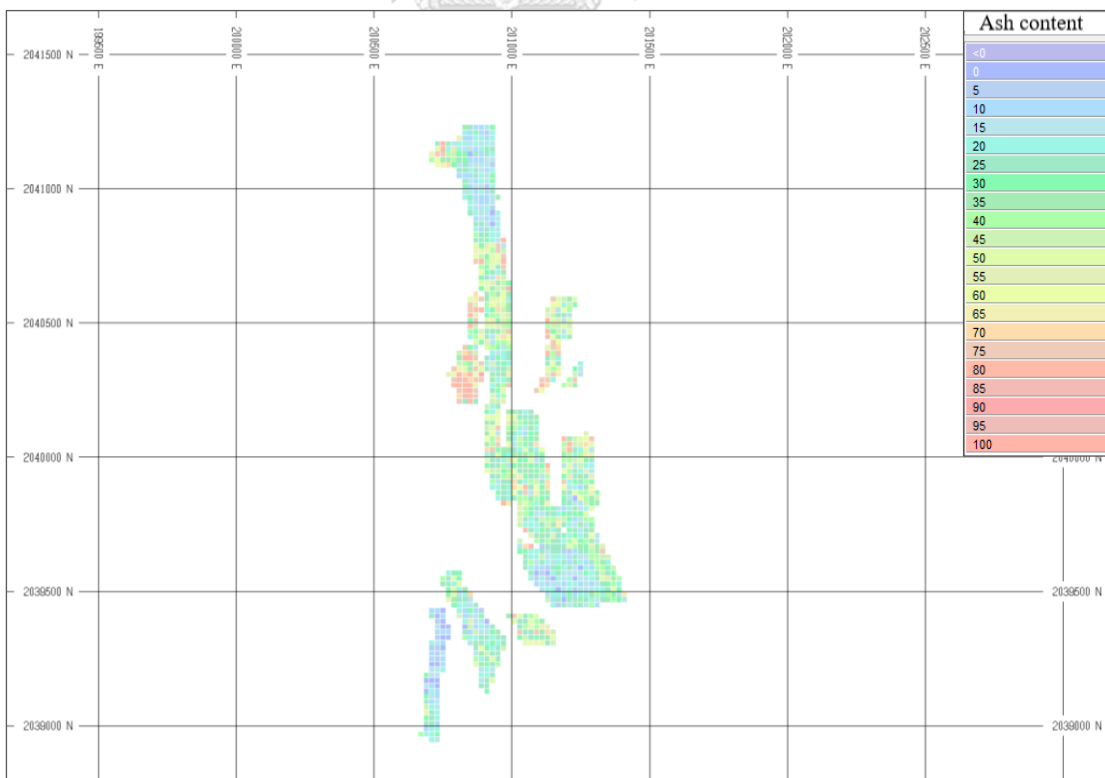


Figure 4.40 Map of realization No. 1 of AC.

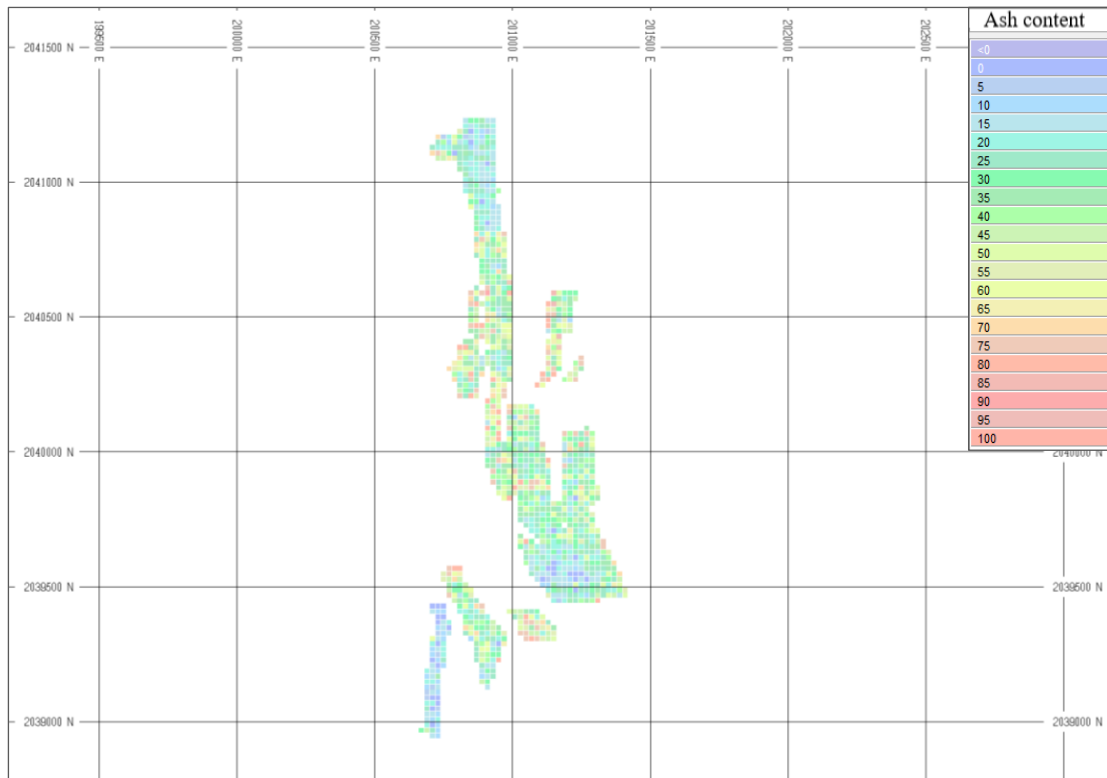


Figure 4.41 Map of realization No. 2 of AC.

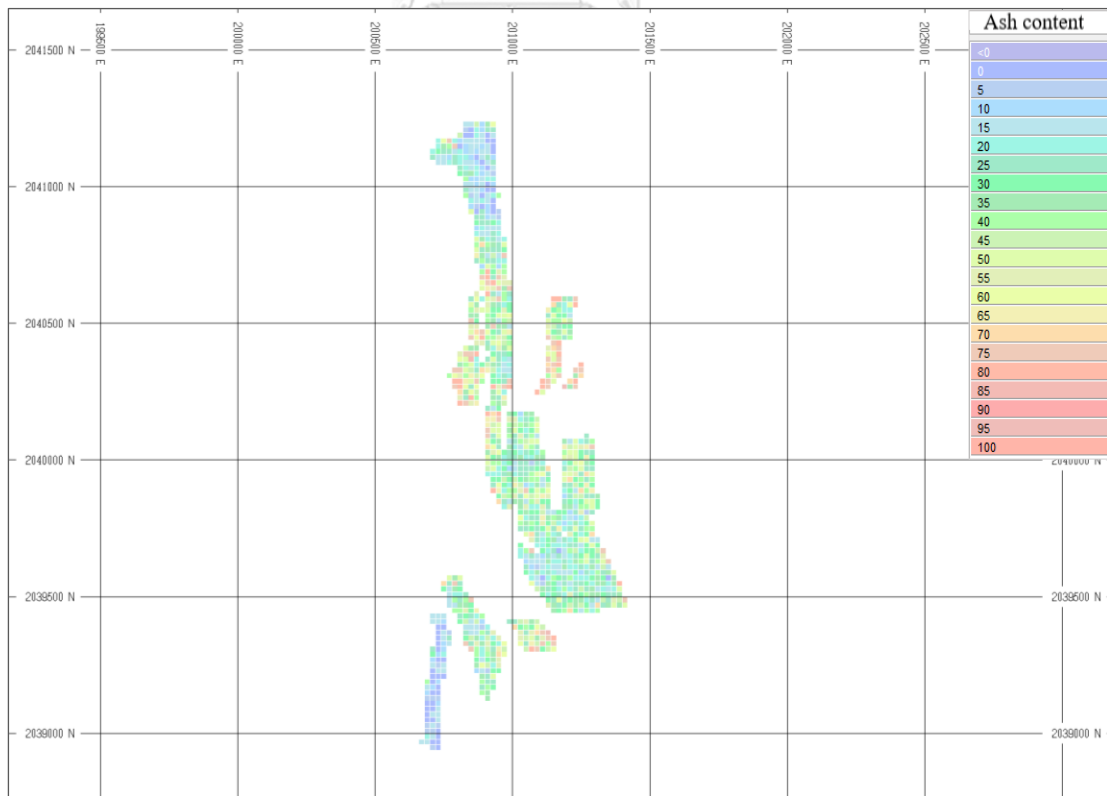


Figure 4.42 Map of realization No. 3 of AC.

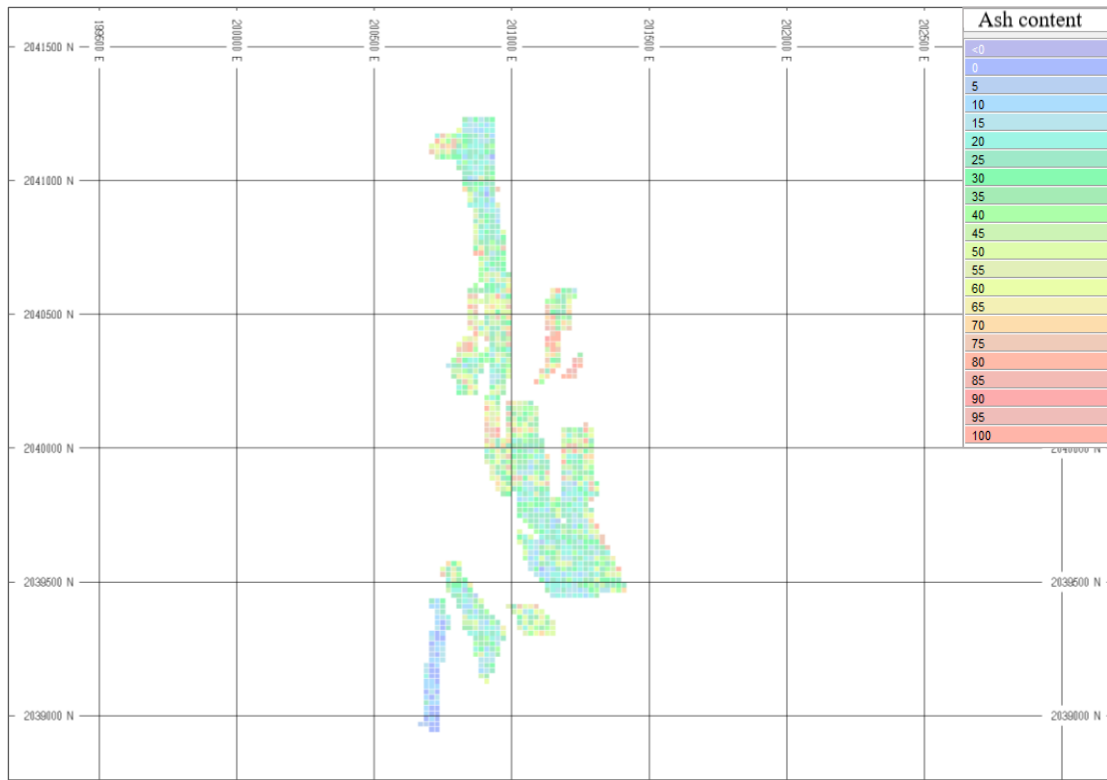


Figure 4.43 Map of realization No. 4 of AC.

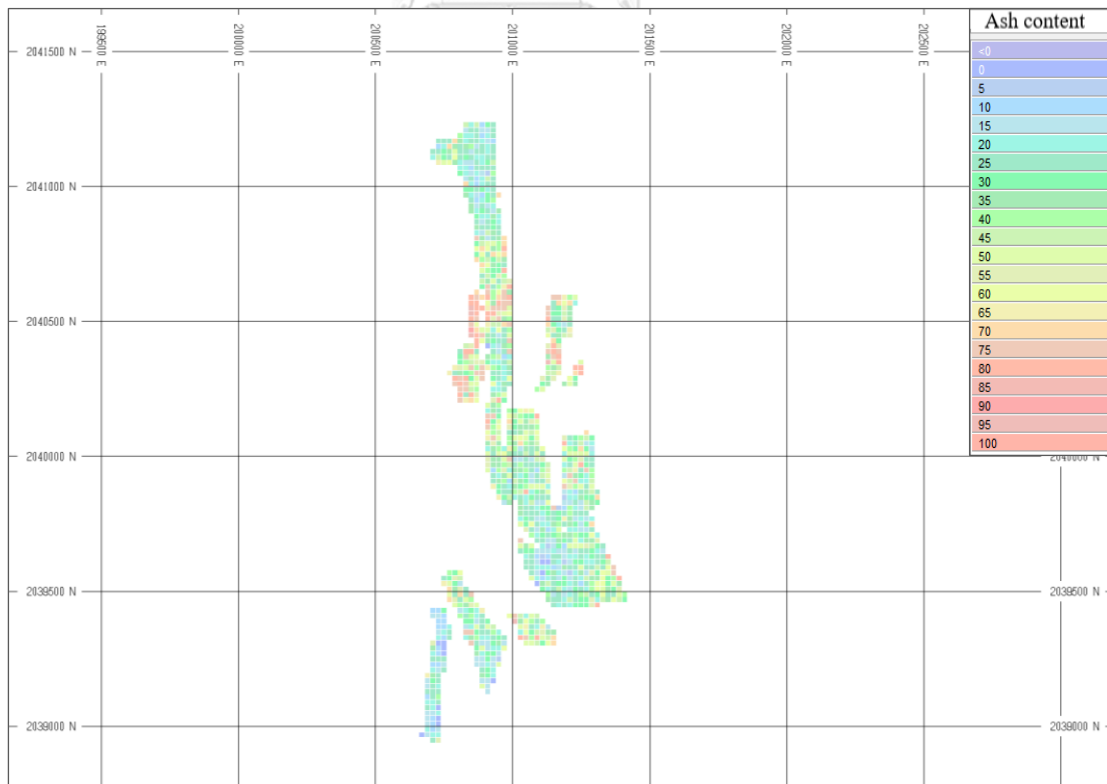


Figure 4.44 Map of realization No. 5 of AC.

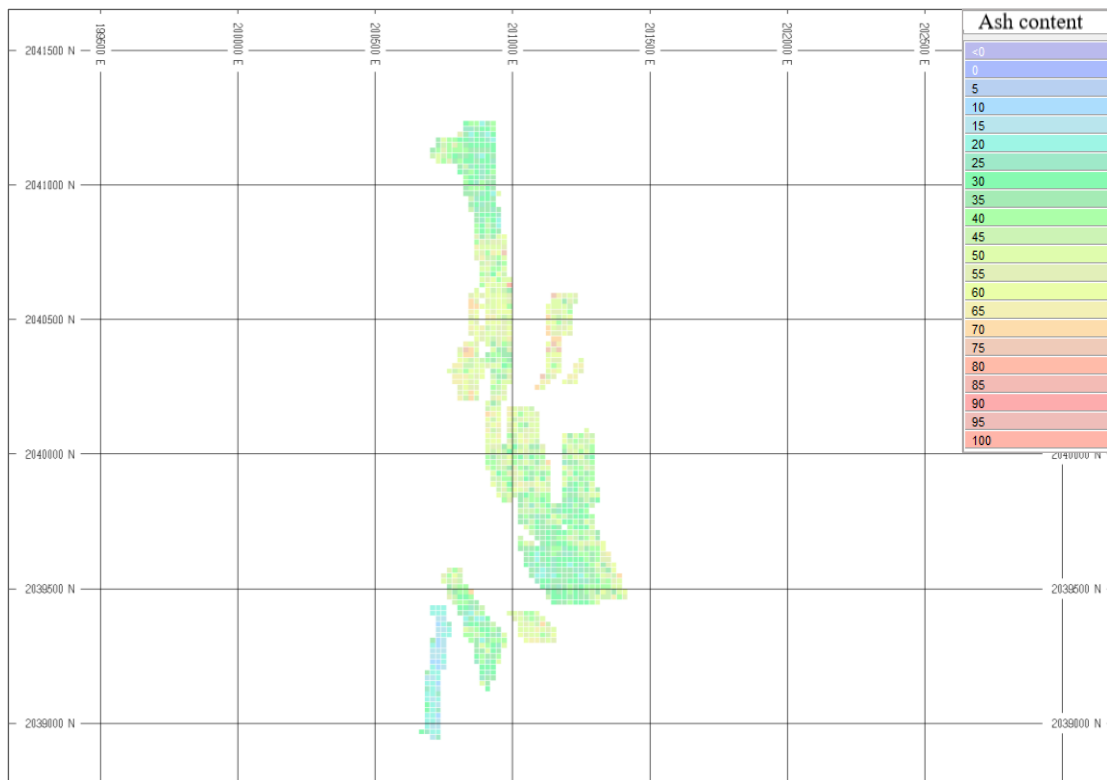


Figure 4.45 Map of E-Type Map (Mean) of AC.



Figure 4.46 Map of variance map of AC.

As mentioned previously, the statistical analysis (histogram) of CV and AC of each realization was carried out prior to E-Type map construction. Therefore, the statistical parameters of both variables are comparable, which illustrated in Table 4.21 and Table 4.22.

Table 4.21 Comparison of statistical parameters of CV for 5 realizations.

Real No.	Min	Max	Mean	Variance	Standard deviation	Coef. of variation
Real 1	0.5	7,999.85	3,348.05	4,427,969	2,104.27	0.63
Real 2	1.45	7,998.62	3,633.40	4,343,488	2,084.10	0.57
Real 3	0.00	7,991.13	3,319.09	4,430,863	2,104.96	0.63
Real 4	0.14	7,945.12	3,724.54	4,292,047	2,071.73	0.56
Real 5	0.21	8,000.00	4,043.44	4,385,375	2,094.13	0.52

Table 4.22 Comparison of statistical parameters of AC for 5 realizations.

Real No.	Min	Max	Mean	Variance	Standard deviation	Coefficient of variation
Real 1	0.01	99.98	46.498	475.30	21.80	0.47
Real 2	0.01	99.94	49.231	481.49	21.94	0.55
Real 3	0.00	99.99	46.957	491.41	22.17	0.47
Real 4	0.00	99.98	50.066	496.05	22.27	0.44
Real 5	0.33	99.98	52.139	463.70	21.53	0.41

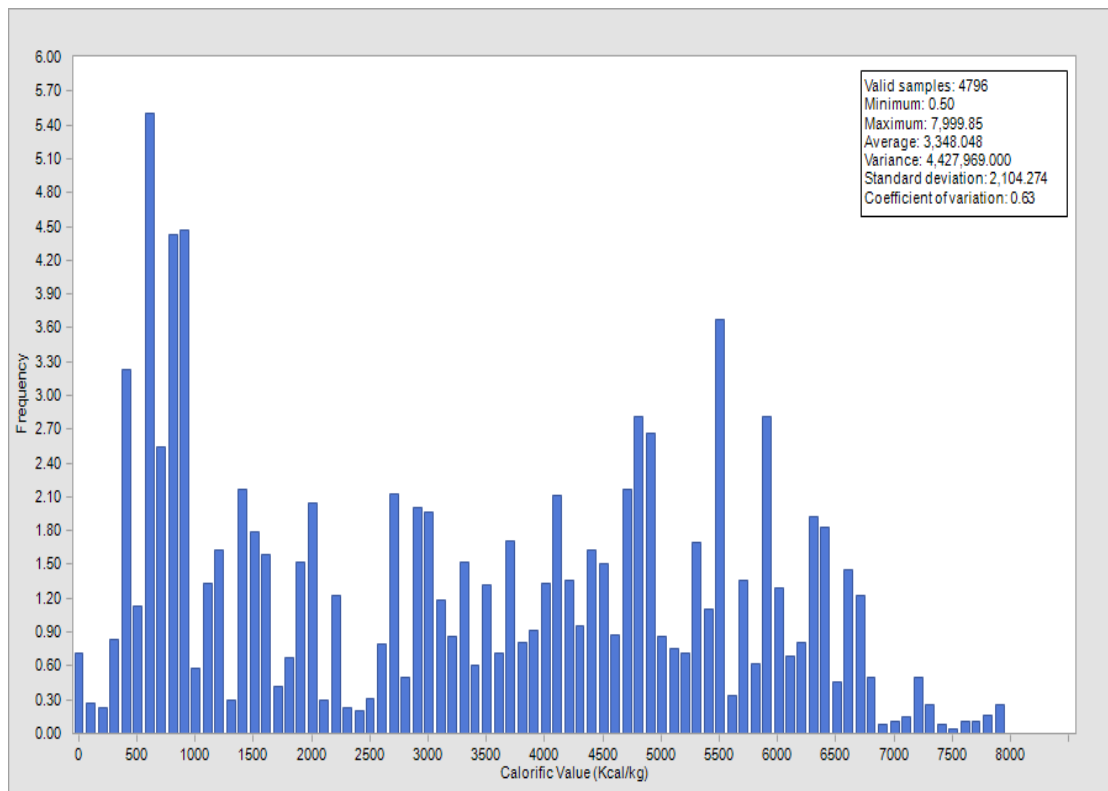


Figure 4.47 Histogram plot of CV's realization No.1.

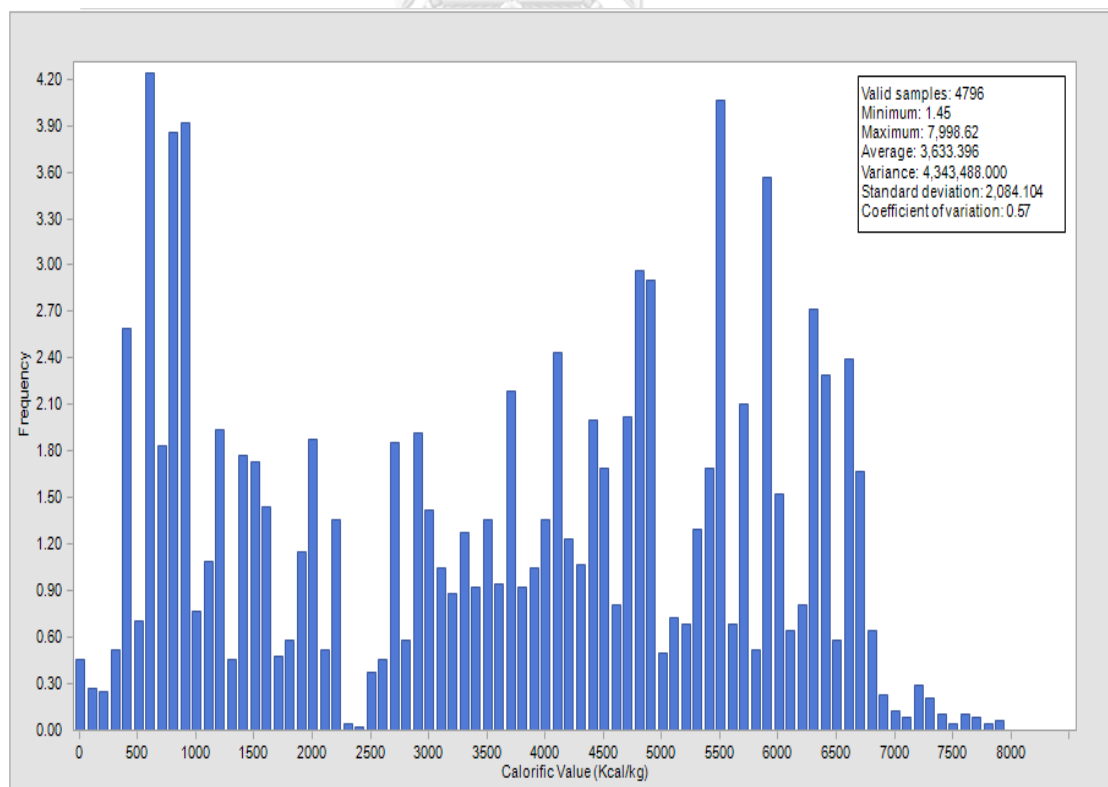


Figure 4.48 Histogram plot of CV's realization No.2.

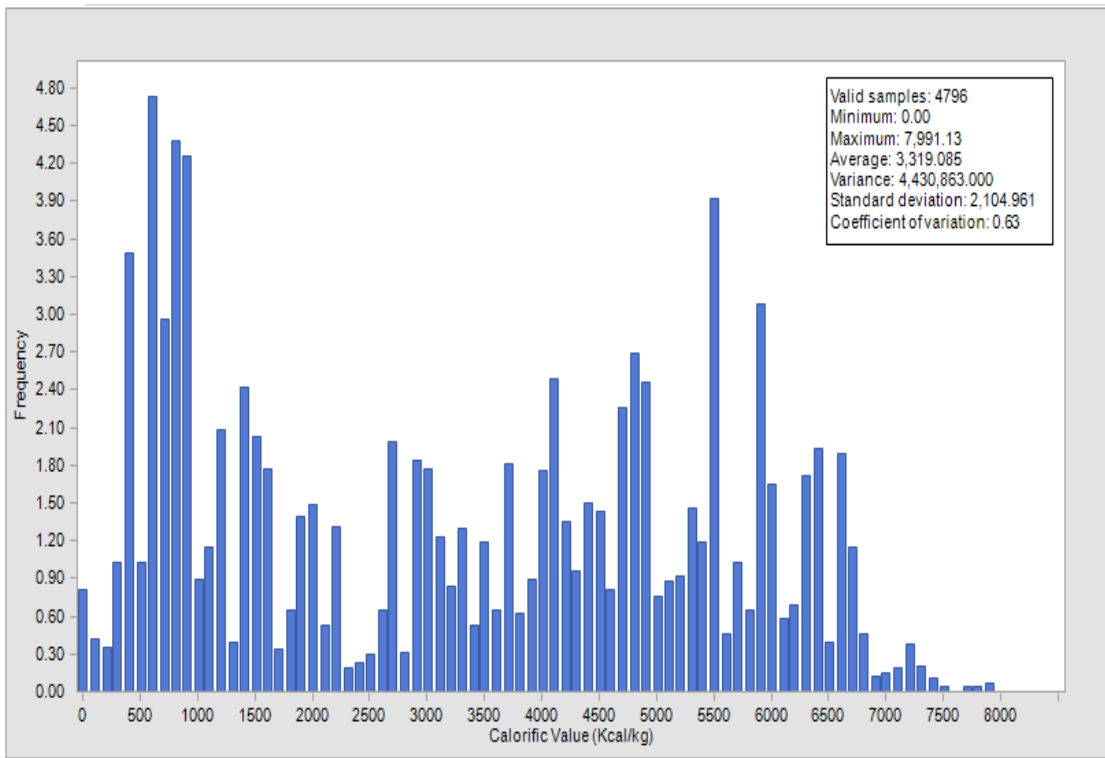


Figure 4.49 Histogram plot of CV's realization No.3.

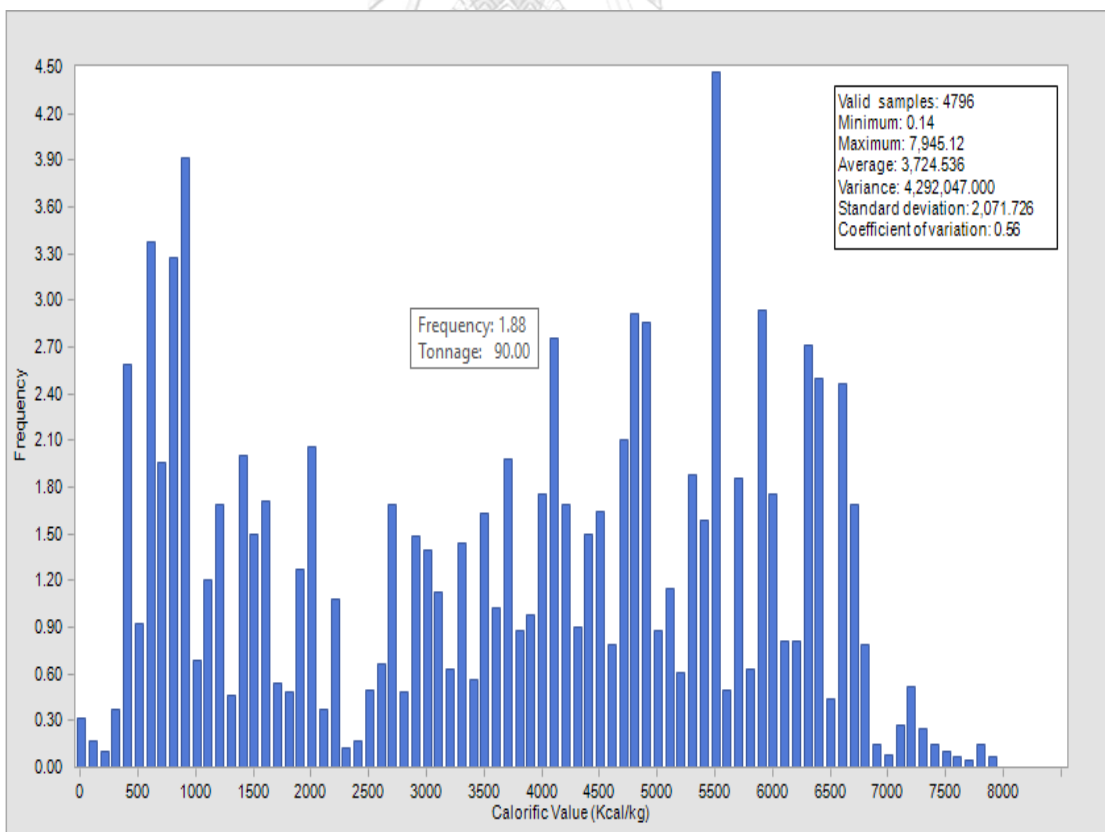


Figure 4.50 Histogram plot of CV's realization No.4.

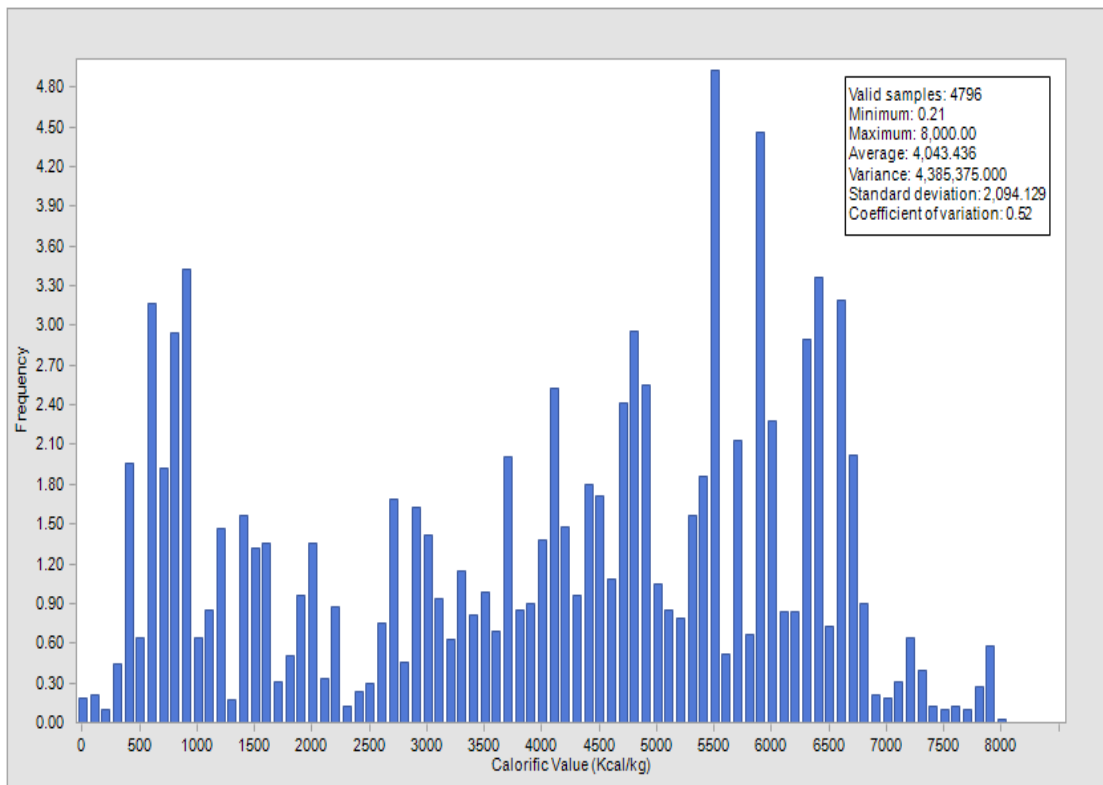


Figure 4.51 Histogram plot of CV's realization No.5.

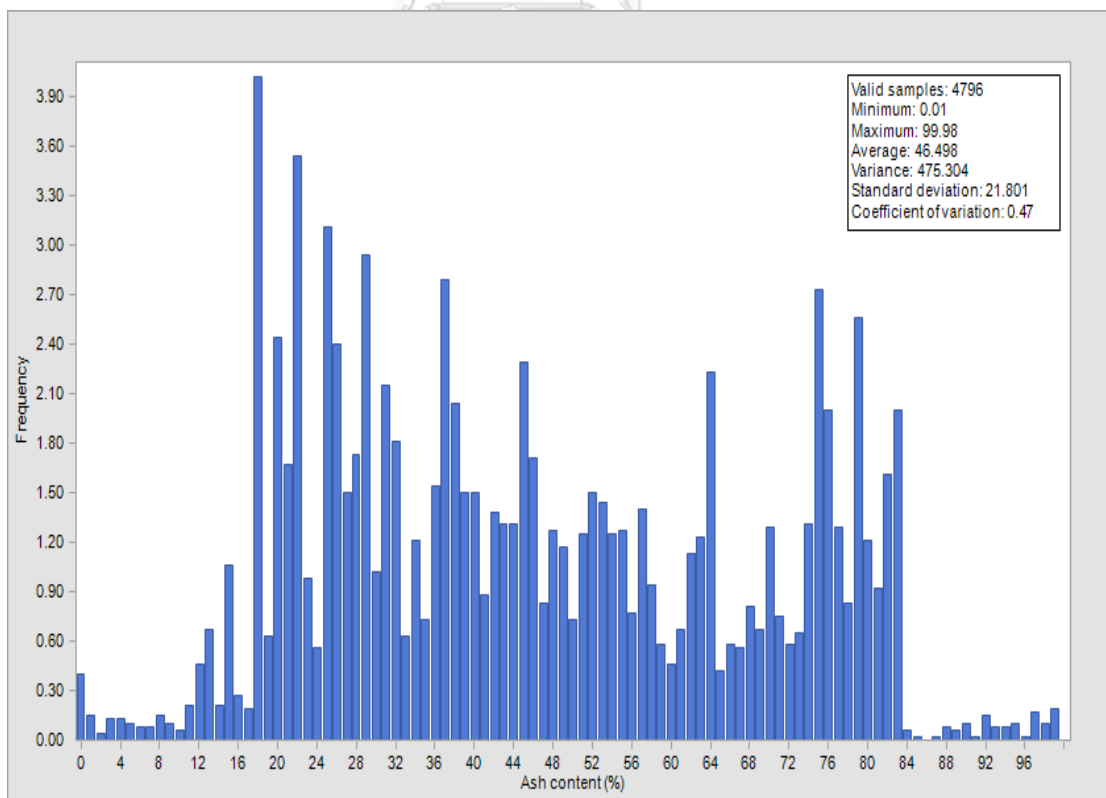


Figure 4.52 Histogram plot of AC's realization No.1.

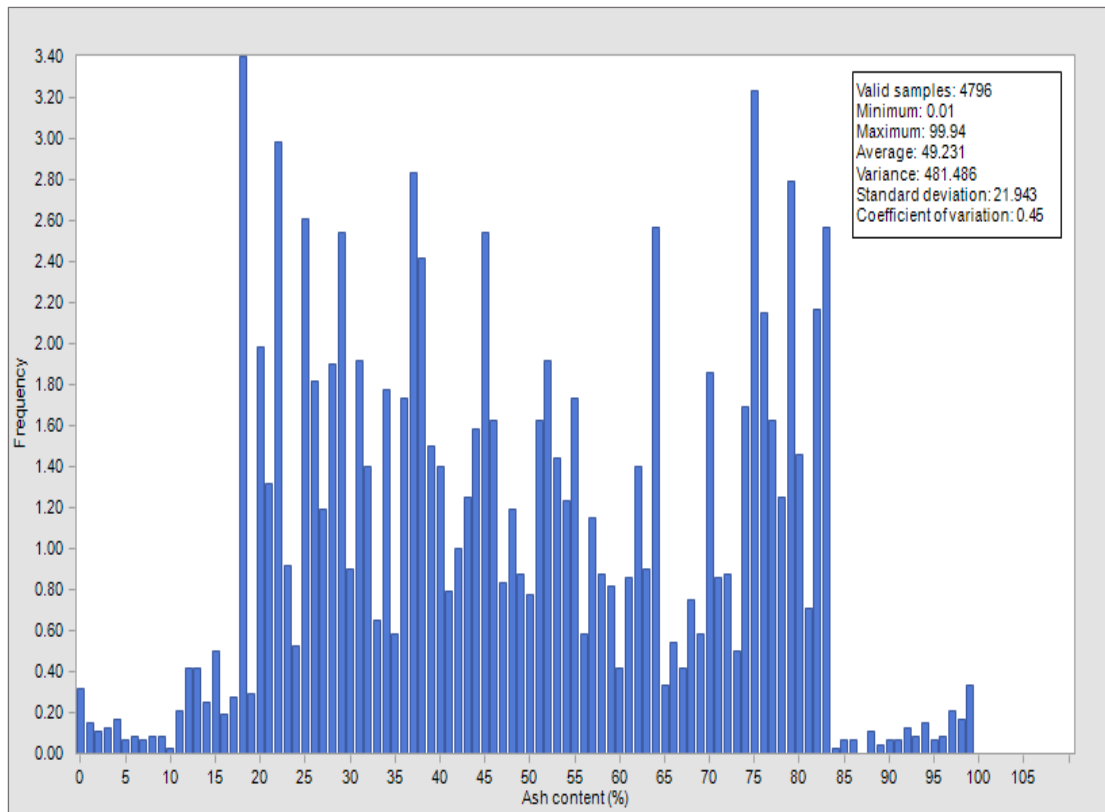


Figure 4.53 Histogram plot of AC's realization No.2.

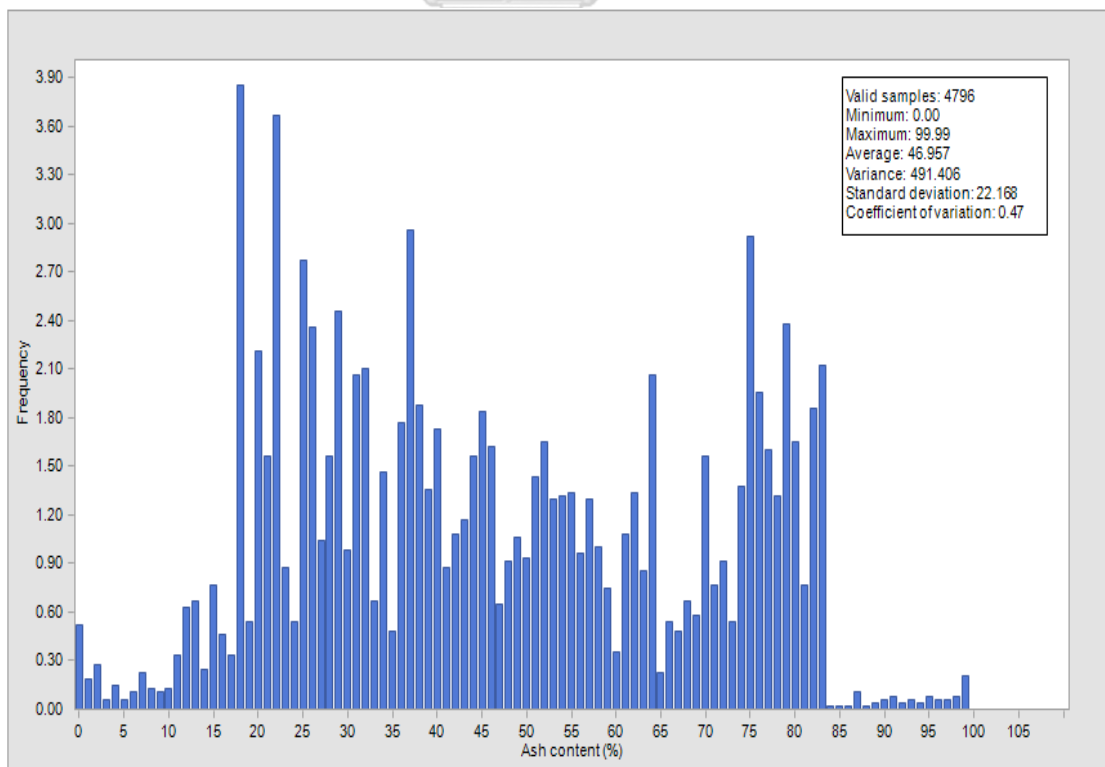


Figure 4.54 Histogram plot of AC's realization No.3.

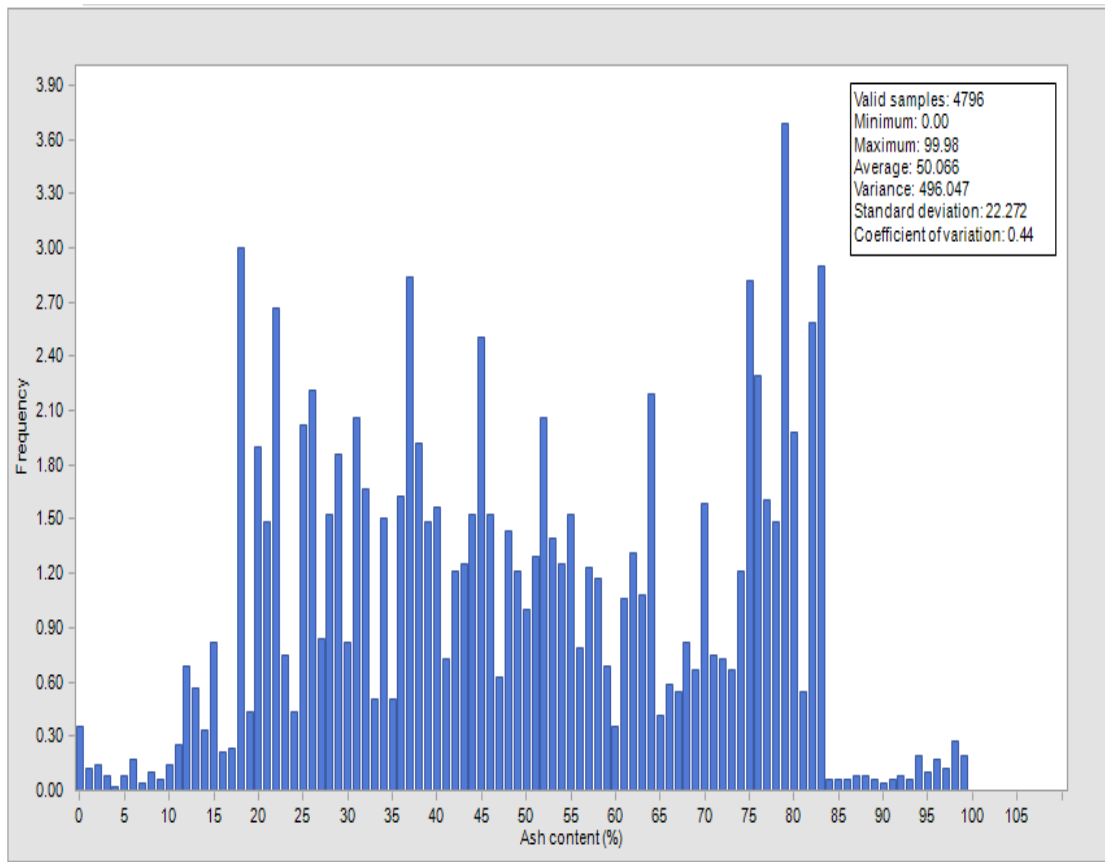


Figure 4.55 Histogram plot of AC's realization No.4.

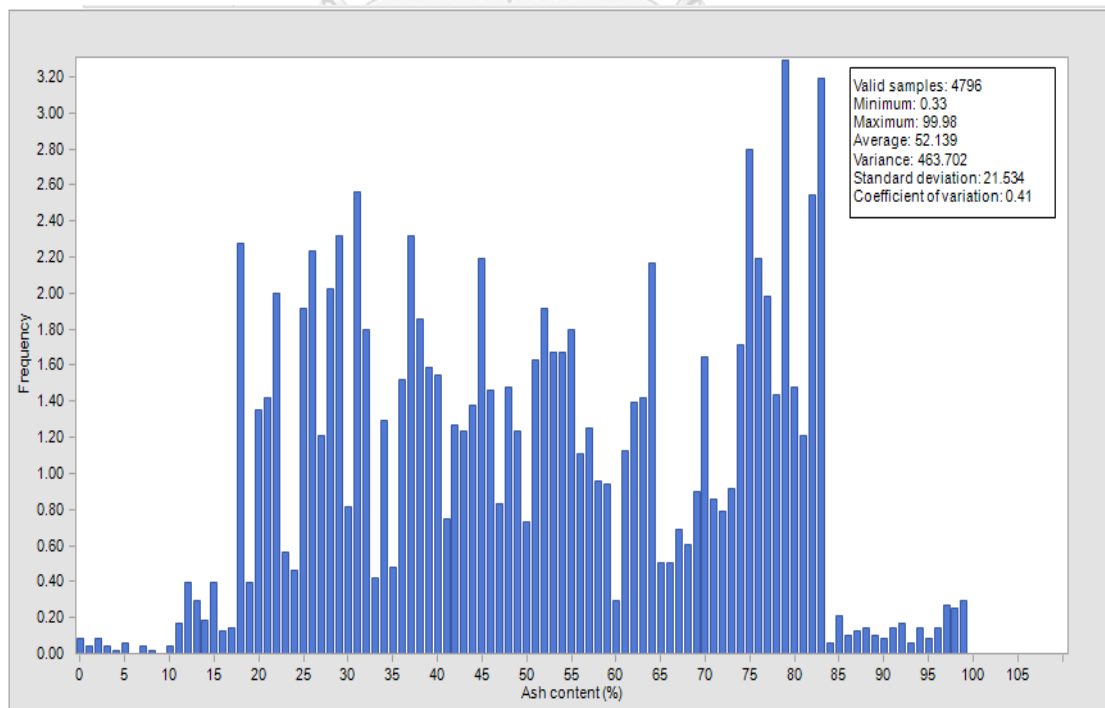


Figure 4.56 Histogram plot of AC's realization No.5.

4.5.3. SGS's Pit optimization and mineable reserves estimation

In this process, the simulated CV averaged from 5 realization maps were used in order to compute the block value for pit optimization. The results show that there are nine optimal pits generated by LG algorithm as shown in Figure 4.57. The most optimum pits consist of narrow pit floor width which caused by the thin coal seams and high-quality variations. The LG pits consist of the lowest bench level at 170 meters above msl. The 2D cross section views of these nine optimal pits are shown in Figures 4.58 – 4.62.

The mineable reserve calculated from optimal pits are 0.65 Mts with an average CV of 3,511.9 kcal/kg, and an average AC of 45.4 %. The mineable reserve presents only 30 % from the original geological resource. The reasons for a huge decrease of mineable reserve are the coal qualities and thickness uncertainties. SGS's mineable reserves are very similar to OK's mineable reserve, only one percent difference. The SGS's total waste materials from all optimum pits are 5.7 Mts, which yielded the stripping ratio to 4.84:1. The SGS's mineable reserve based on CV basis and bench level can be seen in Table 4.23 and Table 4.24, respectively.

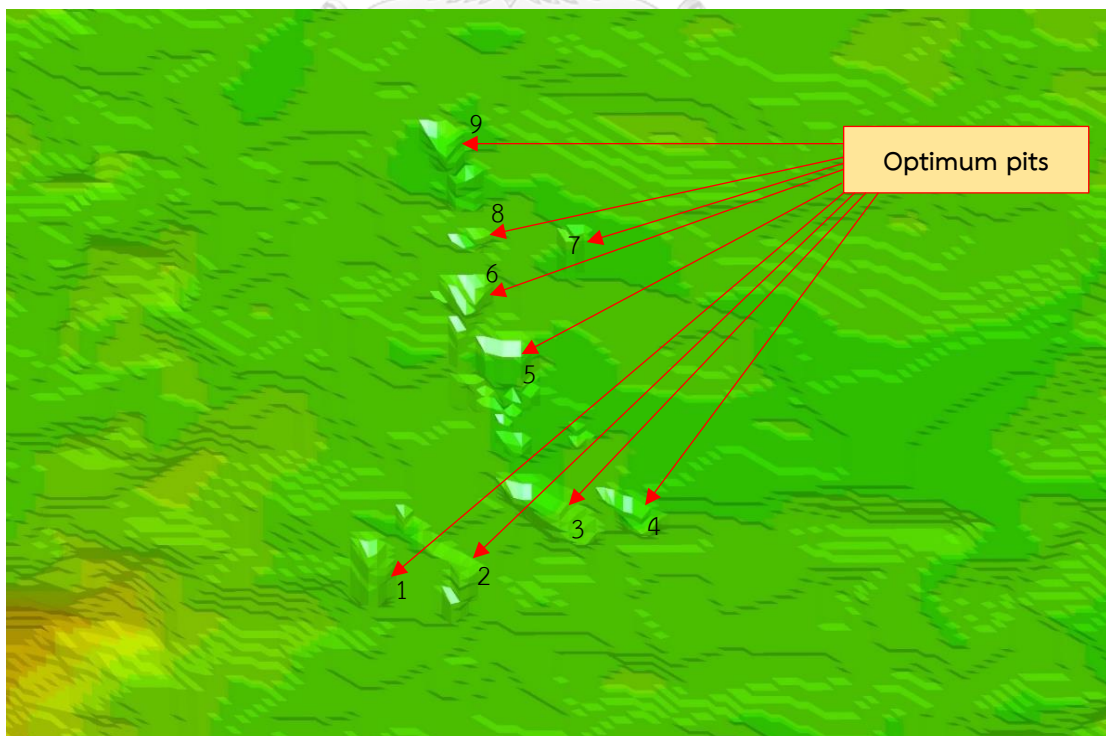


Figure 4.57 SGS's nine ultimate pits from pit optimization.

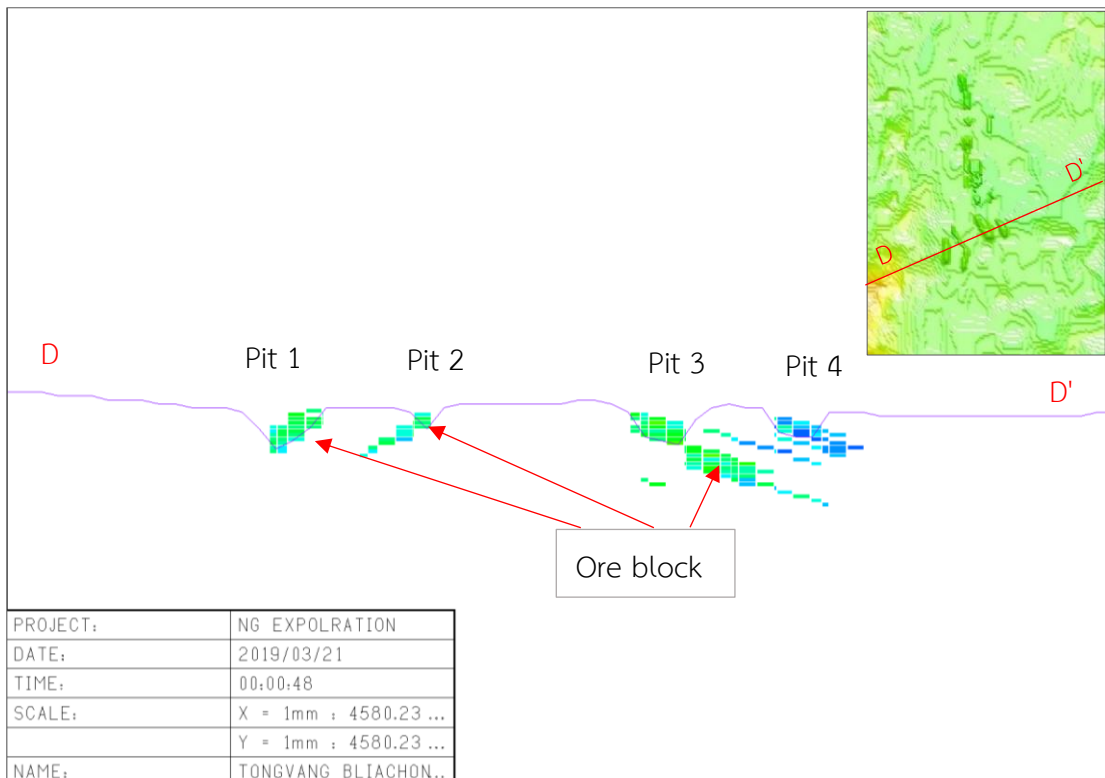


Figure 4.58 2D cross section views of SGS's pits No. 1, 2, 3, and 4.

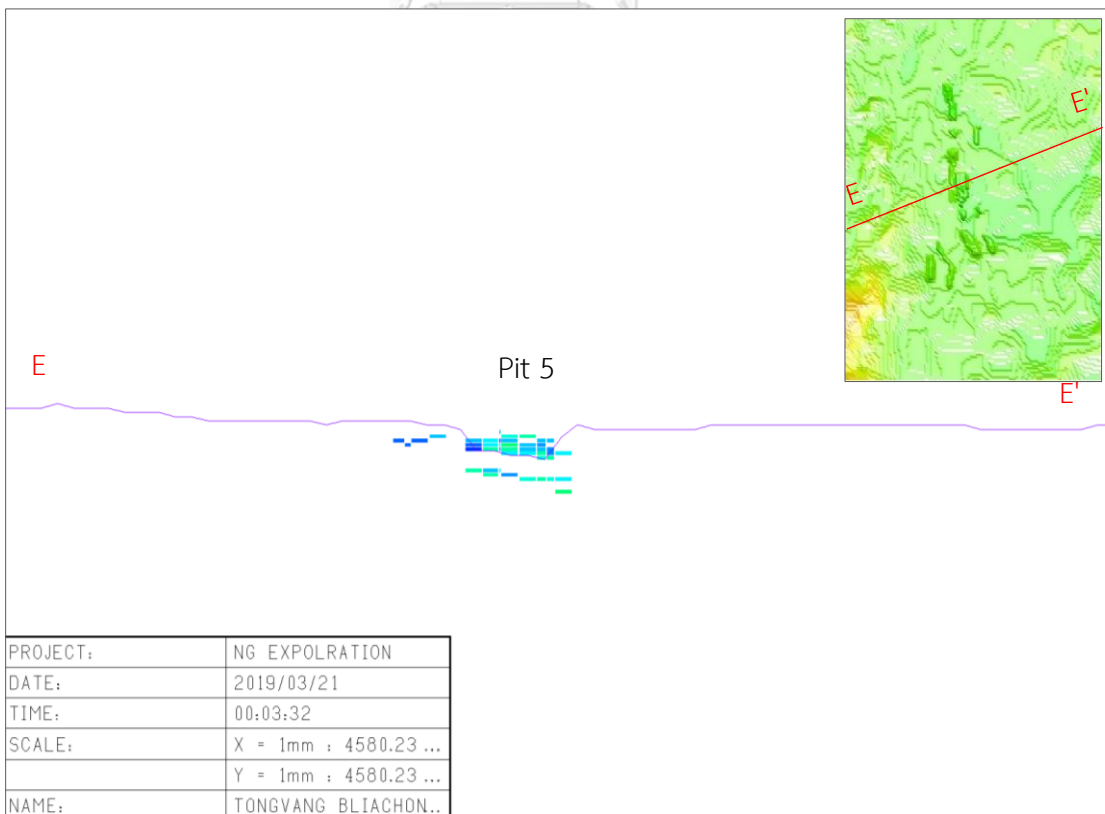


Figure 4.59 2D cross section views of SGS's pit No. 5.

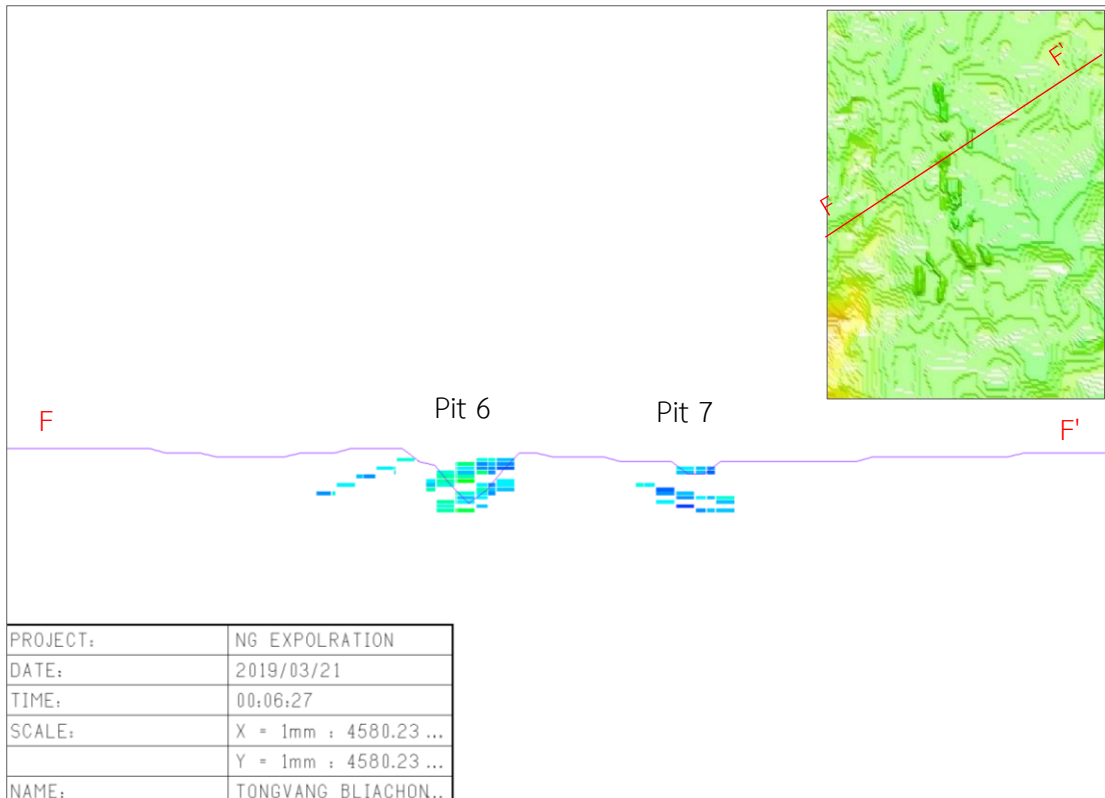


Figure 4.60 2D cross section views of SGS's pits No. 6 and 7.

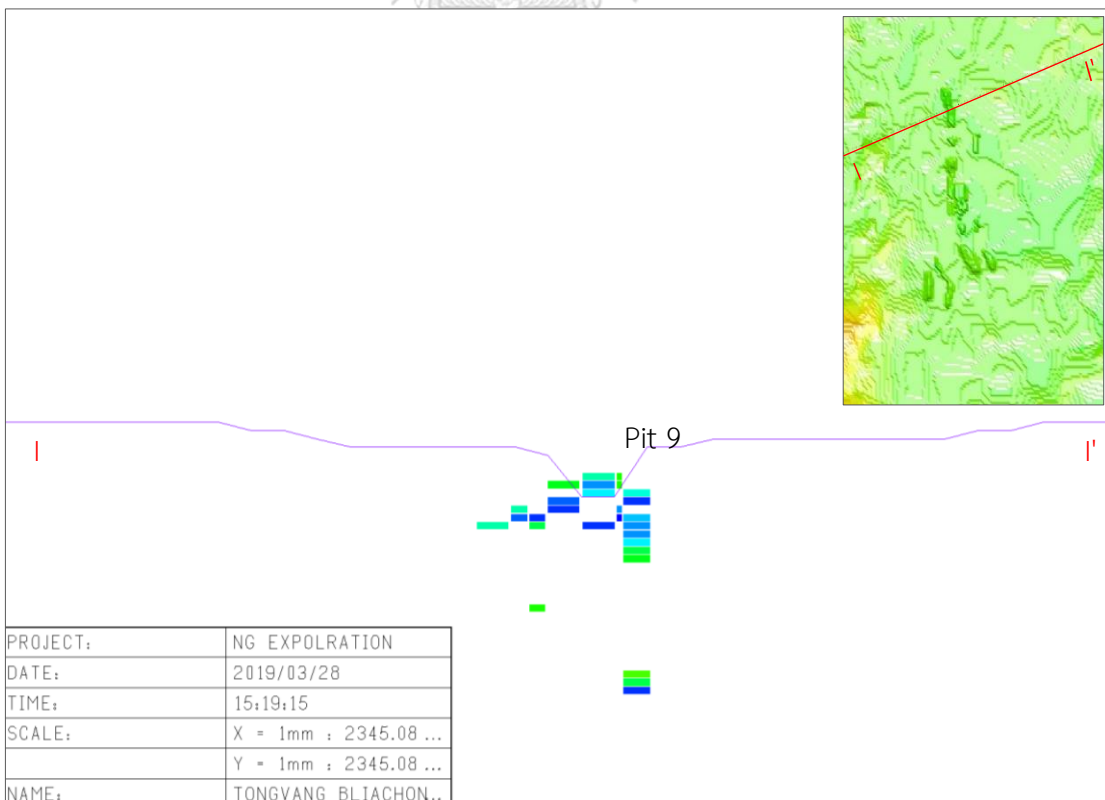


Figure 4.61 2D cross section view of SGS's pit No. 9.

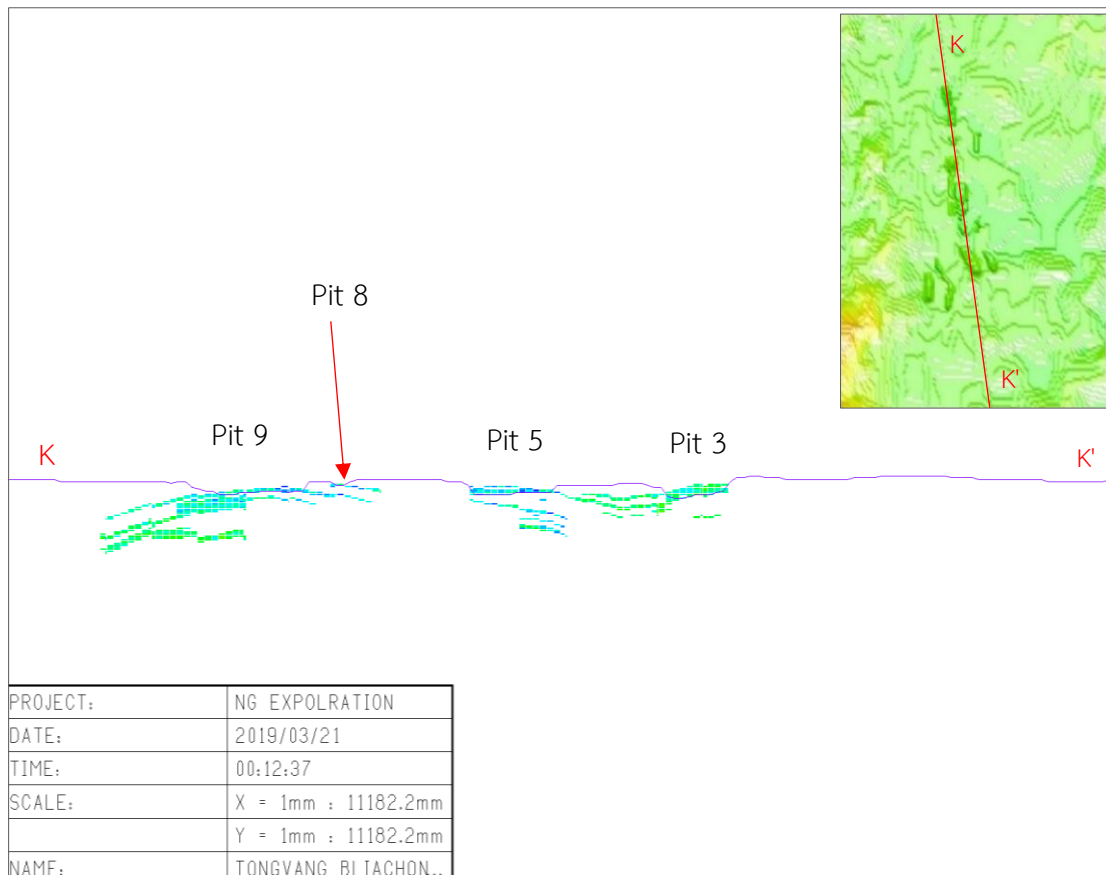


Figure 4.62 2D cross section of long section views of SGS's pits.

Table 4.23 The SGS's mineable reserves from multiple optimal pits by CV basis.

CV basis (kcal/kg)	V_c (m ³)	D_c (T/m ³)	Q_c (T)	Average grade	
				CV (kcal/kg)	AC (%)
500-4000	375,927	1.15	432,316.05	2,913.51	45.52
4000-5000	145,539	1.15	167,369.85	4,445.64	43.48
5000-5500	32,536	1.15	37,416.40	5,203.45	47.50
>= 5500	14,602	1.15	16,792.30	5,841.09	56.15
Total	568,604	1.15	653,894.6	3,511.88	45.39

Table 4.24 SGS's mineable reserve from nine optimum pits generated by LG algorithm by bench level.

Bench level	Minable reserve			Average grade		Waste material			SR (BCM: T)
	V _c (m ³)	D _c (T/m ³)	Q _c (T)	CV (kcal/kg)	AC (%)	V _w (m ³)	D _w (T/m ³)	Q _w (T)	
230	-	-	-	-	-	4,625.00	1.8	8,325.00	-
225	550	1.15	632.50	4,689.97	54.68	139,473.00	1.8	251,051.40	253.59
220	15,912	1.15	18,298.80	3,607.31	44.90	401,622.00	1.8	722,919.60	25.24
215	47,298	1.15	54,392.70	3,773.80	46.15	616,523.00	1.8	1,109,741.40	13.03
210	77,824	1.15	89,497.60	3,511.01	46.05	609,948.00	1.8	1,097,906.40	7.84
205	103,262	1.15	118,751.30	3,409.27	46.92	490,738.00	1.8	883,328.40	4.75
200	108,476	1.15	124,747.40	3,385.87	46.89	351,524.00	1.8	632,743.20	3.24
195	96,620	1.15	111,113.00	3,399.84	46.02	255,380.00	1.8	459,684.00	2.64
190	59,133	1.15	68,002.95	3,576.26	43.87	156,867.00	1.8	282,360.60	2.65
185	35,311	1.15	40,607.65	3,734.53	40.05	86,689.00	1.8	156,040.20	2.46
180	16,129	1.15	18,548.35	4,053.58	37.52	37,871.00	1.8	68,167.80	2.35
175	7,534	1.15	8,664.10	3,603.24	36.55	12,466.00	1.8	22,438.80	1.65
170	555	1.15	638.25	2,628.90	52.15	1,445.00	1.8	2,601.00	2.6
Total	568,604	1.15	653,894.6	3,511.88	45.39	3,165,171.00	1.8	5,697,307.8	4.84

4.5.4. SGS's Pits adjustment, mineable reserve and Grade-Tonnage Curve

The nine optimum pits were designed and adjusted using the minimum pit floor width of 23 meters similarly to Kriging approach. The pit design parameters are illustrated in Table 3.5. In this study, the lowest bench level of SGS's adjusted pits is 180 meters. The proximity pits were combined to create a larger pit allowing the practical mining operation. There are finally five pits created in the pit design and adjustment process. The top and bottom views of 5 adjusted pits are shown in Figure 4.63 – 4.64. The 2D cross section of SGS's pits No. 1 – 5 are shown in Figure 4.65 – 4.67. The mineable reserve from five adjusted pits shown in Table 4.25 by CV basis.

The GTC construction using SGS's mineable reserve was constructed by defining 21 various grades similar to Ordinary Kriging method. The various grades begin at 500 kcal/kg to 5,500 kcal/kg with 250 kcal/kg increasement simultaneously as shown in Figure 4.68. The mineable reserves of 5 pits are presented in Table 4.26 – 4.29 and the stripping ratio among those pits is 10.12: 1 (BCM: T).

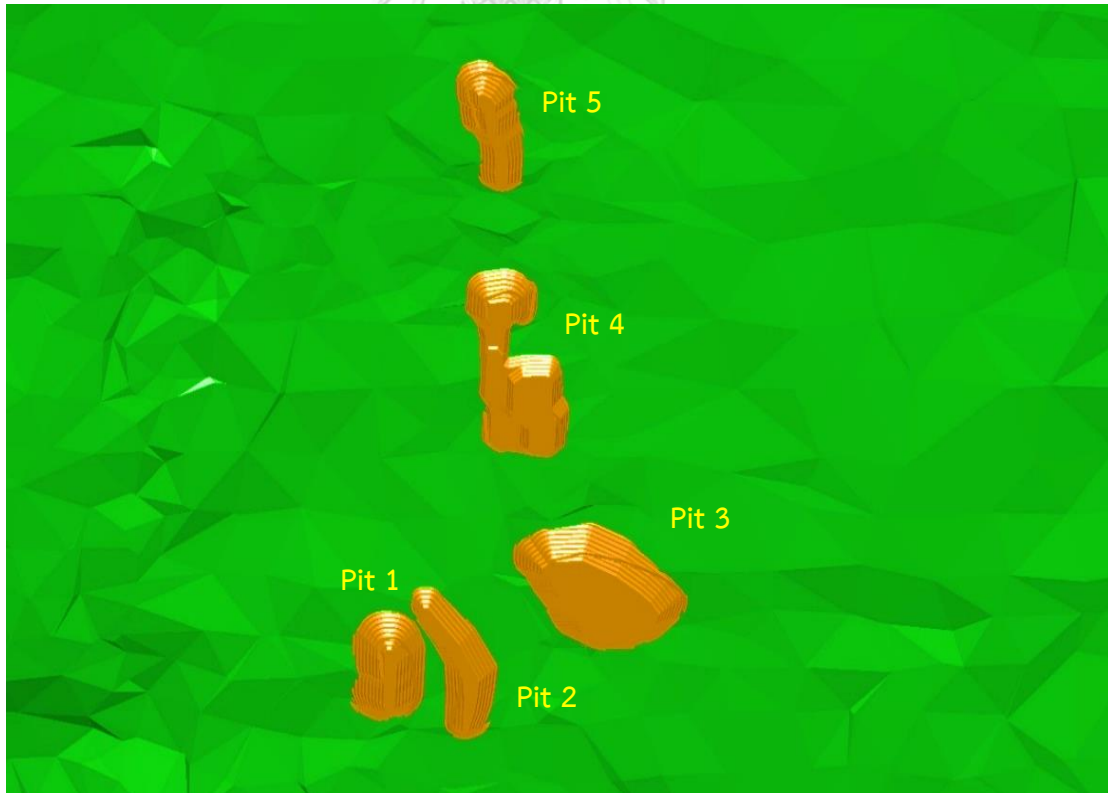


Figure 4.63 Top view of SGS's 5 adjusted pits generated by LG algorithm.

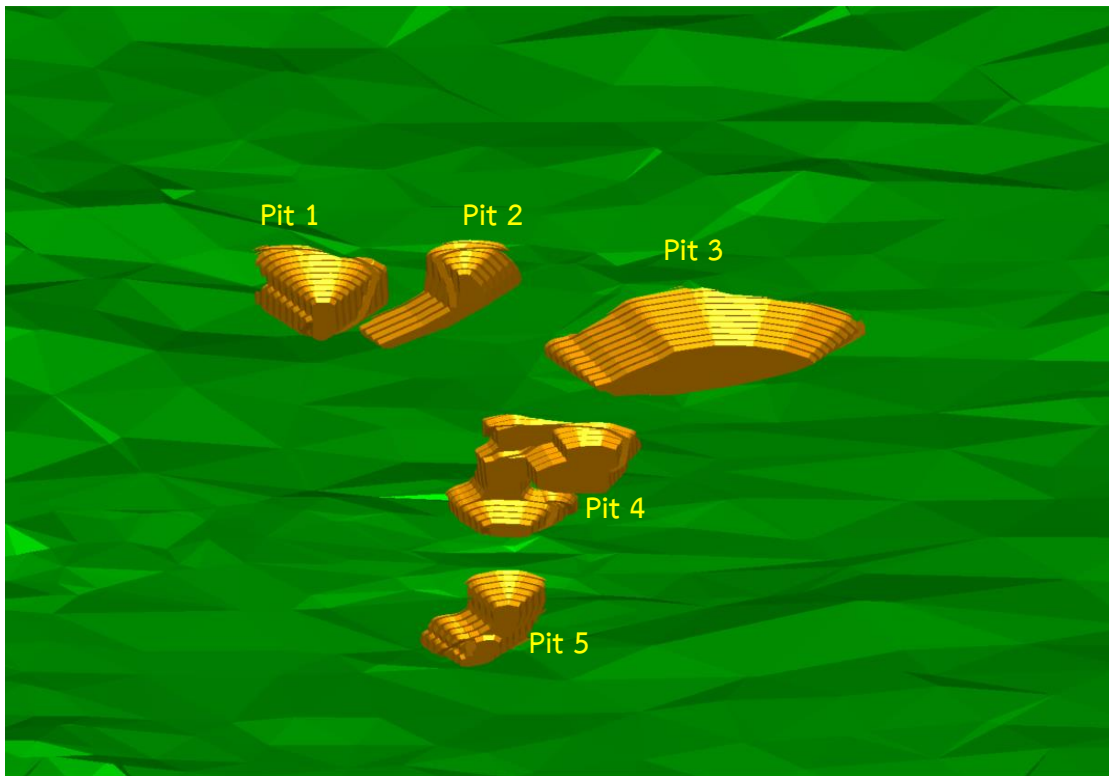


Figure 4.64 Bottom view of SGS's pit adjustment from multiple optimal pits

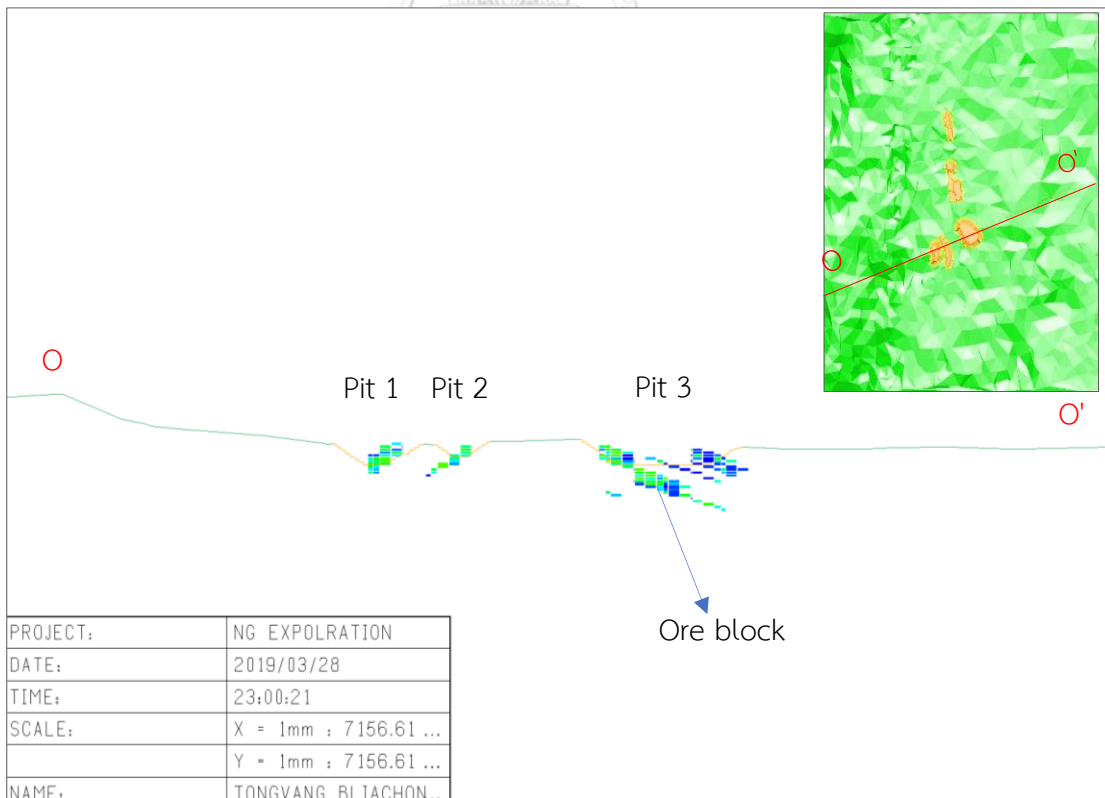


Figure 4.65 2D cross section views of SGS's pits No.1, 2 and 3.

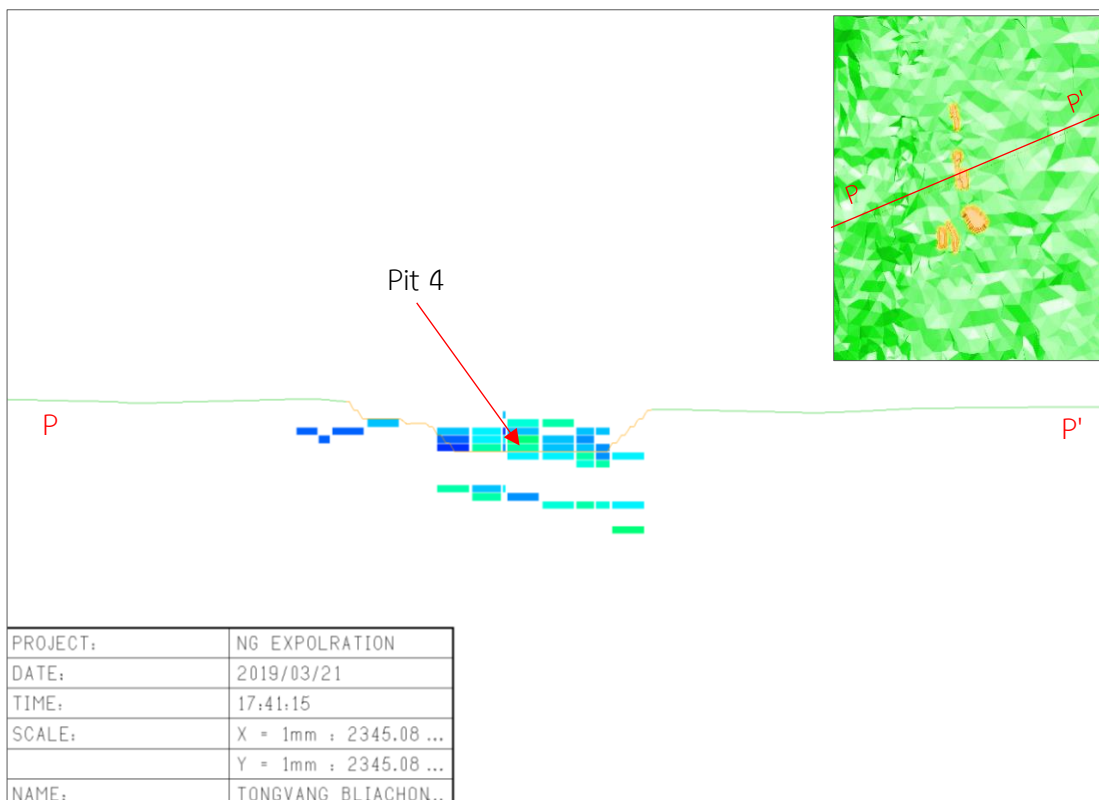


Figure 4.66 2D cross section views of SGS's pit No.4.

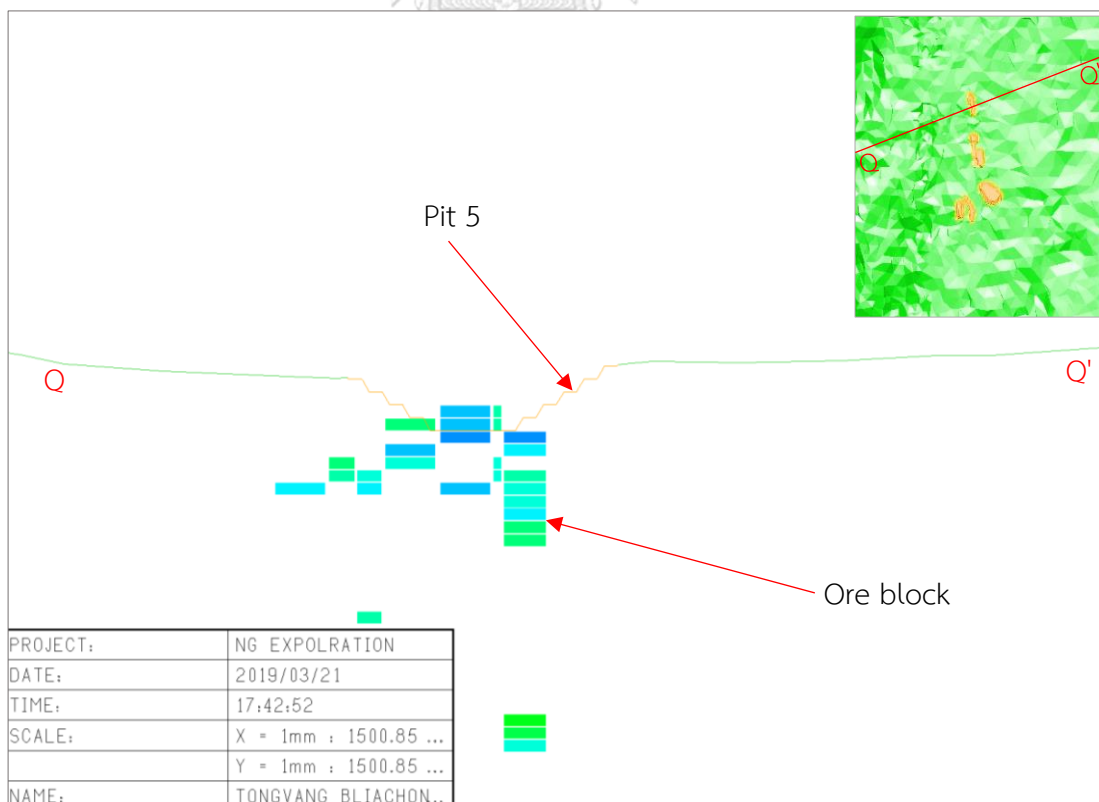


Figure 4.67 2D cross section view of SGS's pit No.5.

Table 4.25 SGS's mineable reserves after pits adjustment based on the CV basis.

CV basis (kcal/kg)	V_c (m ³)	Q_c (T)	Average grade	
			CV (kcal/kg)	AC (%)
500 - 4000	307,333.44	353,433.54	2,879.82	44.31
4000 - 5000	121,720.25	139,978.33	4,392.47	41.98
5000 - 5500	29,480.37	33,902.44	5,146.39	46.27
> = 5500	13,047.07	15,004.12	5,810.45	55.57
Total	471,581.13	542,318.43	3,493.02	44.14

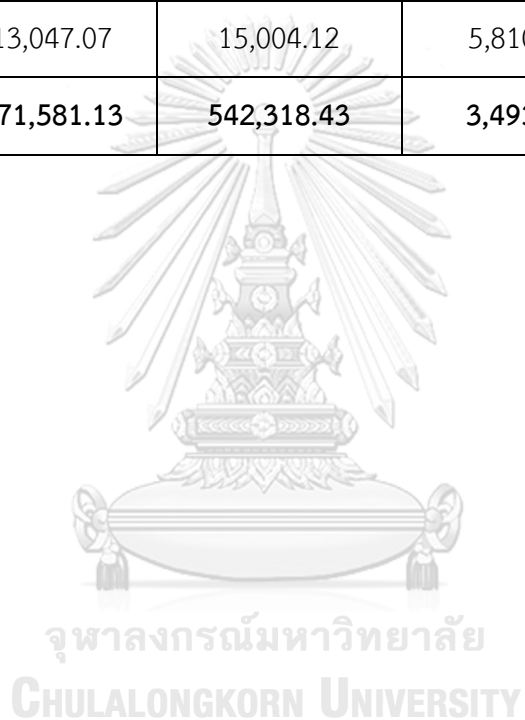


Table 4.26 Summary of mineable reserve after SGS's pits adjustment for pit No.1.

Bench level	CV bin (kcal/kg)	Mineable reserve		Average grade		Waste material		SR (BCM: T)
		V _c (m ³)	Q _c (T)	CV (kcal/kg)	AC (%)	V _w (m ³)	Q _w (T)	
240	-	-	-	-	-	1.60	2.88	
235	-	-	-	-	-	1,144.92	2,060.85	
230	-	-	-	-	-	7,566.42	13,619.55	
225	-	-	-	-	-	22,850.84	41,131.53	
220	500 - 4000	1,327.00	1,526.05	3,049.99	20.28	162,505.79	292,510.42	
	4000 - 5000	302.60	347.99	4,102.15	23.41			
215	500 - 4000	2,668.80	3,069.12	3,632.81	23.53	167,466.90	301,440.41	
	4000 - 4000	2,093.20	2,407.18	4,568.52	31.21			
	5000 - 5500	1,307.20	1,503.28	5,203.24	32.26			
210	500 - 4000	1,534.20	1,764.33	2,449.55	20.98	134,800.94	242,641.70	
	4000 - 5000	6,056.20	6,964.63	4,625.71	28.79			
	5000 - 5500	1,800.00	2,070.00	5,081.37	29.57			

Table 4.27 Mineable reserve after pits adjustment for SGS's pit No.2.

Bench level	CV bin (kcal/kg)	Mineable reserve		Average grade		Waste material		SR (BCM: T)
		V _c (m ³)	Q _c (T)	CV (kcal/kg)	AC (%)	V _w (m ³)	Q _w (T)	
225	4000 – 5000	306.40	352.36	4,022.45	48.29	37,725.66	67,906.18	
	>= 5500	230.00	264.50	5,529.58	62.72			
220	500 – 4000	859.45	988.37	3,441.51	40.04	129,700.78	233,461.38	
	4000 – 5000	1,589.30	1,827.70	4,413.06	50.07			
215	5000 – 5500	516.20	593.63	5,167.28	57.73	155,250.95	279,451.70	
	500 – 4000	3,377.40	3,884.01	3,159.92	40.68			
210	4000 – 5000	2,839.35	3,265.25	4,466.79	50.59	119,329.76	214,793.56	
	5000 – 5500	625.51	719.33	5,255.43	60.08			
205	500 – 4000	6,380.21	7,337.25	3,211.94	38.77	82,991.84	149,385.30	
	4000 – 5000	2,131.26	2,450.96	4,374.80	48.62			
200	5000 – 5500	277.60	319.24	5,046.36	60.26	50,340.93	90,613.67	
	500 – 4000	4,499.04	5,173.89	3,270.54	39.81			
Total	4000 – 5000	3,875.51	4,456.85	4,534.61	46.87	575,339.92	1,035,611.79	13.74
	5000 – 5500	850.12	977.64	5,044.04	56.41			
	500 – 4000	4,429.23	5,093.61	3,368.45	39.34			
	4000 – 5000	3,102.91	3,568.34	4,409.61	46.36			
	5000 – 5500	515.38	592.70	5,242.51	55.57			
		36,404.87	41,865.63	3,869.91	44.36			

Table 4.28 Summary of mineable reserve after SGS's pits adjustment for pit No.3.

Bench level	CV bin (kcal/kg)	Mineable reserve		Average grade		Waste material		SR (BCM: T)
		V _c (m ³)	Q _c (T)	CV (kcal/kg)	AC (%)	V _w (m ³)	Q _w (T)	
235	-	-	-	-	-	315.03	567.05	
230	-	-	-	-	-	10,497.94	18,896.29	
225	-	-	-	-	-	88,082.50	158,548.52	
220	500 – 4000	1,577.60	1,814.24	3,377.82	24.75	252,609.10	454,696.38	
	4000 – 5000	1,124.49	1,293.17	4,649.73	37.05			
	5000 – 5500	833.40	958.41	5,113.60	39.25			
215	500 – 4000	2,460.03	2,829.04	3,568.08	28.51	370,301.17	666,542.07	
	4000 – 5000	6,204.49	7,135.17	4,528.13	37.06			
	5000 – 5500	2,271.14	2,611.81	5,284.49	41.74			
	>= 5500	2,484.40	2,857.06	6,003.66	52.98			
210	500 – 4000	7,934.63	9,124.82	2,944.44	41.26	362,938.50	653,289.31	
	4000 – 5000	6,585.96	7,573.85	4,392.27	38.57			
	5000 – 5500	7,126.30	8,195.24	5,316.53	45.46			
	>= 5500	1,866.20	2,146.13	5,670.90	48.50			
205	500 – 4000	14,783.26	17,000.76	2,978.09	43.99	313,133.63	563,640.55	
	4000 – 5000	12,215.53	14,047.86	4,461.71	40.86			

Table 4.29 Summary of mineable reserves after SGS's pits adjustment for pit No.4.

Bench level	CV bin (kcal/kg)	Mineable reserve		Average grade		Waste material		SR (BCM: T)
		V _c (m ³)	Q _c (T)	CV (kcal/kg)	AC (%)	V _w (m ³)	Q _w (T)	
230		-	-	-	-	6,562.77	11,812.99	
225		-	-	-	-	90,958.22	163,724.79	
220	500 - 4000	5,486.20	6,309.14	2,928.49	53.04	169,399.03	304,918.26	
	4000 - 5000	841.92	968.21	4,425.47	63.96			
215	500 - 5500	16,839.19	19,365.08	2,586.01	53.74	270,475.93	486,856.65	
	4000 - 5000	3,119.55	3,587.48	4,645.77	67.92			
210	500 - 4000	16,618.55	19,111.33	2,497.33	53.96	226,036.85	406,866.31	
	4000 - 5000	816.76	939.28	4,512.08	66.80			
	5000 - 5500	192.02	220.83	5,155.24	68.02			
	>= 5500	325.00	373.75	6,038.07	81.51			
205	500 - 4000	19,793.91	22,763.01	2,485.11	58.43	148,086.10	266,554.99	
	4000 - 5000	2,058.00	2,366.70	4,192.91	61.53			
200	500 - 4000	24,015.15	27,617.42	2,814.94	61.13	111,046.44	199,883.58	
	4000 - 5000	2,612.18	3,004.01	4,289.86	73.99			
	5000 - 5500	0.35	0.40	5,331.84	76.05			
195	500 - 4000	22,164.11	25,488.74	2,802.05	61.92	84,962.00	152,931.62	
	4000 - 5000	1,045.23	1,202.01	4,117.45	75.10			
	5000 - 5500	335.60	385.94	5,250.51	79.00			
Total		116,263.72	133,703.33	2,844.99	59.13	1,107,527.34	1,993,549.19	8.26

Table 4.30 Summary of mineable reserve after SGS's pits adjustment for pit No.5.

Bench level	CV bin (kcal/kg)	Mineable reserve		Average grade		Waste material		SR (BCM: T)
		V _c (m ³)	Q _c (T)	CV (kcal/kg)	AC (%)	V _w (m ³)	Q _w (T)	
220		-	-	-	-	12,567.37	22,621.28	
225		-	-	-	-	175.60	316.08	
215	500 - 4000	412.40	474.26	3,081.26	35.70	112,275.29	202,095.52	
	4000 - 5000	172.60	198.49	4,255.33	50.25			
210	500 - 4000	5,506.66	6,332.66	2,957.27	45.20	144,760.04	260,568.08	
	4000 - 5000	1,388.60	1,596.89	4,421.62	64.90			
205	500 - 4000	9,640.13	11,086.14	2,762.48	49.06	106,377.75	191,479.95	
	4000 - 5000	3,138.20	3,608.93	4,402.86	55.02			
200	500 - 4000	10,410.16	11,971.68	2,844.80	50.37	75,862.35	136,552.25	
	4000 - 5000	2,751.60	3,164.34	4,236.91	61.39			
195	500 - 4000	7,741.94	8,903.24	3,068.84	54.00	52,495.73	94,492.29	
	4000 - 5000	774.25	890.38	4,408.55	58.71			
190	500 - 4000	1,549.65	1,782.10	3,138.01	44.83	19,674.42	35,413.94	
	4000 - 5000	250.43	287.99	4,480.14	59.54			
Total		43,736.62	50,297.10	3,185.14	51.43	524,188.55	943,539.39	10.42

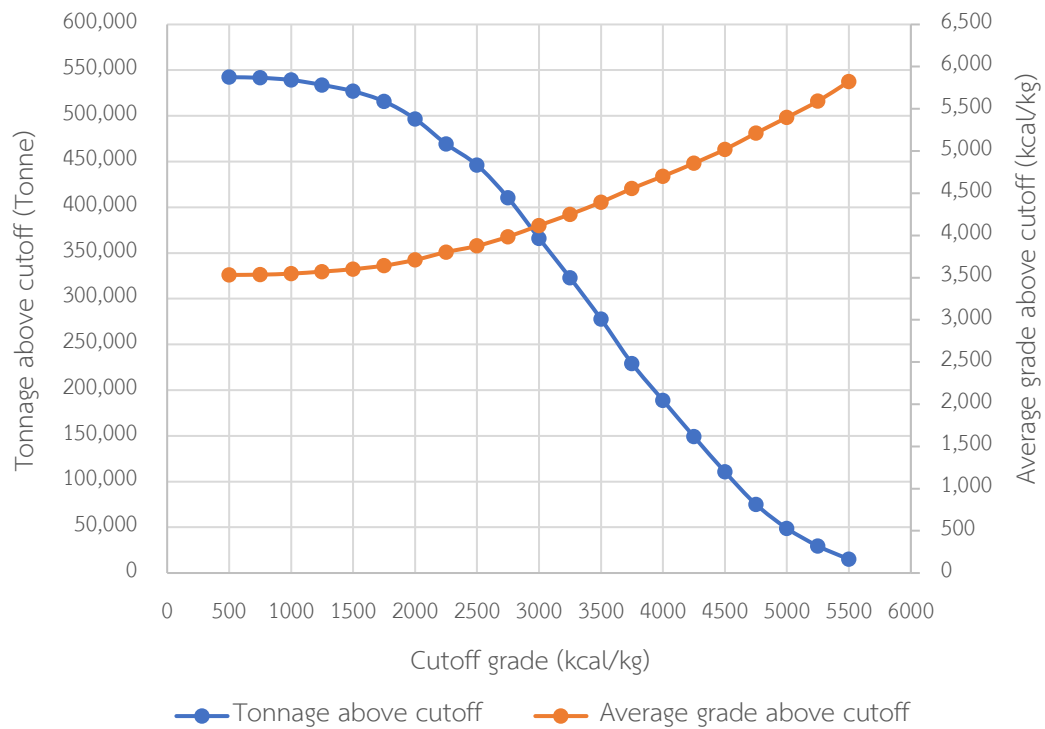


Figure 4.68 SGS's Grade Tonnage Curve of NG coal deposit.

4.6. Compositing data, OK's and SGS's results comparison

The both compositing data and 3D block model results which are estimated by OK and simulated by SGS provide a very similar data distribution as the histograms presented in Figure 4.70 – 4.71 for CV and AC, respectively. This shows that the estimated and simulated values honored the local samples data. The global mean and other statistical parameters among compositing data, OK's results, and SGS's results, are compared to observe the difference of their characteristics.

Table 4.31 Statistical parameters comparison among compositing data, OK's results and SGS's results of CV.

Data source	Mean (kcal/kg)	Variance	Coefficient of variation
Composite	3,793.49	3,252,824.04	0.48
OK's results	3,733.84	1,583,134.6	0.34
Real No. 4	3,724.536	4,292,047	0.56

Table 4.32 Statistical parameters comparison among composited data, OK's results and SGS's results of AC.

Data source	Mean (%)	Variance	Coefficient of variation
Composite	47.83	326.46	0.38
OK's results	48.68	155.65	0.26
Real No. 2	49.23	481.49	0.55

The comparison reveals that OK estimates generates a smoother map than SGS's map. SGS gives a more reliable results while maintaining the variance close to the composited data variance. The mean values of CV from OK's and SGS's results are almost identical to the composite's mean, the same can be said for AC. In general, it can be concluded that SGS method provides better images of spatial relationship of coal qualities. SGS also provides multiple of probable equal images of coal qualities which are necessary for the risk assessment analysis. The GTC between OK estimates and SGS are compared in Figure 4.69. It shows that OK estimates produce a higher grade compared to SGS while the tonnages are quite similar.

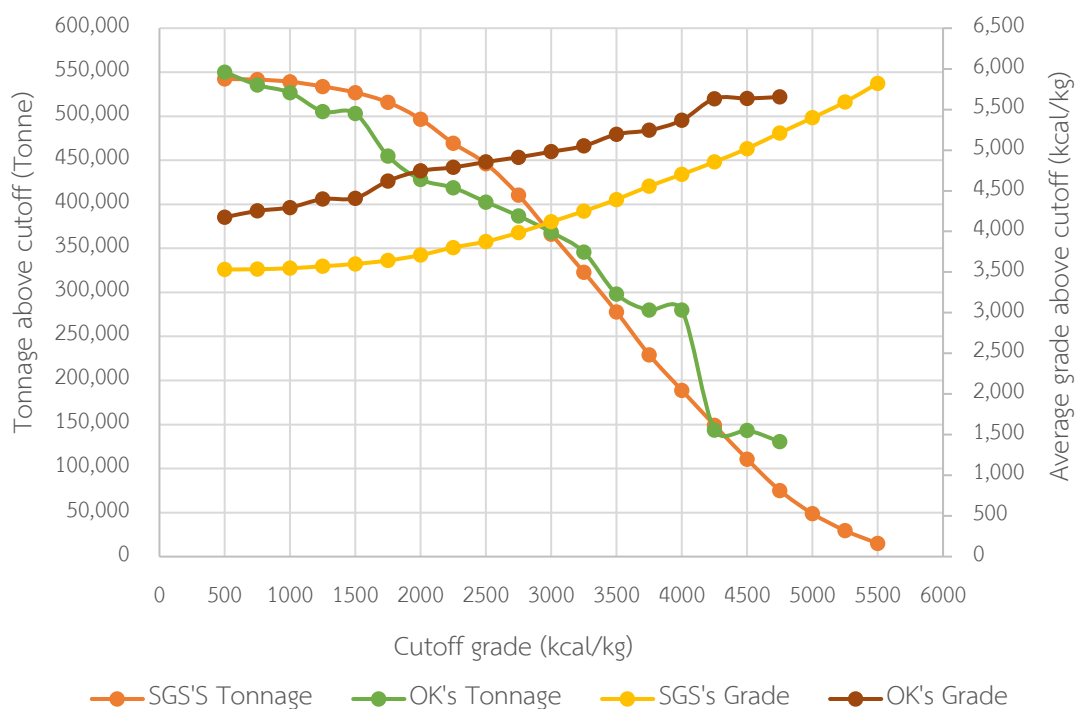


Figure 4.69 Comparing GTC between OK's and SGS's results.

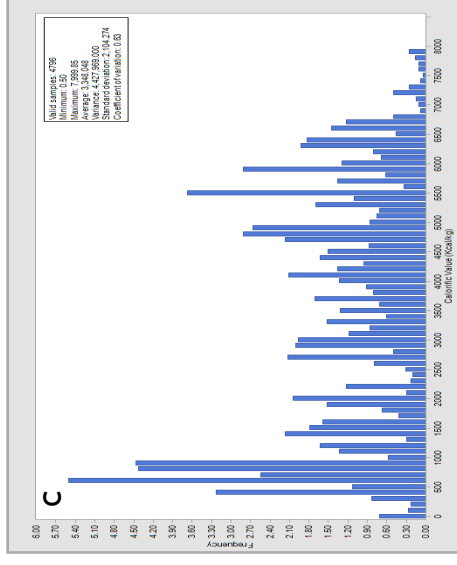
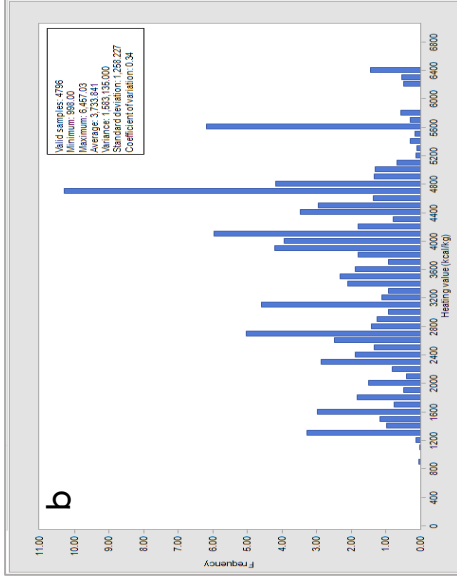
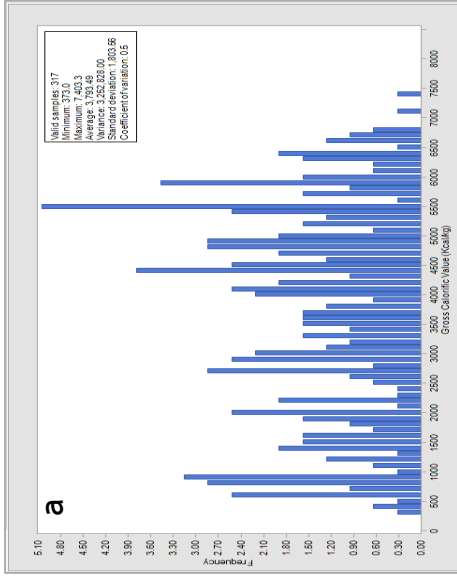


Figure 4.70 Comparing CV's histograms: (a). composited data, (b). OK's estimated values, (c). SGS's realization No.1.

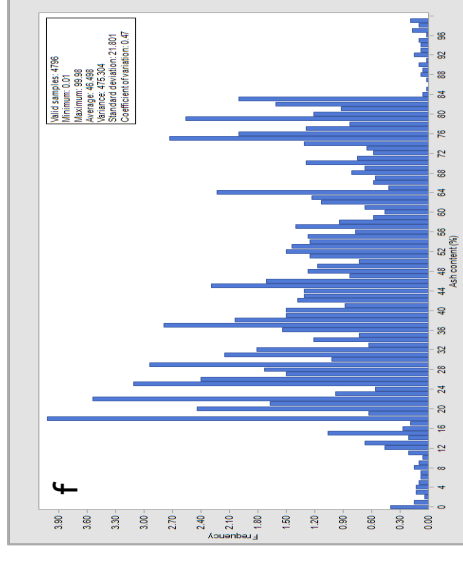
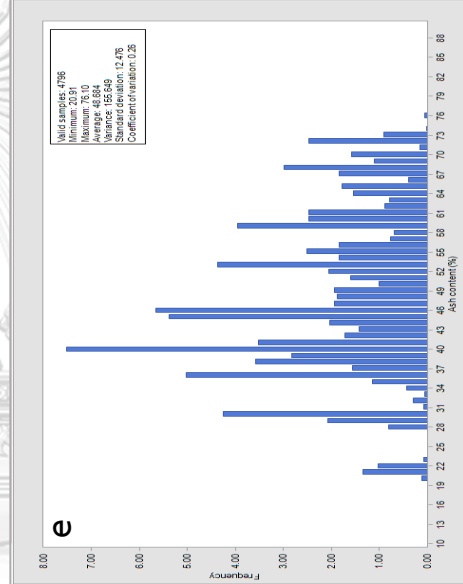
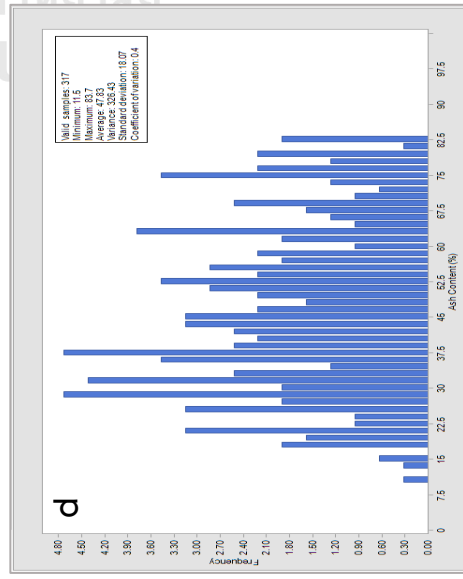


Figure 4.71 Comparing AC's histograms: (a). composited data, (b). OK's estimated values, (c). SGS's realization No.1.

CHAPTER 5

CONCLUSIONS AND RECOMMENDATIONS

5.1. Conclusions

In summary, this research has been carried out with a few objectives which include estimating the coal qualities such as CV and AC using geostatistical estimation approach as linear (OK) and non-linear (SGS) methods. The geological coal resource from estimated blocks have been computed using 3D block model method and estimated grades. The mineable reserve was calculated through the optimal pits and adjusted pits scheme. It was found that NG coal deposit exhibits complex geological structure area causing a high variation for coal seam thickness and coal qualities. The mean values for both CV and AC of composite data are 3,793 kcal/kg, and 47.83 %, respectively.

It can be summarized that OK estimates produces a total geological resource of 2.2 Mts with an average CV of 3,733 kcal/kg, and an average AC of 48.68 %. The LG pit optimization produces nine optimum pits and generates mineable reserve of 0.68 Mts. There are finally five pits adjusted from the LG pits in order to be realistic for mine operations. The mineable reserve after pits adjustment is 0.55 Mts with an average CV of 4,174 kcal/kg and an average AC of 44.2 %. The total waste materials generated from five adjusted pits are 9.32 Mts, yielding the stripping ratio of 10.36:1.

It can be summarized that SGS produces five realization maps for coal qualities distribution of each CV and AC. SGS generates a geological resource of 2.2 Mts, the same as OK approach, with an average CV of 3,769 kcal/kg and an average AC of 46.29 %. The SGS's LG pit optimization produces nine optimum pits and generates mineable reserve of 0.65 Mts. There are five pits adjusted finally to achieve a practical mine operation which produce the mineable reserve of 0.54 Mts with an average CV of 3,493 kcal/kg and an average AC of 44.14 %. The total waste material from the five adjusted pits are 9.5 Mts, yielding the stripping ratio of 10.12:1.

In comparison between OK and SGS methods, they both produce a very similar results throughout the statistical analysis of the findings. The both approaches have

the same geological resource, but different average grades of CV and AC. The Ok estimates generates more mineable reserve with higher grades included CV and AC comparing to SGS method. These two approaches produce the very close stripping ratio in comparison. OK generates a smoother map than SGS's maps. However, SGS provides a closer statistical map to the original data. The local variation is still maintaining in certain extent, as can be observed by the overall variance of the estimated block which is quite close to the original variance. OK approach can be used for coal grades, geological resource and reserve estimation. The SGS method could be considered as a suitable decision-making for a mine planning and mine operation at NG coal deposit.

5.2. Recommendations

Due to the fact that this coal basin presents complex geological structures resulted in coal seams thickness and coal grades variations, it is recommended that the regular drilling grid program should be implemented in order to ensure the coal seam continuities within the entire deposit. The grid dimension for future exploration drill holes has to be within the range of 50 meter according to the range computed from variogram model.

This study is just an attempt to interpolate the coal qualities at NG coal deposit (Block I) and generate a conceptual mine design scheme to achieve a realistic mine operation. Therefore, this research could be taken into account to evaluate the other blocks such as block II and block III with the full exploration area. It is advised that as soon as the pit has been developed, more information regarding to the coal seam thickness and coal grade distribution must be added to the database. Therefore, the estimation model can then be upgraded, and will provide a better coal grade distribution images for future mine plan and operation.

REFERENCES

- Abzalov, M. (2016). *Applied mining geology* (Vol. 12): Springer.
- Abzalov, M. Z. (2006). Localised Uniform Conditioning (LUC): a new approach for direct modelling of small blocks. *Mathematical Geology*, 38(4), 393-411.
- Alastair J, G. H. (2004). *Applied Mineral Inventory Estimation*. United Kingdom: University of Cambridge.
- Arber, S., & Ginn, J. (1991). The invisibility of age: gender and class in later life. *The sociological review*, 39(2), 260-291.
- Asghari, O., Soltni, F., & Amnieh, H. B. (2009). The comparison between sequential gaussian simulation (SGS) of Choghart ore deposit and geostatistical estimation through ordinary kriging. *Aust J Basic Appl Sci*, 3(1), 330-341.
- Asmael, N., Dupuy, A., Huneau, F., Hamid, S., & Coustumer, P. (2015). Groundwater Modeling as an Alternative Approach to Limited Data in the Northeastern Part of Mt. Hermon (Syria), to Develop a Preliminary Water Budget. *Water*, 7(7), 3978-3996.
- Bai, J., Feng, G., Wang, S., Qi, T., Yang, J., Guo, J., . . . Du, Y. (2018). Vertical stress and stability of interburden over an abandoned pillar working before upward mining: a case study. *Royal Society open science*, 5(8), 180346.
- Bohling, G. (2007). Introduction to geostatistics. *Kansas Geological Survey Open File Report no, 26(2007)*, 50.
- COSTA, J. O. F., Zingano, A. C., & KOPPE, J. C. (2000). Simulation—an approach to risk analysis in coal mining. *Exploration and Mining Geology*, 9(1), 43-49.
- David, M. (1977). *Geostatistical ore reserve estimation*: Elsevier Sci. Publ. Co., New York.
- Daya, A. A. (2015). Ordinary kriging for the estimation of vein type copper deposit: A case study of the Chelkureh, Iran. *Journal of Mining and Metallurgy A: Mining*, 51(1), 1-14.
- De Souza, L. E., Costa, J. F. C., & Koppe, J. C. (2004). Uncertainty estimate in resources assessment: a geostatistical contribution. *Natural Resources Research*, 13(1), 1-15.

- Deutsch, C. V., & Journel, A. G. (1992). *GSLIB: Geostatistical Software Library and User's Guide*. Hauptbd: Oxford university press.
- Deutsch, C. V., & Journel, A. G. (1998). Geostatistical software library and user's guide. *Oxford University Press, New York*.
- Dhaene, J., & Goovaerts, M. J. (1997). On the dependency of risks in the individual life model. *Insurance: Mathematics and Economics*, 19(3), 243-253.
- Hustrulid, W., Kuchta, M., & Martin, R. (2013). *Open Pit Mine Planning and Design 3rd Edition–Fundamental*: CRC Press/Balkema: Netherland.
- Irfan Manrwanza, C. N., Ahmad Helman Handani, IyanHaryanto. (2016). Coal resources classification using variogram to describe the spatial variability. *Impact Journals*, 4(10), 151-158.
- Journel, A. G., & Huijbregts, C. J. (1978). *Mining geostatistics* (Vol. 600): Academic press London.
- Lesmana, A., & Hitch, M. (2013). The geostatistical evaluation of coal parameters in Seam H, Malinau area, Indonesia. *International Journal of Oil, Gas and Coal Technology*, 6(6), 705-719.
- Lieskovský, M., Jankovský, M., Trenčiansky, M., & Merganič, J. (2017). Ash content vs. the economics of using wood chips for energy: Model based on data from Central Europe. *BioResources*, 12(1), 1579-1592.
- Olea, R. A., & Luppens, J. A. (2012). Sequential simulation approach to modeling of multi-seam coal deposits with an application to the assessment of a Louisiana lignite. *Natural Resources Research*, 21(4), 443-459.
- Olea, R. A., Luppens, J. A., Egozcue, J. J., & Pawlowsky-Glahn, V. (2016). Calorific value and compositional ultimate analysis with a case study of a Texas lignite. *International Journal of Coal Geology*, 162, 27-33.
- Ortiz Cabrera, J., & Leuangthong, O. (2007). A practical approach to validate the variogram reproduction from geostatistical simulation.
- Pardo-Igúzquiza, E., Dowd, P., Baltuille, J., & Chica-Olmo, M. (2013). Geostatistical modelling of a coal seam for resource risk assessment. *International Journal of Coal Geology*, 112, 134-140.
- Pyrcz, M. J., & Deutsch, C. V. (2006). Semivariogram models based on geometric offsets.

Mathematical Geology, 38(4), 475-488.

Revuelta, M. B. (2017). *Mineral Resources: From Exploration to Sustainability Assessment*: Springer.

Saputra, I. (2008). Shale Volume Calculation. *HRS Jakarta*.

Strebelle, S. (2002). Conditional simulation of complex geological structures using multiple-point statistics. *Mathematical Geology*, 34(1), 1-21.

Vang, S. (2015). *Slope stability assessment and its effect on pit design at Kaolin mine, Ranong province, Thailand*. Chulalongkorn University.

Wang, G., & Huang, L. (2012). 3D geological modeling for mineral resource assessment of the Tongshan Cu deposit, Heilongjiang Province, China. *Geoscience Frontiers*, 3(4), 483-491.

Wierzchowski, K., Chećko, J., & Pyka, I. (2017). Variability of mercury content in coal matter from coal seams of the Upper Silesia Coal Basin. *Archives of Mining Sciences*, 62(4), 843-856.

Wood, I. (1979). The geostatistical evaluation of low-ash coal reserves in No 2 seam, Witbank area. *Journal of the Southern African Institute of Mining and Metallurgy*, 79(12), 348-354.

VITA

NAME	Mr. Tongvang Bliachongvang
DATE OF BIRTH	8 August 1992
PLACE OF BIRTH	Xiengkhouang Province, Lao PDR
INSTITUTIONS ATTENDED	<ul style="list-style-type: none"> - 2017 - Present: Studying Master's degree in Geo-resources Engineering at Chulalongkorn University - 2012 - 2016: Studied Bachelor's degree in Mining Engineering at National University of Laos
HOME ADDRESS	Pek district, Xiengkhouang province, Lao PDR
PUBLICATION	Ore Reserves Estimation of the Nam Nga Coal Deposit, Lao PDR, using Geostatistical Method
AWARD RECEIVED	<ul style="list-style-type: none"> - 2017 - Present: Graduate Scholarship in Geo-resources Engineering from AUN/SEED-Net (JICA) at Chulalongkorn University. - 2016 - 2017: One Semester Scholarship in Geo-resources Engineering at Chulalongkon University